



DOCUMENT NO. 0816-40-TR-101

SYSTEM LEVEL DESIGN REPORT
FOR THE MOBILE-SATELLITE SIMULATION

March 18, 1977

SED SYSTEMS LTD.

Box 1464, Saskatoon, Sask., Canada S7K 3P7

PHONE (306) 244-0976

TELEX 074-2495

TWX 610-731-1476

President: Dr. Alex Kavadas

Vice-Pres. Engineering: Dennis Johnson, P. Eng.

Vice-Pres. Operations: M. P. Hodson

SED SYSTEMS LTD.
SYSTEMS DIVISION

Queen
P
91
C655
P533
1977

SASKATOON

CANADA

Mobile-Satellite Systems Analysis	Document # 0816-40-TR-101	Issue #1
<p>2 SYSTEM LEVEL DESIGN OF THE MOBILE-SATELLITE SIMULATION</p>		

Date of Issue
March 18, 1977

Prepared by:
R.A. Plemel
J.A. Copeck
K.L. Krukewich

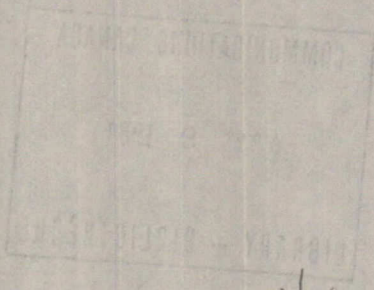
Approved by:
A. Sendyk
A. Sendyk

Industry Canada
Library Queen

JUL 21 1998

Industrie Canada
Bibliothèque Queen

COMMUNICATIONS CANADA
A 9 1984
LIBRARY - BIBLIOTHÈQUE



P
91
C655
P533
1977

DD 4647251
DL 4647299

PREFACE

This report constitutes the systems level design of a computer simulation designed to aid the Department of Communications in assessing the effects of RF interference associated with the operation of a mobile-satellite communications system. This work is the first phase of a two phase program to implement the simulation and was performed by SED Systems Ltd., under Supply and Services contract OPC76-00065 for the Department of Communications.

TABLE OF CONTENTS

	<u>PAGE</u>
i PREFACE	
1.0 INTRODUCTION	1 - 1
1.1 General Description of the Simulation	1 - 1
1.2 Major Factors Considered by the Simulation	1 - 4
1.3 Language Chart Usage	1 - 6
2.0 PROGRAM ORGANIZATION	2 - 1
2.1 Introduction	2 - 1
2.2 Hierarchical Design	2 - 2
2.3 High Level Executive Control Program	2 - 4
2.4 Data Flow	2 - 8
3.0 SITE, LINK and INTERFERENCE ROUTINES	3 - 1
3.1 General	3 - 1
3.2 "SITE" Calculations	3 - 2
3.2.1 General	3 - 2
3.2.2 Site Calculation Initiator (SCINIT)	3 - 3
3.2.3 Loop Controller (SITELC)	3 - 7
3.2.4 SITE Calculation Sequencing Routine (SITE)	3 - 10
3.3 "LINK" Calculations	3 - 12
3.3.1 General	3 - 12
3.3.2 Link Calculation Initiator (LCINIT)	3 - 13
3.3.3 Loop Controller (LINKLC)	3 - 15
3.3.4 LINK Calculation Sequencing Routine (LINK)	3 - 19
3.3.4.1 Subroutine LINK	3 - 19
3.3.4.2 Baseband Transmitter Model for ISI Carriers (BBTX)	3 - 25
3.3.4.3 IF-Type Receiver Model (IFRX)	3 - 25
3.3.4.4 Baseband Receiver Model (BBRX)	3 - 30
3.3.4.5 Path Loss Model (PATHLS)	3 - 33

3.4	Interference Calculations	3 - 38
3.4.1	General	3 - 38
3.4.2	Main Interference Selection Routine (INTERF)	3 - 38
3.4.3	System Interference Routine (SYSINT)	3 - 41
3.4.4	Site Interference Routine (SITINT)	3 - 43
3.4.5	Beam Interference Routine (BMINT)	3 - 45
3.4.6	ESI Interfering Carrier Model (ESITX)	3 - 47
3.4.7	ISI Interfering Carrier Model (ISITX)	3 - 50
3.4.8	Reports Generated in Interference Calculations	3 - 50

4.0	MODEL ROUTINES	4 - 1
4.1	General	4 - 1
4.2	Geometric Models	4 - 2
4.2.1	General	4 - 2
4.2.2	Site Location and Visibility Geometry (STGEOM)	4 - 2
4.2.3	Antenna Pointing Geometry (APGEOM)	4 - 9
4.2.4	Antenna Gain Geometry (ANGEOM)	4 - 12
4.3.5	Antenna Polarizer Geometry Routine (ANPOL)	4 - 14
4.3.6	Linear Polarization Mismatch Angle Geometry (LPMA)	4 - 16
4.3.7	Location of Sun Geometry (SUNLOC)	4 - 17
4.3.8	Spherical Layer Geometry (LAYER)	4 - 20
4.3.9	Specular Point Geometry (SPGEOM)	4 - 21
4.3.10	Geomagnetic Field Geometry (MAGFLD)	4 - 28
4.3	Antenna Models	4 - 31
4.3.1	General	4 - 31
4.3.2	Antenna Gain Model (ANTEN)	4 - 31
4.3.2.1	CCIR Principal Polarization Gain Model (CCIRA)	4 - 34
4.3.2.2	Single Variable Gain Model (SVGAIN)	4 - 35
4.3.2.3	Contour Gain Model (CNGAIN)	4 - 35
4.3.2.4	General Polar Pattern Model (GPGAIN)	4 - 36
4.3.2.5	Single Variable Cross Polarization Gain Model (SVDPOL)	4 - 37
4.3.2.6	Contour Cross Polarization Gain Model (CNDPOL)	4 - 38

4.3.2.7	General Polar Pattern Depolarization Model (GPDPOL)	4 - 39
4.3.2.8	Depolarization Model Routine (DEPOL)	4 - 39
4.3.2.9	Polarizer Mismatch Factor Routine (POLMIS)	4 - 40
4.4	Propagation Models	4 - 43
4.4.1	General	4 - 43
4.4.2	Tropospheric Absorption Model (TROP)	4 - 43
4.4.3	Ionospheric Scintillation Model (ISCINT)	4 - 45
4.4.4	Faraday Rotation Model (FARROT)	4 - 47
4.5	Multipath Interference Model	4 - 49
4.5.1	General	4 - 49
4.5.2	Multipath Interference Path Loss Calculations	4 - 49
4.5.3	Fresnel Reflection Coefficients	4 - 53
4.5.4	Diffuse and Specular Components	4 - 58
4.5.5	Doppler Spread	4 - 58
4.5.6	Implementation of the Multipath Model (MLTINT)	4 - 59
4.5.7	Reflection Coefficient Routine (REFLEC)	4 - 61
4.5.8	Effective RX Antenna Gain Calculation (ERGAIN)	4 - 63
4.6	Baseband Signal Processing Models	4 - 65
4.6.1	Delta Modulation Coding and Decoding of Analog Voice Signals	4 - 65
4.6.1.1	General	4 - 65
4.6.1.2	Delta Modulation Decoding Subroutine (DLTDEC)	4 - 65
4.6.2	Forward Error Correction Coding and Decoding of Digital Signals	4 - 70
4.6.2.1	General	4 - 70
4.6.2.2	FEC Decoding Subroutine (FECDEC)	4 - 70
4.6.3	Companding of Analog Voice Signals	4 - 76
4.6.4	Preamphasis and Deemphasis Models	4 - 77
4.7	RF Spectrum Models	4 - 79
4.7.1	General	4 - 79
4.7.2	FM Single Channel Voice (FMVOIC)	4 - 79
4.7.3	Binary FSK Model (FSKSPC)	4 - 83
4.7.4	PSK Spectrum Model (PSKSPC)	4 - 84

4.7.5	FM Television Spectrum Model (FMTV)	4 - 85
4.7.6	Gaussian Noise Spectrum Model (GAUSS)	4 - 85
4.7.7	Bandlimited White Noise Model (WHITE)	4 - 86
4.7.8	General Spectrum Model (GENSPC)	4 - 87
4.8	Demodulator Models	4 - 91
4.8.1	General	4 - 91
4.8.2	Digital Demodulator Models	4 - 91
4.8.3	FSK Demodulator Model	4 - 94
4.8.4	PSK Demodulator Model	4 - 101
4.8.5	Binary DPSK Demodulator Routine (BDPSK)	4 - 103
4.8.6	Binary CPSK Demodulator Routine (BCPSK)	4 - 104
4.8.7	M-ary DPSK Receiver Model (MDPSK)	4 - 105
4.8.8	M-ary CPSK Receiver Model (MCPSK)	4 - 107
4.8.9	FM Demodulator Model (FMDMD)	4 - 108
4.9	Filter Models	4 - 117
4.9.1	General	4 - 117
4.9.2	Filter Model Selector Routine (FILTER)	4 - 117
4.9.3	Ideal Bandpass Filter Model (IBPFIL)	4 - 119
4.9.4	Butterworth Filter Model (BUTFIL)	4 - 120
4.9.5	Chebyshev Filter Model (CHBFIL)	4 - 121
4.9.6	General Filter Model (GENFIL)	4 - 124
4.10	High Power Amplifier Model (HPA)	4 - 127
4.10.1	General	4 - 127
4.10.2	HPA Power Transfer Characteristic (HPAPWR)	4 - 128
4.10.3	HPA Intermodulation Distortion Routine (HPAIMD)	4 - 137
4.10.4	"Linear" Amplifier Distortion to Carrier Ratio Subroutine (SLMDCR)	4 - 143
4.10.5	Soft Limiter Distortion to Carrier Ratio Subroutine (SLMDCR)	4 - 145
4.10.6	Gaussian Distortion Spectrum Model (GAUSIM)	4 - 148
4.10.7	White Noise Distortion Spectrum Model (WNIMD)	4 - 149
4.11	Low Noise Amplifier Model (LNA)	4 - 152
4.11.1	General	4 - 152
4.11.2	Low Noise Amplifier Subroutine (LNA)	4 - 152

4.12	Antenna Noise Temperature	4 - 158
4.12.1	General	4 - 158
4.12.2	Antenna Noise Temperature Subroutine (ANTEMP)	4 - 159
5.0	FILE DESIGN	5 - 1
5.1	Introduction	5 - 1
5.2	Database	5 - 1
5.2.1	File Orgainziation and Record Format	5 - 2
5.2.2	Creation (CREATE)	5 - 17
5.2.3	Insertion	5 - 17
5.2.3.1	Introduction (INSERT)	5 - 17
5.2.3.2	System Record Insertion (SYSI)	5 - 18
5.2.3.3	Satellite Site Record Insertion (SSITI)	5 - 20
5.2.3.4	Non-Satellite Site Record Insertion (NSSITI)	5 - 20
5.2.3.5	Satellite Beam Record Insertion (SBMI)	5 - 23
5.2.3.6	Non-Satellite Beam Record Insertion (NSBMI)	5 - 23
5.2.3.7	ISI TX Carrier Record Insertion (ITXCRI)	5 - 25
5.2.3.8	RX Carrier Record Insertion (ITXCRI)	5 - 30
5.2.3.9	ESI TX Carrier Record Insertion (ETXCRI)	5 - 30
5.2.4	Deletion (DELETE)	5 - 34
5.2.5	Dumping (DUMP)	5 - 34
5.2.6	Updating (UPDATE)	5 - 34
5.2.7	Reorganization (REORG)	5 - 37
5.3	Pattern File	5 - 40
5.3.1	File Organization and Record Format	5 - 40
5.3.2	Creation (CREATE)	5 - 40

5.3.3	Insertion	5 - 41
5.3.3.1	Single Variable and Contour Patterns	5 - 41
5.3.3.2	Polar Patterns (POLPAT)	5 - 41
5.3.4	Deletion (DELETE)	5 - 44
5.3.5	Dumping (DUMP)	5 - 44
5.3.6	Reorganization (PATRG)	5 - 47
5.4	Spectrum and Filter File	5 - 49
6.0	MISCELLANEOUS	6 - 1
6.1	Antenna Pattern Display	6 - 1
6.1.1	Display Command Processor (DSPLAY)	6 - 1
6.1.2	Display Plot Utility (PATPLT)	6 - 4
6.2	Status and Error Messages	6 - 6
7.0	SYSTEM RESOURCE REQUIREMENTS	7 - 1
7.1	Device and Memory Requirements	7 - 1
7.1.1	Input	7 - 1
7.1.2	Output	7 - 2
7.1.3	Processing	7 - 3
7.2	Language Requirements	7 - 5

1.0 INTRODUCTION

1.1 General Description of the Simulation

The computer simulation described in this report can be used to aid systems planners and analysts to assess the extent of and the effects of RF interference associated with the operation of a mobile-satellite communications system. The simulation will be capable of:

- o assessing the levels of RF interference into other existing or proposed communications systems caused by the operation of a mobile-satellite system.
- o assessing the effects of RF interference on the operation of a mobile-satellite system caused by other communications systems and by transmitters in the mobile-satellite system
- o providing results that will be useful in the coordination of a mobile-satellite system with other existing or proposed Canadian and international communications systems.

To use the simulation to assess the effects of interference associated with the operation of a mobile-satellite system, the following steps are followed:

- o data describing the transmitters in the mobile-satellite system is presented to the simulation. The simulation then stores this information, for later use, in a specially formatted "database".
- o data describing any "outside" (extra-system) interferors is collected and presented to the simulation. The simulation then stores this information in the database.
- o communications links between stations in the mobile-satellite system are defined by the user. The simulation then calculates the effect of the catalogued interferors on the quality of voice or data signals transmitted over these links, and generates reports describing the results of the calculations.

- o a number of sites at arbitrary locations are specified by the user. The simulation then calculates the interference received at the sites due to transmitters in the database.

Data describing the transmitters and receivers must be organized in a hierarchical fashion. The simulation design and operation have been based on this hierarchical structure. Basically, transmitters are grouped into two types of systems. The first is the collection of receiving and transmitting sites in the designated mobile-satellite system, and is called the ISI system. All "outside" transmitters are grouped into collections called ESI systems. Any site within a system can have an arbitrary number of antenna beams associated with it, and each beam can transmit or receive an arbitrary number of carriers. This hierarchy of SYSTEM, SITE, BEAM, and CARRIER is discussed in more detail in the remaining chapters of this report.

The calculations described above have been denoted "LINK" and "SITE" calculations and are controlled by the simulation user through a "command language" consisting of keywords and numeric parameters. In addition to these calculations, all operations of the simulation are controlled by the command language. This "language" is used to:

- o insert data describing receivers and transmitters into the database
- o update and display this data and perform other database maintenance operations
- o request SITE or LINK calculations
- o specify the control parameters and instructions required by these routines
- o select systems of interferors for analysis in SITE and LINK calculations
- o select reports and plots describing the results of calculations
- o override simulation-provided defaults when inserting data into the database or performing calculations.

The control language is a major feature of the simulation. Throughout the report, it is described in "language charts". Section 1.3 describes the meaning and usage of these charts.

1.2 Major Factors Considered by the Simulation

This section lists the major features and models of the simulation. Detailed descriptions of these constitute the remainder of this report.

- o the simulation can consider receivers and transmitters located at sites on or near the earth's surface (earth stations, aircraft, and non aeronautical-mobile stations, called ships in this report) or on satellites (geosynchronous or non-geosynchronous orbital).
- o the simulation can consider carriers operating from 200 MHz to 20 GHz.
- o the effects of atmospheric propagation phenomena on interference levels and communication link performance is considered. These include tropospheric absorption, ionospheric scintillation, Faraday rotation, multipath interference, and antenna thermal noise effects.
- o antenna principal and cross-polarization response patterns are considered. A number of analytical and general models are included.
- o multi-hop communications links (up to a maximum of four hops) can be considered. Hops between any two sites can be analysed, including inter-satellite hops.
- o a communications link can include IF-type repeaters and remodulation (or baseband-type repeaters). For IF-repeaters, non-linear amplifier power transfer characteristics can be modelled (ie: biased, soft and hard limiting amplifiers). For all amplifiers, intermodulation distortion is also considered.
- o the simulation can analyse the performance of single-channel analog voice and digital data basebands, and their associated baseband processors (preemphasis/deemphasis, companding, delta-modulation coding and decoding, forward error correction encoding and decoding), and FM (for analog VOICE), PSK and FSK (for digital data), modulators and demodulators.

- o the simulation also considers the effects of band-limiting filters used in receivers and transmitters.
- o for ESI interferors, the simulation can consider FM/VOICE, FM/TV, PSK, and FSK signals. Models are also included for Gaussian and white band-limited noise-like interferors and for carriers with arbitrary RF spectra.
- o the simulation can repeat SITE or LINK calculations while varying selected parameters over a specified range.

1.3 Language Chart Usage

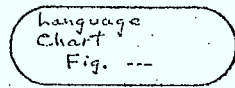
In order to give the user the capability of specifying and controlling the operations of the simulation, a special-purpose language has been designed. The elements of this language are:

- o keywords (maximum of 8 symbols)
- o numbers
- o quoted strings (used to provide text material such as names or comments, and begin and end with quote marks)
- o special symbols:
 - single quote mark ('), used to start and end quoted strings
 - asterisk (*), used to request a simulation default
 - semi-colon (;), used to end certain collections of language elements and to initiate the processing associated with them
- o separators (blanks), used to separate the other language elements

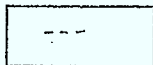
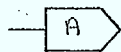
The correct ways of putting language elements together to form commands are described by means of language charts. A language chart is composed of a number of boxes joined by lines. The user constructs a command by beginning at the starting point of the diagram and following the lines from box to box, adding the indicated language element to the sequence forming the command, in the order that it is encountered.

Command options, and optional data items that need not always be provided, correspond to decision points on the language charts. The user selects from the available options at that point by following the corresponding line on the chart.

The symbols appearing in the language charts will now be described:

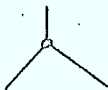


- a starting point of the language chart
- an ending point of the language chart
- an "off-page connector"
- a reference to a different language chart (indicated inside the box)
 - o begin at the starting point of this new language chart
 - o when finished with this other chart, continue out of this box and proceed as usual



- an "on-page connector" starting point
- marks a point that is taken to be immediately connected to certain other points in the diagram, though no line is used to join them
- an "on-page connector" ending point
- go to the "on-page connector" starting point with the same internal letter, and then proceed as usual
- contains a language element which is either:
 - o a keyword, written exactly as it must appear
 - o a description of a numeric value expected
 - o a special symbol
 - o a description of text material expected
- where applicable, units for values will be indicated

direction
of
travel ↓



direction
of
travel ↓



- junction point
- indicates a point where the user has a choice as to which line to follow
- collection point

direction
or
travel ↓



- another type of collection point
 - o curvature of the point of connection indicates the direction of travel on the common line

[---]

- a default value
- this notation is used to label a path which permits the user to skip a particular language item. It means that the default value in the square brackets will be used by the program in the place of the omitted item.
- the symbol 'd' denotes a default whose value will be determined during implementation of the simulation

(---)

- a branch label
- used to label the paths proceeding away from a junction point
 - o a junction point whose outgoing paths are labelled is a case of a conditional choice the user must make. He must choose the path whose label describes the situation at hand.

Occasionally, a language chart will begin with one or two keywords that appear on another language chart just before an "off-page connector" reference. This is done simply to assist in joining together different language charts. The language elements that are repeated on the two charts are not to be repeated in the command being formed; only one occurrence of the language elements is permitted in the command.

2.0 PROGRAM ORGANIZATION

2.1 Introduction

This simulation will be developed in a "top-down" fashion whereby the higher-level routines are developed and tested first, and then, once operational, they can serve as a natural test framework into which lower-level routines can be incorporated for development and testing. This hierarchical structure assists in the design and analysis phases of program development.

The "top-down" design philosophy also encourages modularity of design. Program modules are relatively independent, each having only one or two specific tasks to perform. In this way, the simulation can be modified to add or replace various models and functions without unreasonable amounts of effort.

The following sections discuss in more detail the hierarchical structure of the simulation, the higher-level executive programs which control the operation of the simulation (according to user commands), and the data flow between various components of the simulation.

2.2 Hierarchical Design

The major functional components of the simulation are displayed in Figure 2.2/1; which illustrates the hierarchical structure of the program. Individual subroutines are not indicated, and neither are utility-type subprograms. Aside from these differences, and those changes imposed by differing requirements, this structure of this simulation bears considerable resemblance to that of OFUS, as illustrated in Section 1.2 of Reference 2.2/1.

References

- 2.2/1: SED 0710-44-SW-103, Issue 3; "Orbit Frequency Utilization Simulation - Volume 2 - Program Description", February 28, 1977.

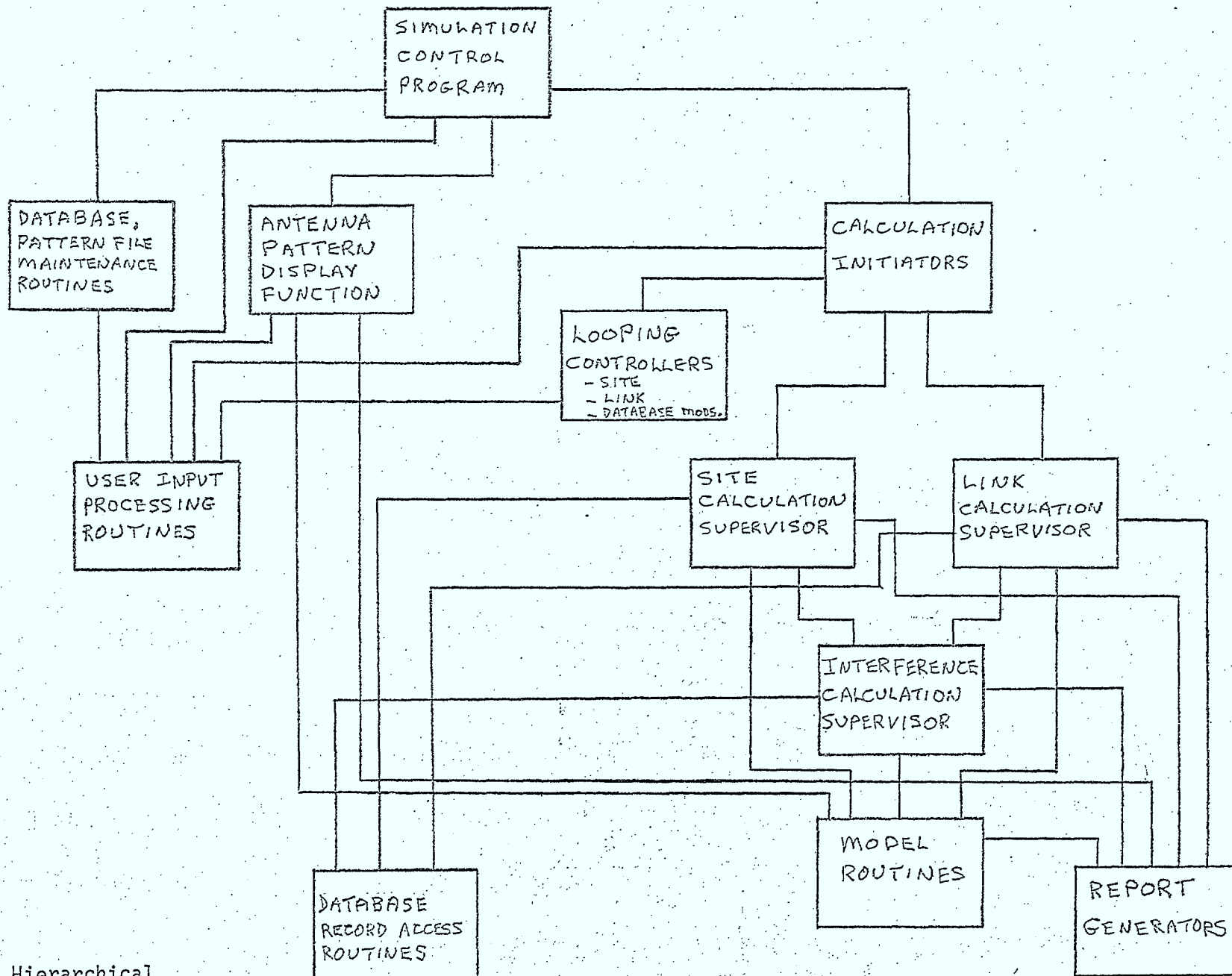


Figure 2.2/1 Hierarchical Structure

2.3 High Level Executive Control Program (SCP)

Purpose

To read and interpret user commands specifying operations the simulation is to perform, and to invoke the appropriate subprograms that implement the operations requested.

Method

This control program will function in a manner similar to the corresponding program in OFUS, as described in Section 2.2 of Reference 2.3/1.

Figure 2.3/1 is a flowchart illustrating the structure of the simulation control program SCP, while the language chart in Figure 2.3/2 indicates the form of the command language structure available to the user.

Inputs

0 none

Outputs

0 none

Figure 2.3/1 Flowchart of SCP

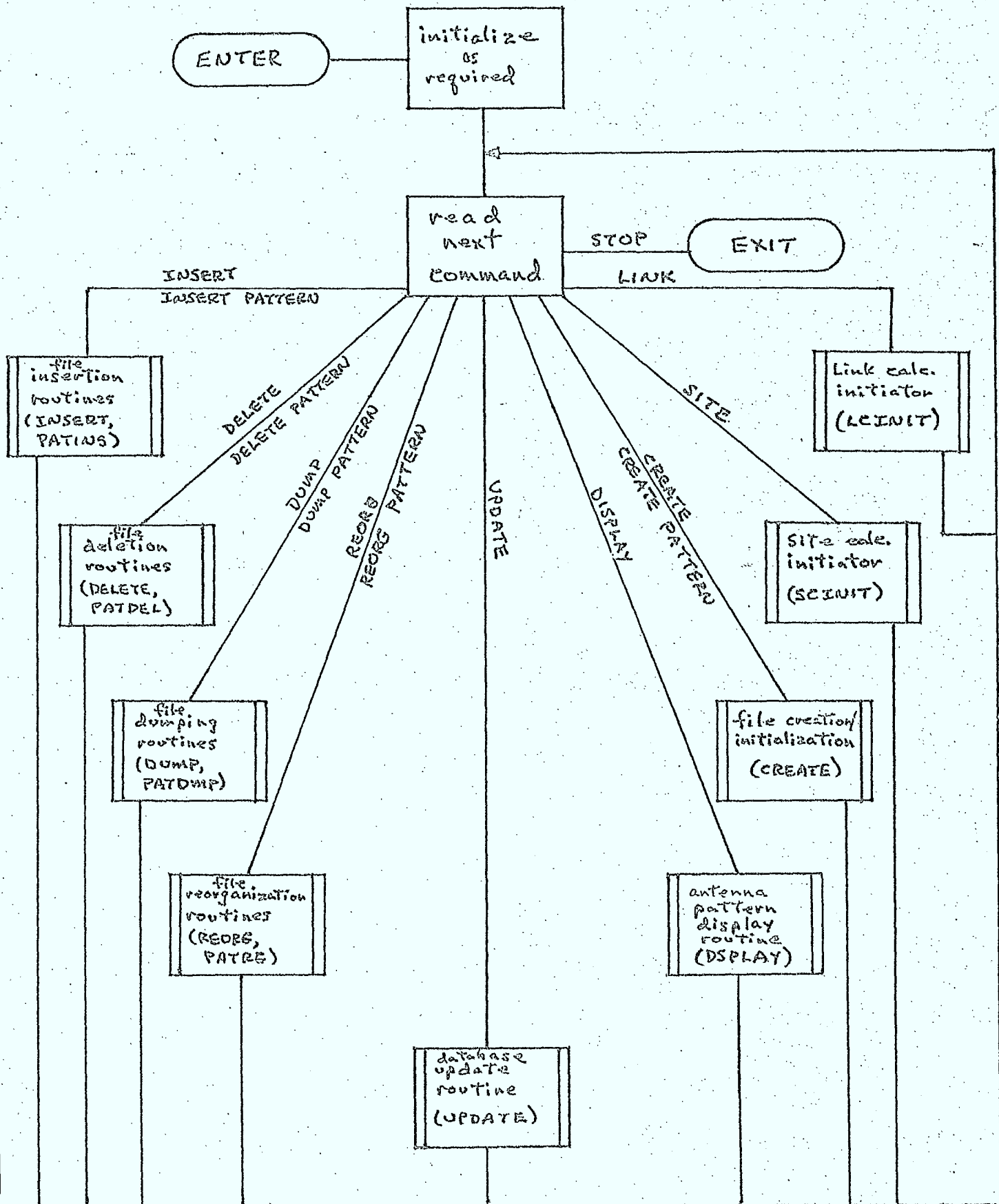
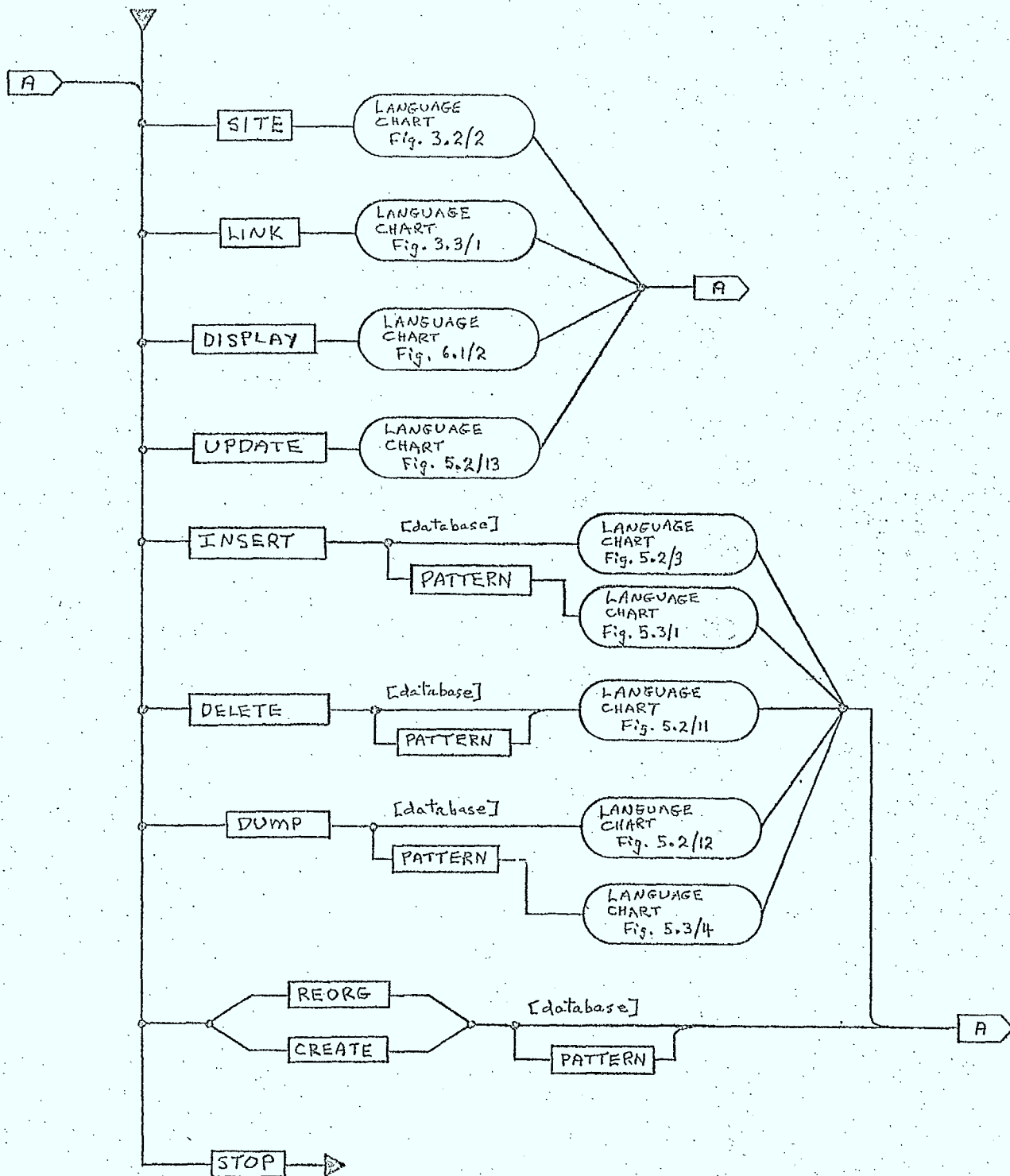


Figure 2.3/2 Language Chart of Simulation Commands



References

- 2.3/1: SED 0710-44-SW-103, Issue 3; "Orbit Frequency Utilization Simulation - Volume 2 - Program Description", February 28, 1977.

2.4 Data Flow

The data processed by this simulation can be classified as follows:

- input data, which can be of several kinds:
 - o for the database, describing transmitters and receivers that will be used in link and site calculations;
 - o for the pattern file, describing gain response patterns for various antennas in the database;
 - o for simulation control, commanding various program operations, specifying parameters for various calculations, controlling the form of the reports associated with calculations, etc.;
- processing data, obtained from the following sources:
 - o the database;
 - o the pattern file;
 - o a spectrum and filter file provided by the user containing data in a pre-defined format that describes spectrum and filter characteristics;
 - o internal memory, used for the common blocks, parameter lists, and local variable storage required for data communications between various subprograms;
- output data, of the following kinds:
 - o reports and plots describing the results of site and link calculations;
 - o plots of antenna gain response;
 - o status and error messages.

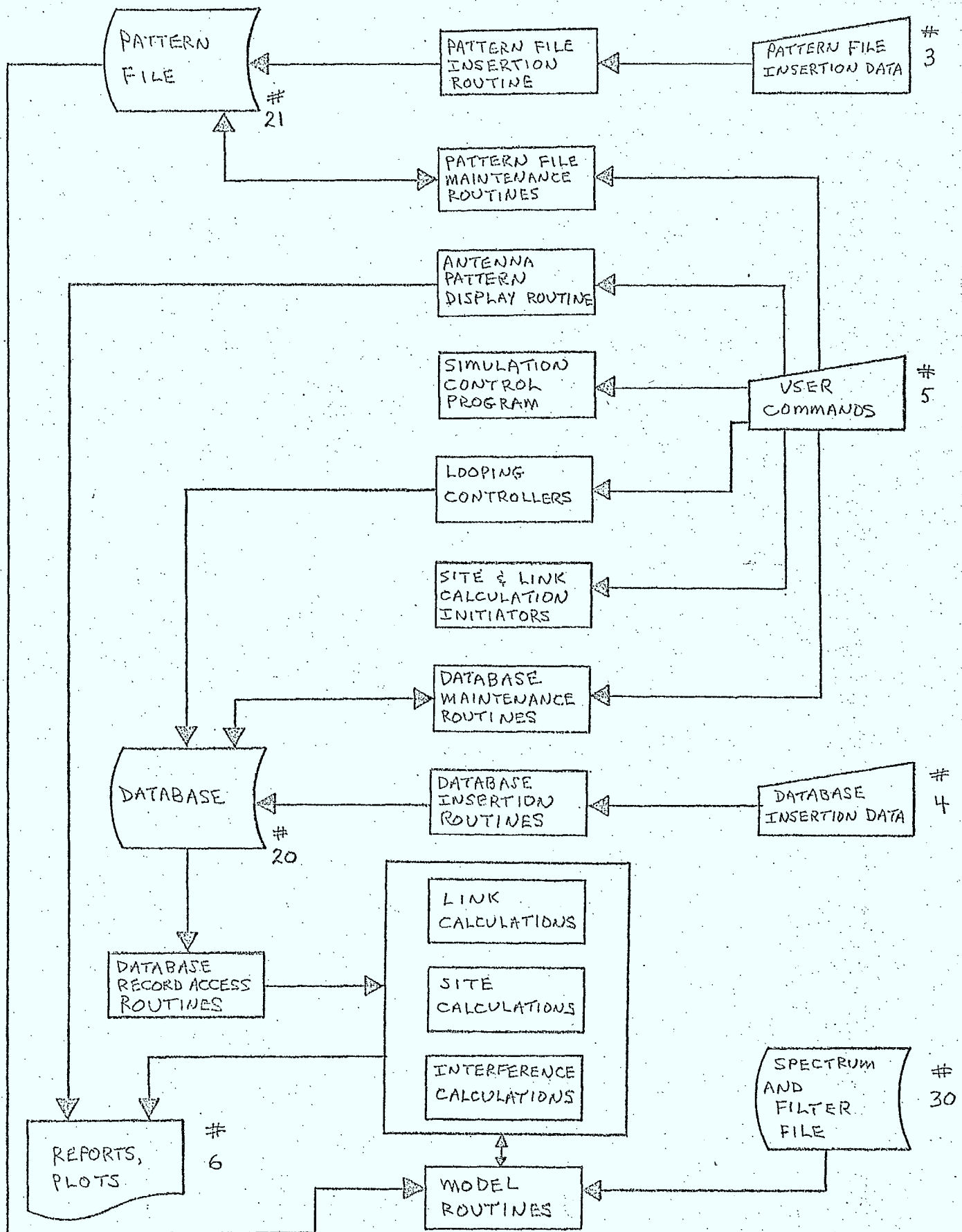
FORTTRAN logical I/O unit numbers are associated with certain of these data collections in order to permit the user to make use of various physical devices such as card readers, printers, terminals, and disc files to be attached to the various datasets. These assignments are given in Table 2.4/1.

TABLE 2.4/1 DEVICE ASSIGNMENTS AND CHARACTERISTICS

<u>Unit No.</u>	<u>Type of Dataset</u>	<u>Contents</u>
3	sequential	insertion data for the pattern file
4	sequential	insertion data for the database
5	sequential	user commands, parameters, etc.
6	sequential	all simulation output
20	FORTTRAN direct access	the database
211	FORTTRAN direct access	the pattern file
30	FORTTRAN direct access	the spectrum and filter file

Some of the relationships between the data associated with these devices and the various program segments that use this data are shown in the data flow diagram in Figure 2.4/1. In this diagram the arrows are intended to indicate the direction of data transmission, not subroutine calls/returns.

Figure 2.4/1 Data Flow Diagram



3.0 SITE, LINK, and INTERFERENCE ROUTINES

3.1 General

In this chapter, the routines required to perform "SITE" and "LINK" calculations are described. For each routine, the user-specified inputs and program generated reports are described, together with the "looping" control routines required to repeat either SITE or LINK calculations while iteratively changing selected parameters. As both of these calculation supervisor routines make use of the same RF interference calculation routine, this routine, INTERF, and its associated lower level routines are also discussed in this chapter.

3.2 "SITE" Calculations

3.2.1 General

In a SITE calculation, the RF interference at a receiving site, across some specified bandwidth, is calculated. If no antenna is specified for the site, the simulation calculates the flux density and associated interference spectrum at the site. If an antenna is specified, the received power is also determined. The simulation user will specify the antenna by giving the program the record number in the database of the RX beam record describing the antenna (see Chapter 5). If no antenna is present, the site can be specified in two ways, ie:

- o the user specifies the record number in the database of the site record containing the receiver site location parameters
- or
- o the user specifies the type of site and location parameters directly.

The interference at the receiving site is calculated using the following criteria to select interfering transmitters from those stored in the database:

- o first, the user specifies collections of interfering transmitters, ie: systems, using the keyword instructions discussed in Section 3.2.2.
- o within the selected systems, only those sites visible to the receiver are considered further
- o only those TX carriers originating at the visible sites whose RF bandwidth lies within some portion of the user-specified "simulation bandwidth" are then considered in the interference calculations.

The simulation bandwidth can range from 1 kHz to 2MHz, and can be centered on any frequency from 201 MHz to 19.999 GHz.

The implementation of the SITE calculation is discussed in the remainder of this section.

3.2.2 Site Calculations Initiator (SCINIT)

Purpose

This routine is used to read and interpret the user commands and parameters specifying simulation control information for site calculations; this would include frequency, bandwidth, location data, report selection, interference selection, etc.

Method

Tables are constructed to store the user-specified information (including those items definable by default). Data in these tables are then made available to SITE, the subroutine which sequences the "SITE" calculations for the specified receiving site. The capability to repeat a SITE calculation while iteratively changing key parameters is implemented by making regular updates of the information stored in these tables, or to information stored in the database.

Figure 3.2/1 is a flowchart illustrating the operation of SCINIT. A language chart in Figure 3.2/2 describes the language format available to the user to specify and control the SITE calculations. It also illustrates the selection of interfering systems and report selection.

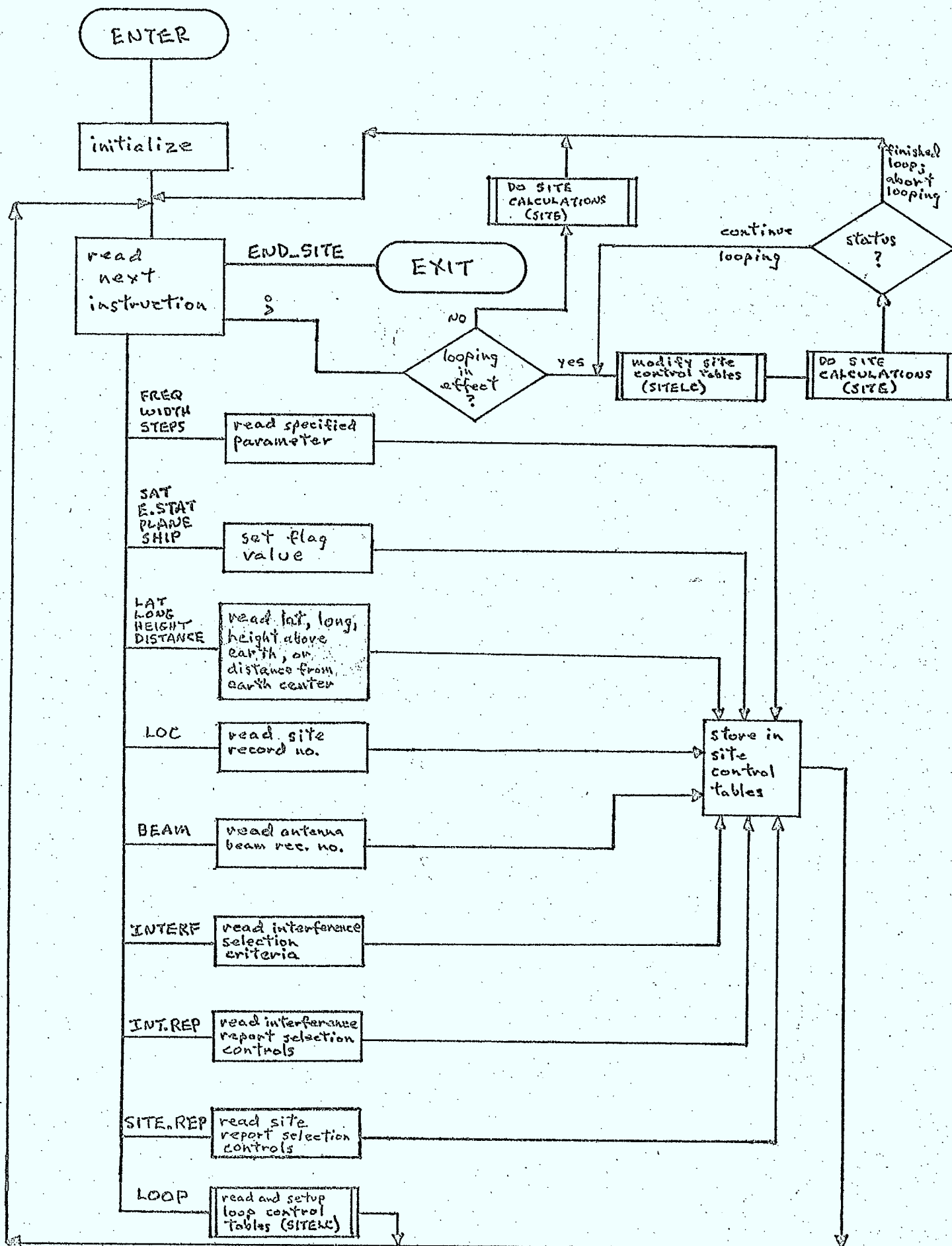
Inputs

- ① input device unit no. and characteristic parameters

Outputs

- ① none

Figure 3.2/1 Flowchart of SCINIT



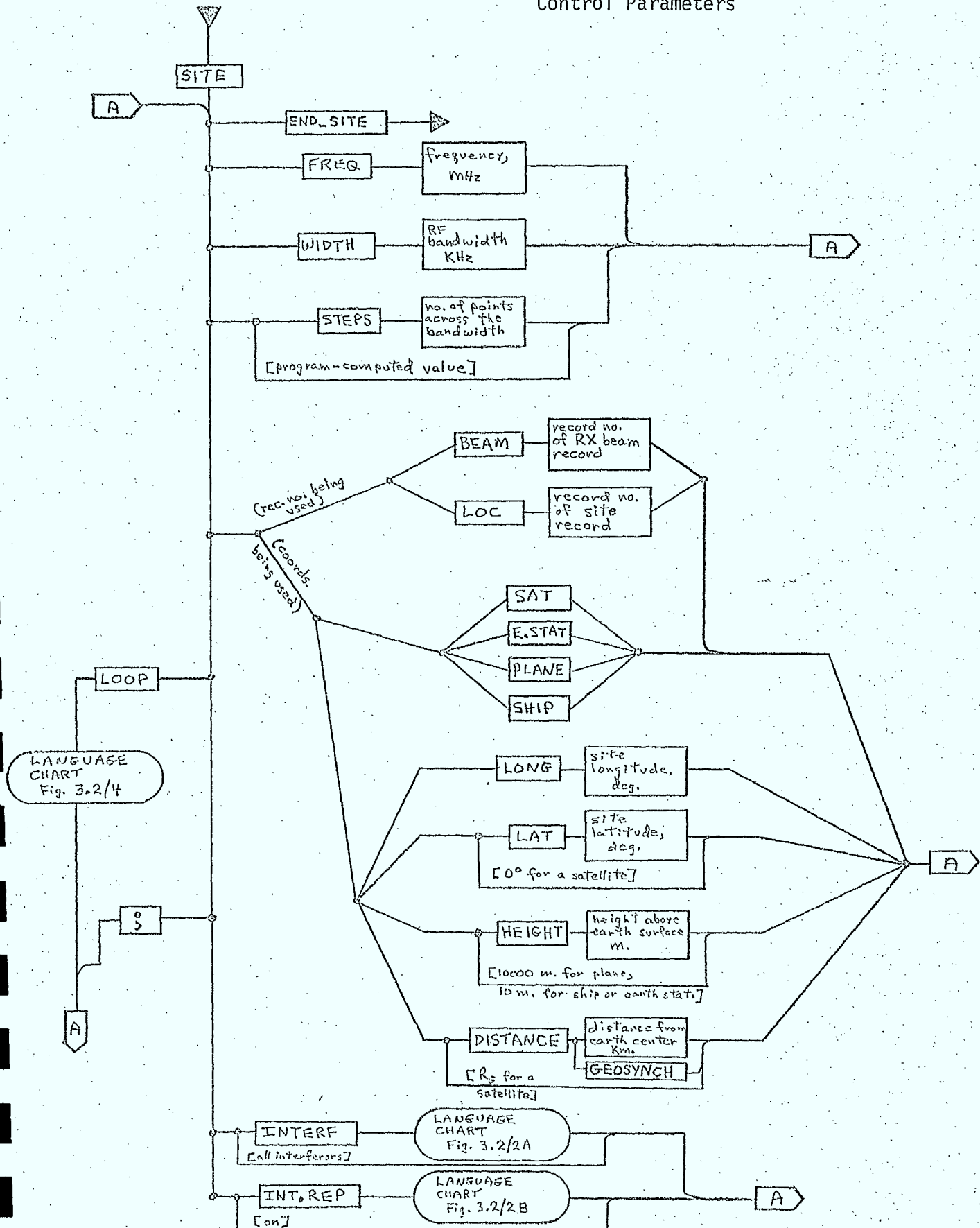


Figure 3.2/2A Language Chart of Site Control Parameters
- Interference Selection Sub-Chart

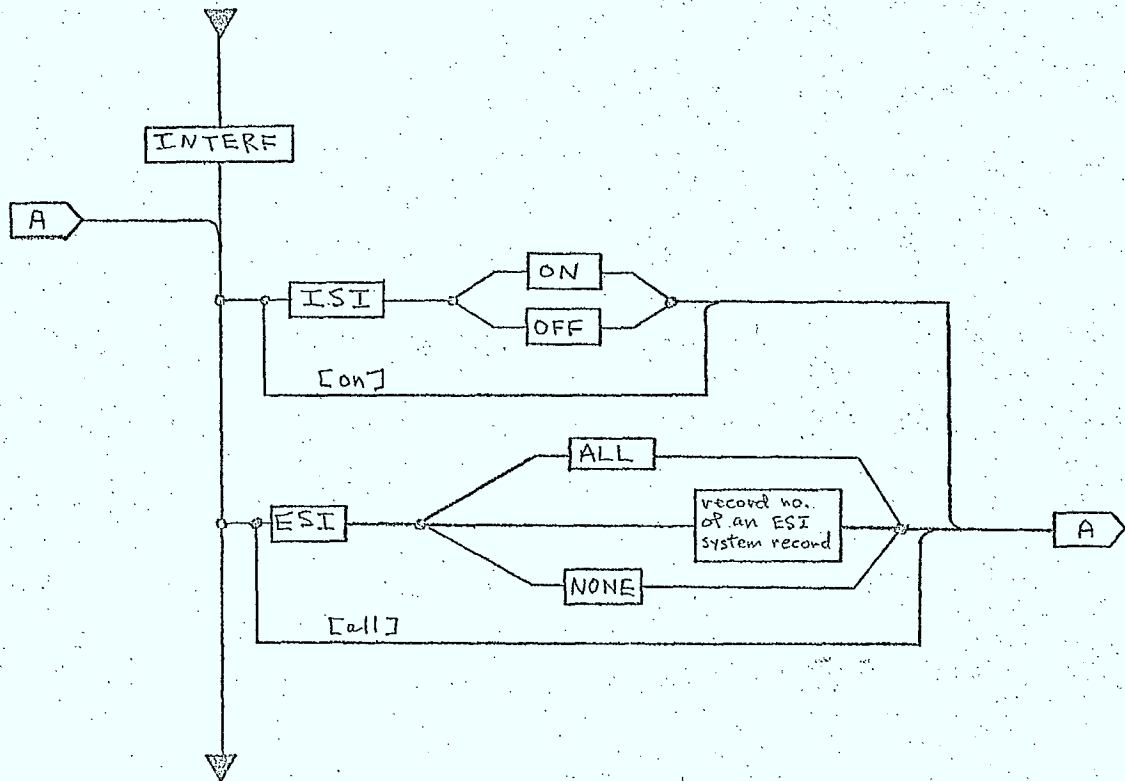
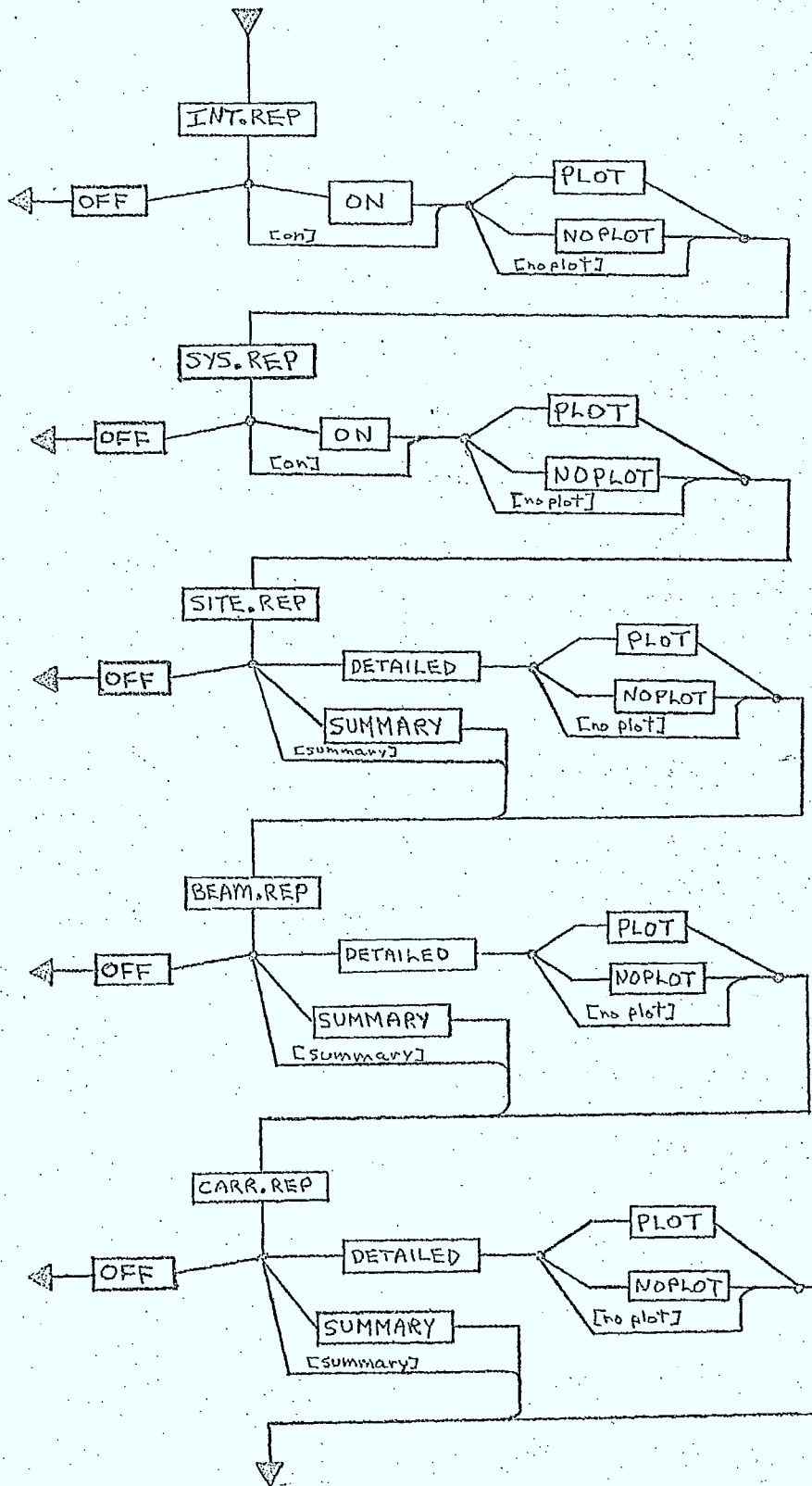


Figure 3.2/2B Language Chart of Site Control Parameters
- Interference Report Selection Sub-Chart



3.2.3 Loop Controller (SITELC)

Purpose

This routine is used to read loop control instructions used to modify the site control tables and information stored in the database, thus permitting repeated site calculations to be performed while varying selected parameters over a range of values.

Method

Starting and terminating values are read for certain of the user-specifiable site definition parameters and for those fields in database records the user has chosen for incremental variation. These values, along with the number of times the loop is to execute, are used to construct loop control tables. When the site control tables are to be modified for iterated site calculation, reentry into this routine permits the desired modifications to be made.

Figure 3.2/3 is a flowchart indicating the structure of subroutine SITELC. The language chart in Figure 3.2/4 illustrates the form the site loop control instructions take.

Inputs

- ① input device unit no. and characteristic parameters
- ① site control tables

Outputs

- ① site control tables

Figure 3.2/3 Flowchart of SITELC

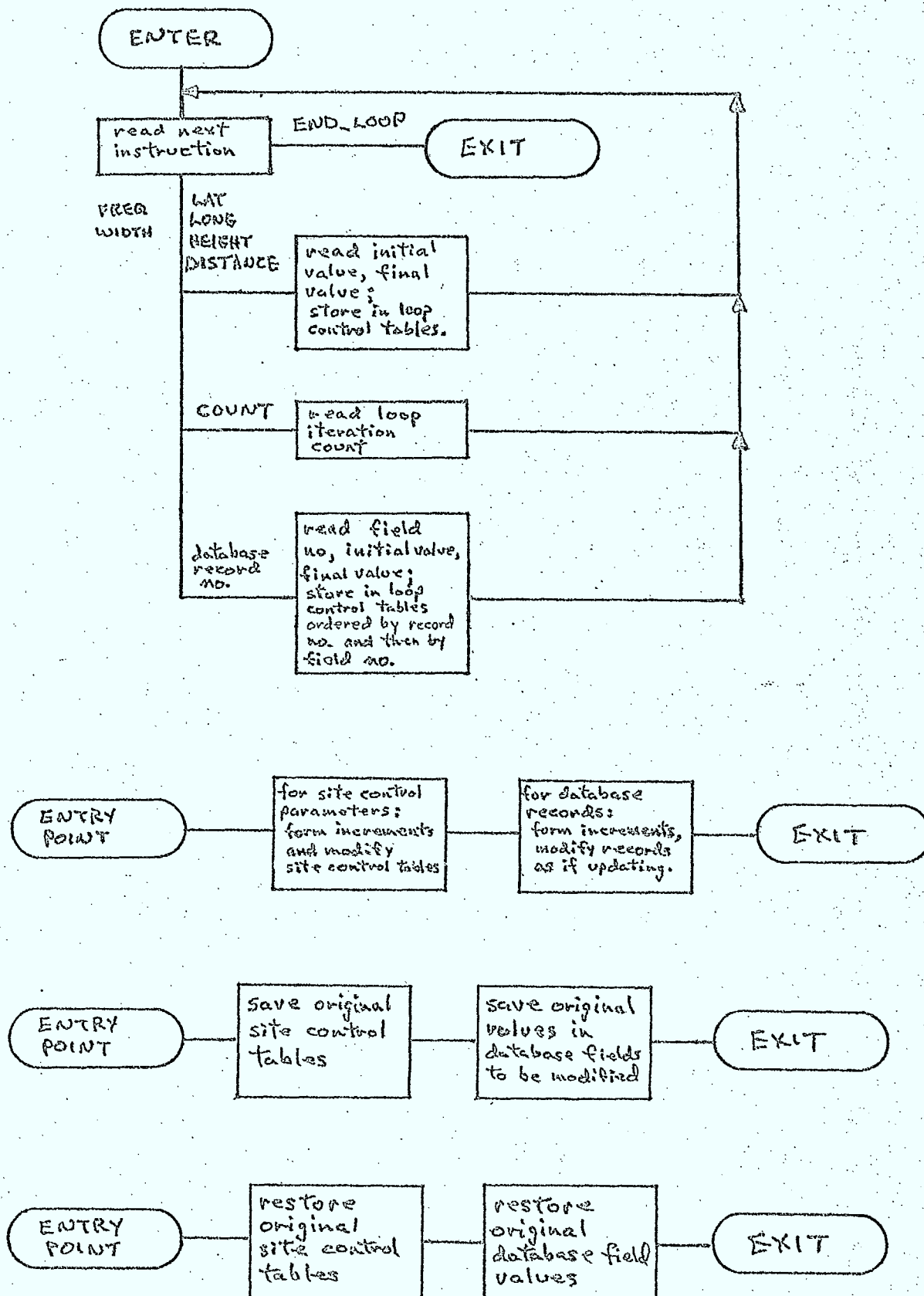
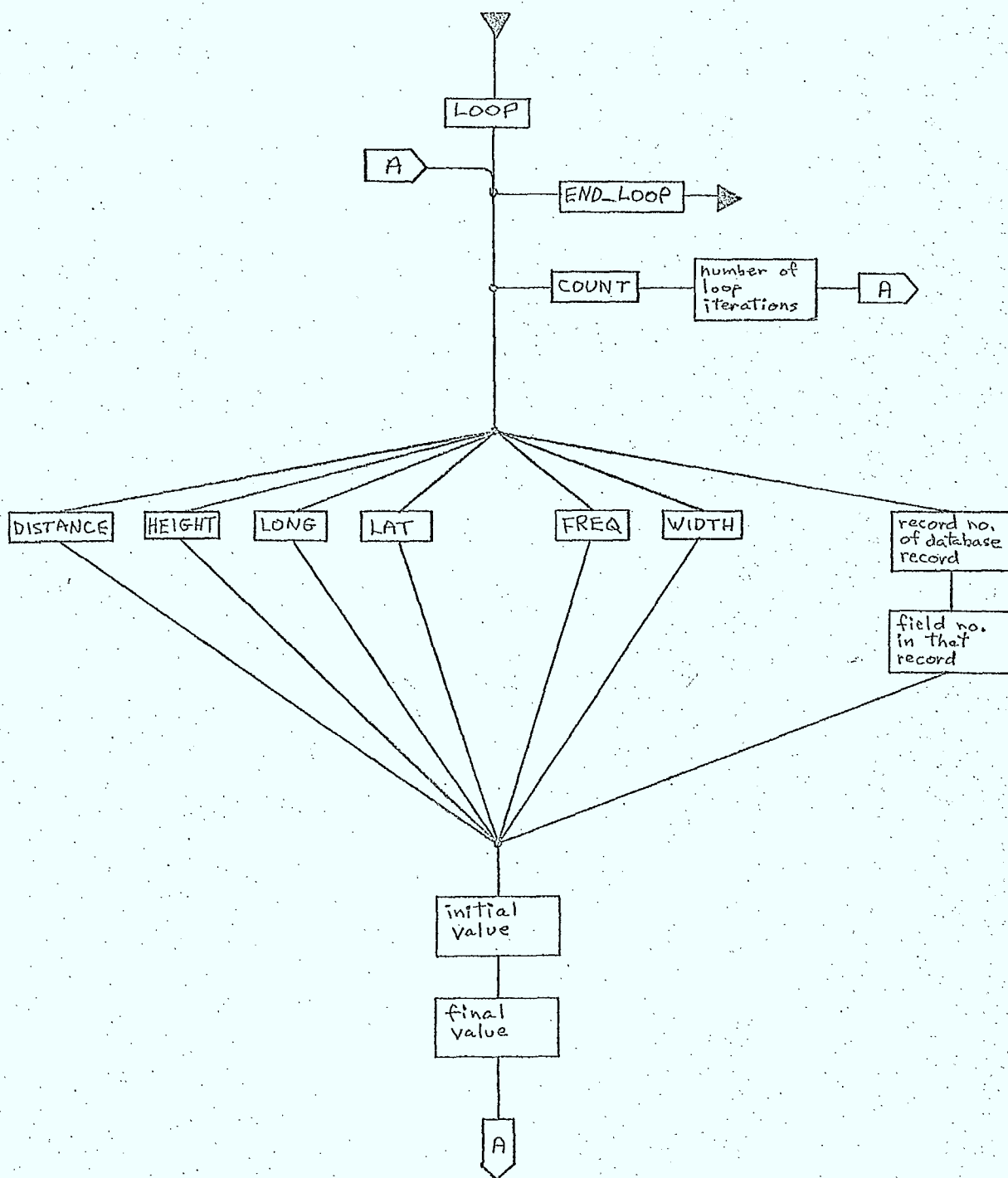


Figure 3.2/4 Language Chart of Site Calculation
Looping Control Instructions



3.2.4 SITE Calculation Sequencing Routine (SITE)

Purpose

This routine is used to calculate the cumulative RF interference spectrum and its total flux or power at a receiving site, using the instructions contained in the SITE control tables specified by the user.

Description

A flowchart illustrating the implementation of the SITE calculation is given by Figure 3.2/5. Basically, this routine determines the location vector and antenna parameters of the receiving site and calls a lower level subroutine (INTERF, described in Section 3.4) which actually does the interference calculations for the site. The routine SITE also generates a "SITE DEFINITION" report that describes the RX site location and antenna (if present) parameters used in the calculation. It should be noted that the only propagation phenomena considered on paths between the receiver and the interfering transmitters is tropospheric absorption.

This routine also checks the validity of the user-specified control data (ie: record type, etc) and terminates the current SITE calculation if an error condition is detected.

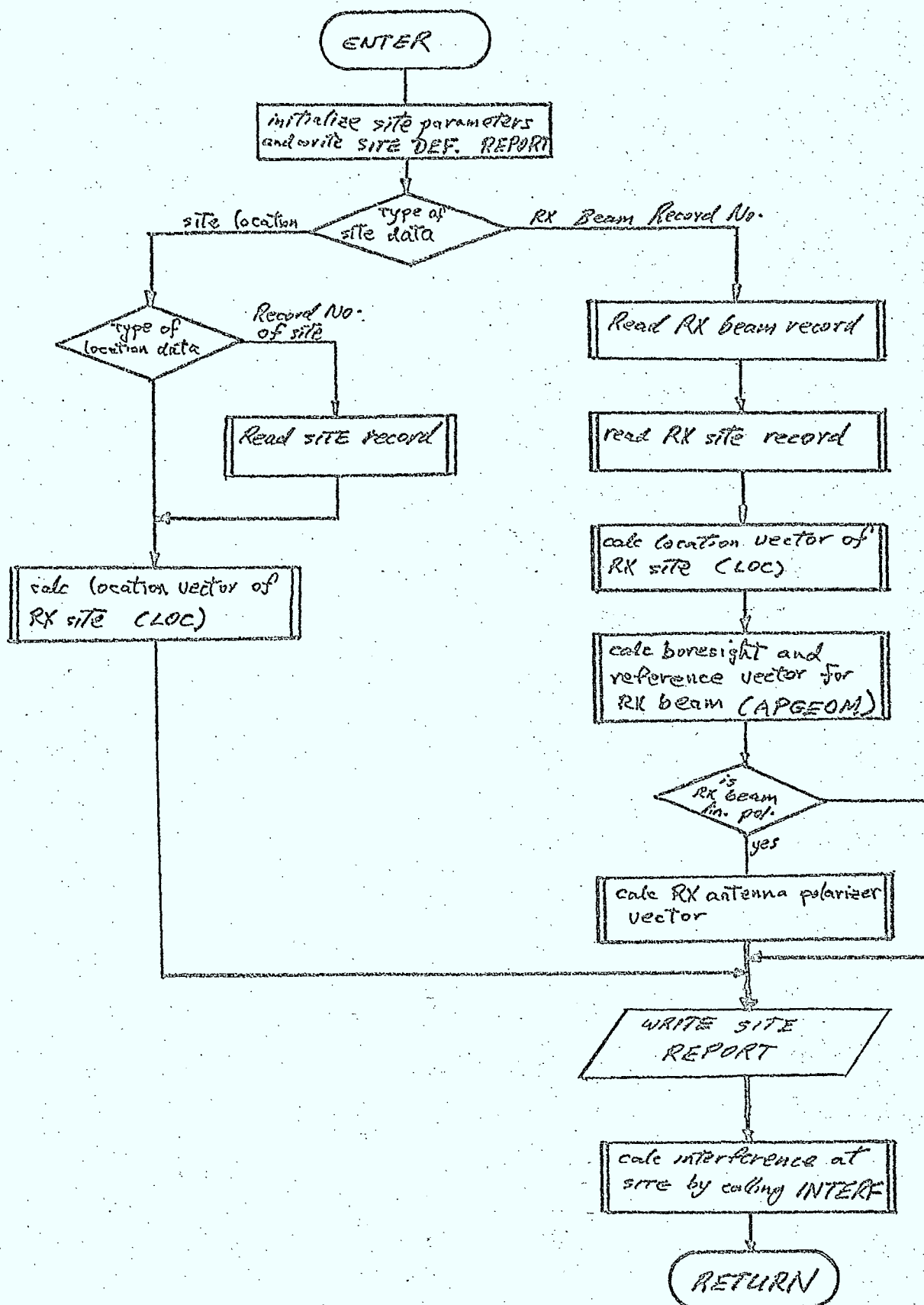
Inputs

- o site control table, containing receiving site location and antenna parameters, simulation frequency, resolution, and bandwidth, interference selection and report control instructions.

Outputs

- o error flag indicating whether or not an error condition occurred while attempting the SITE calculation.

Figure 3.2/5 Flowchart of Site



3.3 "LINK" Calculations

3.3.1 General

In a LINK calculation, the performance of a communications link operated in the presence of RF interference, is determined. The communications LINK can consist of a maximum of four hops, each starting at a transmitter and ending at a receiver. For simulation purposes, it is useful to define the following type of transmitters and receivers:

- o baseband transmitter - consisting of a modulator, associated RF filters, and a high power amplifier (HPA), and may be the first transmitter on a LINK or the transmitter portion of a remodulation repeater (also called a baseband repeater).
- o IF-type transmitter - consisting of a high power amplifier and associated filter, and is used as the transmitter portion of an IF-type repeater.
- o baseband receiver - consisting of a low noise amplifier (LNA) associated RF filters and a demodulator, and may be the final receiver on a link or the receiving section of a remodulation repeater.
- o IF-type receiver - consisting of an LNA and associated filter, and is used as the receiving section of an IF-type repeater.

Each hop of a link is defined by the user by specification of the record numbers of the transmitter and receiver carrier records in the database, as is done in OFUS. (Note, only ISI transmitters can be used in a LINK calculation). Each hop can also have propagation phenomena associated with it. The simulation will include the following phenomena:

- o tropospheric absorption (considered on all paths including those to interferors)
- o multipath interference (considered only on satellite-to-aircraft or satellite-to-ship paths involving the wanted carrier in a link calculation)
- o ionospheric scintillation (user-selected, considered on trans-ionospheric paths involving the wanted carrier)
- o Faraday rotation (user-selected, considered on transionospheric paths involving any linearly polarized carrier).

The antenna and location parameters associated with the sites used in the link are not specified by the user when defining a link since this data can be obtained from the database by the LINK routine from the information stored in the carrier records defining the link. It is assumed that the database contains information on all of the transmitters and receivers used in LINK and interference calculations.

The operation of the LINK calculation is illustrated in Figure 3.3/1. Basically, the routine calculates the degradation of the wanted carrier along the link and produces reports describing the thermal noise, RF interference, intermodulation distortion, and multipath interference at each receiver in the link. Whenever a baseband receiver is encountered, the resulting signal-to-noise ratio or bit error probability (depending on whether analog voice or digital data is being considered) is calculated. This routine is discussed in more detail in Section 3.3.4.

The RF interference corrupting the signal is determined using the routine INTERF, described in Section 3.4.

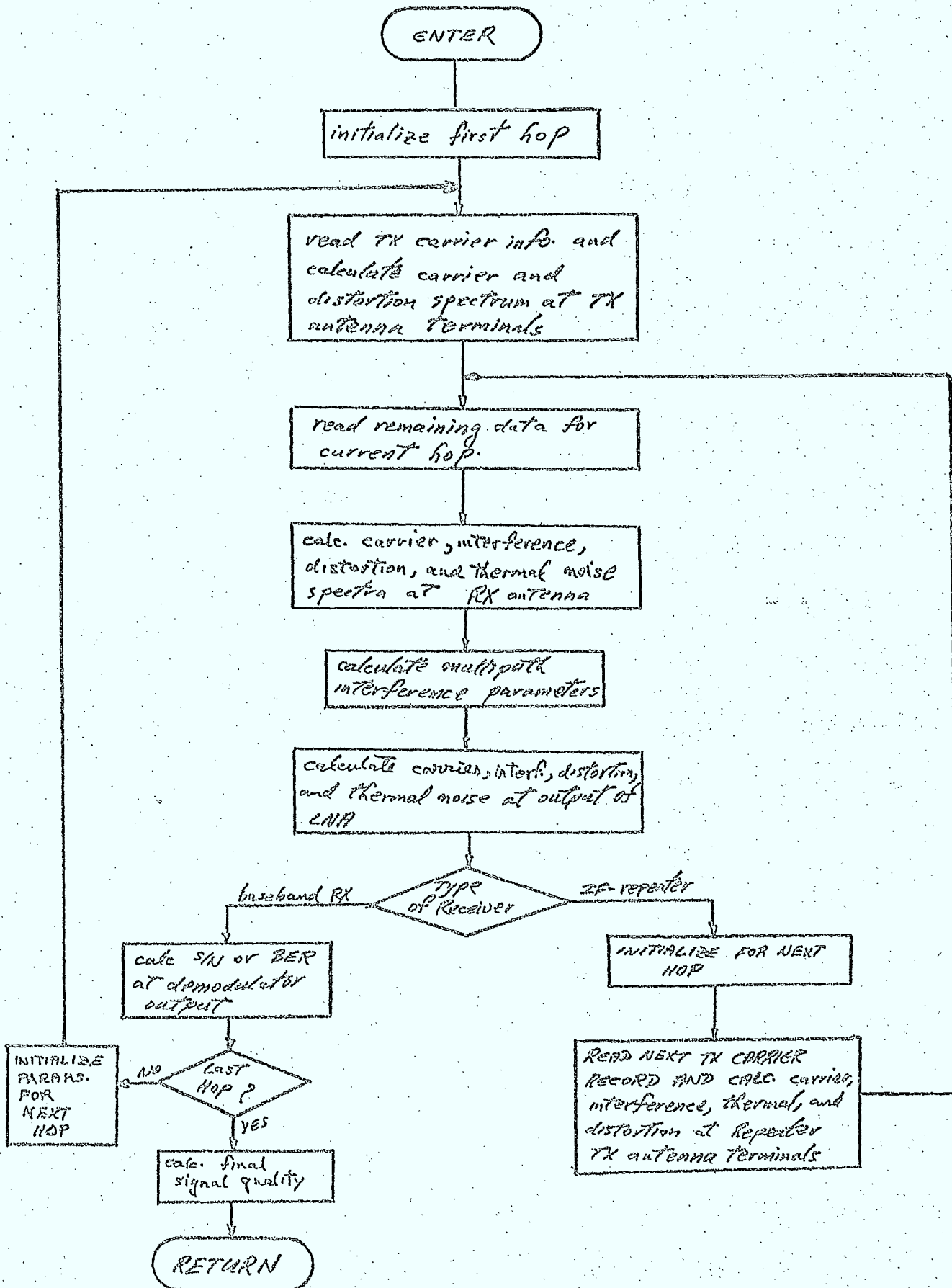
The specification of the LINK definition and control instructions and interference and report selection, is described in Section 3.3.2. As in SITE calculations, it is possible to repeat a LINK calculation a number of times while iteratively changing certain key parameters. The implementation of this "looping" capability is discussed in Section 3.3.3.

3.3.2 Link Calculation Initiator (LCINIT)

Purpose

This routine is used to read and interpret user commands and parameters specifying simulation control information for link calculations. This information can include day, time, sunspot data, minimum acceptable signal quality levels, report selection, interference selection, transmitters, receivers, and propagation effects for the hops on a link, etc.

Figure 3.3/1 Summary of LINK Calculation



Method

The routine will generate link control tables similar to those of SCINIT, with obvious exceptions being made for the different types of commands available. Because of this similarity, a flowchart is omitted. The language chart in Figure 3.3/2 illustrates the form of the command language available.

Inputs

- o input device unit no. and characteristic parameters

Outputs

- o none

3.3.3 Loop Controller (LINKLC)Purpose

This routine is used to read loop control instructions used to modify the link control tables and data in the database, thus permitting repeated link calculations to be performed while varying selected parameters over a range of values.

Method

This routine will be implemented in the same way as the site looping controller, SITELC. The language chart in Figure 3.3/3 illustrates the form of language available for specification of looping for link calculations.

Inputs

- o input device unit no. and characteristic parameters
- o link control tables

Figure 3.3/2 Language Chart of LINK Calculation Control Parameters

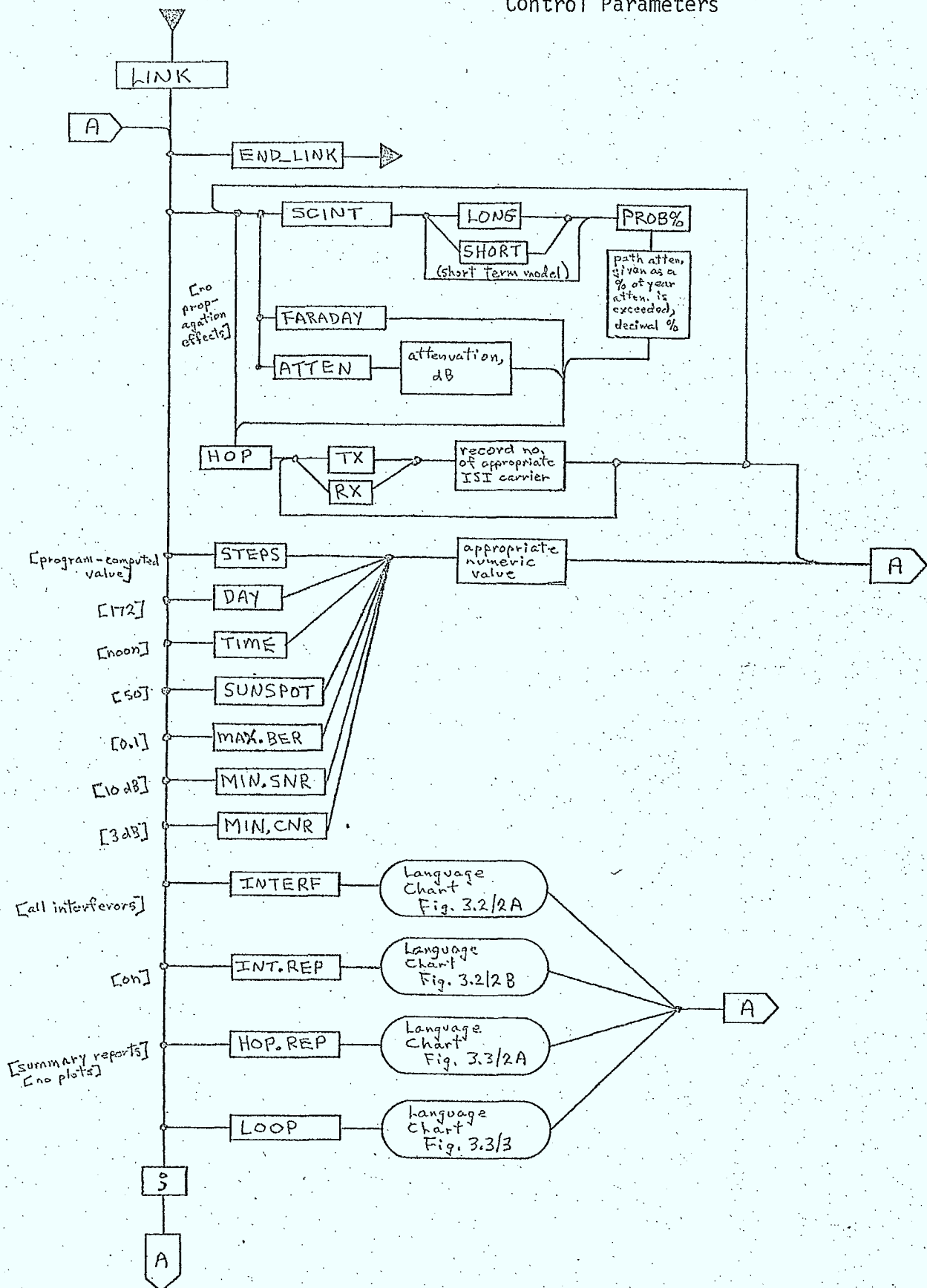


Figure 3.3/2A Language Chart of LINK Control Parameters
- Hop Report Selection Sub-Chart

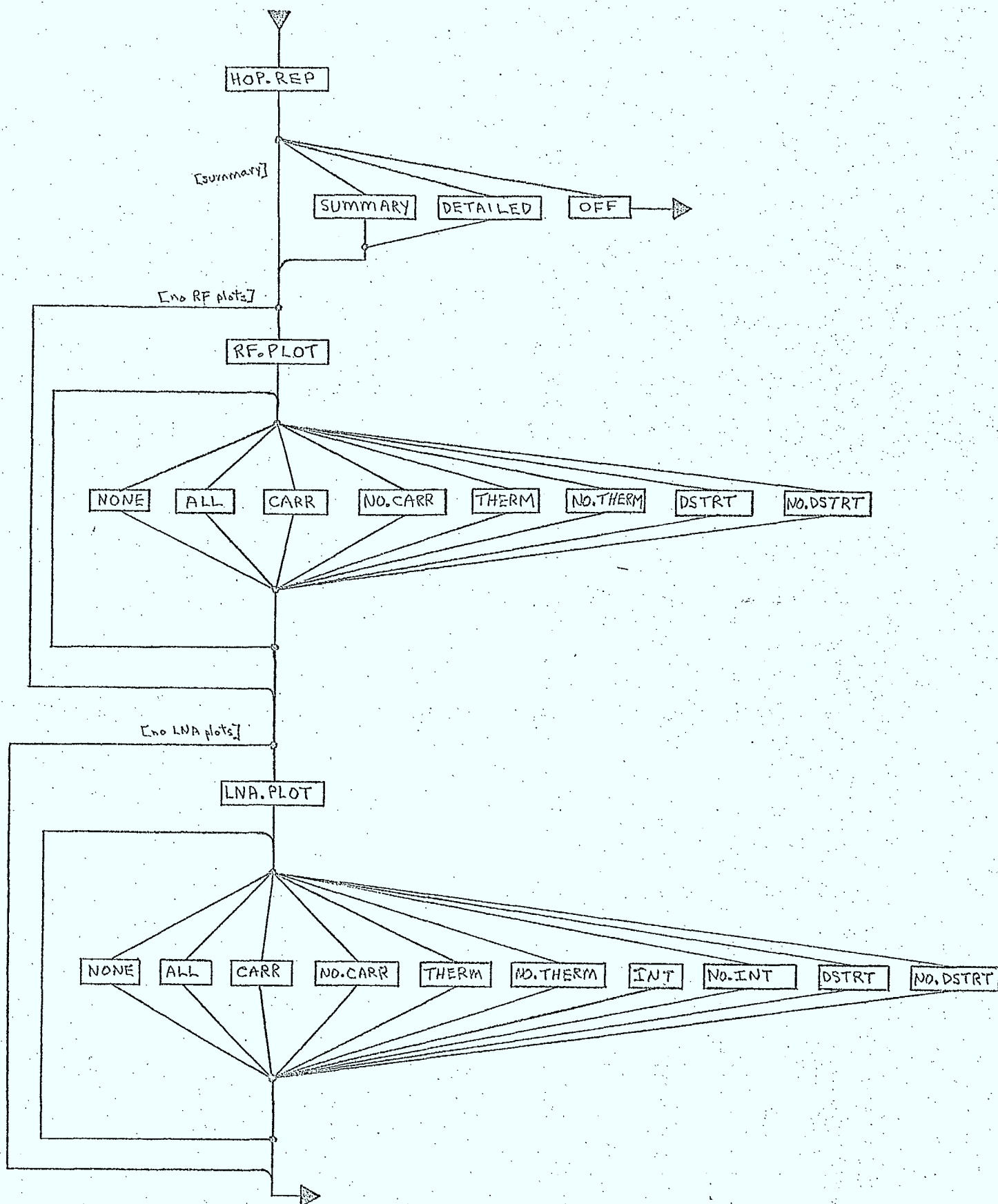
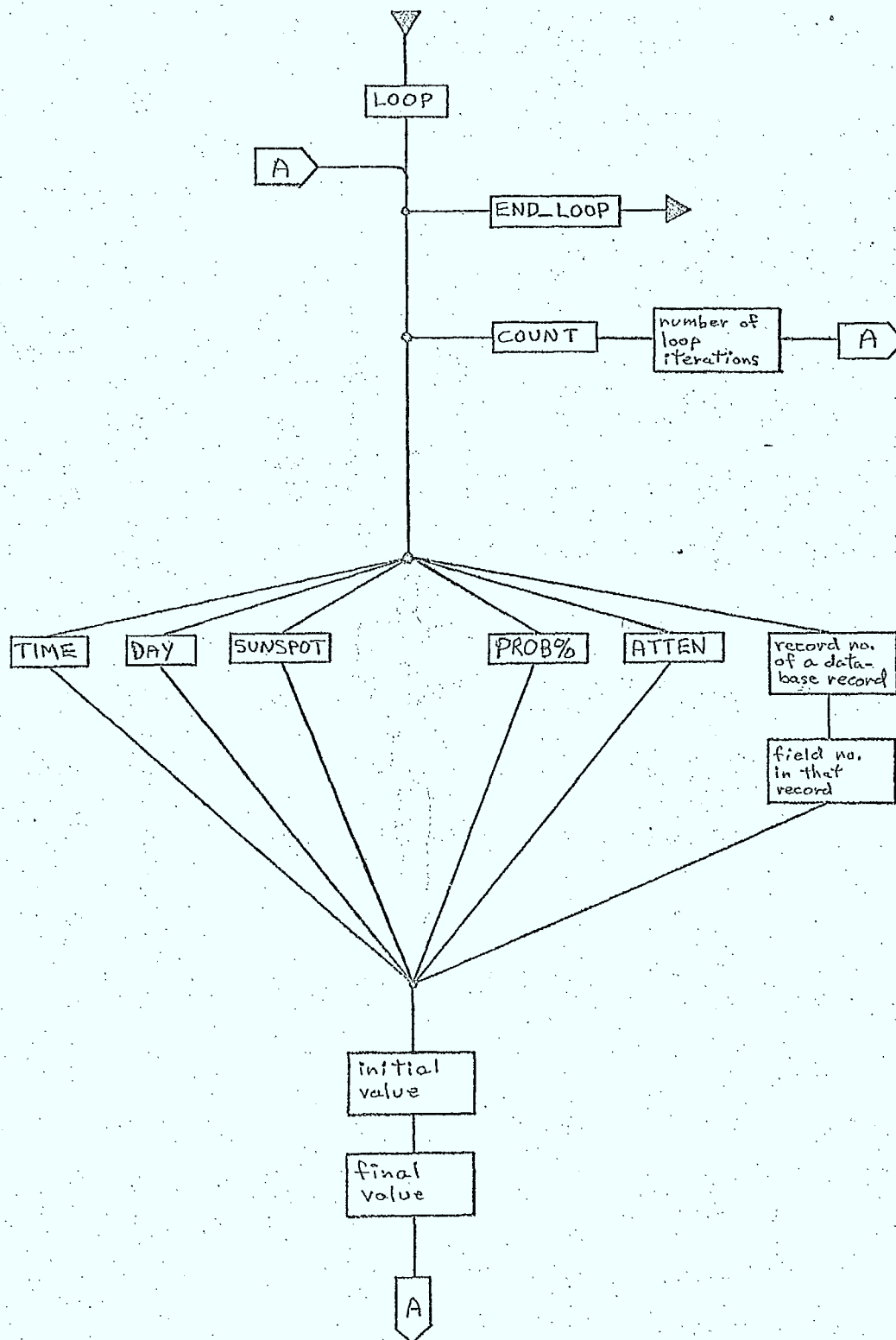


Figure 3.3/3 Language Chart of LINK Calculation
Looping Control Instructions



Outputs

- o link control tables

3.3.4 LINK Calculation Sequencing Routine (LINK)3.3.4.1 Subroutine LINKPurpose

This routine is used to calculate the signal-to-noise ratio or bit error probability describing the quality of a communications link operated in the presence of RF interference.

Description

This routine will be one of the largest subroutines in the simulation due to the complex and lengthy nature of the LINK calculation. A flowchart illustrating its implementation is shown in Figure 3.3/4.

Certain segments of the calculation will be implemented as subroutines called by LINK. These include:

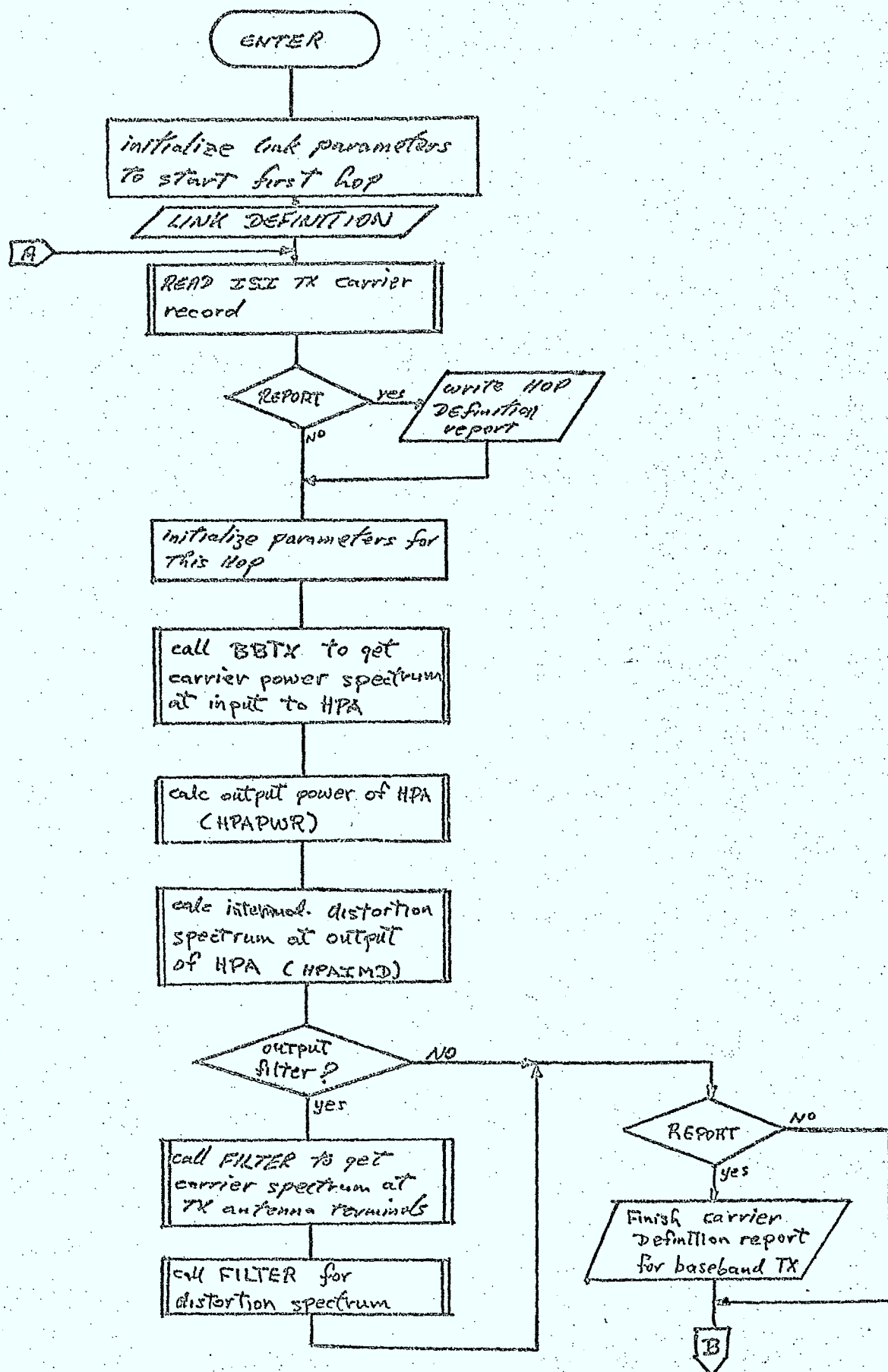
- o BBTX - a routine to model the baseband transmitter
- o IFRX - a routine to model the IF-receiver
- o BBRX - a routine to model the demodulation and signal processing sections of a baseband repeater or a baseband receiver
- o PATHLS - a routine to determine the path loss factor for a hop (ie: the ratio of received-to-transmitted power)

These routines are discussed in Sections 3.3.4.2 to 3.3.4.5.

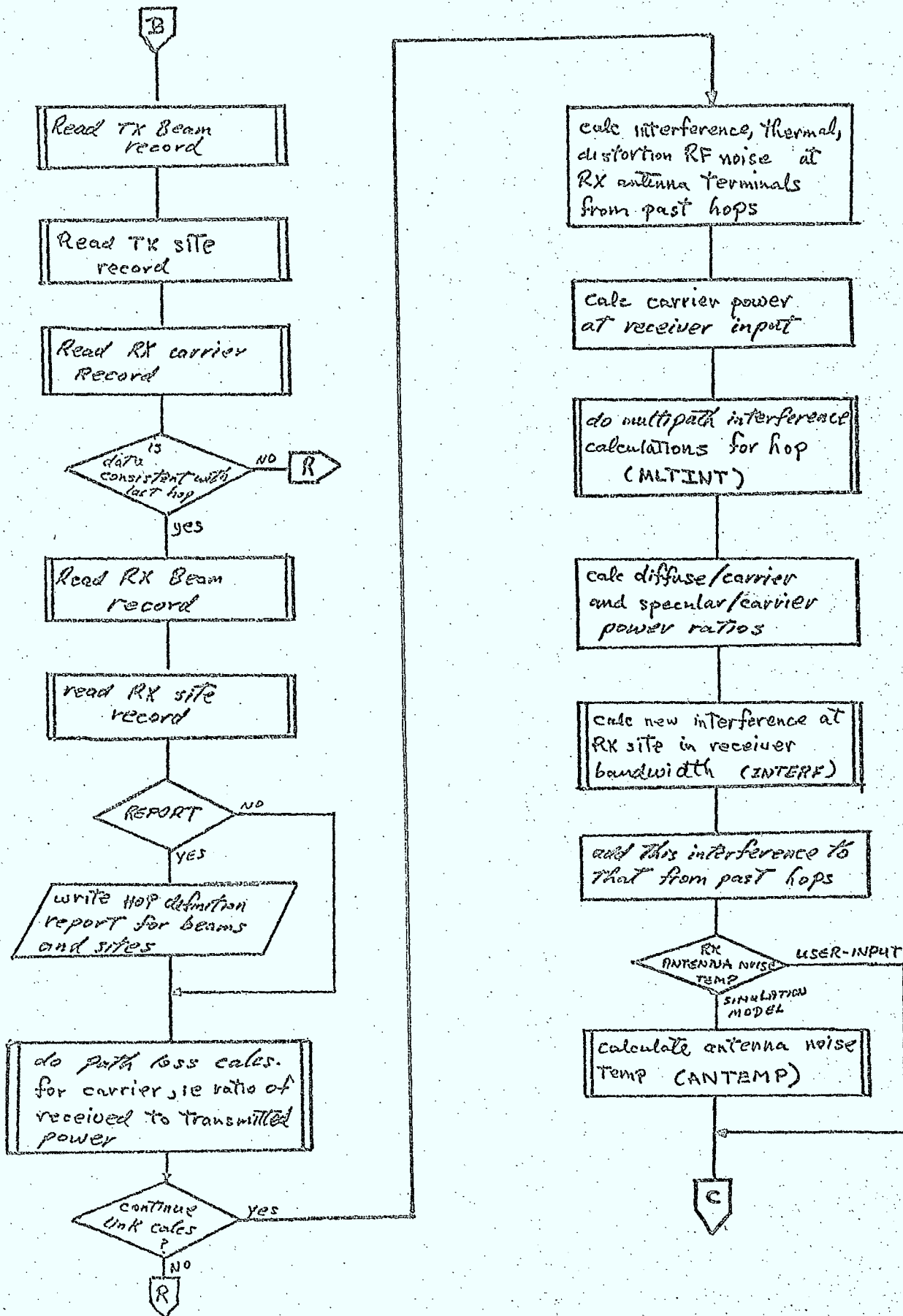
The LINK routine also uses the following routines, described in other sections of this report:

- o INTERF - calculates the RF interference accepted by the receiving antennae on the link

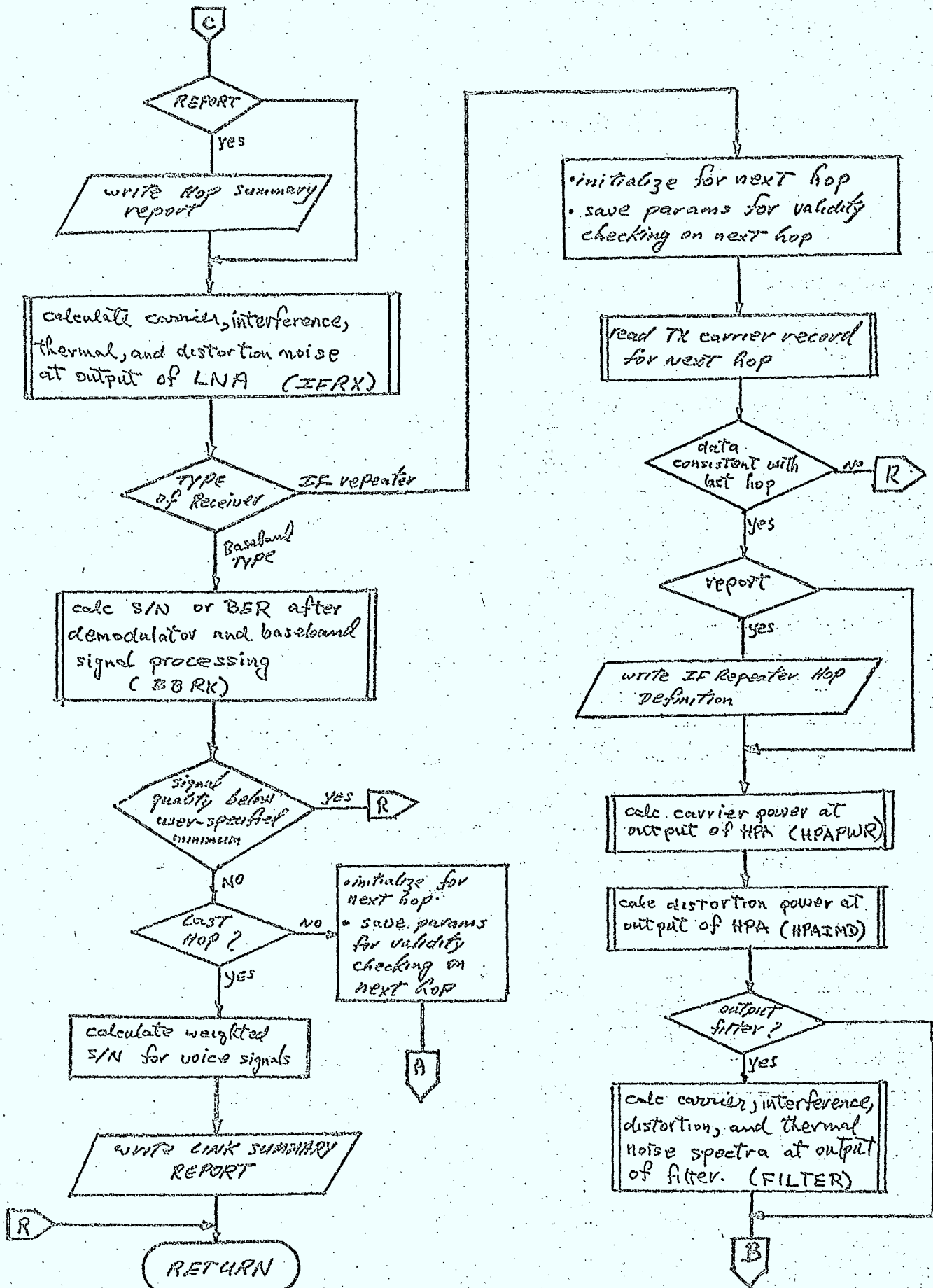
Figure 3.3/4 Flowchart of LINK



LINK Flowchart (continued)



LINK Flowchart (continued)



- o MLTINT - calculates the multipath interference on a hop
- o ANTEMP - calculates the noise temperature of each of the receiving antenna in the link.

In addition, many of the geometric, antenna, propagation, amplifier, and filter models are used in a LINK calculation.

While performing its calculations, the LINK routine will do validity testing on all of the user-specified data to ensure that erroneous calculations are not continued. The routine will also terminate the calculation if any of the following are detected during a calculation:

- o RX and TX sites defining a hop or used in antenna pointing are not visible
- o attempting a LINK calculation with two sites at the same location
- o attempting to terminate a link at an IF-type repeater
- o file read errors occurring while attempting to read from the database, the pattern file, or the spectrum and filter file
- o RX and TX data inconsistent (ie: PSK modulator, FM demodulator, etc)
- o attempting to use an ESI carrier as a "wanted carrier" in a LINK calculation
- o attempting to use an IF-repeater whose TX and RX record numbers differ
- o bit error rate at demodulator output greater than the threshold value for an FEC decoder
- o signal-to-noise ratio at demodulator output falls below the threshold value for a compander
- o bit error probability greater than user-specified maximum
- o signal-to-noise ratio at demodulator output less than user-specified minimum
- o carrier-to-noise ratio at LNA input lower than user-specified minimum
- o carrier power less than bias point at input to biased-limiting HPA

The LINK routine also generates a number of reports during calculations. A "LINK DEFINITION" report is always produced and describes the TX and RX carriers making up the link. A "LINK SUMMARY" report is also produced describing the final signal quality of the link. In addition to these reports optional reports and plots that can be selected by the user will be available. These include:

- o HOP DEFINITION report, giving geometric, antenna, and carrier parameters of the transmitter and receiver used in a hop.
- o MULTIPATH report, giving geometric, antenna, reflection coefficients, and other key parameters whenever multipath interference calculations are performed.
- o HOP SUMMARY report, giving RF thermal noise, distortion, interference, and carrier parameters at the receiving antenna at the end of a hop. Spectrum plots will be available as an option in this report.
- o LNA report, giving these same parameters at the output of the LNA. Spectrum plots will be available as an option in this report.
- o DEMODULATOR report, giving demodulation and baseband signal processing parameters and the signal quality at the output of a baseband receiver.

The interference reports produced by INTERF will also appear, if selected by the user, on each hop of the link.

Inputs

- o LINK control table containing hop definitions, propagation phenomena control instructions, report selection instructions, interference selection instructions, etc.

Outputs

- o error flag indicating whether or not an error condition was detected during calculations.

3.3.4.2 Baseband Transmitter Model for ISI Carriers (BBTX)

The baseband transmitter model used in LINK and ISI interference calculations is illustrated in Figure 3.3/5 for both analog voice and digital data basebands. This model is implemented as a routine (BBTX) (see Figure 3.3/5) that determines the RF spectrum of the carrier at the input to the high power amplifier. The spectrum is normalized such that the total power is unity.

Inputs

- o type of baseband (VOICE or data)
- o baseband processing control flags and parameters
- o type of modulator and associated parameters
- o spectrum shaping filter flag and associated parameters

Outputs

- o normalized carrier power spectrum
- o flag indicating whether or not file read error occurred
- o flag indicating whether or not carrier power is zero

3.3.4.3 IF-Type Receiver Model (IFRX)

The IF-type receiver model used as the front end amplifier section of IF-type repeaters and baseband receivers is illustrated in Figure 3.3/7. This model is implemented as a routine (IFRX), as illustrated in Figure 3.3/8. This routine is used to determine the RF spectra and power level of the wanted carrier, RF interference, thermal noise, and intermodulation distortion at the output of the receiver.

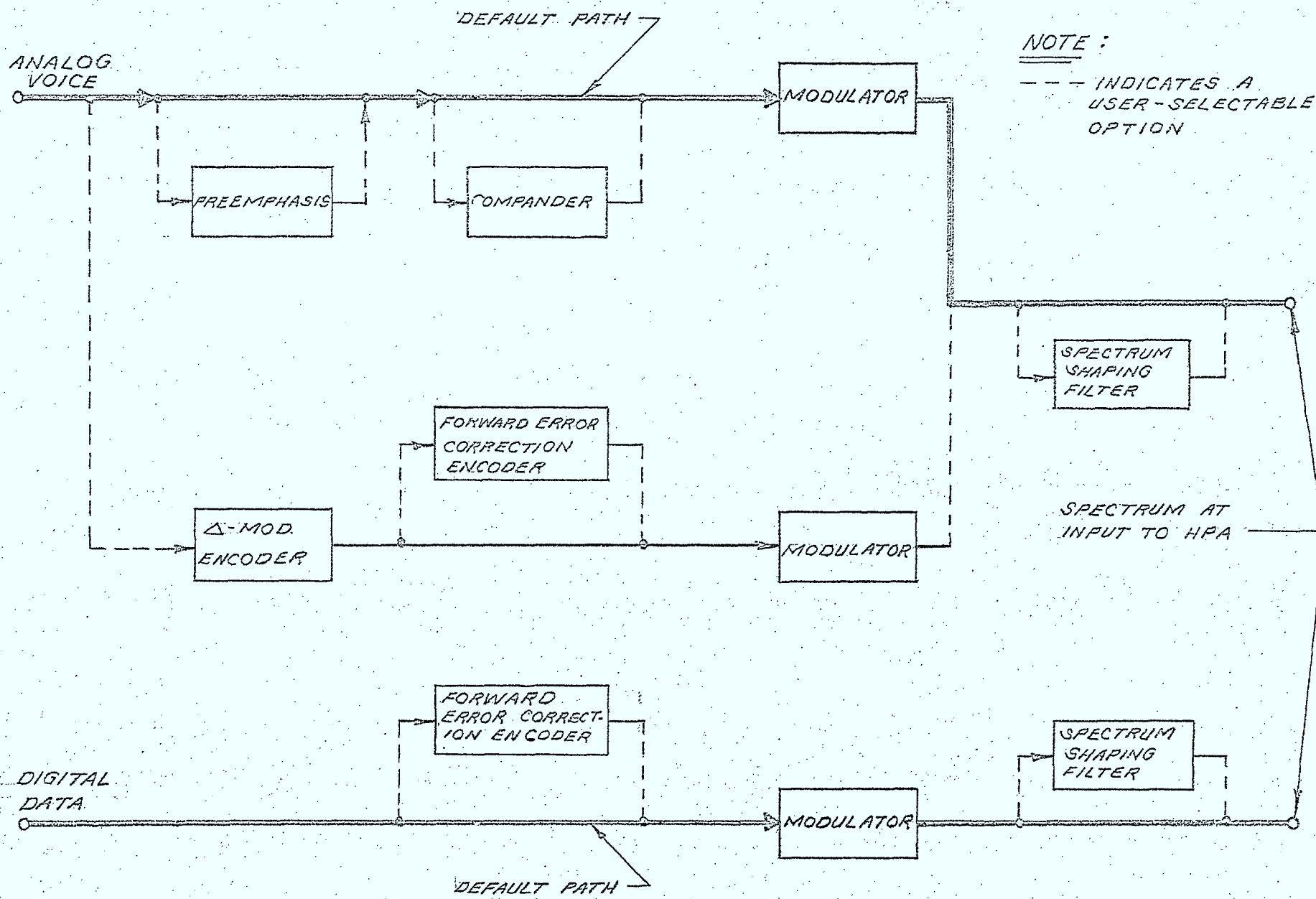
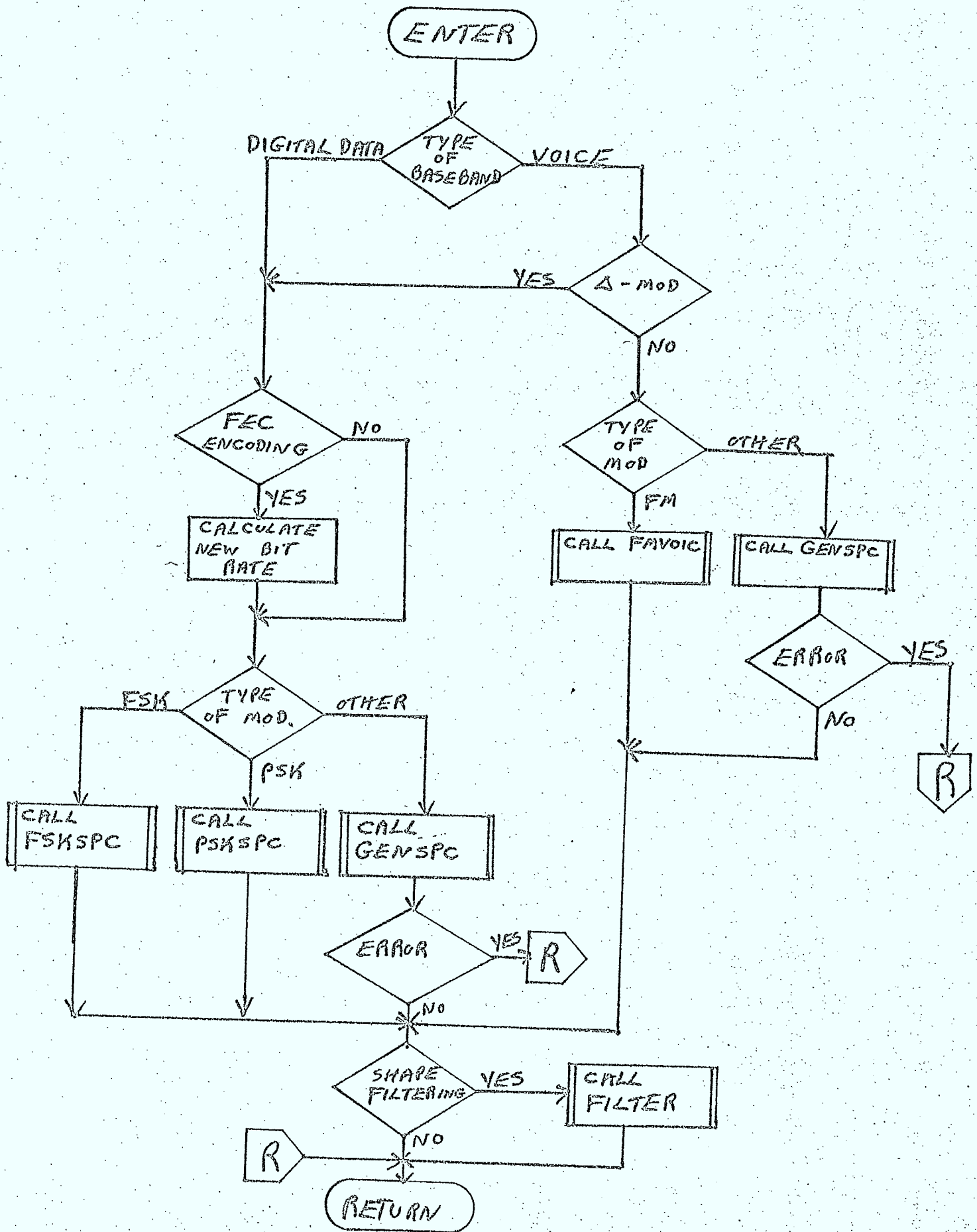


FIG. 3.3/5 BASEBAND TRANSMITTER MODEL FOR ISI TRANSMITTERS

Figure 3.3/6 Flowchart of BBTX



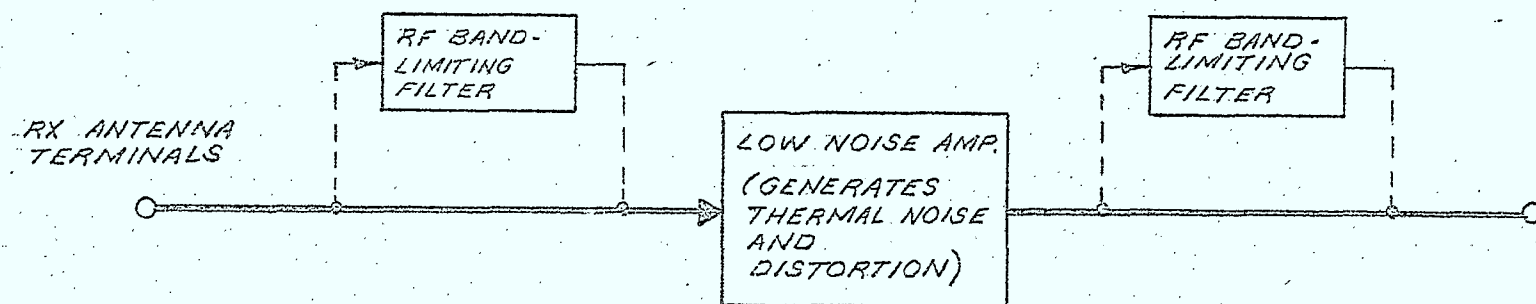
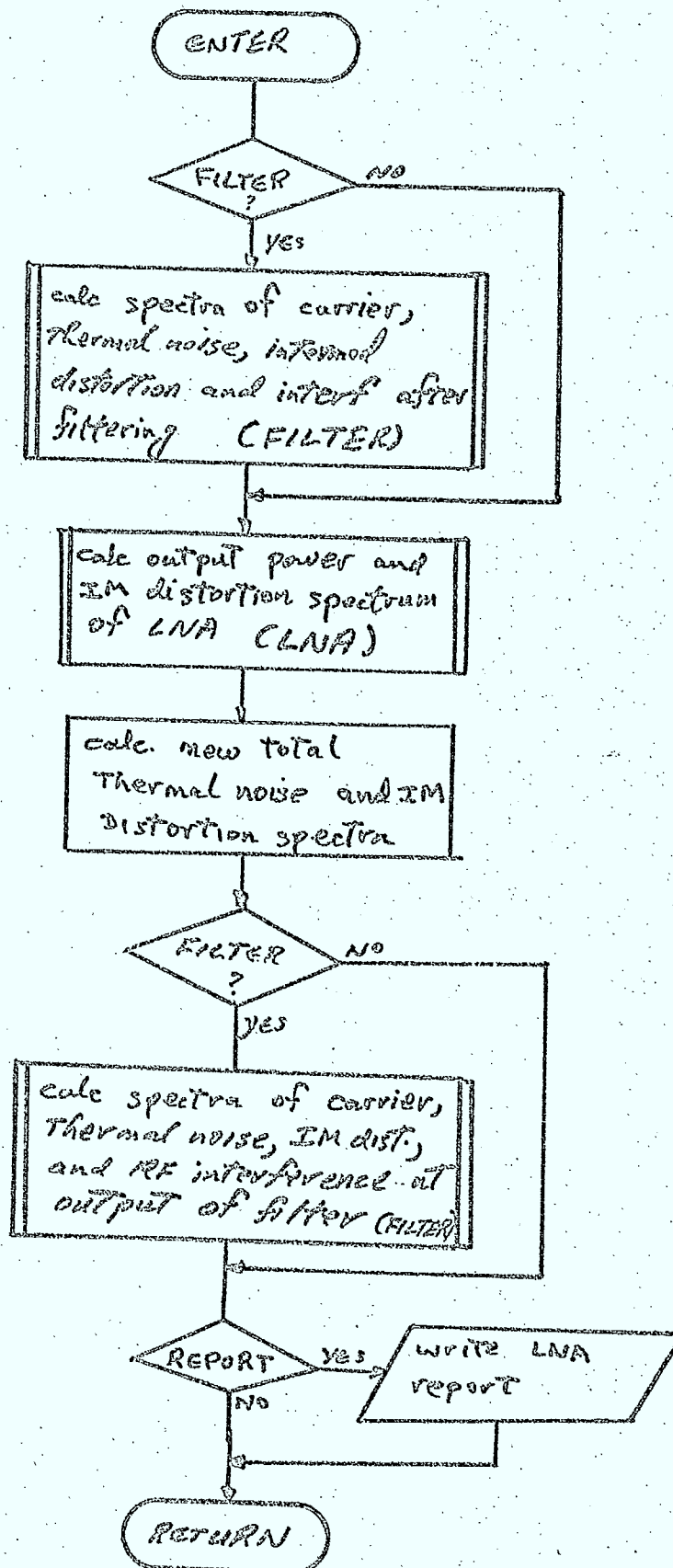


FIG: 3.3/7 IF - TYPE RECEIVER MODEL

Figure 3.3/8 Flowchart of IFRX



Inputs

- o filter parameters
- o LNA noise temperature
- o LNA distortion parameters
- o RF spectra of carrier, interference, distortion, and thermal noise at RX antenna terminals

Outputs

- o RF spectra at receiver output
- o flag indicating whether or not file read error occurred

3.3.4.4 Baseband Receiver Model (BBRX)

The demodulation and baseband processing sections of a baseband receiver, as modelled in the simulation, are illustrated in Figure 3.3/9. This model is implemented as a routine (BBRX) illustrated in Figure 3.3/10. This routine is used to calculate the signal-to-noise ratio of voice basebands and the bit error probability of digital basebands at the receiver output.

Inputs

- o type of baseband signal (analog or digital)
- o type of demodulator
- o demodulator parameters
- o baseband signal processing parameters
- o RF carrier, interference, thermal, and intermodulation distortion spectra at demodulator input

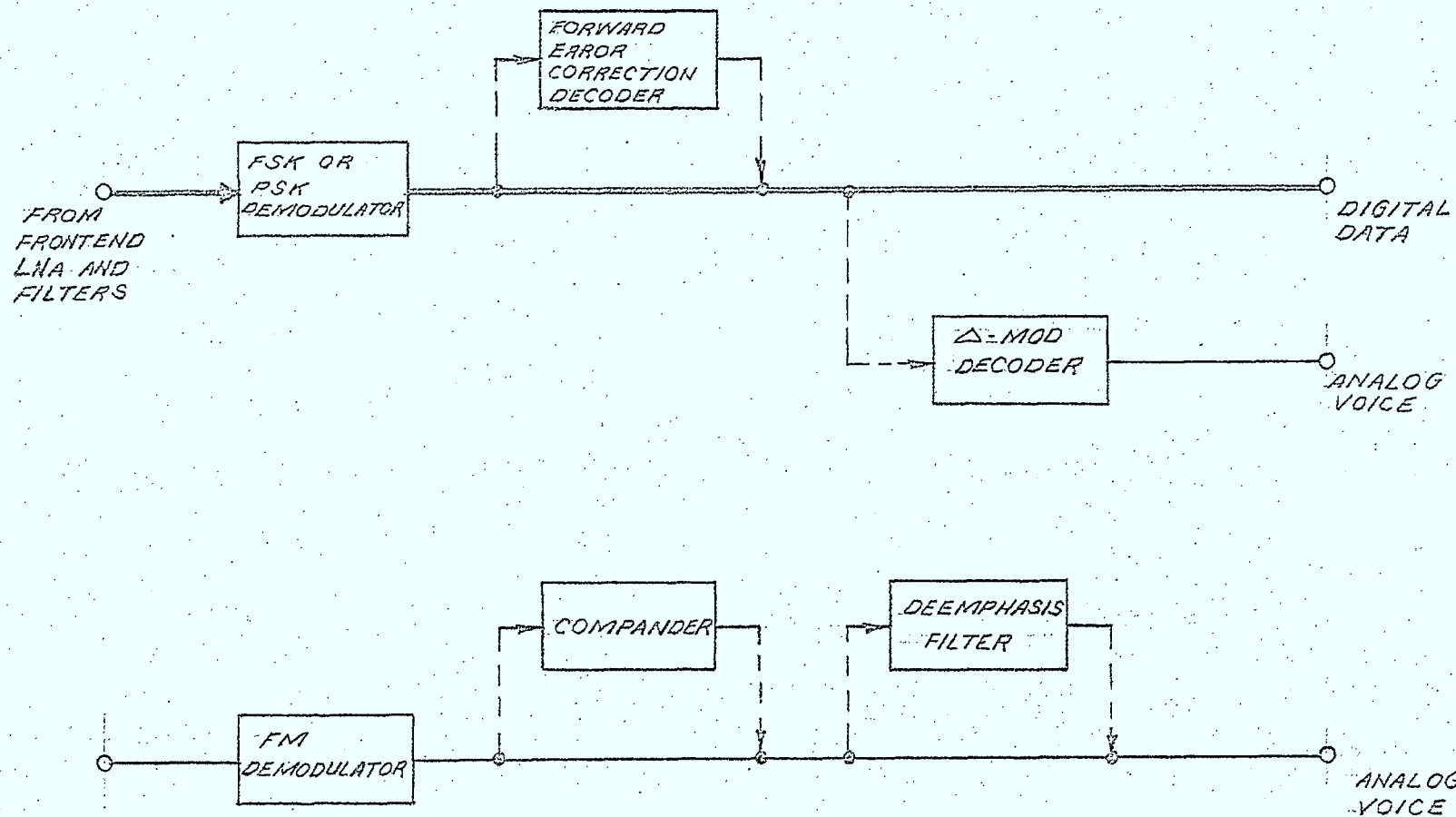
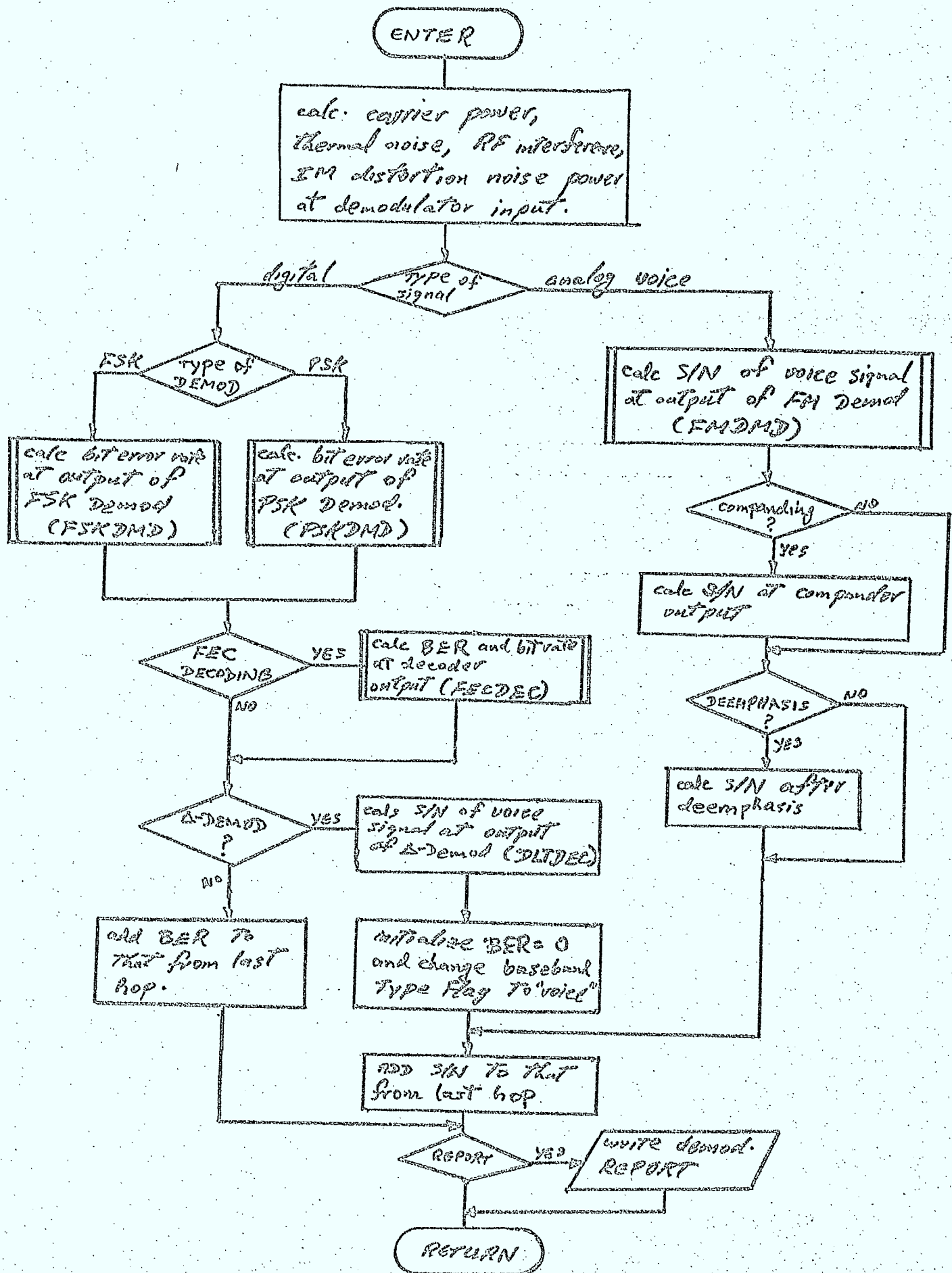


FIG: 3.3/3 BASEBAND RECEIVER MODELS FOR FM, FSK, AND PSK RECEIVERS.

Figure 3.3/8. Flowchart of BBRX



Outputs

- o bit error probability for digital signals
- o signal-to-noise ratio for VOICE basebands
- o flag indicating whether or not FEC decoder is below threshold
- o flag indicating whether or not compander is below threshold

3.3.4.4 Path Loss Model (PATHLS)Calculation of Path Loss for a LINK Carrier

The path loss for the "wanted" carrier in a LINK calculation depends on a variety of antenna, propagation, and geometric parameters. The path loss, defined as the ratio of received-to-transmitted carrier power is given by (Reference 3.3/1):

$$L = \frac{G_R \lambda^2 A_T A_P}{(4\pi r)^2} [G_{TP} M_P + G_{TC} M_C] \quad (3.3.1)$$

where:

- G_R - principal polarization gain of RX antenna in the direction of the TX site
- λ - wavelength
- A_T - nominal tropospheric absorption loss factor
- A_P - propagation loss factor due to scintillation or other phenomena (excluding Faraday rotation)
- G_{TP} - principal polarization gain of the transmitting antenna in the direction of the receiver
- G_{TC} - cross polarization gain of the transmitting antenna in the direction of the RX antenna
- M_P - principal polarization mismatch factor
- M_C - cross polarization mismatch factor
- r - separation distance between the RX and TX sites

Models for all of the parameters used in this equation are described in Chapter 4. The sequencing of geometric and model routines required to calculate the path loss on a hop is illustrated in Figure 3.3/11.

Another parameter used in the simulation calculations is the ratio of the received power-to-the ratio of the power that would be received if the user had not selected a propagation phenomenon. This ratio, denoted, ΔP_{PROP} , is given by:

$$\Delta P_{PROP} = A_p \left[\frac{M_p(\theta_F) G_{TP} + M_p(\theta_F) G_{RC}}{M_p(\theta_F=0) G_{TP} + M_p(\theta_F=0) G_{RC}} \right] \quad (3.3.2)$$

This expression depends on both the optional propagation attenuation, A_p , and the dependence of the polarization mismatch factors on the Faraday rotation angle (if non-zero).

This ratio, ΔP_{PROP} , is used to determine the input backoff of LNA's and HPA's used in the link, and is required since the simulation will consider non-linear amplifiers, and amplifiers with automatic gain control (AGC).

Figure 3.3/11 Flowchart of PATHLS

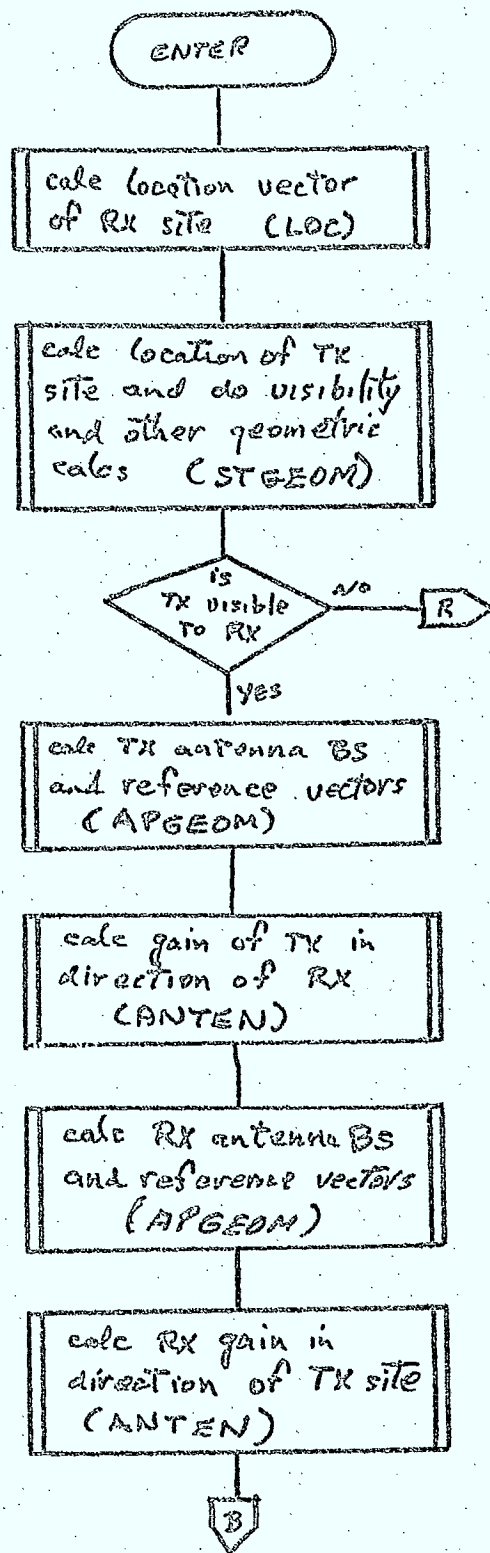


Figure 3.3/11 (continued)

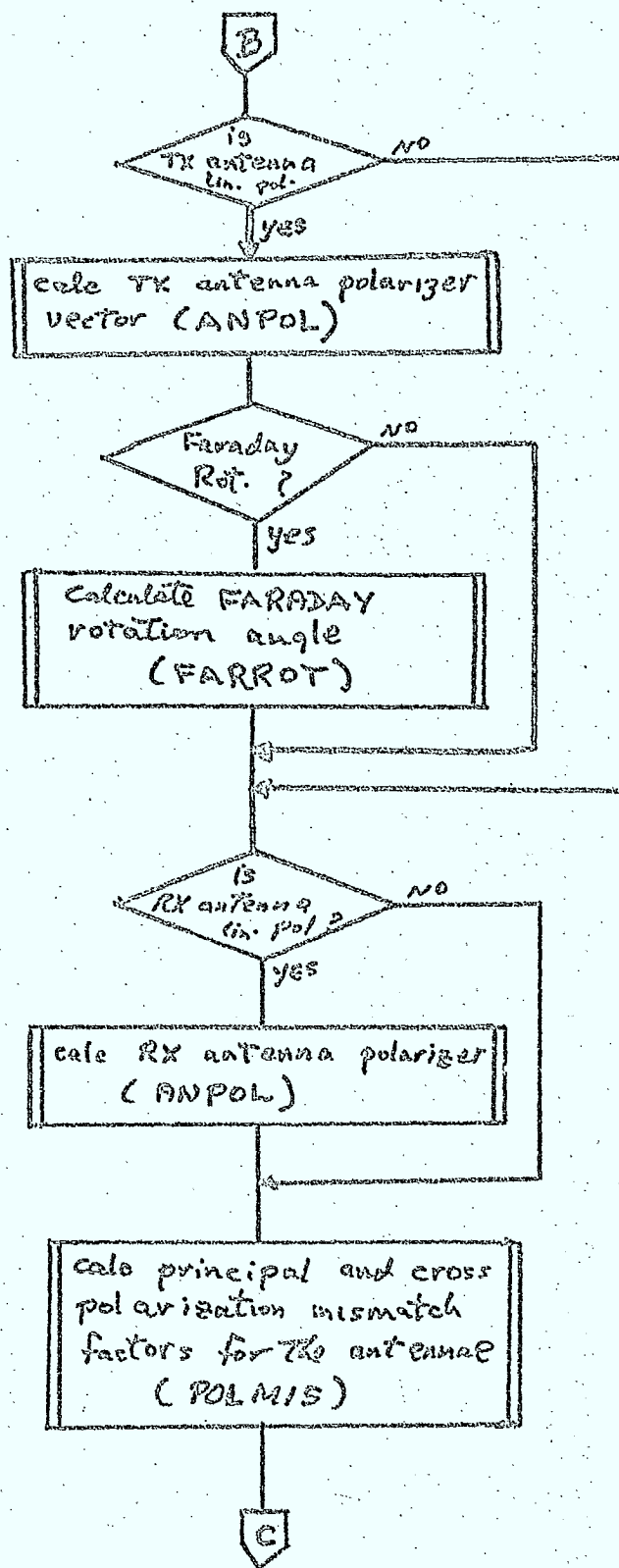
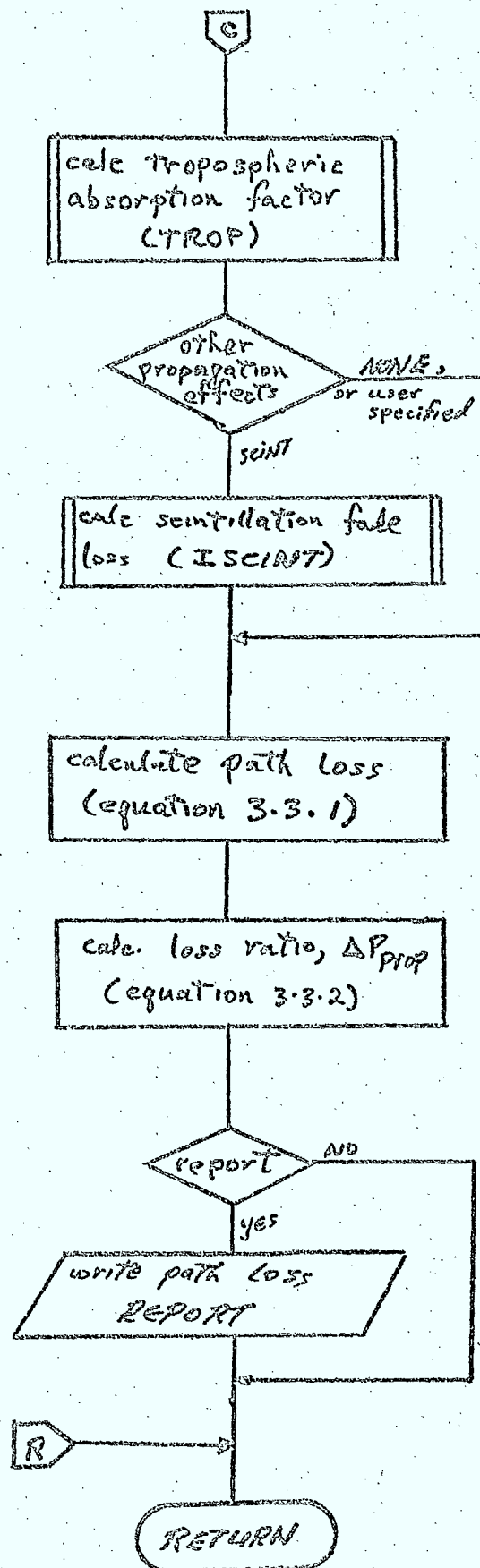


Figure 3.3/11 (continued)



3.4 Interference Calculations

3.4.1 General

The implementation of the RF interference calculation required in SITE and LINK calculations is discussed in this section. The interference calculation is performed by a hierarchical set of subroutines whose purpose is to calculate the cumulative interference power spectrum across the simulation bandwidth. This hierarchy is illustrated in Figure 3.4/1. The hierarchical structure is imposed by the database design and data organization.

As indicated in Sections 3.2 and 3.3, the following types of interferers can be selected in interference calculations:

- o all transmitters in database
- o all ISI transmitters in database
- o one particular system of ESI transmitters
- o all ESI transmitters in database
- o one particular system of ESI transmitters and all ISI transmitters
- o no transmitters

3.4.2 Main Interference Selection Routine (INTERF)

Purpose

This routine is used to calculate the cumulative RF interference at a receiving site due to interferers in those systems selected by the user.

Description

The implementation of this routine is illustrated in Figure 3.4/2. This routine sequences calls to a routine (SYSINT) that calculates the received interference from a single system. It also produces a user-selectable CUMULATIVE INTERFERENCE REPORT describing the total interference power and spectrum across the simulation bandwidth.

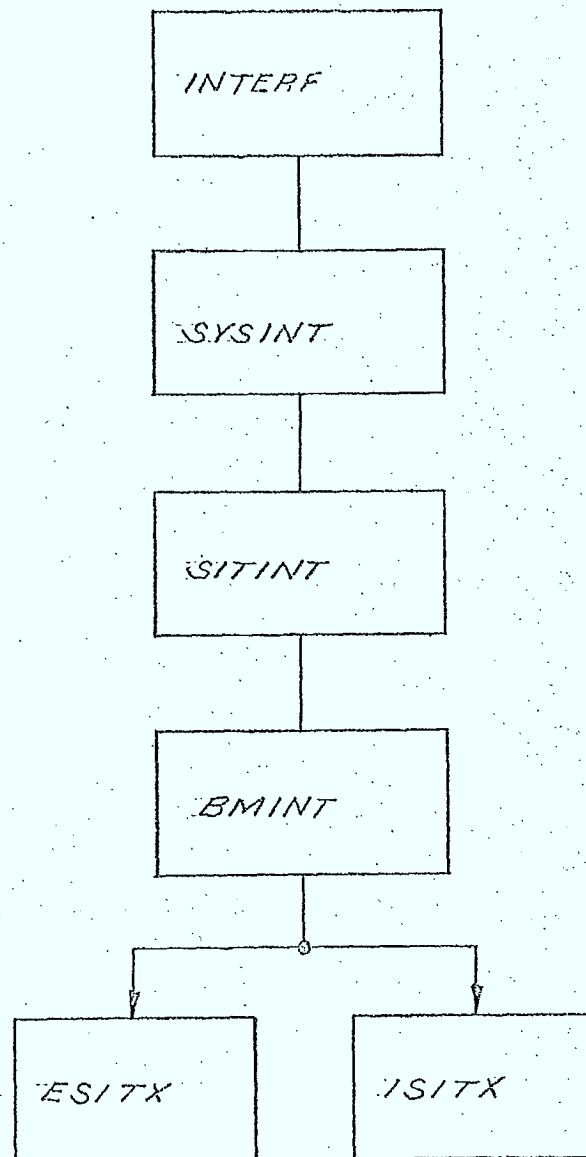
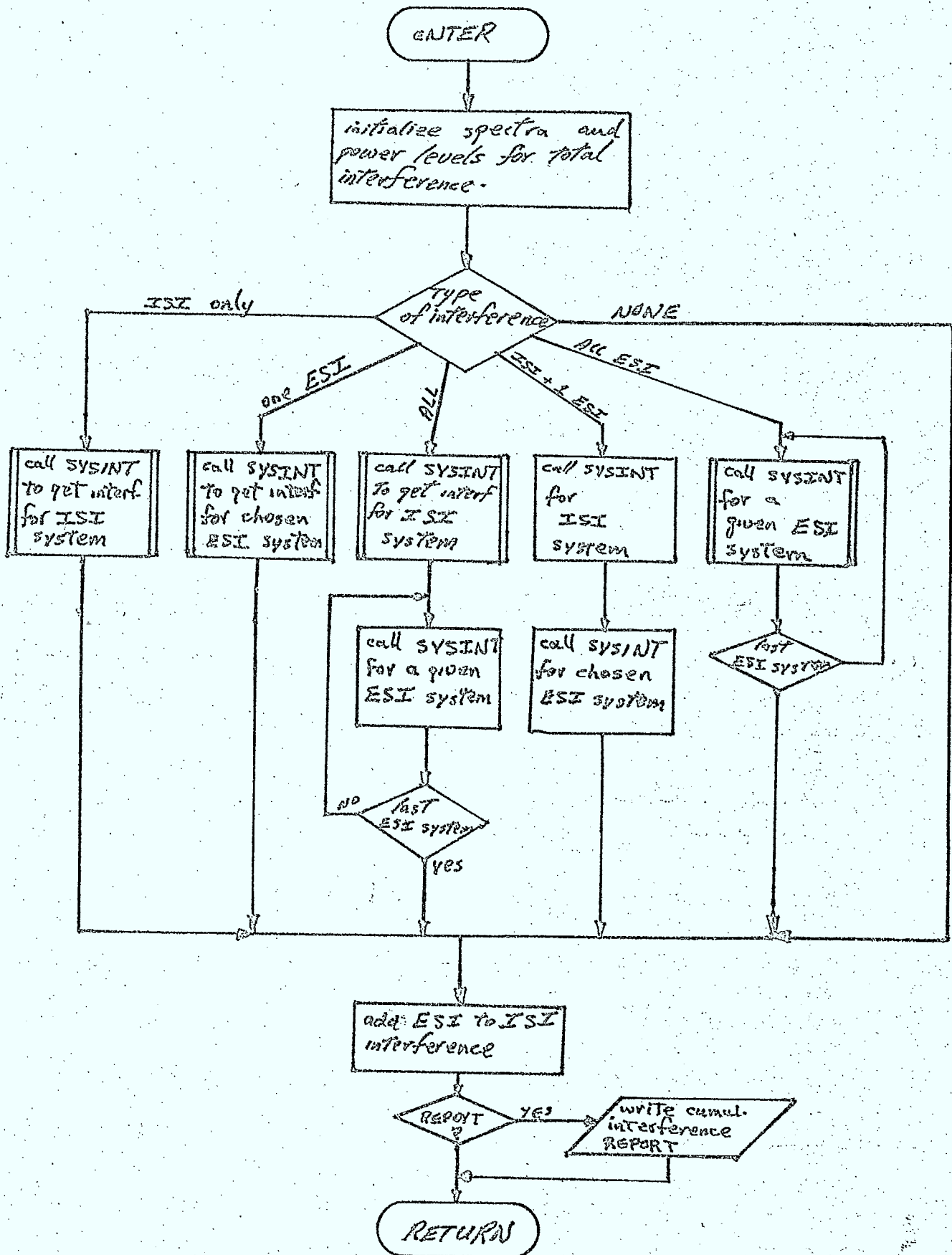


FIG: 3-4/1 HIERARCHY OF INTERFERENCE ROUTINES

Figure 3.4/2 Flowchart of INTERF



Inputs

- o interference selection instructions
- o report control instructions
- o receiver site and beam parameters
- o simulation bandwidth parameters

Outputs

- o cumulative interference spectrum across the simulation bandwidth at a receiving site

3.4.3 System Interference Routine (SYSINT)

Purpose

This routine is used to calculate the interference spectrum across the simulation bandwidth at a receiving site due to all potential interferors in a specified system.

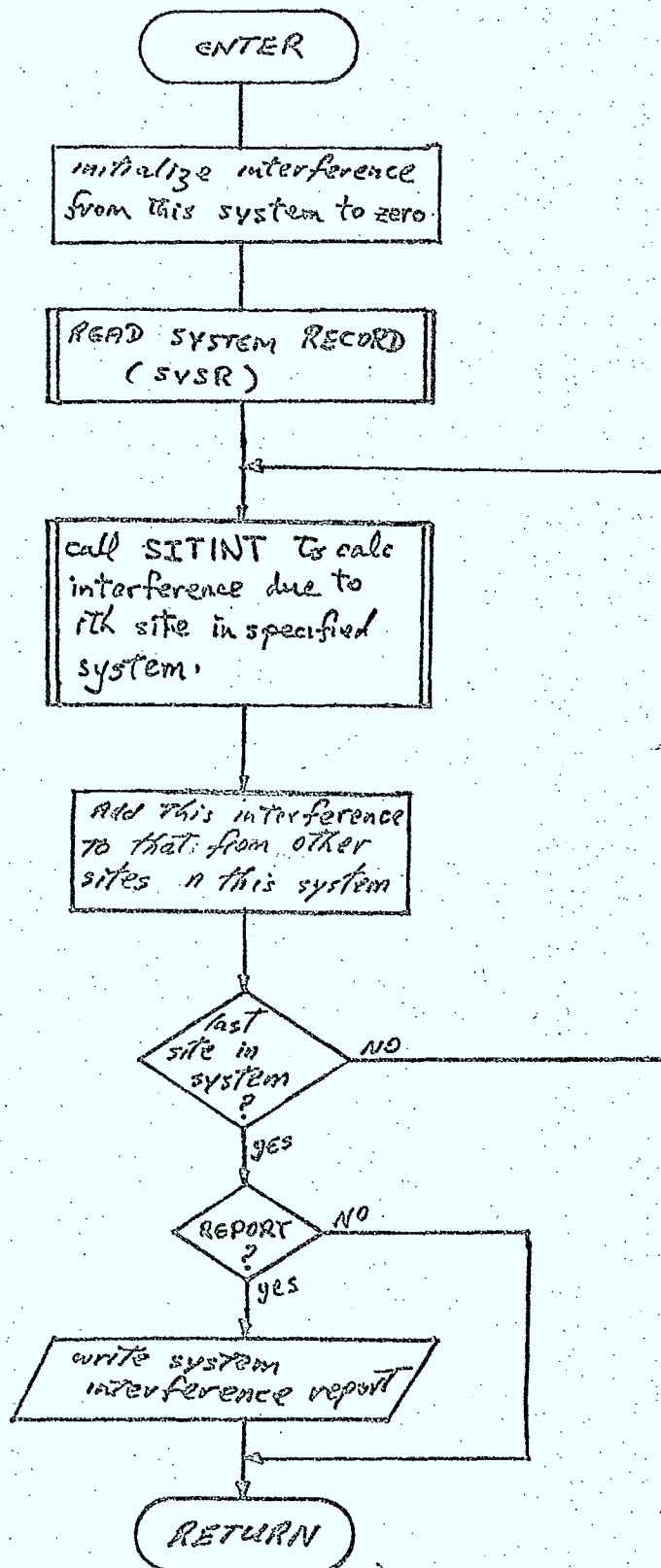
Description

The implementation of this routine is illustrated in Figure 3.4/3. This routine sequences calls to a routine (SITINT) that calculates the received interference from a single site within the system. It also produces a user-selectable SYSTEM INTERFERENCE REPORT describing the total interference power and spectrum across the simulation bandwidth at the receiving site.

Inputs

- o system record number in database
- o report control instructions
- o receiver site and antenna parameters
- o simulation bandwidth parameters

Figure 3.4/3 Flowchart of SYSINT



Outputs

- o interference spectrum at the receiving site due to interferors at all of the sites within the system

3.4.4 Site Interference Routine (SITINT)Purpose

This routine is used to calculate the interference at a receiving site due to all potential interfering carriers originating from a specified transmitting site.

Description

The implementation of this routine is illustrated in Figure 3.4/4. This routine calculates the location of the transmitting site, and the receiving antenna gain in its direction, and sequences calls to a routine (BMINT) that determines the interference due to carriers on a single antenna at the site (Note, multibeam satellites may have an arbitrary number of beams). It also produces a user-selectable SITE INTERFERENCE REPORT describing the total interference power and spectrum from the TX site across the simulation bandwidth at the receiving site.

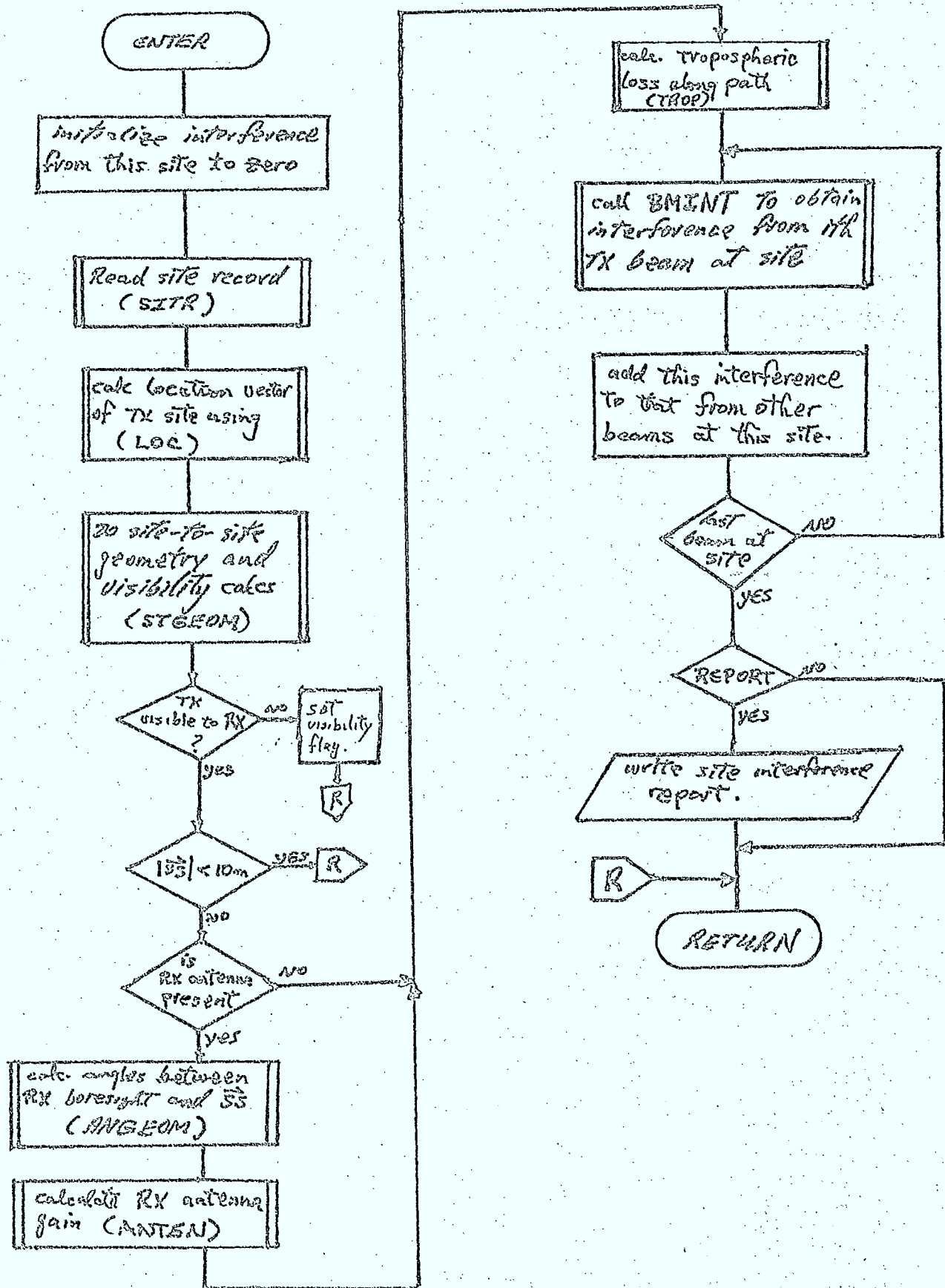
Inputs

- o site record number in database
- o receiving site and antenna parameters
- o report control instructions
- o simulation bandwidth instructions

Outputs

- o interference spectrum at receiving site due to all of the interfering carriers originating at the specified transmitting site.

Figure 3.4/4 Flowchart of SITINT



3.4.5 Beam Interference Routine (BMINT)

Purpose

This routine is used to calculate the interference at a receiving site due to all potential interfering carriers originating from a specified antenna at a TX site.

Description

The implementation of this routine is illustrated in Figure 3.4/5. This routine calculates the TX antenna gain in the direction of the receiving site and sequences calls to routines (ESITX and ISITX) that calculate the power spectrum of single carriers at the transmitting antenna terminals. This routine also produces a user-selectable BEAM INTERFERENCE REPORT describing the total interference power and spectrum at the receiving site due to all of the interfering carriers on the specified TX beam.

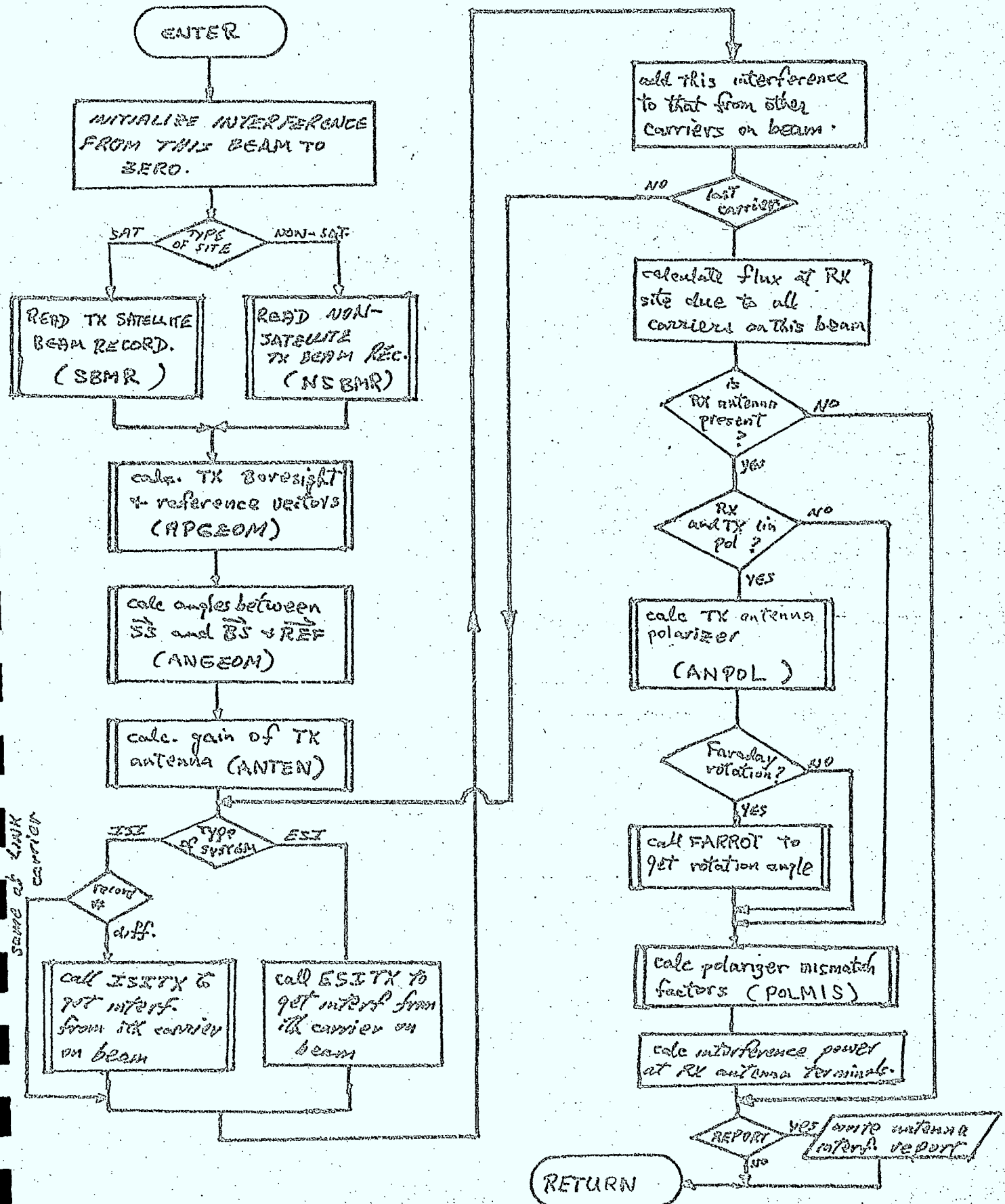
Inputs

- o TX beam record number
- o TX site parameters
- o TX site and antenna parameters
- o propagation phenomena control instructions
- o report control instructions
- o simulation bandwidth parameters

Outputs

- o interference spectrum at the receiving site due to all of the interfering carriers on the specified TX beam

Figure 3.4/5 Flowchart of BMINT



3.4.6 ESI Interfering Carrier Model (ESITX)

Purpose

This routine is used to calculate the RF spectrum and power level of a specified ESI carrier at its transmitting antenna terminals.

Description

The model used for ESI transmitters is shown in Figure 3.4/6. The following spectrum models will be used in ESI interference calculations:

- o single channel FM voice (FMVOIC)
- o binary or M-ary PSK (PSKSPC)
- o binary FSK (or FFSK) (FSKSPC)
- o FM/TV (FMTV)
- o Gaussian shaped, band-limited noise (GAUSS)
- o Band-limited white noise (WHITE)
- o arbitrary spectra (GENSPC)

These models are discussed in Chapter 4.

The implementation of the ESI transmitter model is illustrated in Figure 3.4/7. The routine also generates a user-selectable ESI CARRIER INTERFERENCE that describes the spectrum and power of the specified ESI at its TX antenna terminals.

Inputs

- o TX carrier records number in database
- o simulation bandwidth parameters
- o report control instructions

Outputs

- o spectrum of specified ESI carrier, (if in the simulation bandwidth), at the TX antenna terminals

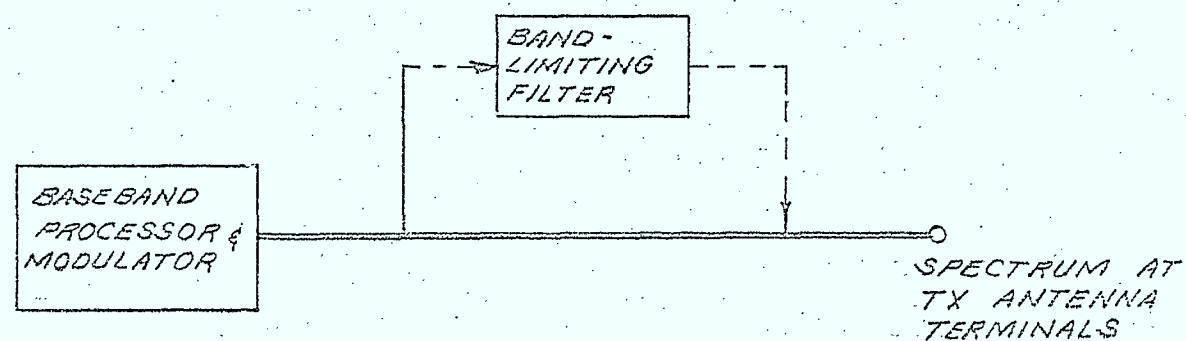
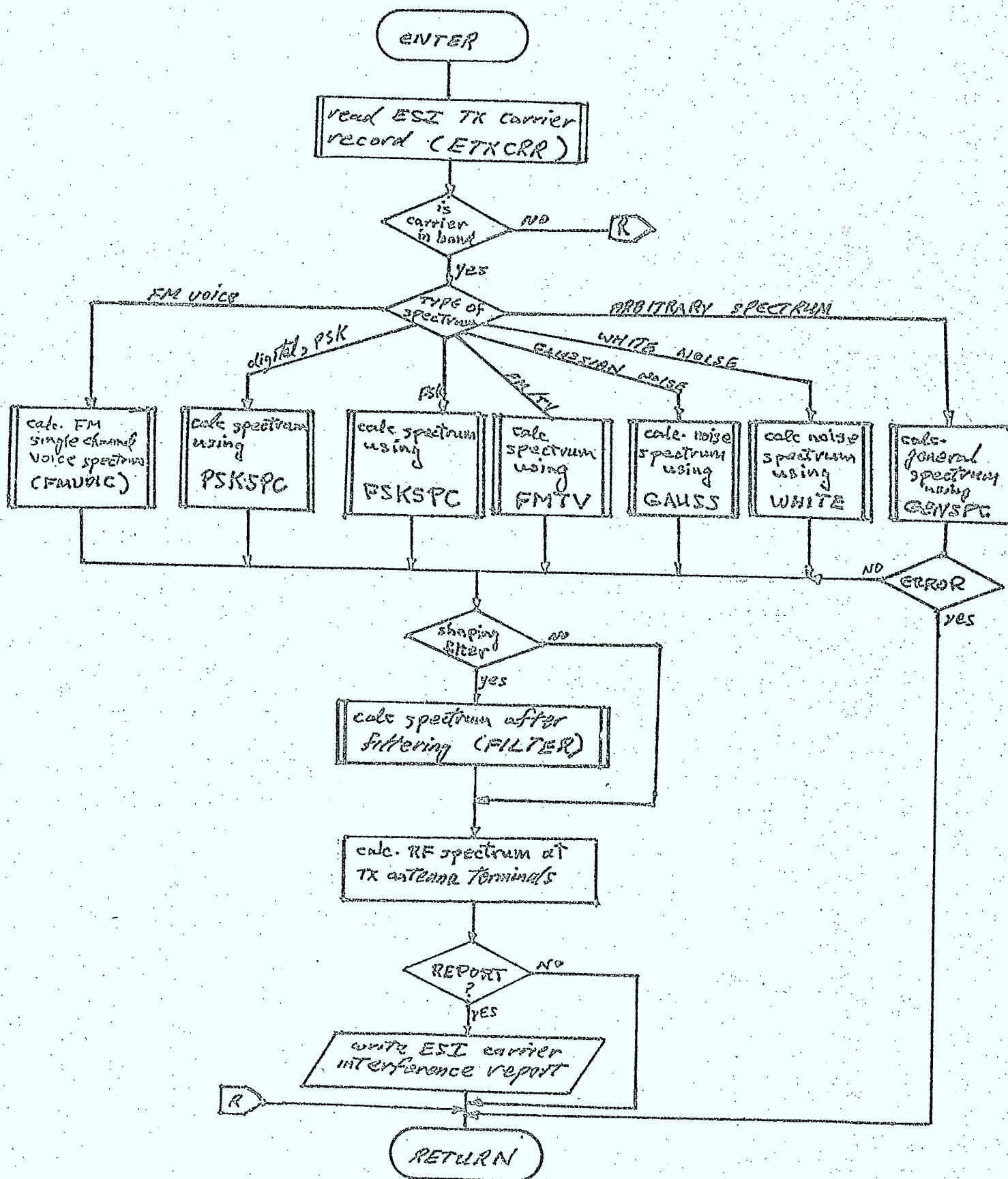


FIG: 3.4/6 ESI TRANSMITTER MODEL

Figure 3.4/7 Flowchart of ESITX



3.4.7 ISI Interfering Carrier Model (ISITX)

Purpose

This routine is used to calculate the RF spectrum and power level of a specified ISI carrier at its transmitting antenna terminals.

Description

The baseband transmitter model is used to determine the carrier spectrum and power levels at the outputs of both IF-type repeaters and baseband-transmitters used as interferors. The implementation of the routine (ISITX) is shown in Figure 3.4/8. The routine also generates a user-selectable ISI CARRIER INTERFERENCE report.

Inputs

- o TX carrier record number
- o simulation bandwidth parameters
- o report control instructions

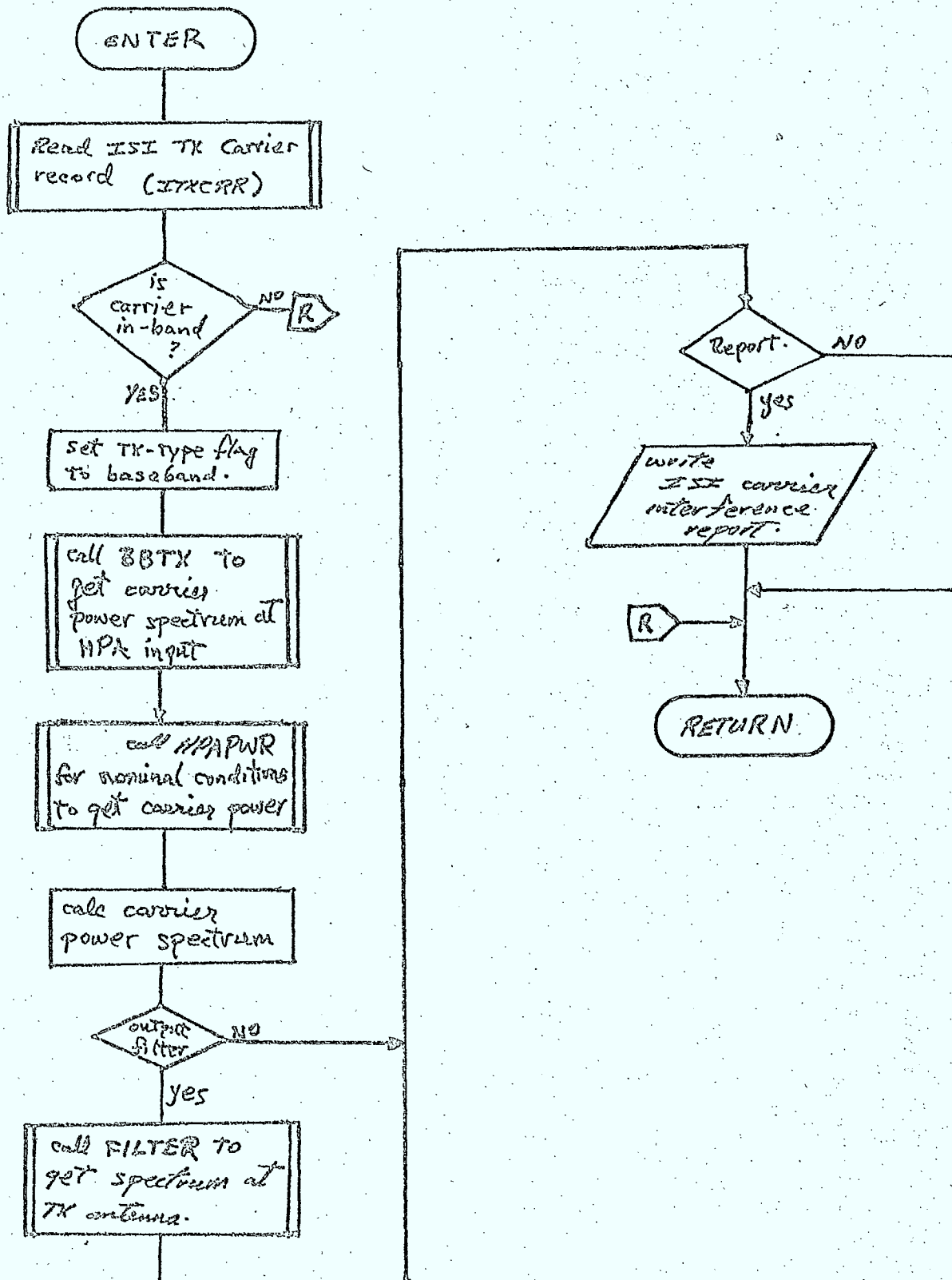
Outputs

- o spectrum of specified ISI carrier at the TX antenna terminals

3.4.8 Reports Generated in Interference Calculations

The interference calculation routines described in this section generate a number of tables and line printer plots of the computed interference. All of these reports are user-selected and are hierarchical in nature due to the way in which interference calculations are sequenced. The selection of these reports and plots is done via keywords when specifying the control parameters for SITE or LINK calculations, as described in Section 3.2 and 3.3.

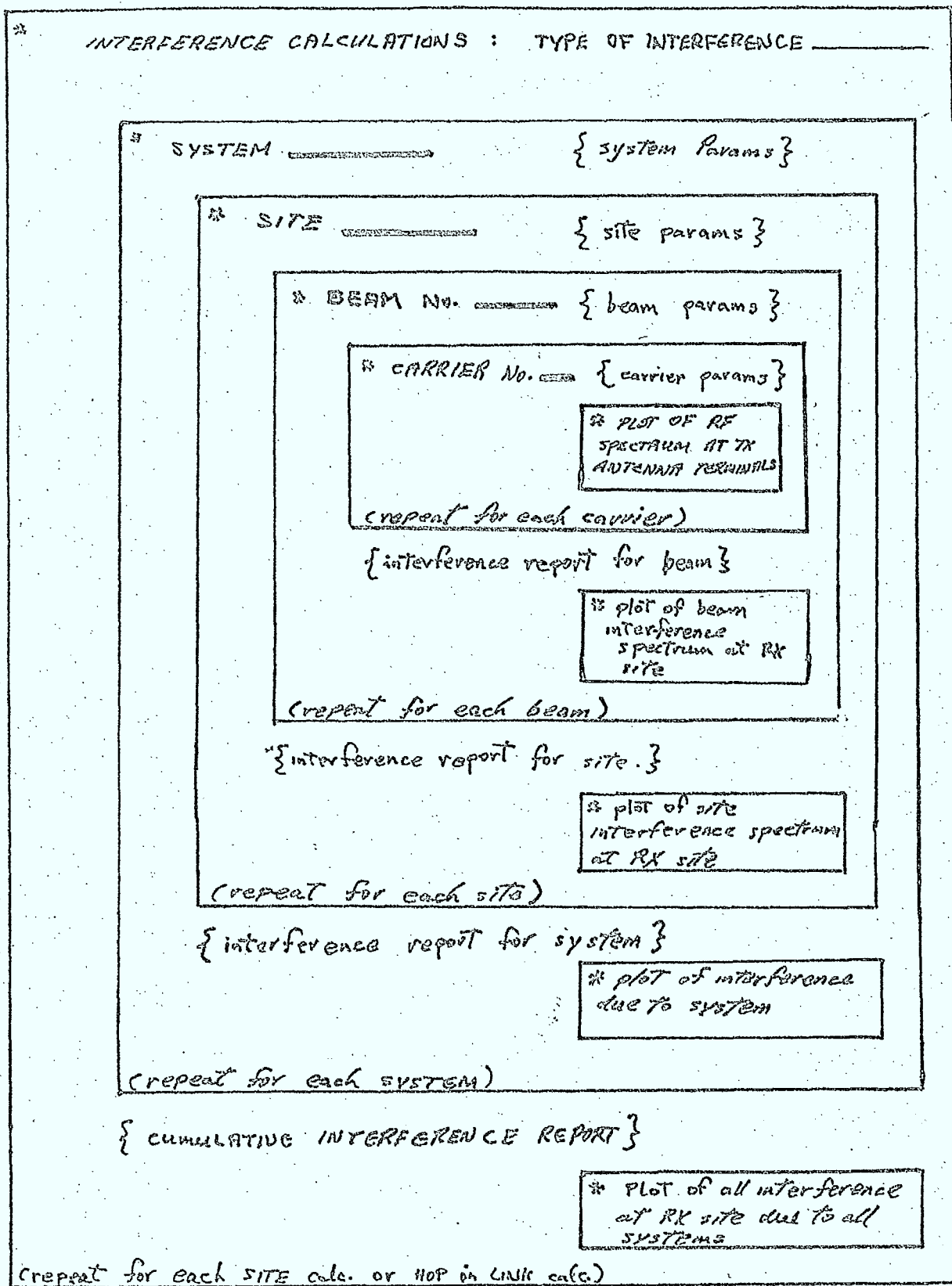
Figure 3.4/8 Flowchart of ISITX



The order in which the reports appear is illustrated in Figure 3.4/9. As indicated in the figure, plots of the RF interference spectrum due to individual carriers, beams, sites, and systems, in addition to the cumulative interference due to all of the selected interferors can be obtained.

Summary, or an optional detailed interference report, can be obtained for each of the carrier, beam and site, levels of the report. These reports will describe the geometric and antenna parameters, frequencies, spectrum and power parameters, and a count of the number of interfering carriers contributing to the interference at each level. If the report for a given level is "turned off" by the user, the reports at all lower levels are automatically suppressed.

Figure 3.4/9 Interference Reports



4.0 MODEL ROUTINES

4.1 General

In this chapter, all of the model routines used in the simulation are discussed. In many cases, these models are the same, or very similar to those used in OFUS. For those models, only brief descriptions are given, as the details can be found in the OFUS documentation. Several new models have been developed for this simulation to model a variety of phenomena, equipment, and effects, unique to mobile-satellite communications systems. These models are described in more detail. In all cases however, all of the inputs and outputs required by the model routines have been identified.

Before describing the models to be used in the simulation, the following points should be noted:

- the level of approximation, when required, has been made consistent throughout the simulation,
- defaults can be applied to many of the parameters used to characterize equipment, as indicated in the INSERTION LANGUAGE CHARTS presented in Chapter 5,
- the flowcharts presented in this Chapter are part of the model descriptions and indicate flow-of-control, model options, sequencing of calculations, and selection of models. (Note, double horizontal bars used in the flowcharts indicate use of the subroutine whose name appears in brackets)

4.2 Geometric Models

4.2.1 General

In this section, the model routines required to calculate a variety of geometric parameters are presented. Much of the basis for these models comes from Reference 4.2/1. Among the geometric models required are location and site visibility algorithms for earth stations, ships and aircraft ; antenna boresight and reference vector algorithms; polarizer and mismatch angle geometry for linearly polarized antennae; and specialized geometric algorithms for multipath, antenna noise, and ionospheric propagation model calculations.

4.2.2 Site Location and Visibility Geometry (STGEOM)

Purpose

This routine calculates the site-to-site vector between a receiving site and transmitting site, and determines if the sites are visible to each other.

Description

The types of sites to be considered are:

- o earth stations
- o aircraft
- o ships
- o spacecraft

The location vector of a receiving site is computed by higher level routines and passed to this routine.

STGEOM calls subroutine LOC (described in the next section), to compute the location vector of a transmitting site.

The site-to-site vector and the zenith angle, χ , of the site-to-site vector is calculated using the geometric equations described in Reference 4.2/1 (equation 2.2.3, and 2.2.8).

A visibility algorithm has been developed which is applicable to all types of sites. The visibility geometry is sketched in Figure 4.2/1.

For site A, with an antenna located a distance h_A above sea level, site B is visible to A provided that $\chi_{SS} < \chi_C$, where χ_C is found by:

$$\chi_C = \frac{\pi}{2} + \Theta \quad , \quad (4.2.1)$$

and

$$\Theta = \cos^{-1} \left(\frac{R_E}{R_E + h_A} \right) \quad . \quad (4.2.2)$$

For $h_A < 10$ km, the following small angle approximation is used to determine Θ :

$$\frac{R_E}{R_E + h_A} = \begin{cases} \cos \Theta \\ 1 - \frac{\Theta^2}{2} \end{cases} \quad . \quad (4.2.3)$$

Θ can be written as:

$$\Theta \approx \sqrt{\frac{2h_A}{R_E}} \quad , \quad \text{radians} \quad (4.2.4)$$

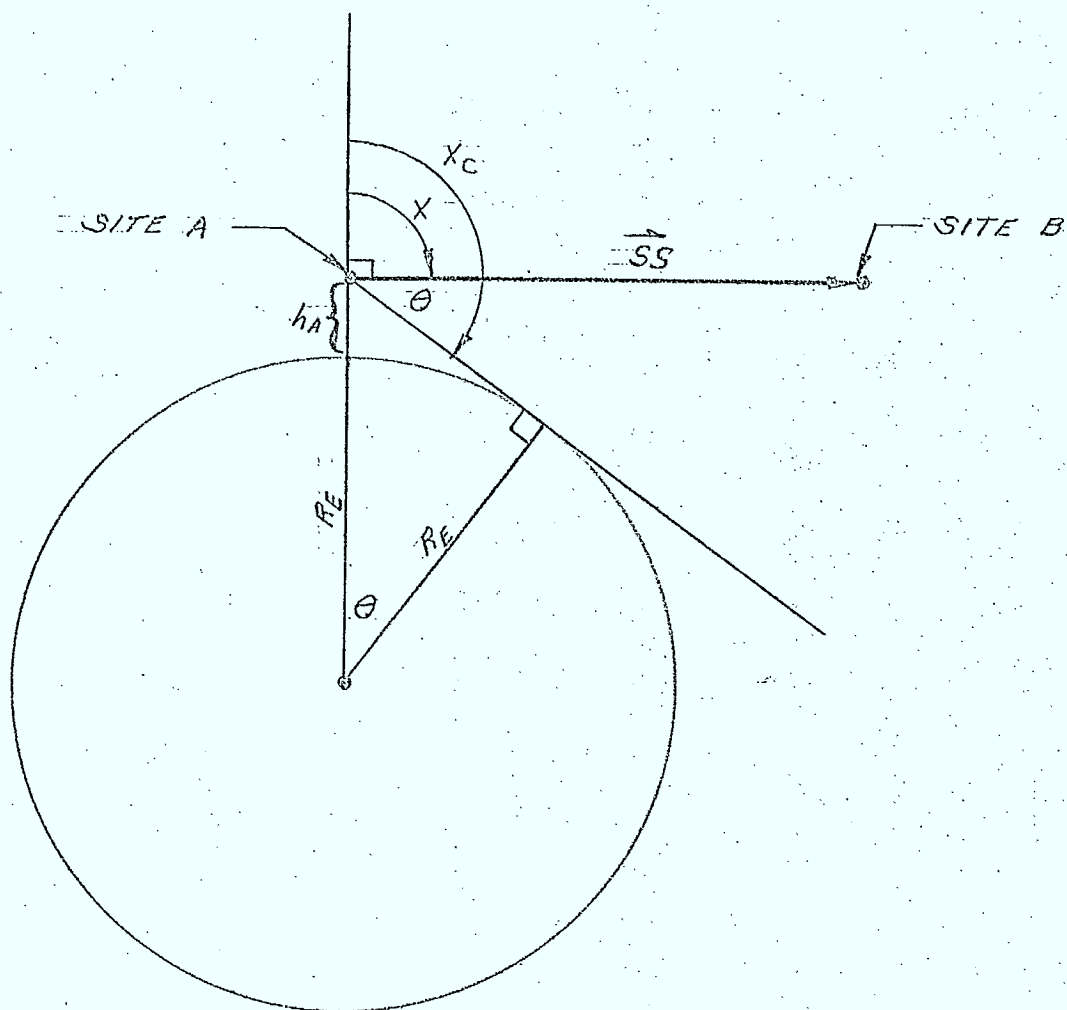


FIG. 4.2/1 VISIBILITY GEOMETRY

Additional parameters calculated by this routine are (see section 2.2, reference 4.2.1):

- o the azimuth and elevation of the site-to-site vector at both the receiver and transmitter sites
- o the great circle separation distance on the earth's surface between the receiving and transmitting sites.

A flowchart of this routine is given in Figure 4.2/2.

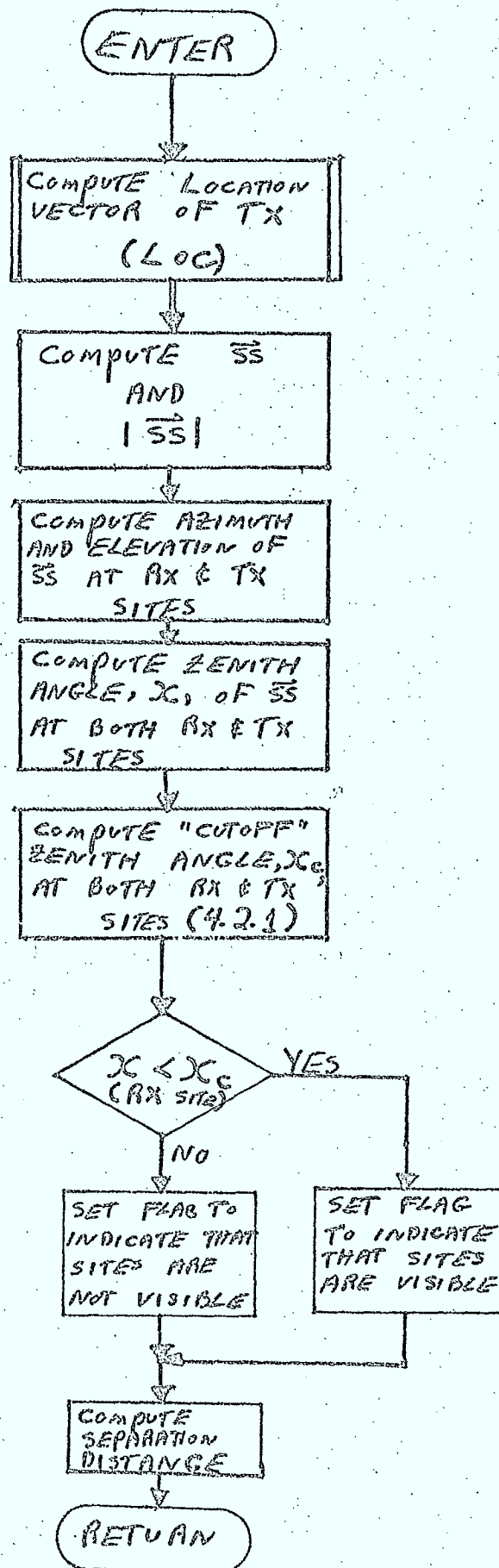
Inputs

- o flag indicating type of transmitter site
- o height of transmitter antenna above sea level
- o the location vector of the receiver site
- o longitude of transmitter site
- o latitude of transmitter site
- o longitude of receiver site
- o latitude of receiver site

Outputs

- o the site-to-site vector pointing from the receiver to the transmitter site
- o site separation distance
- o azimuth and elevation of \vec{SS} computed at both the receiver and transmitter sites
- o the great circle separation distance between the receiver and transmitter sites
- o flag indicating if the two sites are visible to each other.

Figure 4.2/2 Flowchart of STGEOM



Site Location Subroutine (LOC)Purpose

This routine computes the location vector of any site.

Description

The location vector of any site is given by:

$$\vec{LOC} = R \begin{pmatrix} \sin \theta \cos \lambda \\ \sin \theta \sin \lambda \\ \cos \theta \end{pmatrix} \quad (4.2.5)$$

where θ is the site co-latitude, λ is longitude measured east of Greenwich and R is the distance of the site antenna from the earth's center.

For earth stations, ships and aircraft, R is given by:

$$R = R_E + h \quad (4.2.6)$$

where R_E is the earth radius (6366 km) and h is the antenna height above sea level.

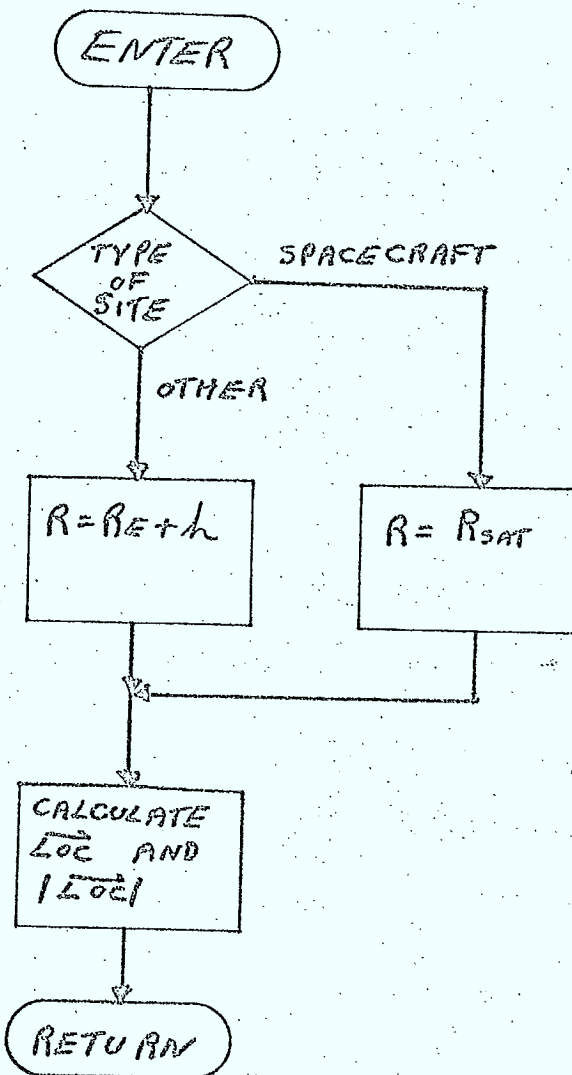
For spacecraft, R is given by:

$$R = R_{SAT} \quad (4.2.7)$$

where R_{SAT} is the spacecraft distance from the earth's center.

A flowchart of this routine is given in Figure 4.2/3.

Figure 4.2/3 Flowchart of LOC



Inputs

- o site latitude
- o site longitude
- o radius of spacecraft orbit
- o the antenna height above sea level
- o flag indicating type of site

Outputs

- o the location vector of the site
- o the distance of the site from the earth's center

4.2.3 Antenna Pointing Geometry (APGEOM)Purpose

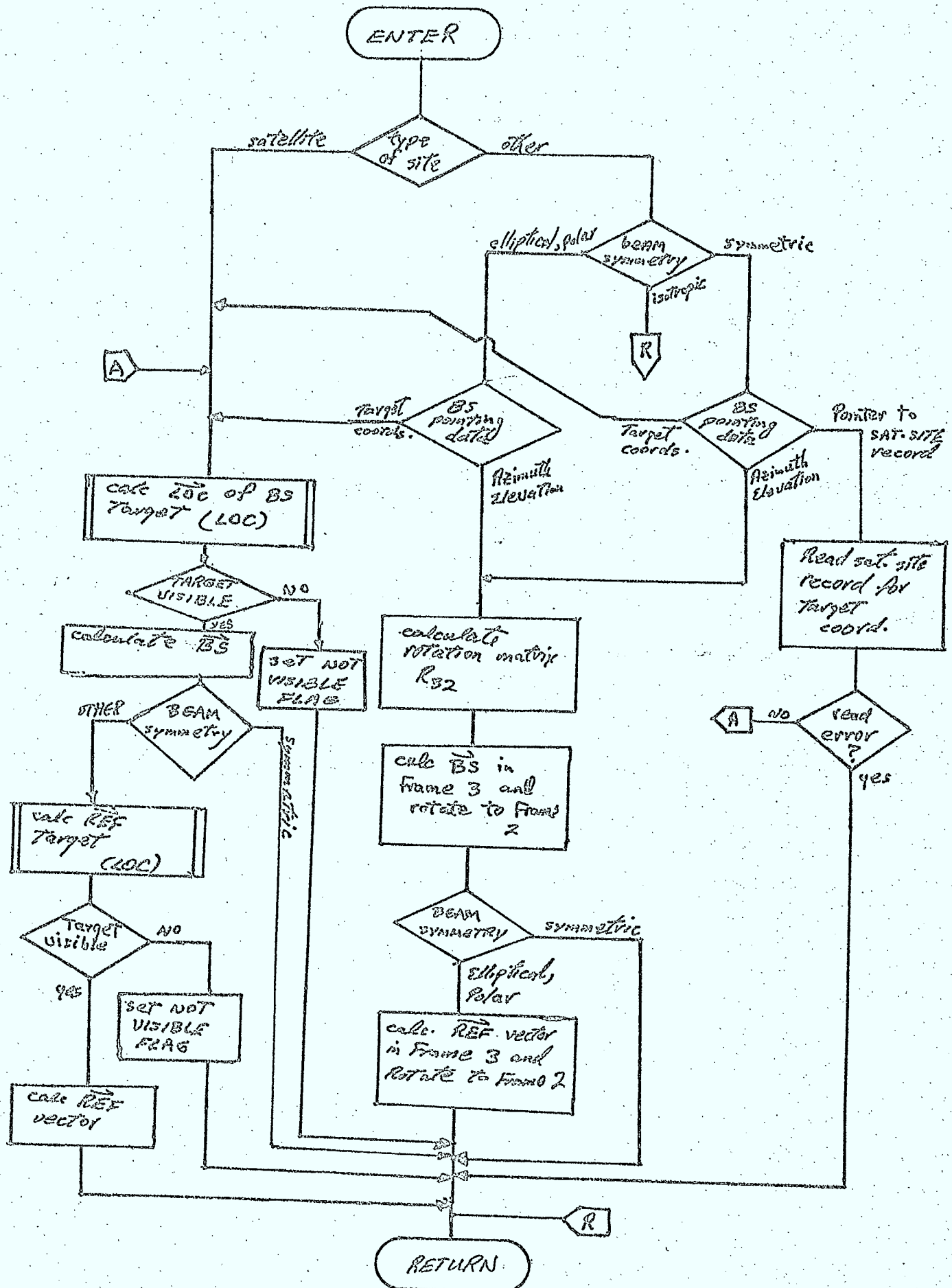
This routine calculates the boresight vector and reference vector at a site.

Description

A detailed description of this routine is given in section 2.3 of reference 4.2/1. A flowchart is illustrated in Figure 4.2/4.

Inputs

- o flag indicating type of site
- o latitude of site
- o longitude of site
- o orbital radius for spacecraft sites
- o height of antenna above sea level (earth stations, aircraft, ships)
- o the location vector of the site



- 0 flag indicating type of beam symmetry:
 - isotropic
 - single variable symmetric
 - elliptical
 - contour
 - polar
- 0 latitude of boresight target
- 0 longitude of boresight target
- 0 distance of boresight target from earth's center
- 0 latitude of reference target location
- 0 longitude of reference target location
- 0 distance of reference target location from earth's center
- 0 boresight azimuth
- 0 boresight elevation
- 0 reference target azimuth
- 0 reference target elevation
- 0 pointer to a satellite site if target location is specified as a particular satellite
- 0 unit number of database

Outputs

- 0 boresight vector components in frame 2
- 0 reference vector components in frame 2
- 0 error flag indicating pointer data is not valid
- 0 visibility flag indicating whether or not target is visible to the site
- 0 boresight azimuth
- 0 boresight elevation

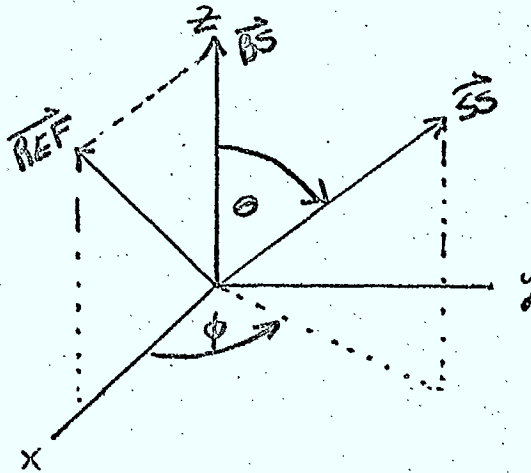
4.2.4 Antenna Gain Geometry (ANGEOM)

Purpose

This routine calculates the off-axis angle and rotation angle of the site-to-site vector relative to the antenna boresight and the reference plane (see sketch below).

Description

This routine is described in detail in section 2.3 of reference 4.2/1. The flowchart for this routine is sketched in Figure 4.2/5.

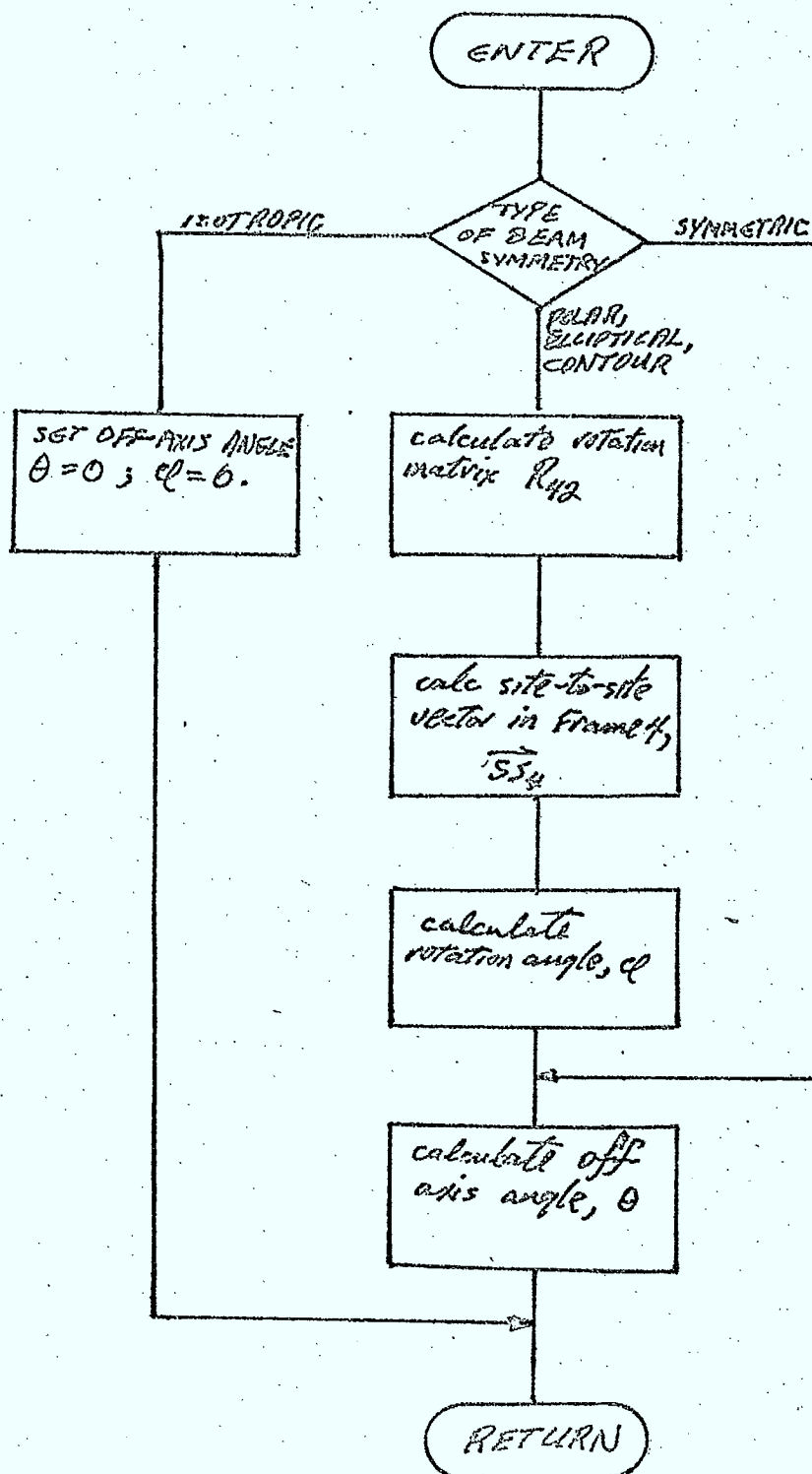


Inputs

- o boresight vector
- o antenna symmetry flag
- o reference direction vector
- o site-to-site vector

Outputs

- o the off-axis angle
- o the rotation angle



4.2.5 Antenna Polarizer Geometry Routine (ANPOL)Purpose

This routine calculates the polarizer vector of a transmitting or receiving antenna.

Description

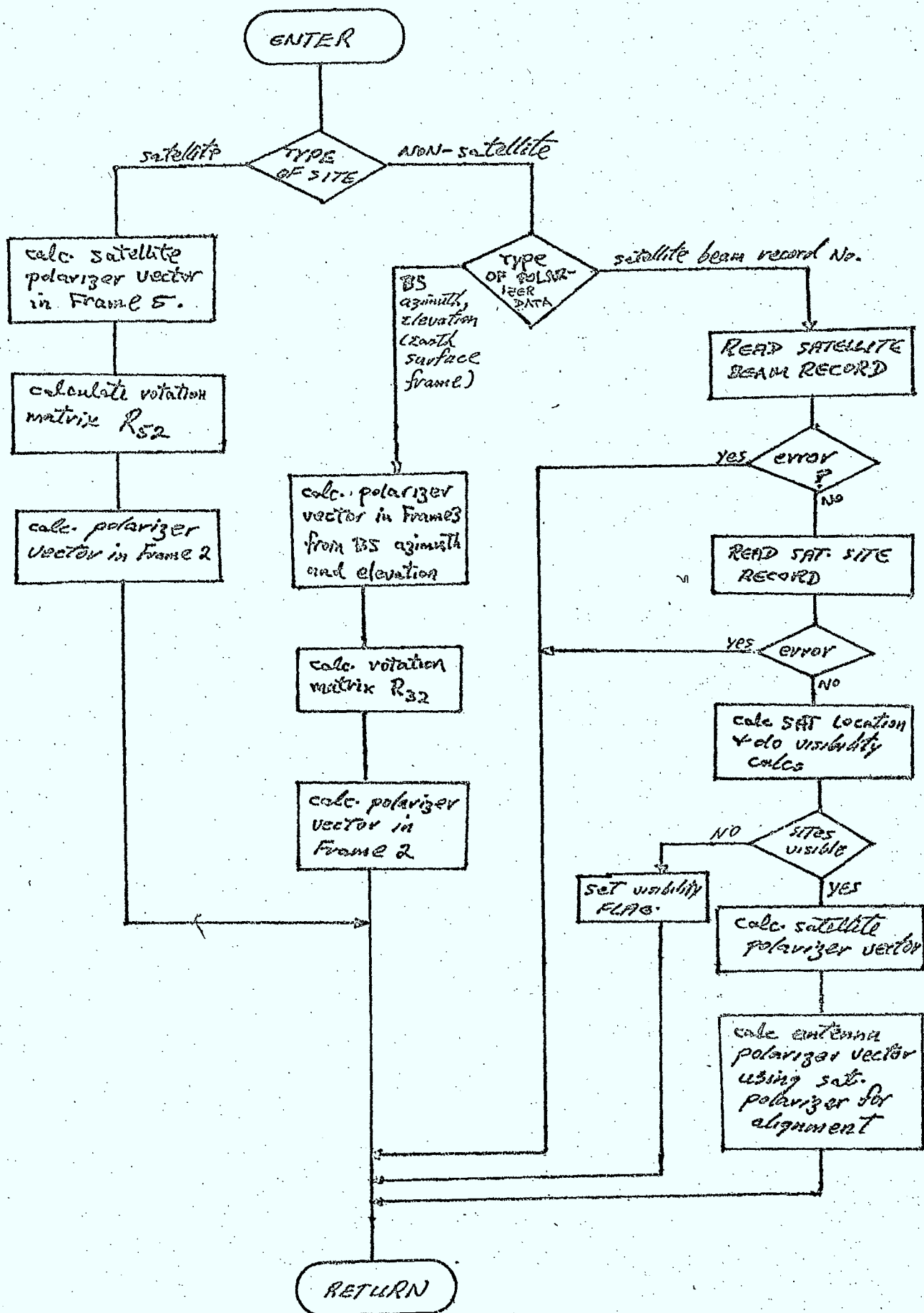
A detailed description of the analytics used in this routine is given in section 2.3 of reference 4.2/1.

A flowchart of this routing is given in Figure 4.2/6.

Inputs

- ① flag indicating type of site
- ① flag indicating type of polarizer orientation data specified (see next two items)
- ① polarizer rotation angle about the boresight
- ① a satellite beam record number with which the earth station, ship or aircraft polarizer vector is aligned.
- ① unit number of database
- ① flag indicating type of polarization (V, H, L, R)
- ① site longitude
- ① site latitude
- ① orbital radius for spacecraft sites
- ① height of antenna above sea level for earth stations, aircraft, and ships
- ① the location vector of the site
- ① antenna boresight vector
- ① antenna boresight azimuth
- ① antenna boresight elevation

Figure 4.2/6. Flowchart of ANPOL



Outputs

- o the polarizer vector
- o flag indicating whether or not error occurred using pointer data
- o flag indicating whether or not target site is visible

4.2.6 Linear Polarization Mismatch Angle Geometry (LPMA)

Purpose

This routine calculates the polarizer mismatch angle for linearly polarized RX and TX antennae.

Description

A detailed description of this routine is given in section 2.3 of reference 4.2/1 (equations 2.3.38, 2.3.39, 2.3.40).

Inputs

- o transmitting antenna polarizer vector
- o receiving antenna polarizer vector
- o site-to-site vector
- o Faraday rotation angle

Outputs

- o the polarizer mismatch angle

4.2.7 Location of Sun Geometry (SUNLOC)Purpose

This routine calculates the azimuth and elevation of the sun, for use by the antenna noise temperature and the ionospheric propagation models.

Description

A simple model to determine the approximate location (to within a few degrees) is recommended. It is assumed that the sun crosses the Greenwich meridian at 12:00 GMT. In actual fact, the time of meridian crossing deviates by approximately ± 16 minutes during the course of the year. It is also assumed that the sun declination varies sinusoidally over the course of the year with an amplitude of 23.5° and a period of 365 days. At day 80 (spring equinox) the sun declination is assumed to be zero. The sun location geometry is shown in Figure 4.2/7.

The location vector is given by:

$$\vec{Loc}_{SUN} = \begin{pmatrix} \cos \delta \cos \left(\frac{2\pi t}{24} - \pi \right) \\ - \cos \delta \sin \left(\frac{2\pi t}{24} - \pi \right) \\ \sin \delta \end{pmatrix} \quad (4.2.8)$$

where t is time of day (hours GMT) and the sun declination, δ , is given by:

$$\delta = 23.5^\circ \sin \left(\frac{2\pi D}{365} - .2192(2\pi) \right) \quad (4.2.9)$$

where D is the day of the year.

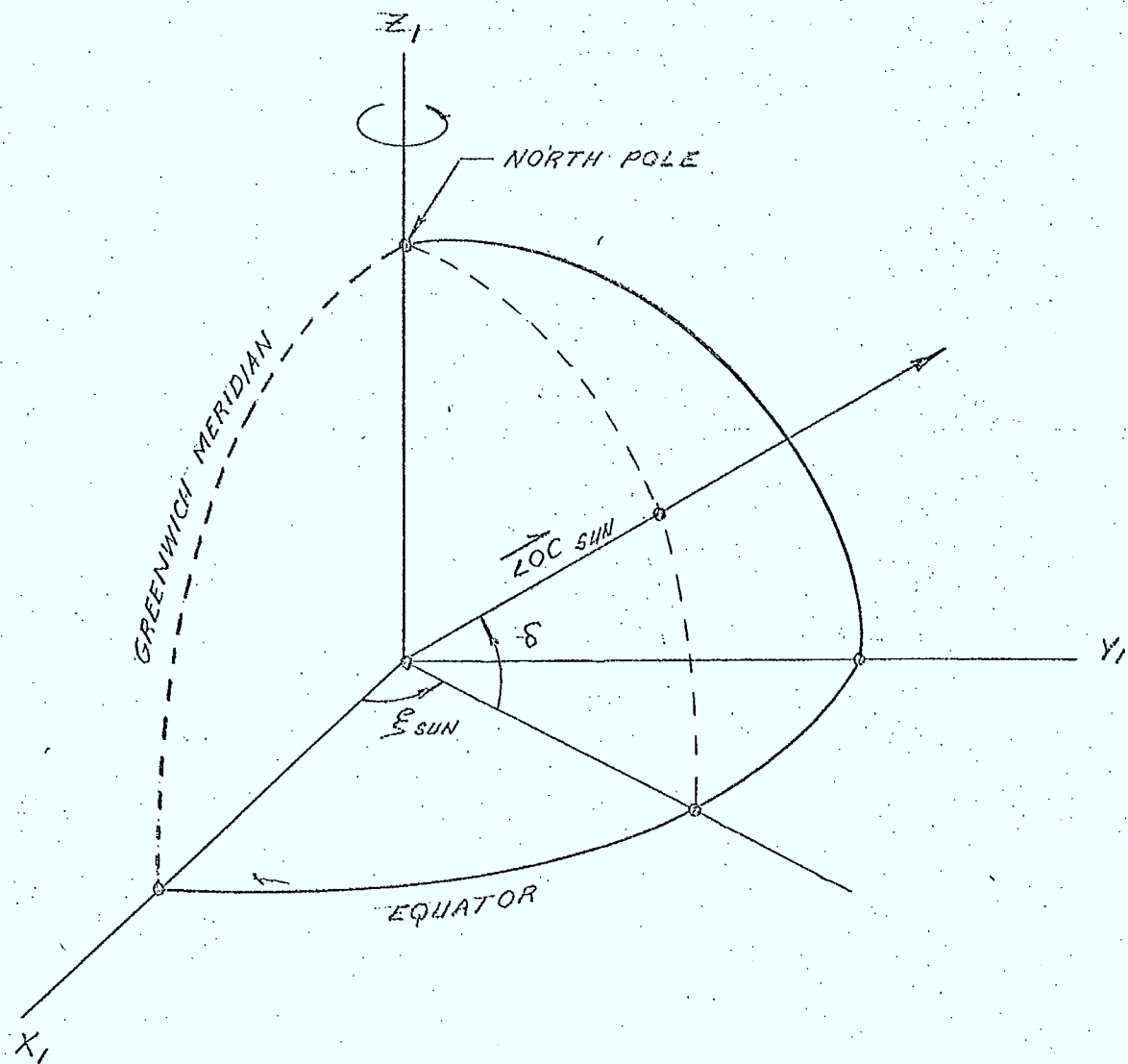


FIG: 4.2/7 SUN LOCATION GEOMETRY

Since the distance to the sun is large relative to the earth radius, the normalized sun vector in frame 2 (parallel to frame 1), \vec{SS} , is given by:

$$\vec{SS} = \vec{LOC}_{SUN} \quad (4.2.10)$$

To determine the solar zenith angle, the components of the site-to-site vector are expressed in frame 3:

$$\vec{SS}_3 = R_{23} \vec{SS}_2 \quad (4.2.11)$$

where R_{23} is given by equation (2.2.5) of reference 4.2/1.

The solar zenith angle, χ_{SUN} , is given by:

$$\chi_{SUN} = \frac{\pi}{2} - \sin^{-1} \left(\frac{SS_{23}}{|\vec{SS}|} \right) \quad (4.2.12)$$

Inputs

- 0 latitude of site
- 0 longitude of site
- 0 time of day (GMT)
- 0 day of year

Outputs

- 0 normalized solar location vector
- 0 the solar zenith angle
- 0 solar declination

4.2.8 Spherical Layer Geometry (LAYER)

Purpose

This routine is used to calculate a number of geometric parameters required in ionospheric propagation model calculations, related to the intersection of a spherical ionospheric layer by the propagation path.

Method

This routine is a direct implementation of the geometric model described in Section 2.2.6 of Reference 4.2/1.

Inputs

- o line of site vector pointing from earth station or aircraft to a satellite
- o latitude, longitude, radius of the earth station
- o height of layer

Outputs

- o latitude, longitude of intersection point of line of site and spherical layer
- o distance from earth station to layer along line of site
- o distance from layer to satellite along line of site
- o zenith angle of line of site at earth station
- o incidence angle of the line of site at the layer

4.2.9 Specular Point Geometry (SPGEOM)Purpose

This routine is used to calculate a variety of geometric parameters associated with multipath interference for any two sites.

Description

Several geometric models are required when calculating the effects of multipath interference when mobile transmitters and receivers are involved in a communications link. These geometric parameters are dependent only on the locations of the two sites involved. The situation is sketched in Figure 4.2/8. Among the parameters that must be calculated in this routine are:

- o vector pointing from the TX site to the specular point, \vec{SS}_T
- o vector pointing from the RX site to the specular point, \vec{SS}_R
- o the distance from the TX site to the specular point, d_T
- o the distance from the RX site to the specular point, d_R
- o the reflection angle at the specular point, θ_S

These parameters are indicated in the figure. The specular point, S, is the point of reflection on the earth's surface of the specular multipath component. If h_T is the height of the transmitter above the earth's surface, h_R is the height of the receiver above the earth's surface, and assuming a smooth spherical earth of radius R_E , then the following relationships hold:

$$(h_R + R_E)^2 = R_E^2 + d_R^2 - 2 R_E d_R \cos(90 + \theta_S) \quad (4.2.13)$$

$$(h_T + R_E)^2 = R_E^2 + d_T^2 - 2 R_E d_T \cos(90 + \theta_S) \quad (4.2.14)$$

$$d^2 = d_T^2 + d_R^2 - 2 d_T d_R \cos(180 - 2\theta_S) \quad (4.2.15)$$

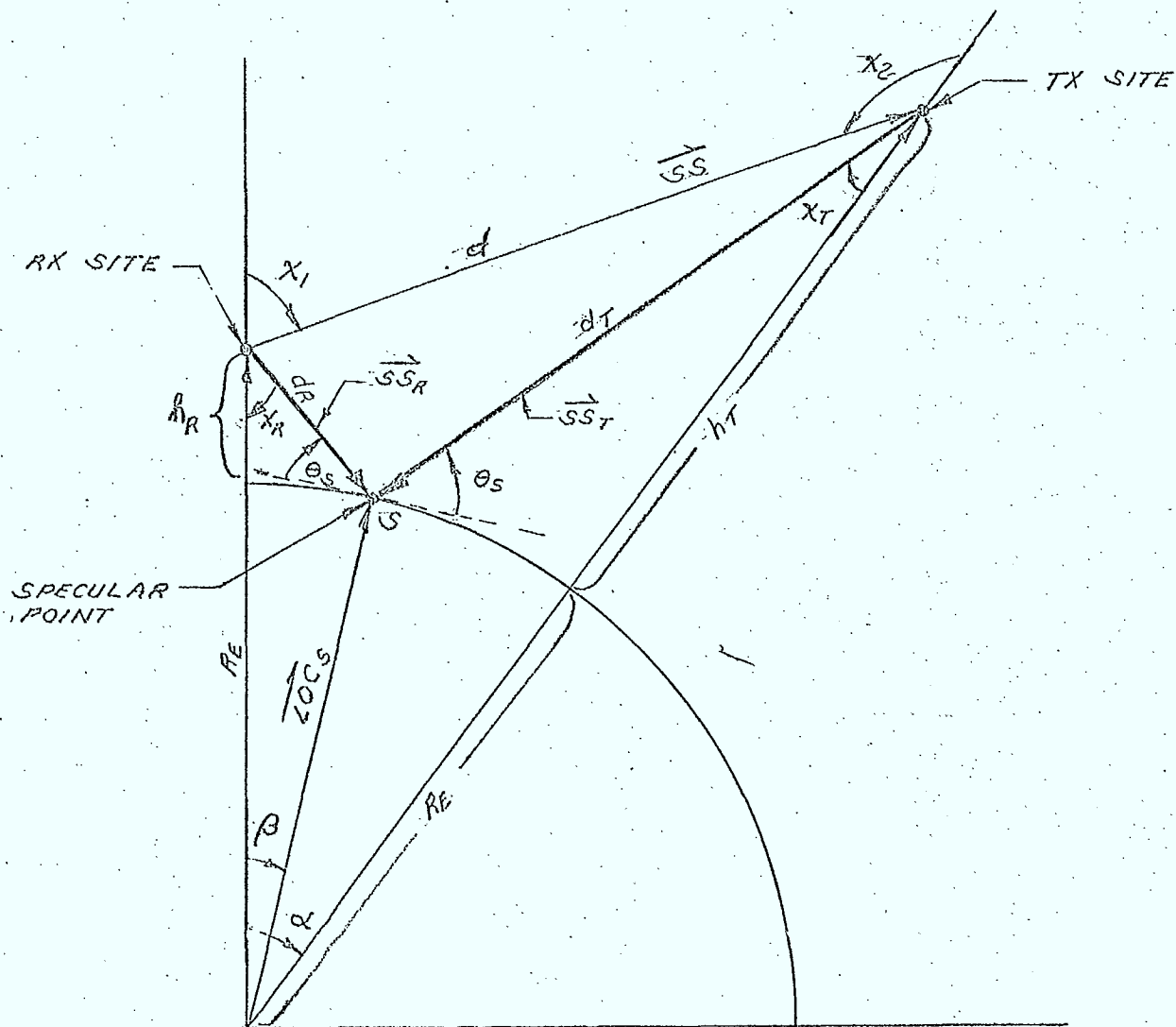


FIG: 4.2/8 SPECULAR POINT GEOMETRY

These equations can be rearranged to yield:

$$d_R = R_E \left[\sin \theta_S + \left\{ \left(\frac{h_R + R_E}{R_E} \right)^2 - \cos^2 \theta_S \right\}^{\frac{1}{2}} \right] \quad (4.2.16)$$

$$d_T = R_E \left[-\sin \theta_S + \left\{ \left(\frac{h_T + R_E}{R_E} \right)^2 - \cos^2 \theta_S \right\}^{\frac{1}{2}} \right] \quad (4.2.17)$$

$$\theta_S = \frac{1}{2} \cos^{-1} \left[\frac{d^2 - d_T^2 - d_R^2}{2 d_T d_R} \right] \quad (4.2.18)$$

These equations can be solved for d_T , d_R , and θ_S using an iterative technique. First a value of θ_S is estimated and equations 4.2.16 and 4.2.17 are used to obtain values for d_R and d_T . These values are then used to improve the estimate of θ_S and the procedure repeated until all values converge. This procedure will converge if a starting value of θ_S is obtained using the following values of d_R and d_T :

$$d_{R, \text{INITIAL}} = \left[(R_E + h_R)^2 + R_E^2 - 2 h_R R_E \cos\left(\frac{\alpha}{2}\right) \right]^{\frac{1}{2}} \quad (4.2.19)$$

$$d_{T, \text{INITIAL}} = \left[(R_E + h_T)^2 + R_E^2 - 2 h_T R_E \cos\left(\frac{\alpha}{2}\right) \right]^{\frac{1}{2}} \quad (4.2.20)$$

where α is the angle between the location vectors to the two sites.

The vectors \vec{SS}_R and \vec{SS}_T can be determined once the location vector of the specular point, \vec{LOC}_S , is obtained, ie:

$$\vec{SS}_R = \vec{LOC}_S - \vec{LOC}_R \quad (4.2.21)$$

$$\vec{SS}_T = \vec{LOC}_S - \vec{LOC}_T \quad (4.2.22)$$

where \vec{LOC}_R and \vec{LOC}_T are the location vectors of the receiver and the transmitter.

The vector $\overrightarrow{LOC_S}$ is given by:

$$\overrightarrow{LOC_S} = R_E \vec{s} \quad (4.2.23)$$

where \vec{s} is a unit vector. From Figure 4.2/8 it is seen that:

$$\vec{s} \cdot \frac{\overrightarrow{LOC_R}}{|\overrightarrow{LOC_R}|} = \cos \beta \quad (4.2.24)$$

$$\vec{s} \cdot \frac{\overrightarrow{LOC_T}}{|\overrightarrow{LOC_T}|} = \cos(\alpha - \beta) \quad (4.2.25)$$

These equations, together with the condition that $|\vec{s}| = 1$ can be used to obtain the components of \vec{s} .

Let

$$\begin{aligned} B &= \cos \beta \\ A &= \cos(\alpha - \beta) \end{aligned} \quad (4.2.26)$$

Then

$$B = \frac{1}{2} \cos^{-1} \left\{ \frac{d_R^2 - R_E^2 - (R_E + h_R)^2}{2(R_E + h_R)} \right\} \quad (4.2.27)$$

$$A = \frac{1}{2} \cos^{-1} \left\{ \frac{d_T^2 - R_E^2 - (R_E + h_T)^2}{2(R_E + h_T)} \right\} \quad (4.2.28)$$

Letting

$$\vec{r} = \frac{\overrightarrow{LOC_R}}{|\overrightarrow{LOC_R}|} \quad (4.2.29)$$

$$\vec{t} = \frac{\overrightarrow{LOC_T}}{|\overrightarrow{LOC_T}|}$$

then substituting into equations 4.2.24 and 4.2.25 yields:

$$\left. \begin{aligned} S_x r_x + S_y r_y + S_z r_z &= B \\ S_x \tau_x + S_y \tau_y + S_z \tau_z &= A \\ S_x^2 + S_y^2 + S_z^2 &= 1 \end{aligned} \right\} \quad (4.2.30)$$

These equations can then be solved for S_x , S_y , S_z .

The final geometric parameter required in multipath calculations is the "power divergence factor", D . This factor may be interpreted geometrically as the ratio of the cross section S formed at the receiver by a narrow beam originating at the transmitter and reflected from the smooth earth to the cross section S' that would be obtained if the spherical earth were replaced by a plane (see Figure 4.2/9). From Reference 4.2/2, the divergence factor is given by:

$$D = \frac{[R_E(d_T + d_R)]^2 \sin \theta_S \cos \theta_S}{(R_E + h_R)(R_E + h_T) \sin \alpha [d_R(R_E + h_T) \cos \chi_T + d_T(R_E + h_R) \cos \chi_R]} \quad (4.2.31)$$

For θ_S greater than $\approx 20^\circ$, $D \approx 1$.

A flowchart illustrating the implementation of these models in subroutine SPGEOM is given in Figure 4.2/10.

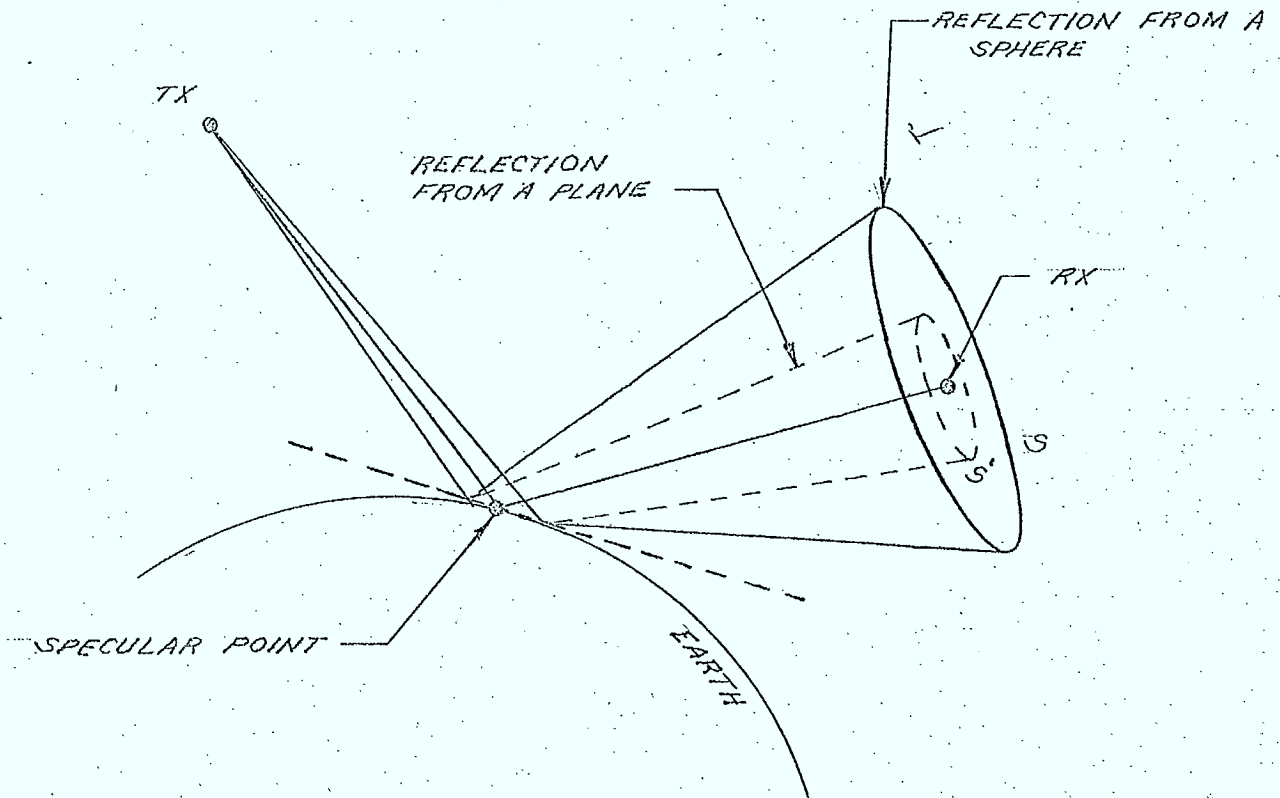
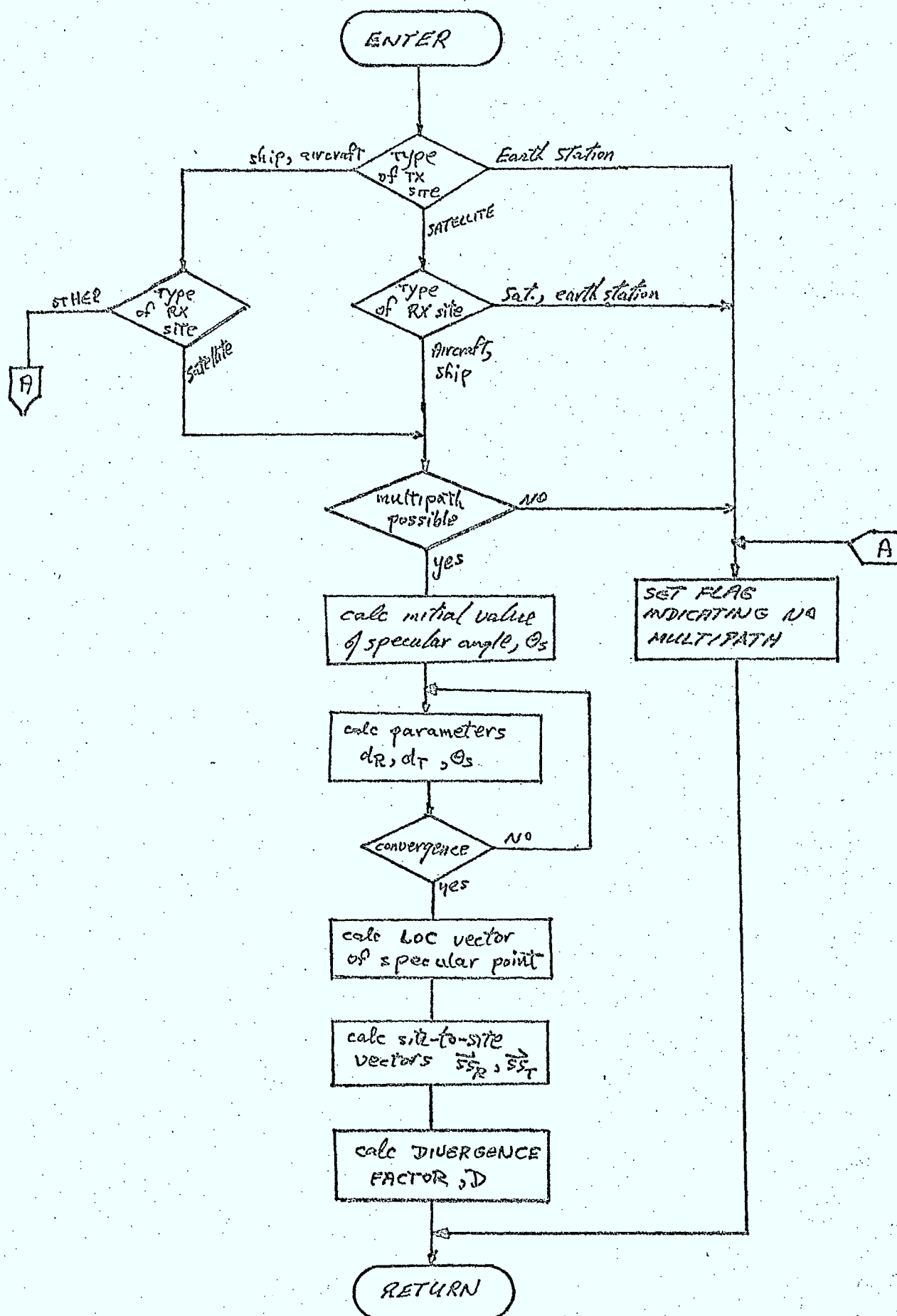


FIG. 4.2/9 GEOMETRIC INTERPRETATION OF DIVERGENCE FACTOR

Figure 4.2/10 Flowchart of SPGEOM



Inputs

- o type of TX site
- o type of RX site
- o location parameters of TX site: height, lat, long, radius, and \vec{LOC}
- o location parameters of RX site: height, lat, long, radius, and \vec{LOC}
- o length of the site-to-site vector connecting the RX and TX sites, d
- o zenith angles and critical zenith angle of \vec{SS} at RX and TX

Outputs

- o \vec{SS}_R , \vec{SS}_T , θ_S , d_R , d_T , D (described in this section)
- o flag indicating whether or not multipath can occur between sites

4.2.10 Geomagnetic Field Geometry (MAGFLD)Purpose

This routine is used to calculate the earth's magnetic field vector and geomagnetic coordinates for any geographic location on or above the earth's surface.

Description

The models described in Section 2.5 of Reference 4.2/1 are used directly in this routine.

Inputs

- ① geographic latitude, longitude of site
- ② height of site above the earth's surface

Outputs

- ① geomagnetic latitude and longitude of site
- ② magnetic field vector at site

References

4.2/1: SED 0710-44-TR-102, Issue 4; "Orbit Frequency Utilization Simulation - Volume 1 - Analytical Foundation", February 28, 1977.

4.2/2: "Radio Wave Propagation and the Ionosphere", Vol. 2;
"Propagation of Electromagnetic Waves Near The Earth",
Yakov L. Al'Pert, Consultants Bureau, New York, 1974.

4.3 Antenna Models

4.3.1 General

In this section, models are presented that are used in all of the antenna gain calculations performed by the simulation. These models are used to calculate the principal and cross polarization gain of the antenna, and the polarization mismatch factors used in LINK and SITE calculations. The antenna models to be included in the simulation for satellite beams are:

- CCIR principal polarization gain model
- single variable general antenna pattern model (principal and cross polarizations)
- OFUS antenna depolarization ratio model
- contour gain pattern model
- general polar pattern model.

The first three models are used for symmetric and elliptical antenna beams while the last two are used for satellite beams with arbitrary gain patterns.

For earth-stations, aircraft, and ships, the same models are used, with the exception of the contour pattern model, and the addition of an isotropic antenna model. In all cases (except isotropic) the OFUS depolarization ratio model is used as the default model when an actual cross polarization pattern is not specified by the user.

4.3.2 Antenna Gain Model (ANTEN)

Purpose

This routine calculates the antenna principal and cross polarization gains and the depolarization ratio for the different types of antenna gain models included in the simulation.

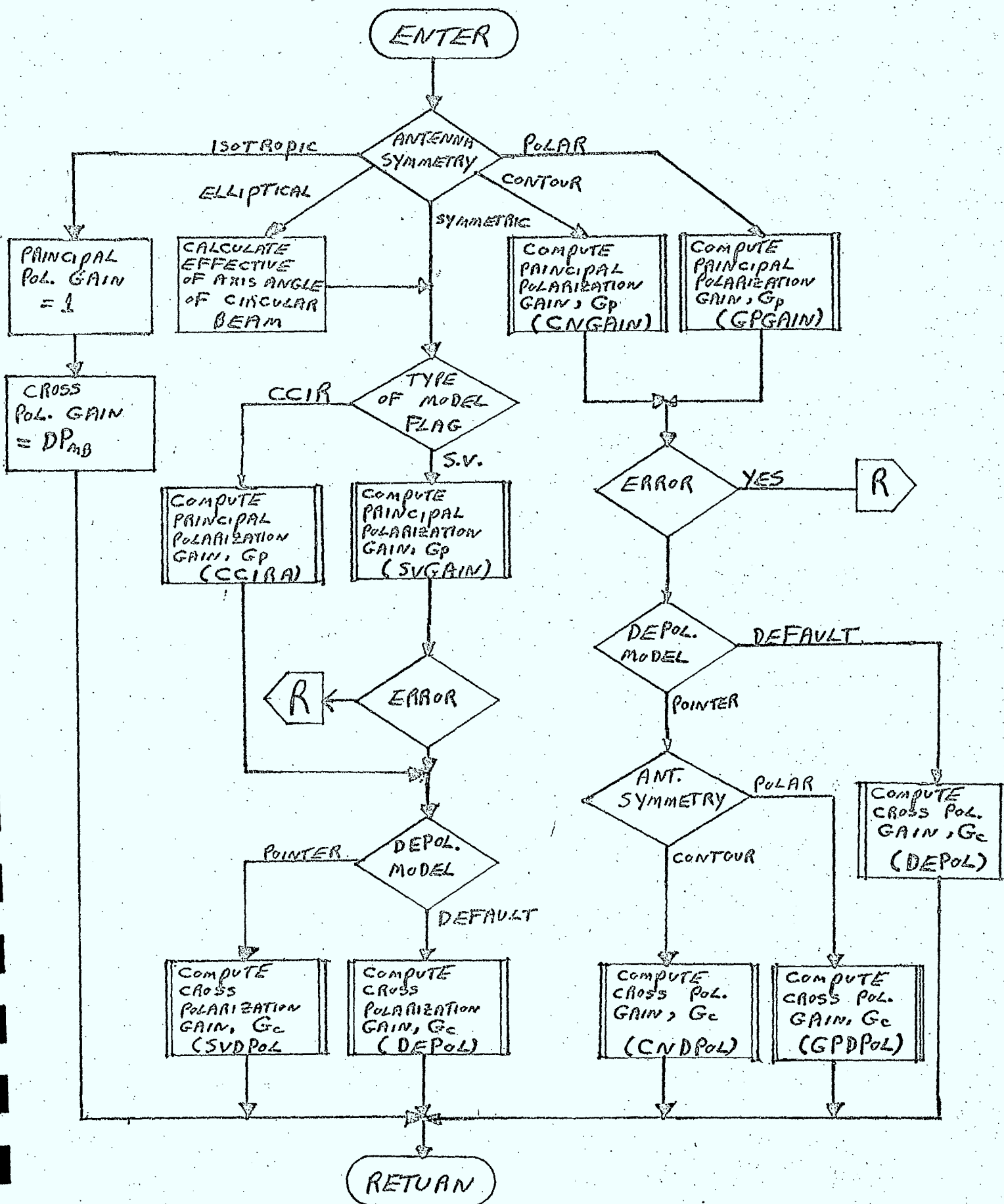
Description

This routine is primarily an executive type routine which controls the calling sequence to the other routines described later in this section. The main control logic of subroutine ANTEN is shown in Figure 4.3/1.

Inputs

- ① flag indicating type of site
- ① flag indicating type of beam symmetry
 - isotropic
 - symmetric (circular)
 - elliptical
 - contour
 - polar projection
- ① flag indicating type of antenna model for symmetric or elliptical patterns
 - CCIR
 - single variable
- ① the on-axis gain
- ① major axis beamwidth (for elliptical beams only)
- ① minor axis beamwidth (for elliptical beams only)
- ① pattern file characteristic parameters
- ① pointer to principal polarization pattern
- ① pointer to cross polarization pattern
- ① main beam depolarization ratio
- ① side lobe depolarization ratio
- ① back lobe depolarization ratio
- ① the off axis angle
- ① the rotation angle

Figure 4.3/1 Flowchart of ANTEN



Outputs

- o depolarization ratio
- o the principal polarization gain in direction, (θ, ϕ)
- o the cross polarization gain in direction, (θ, ϕ)
- o error flag indicating if pattern file data is incorrect

4.3.2.1 CCIR Principal Polarization Gain Model (CCIRA)Purpose

This routine calculates the principal polarization gain for a given off-axis angle, for the CCIR model.

Description

A detailed description of this model is given in section 3.2 of reference 4.3/1.

Inputs

- o the off axis angle
- o the on axis gain
- o the diameter-to-wavelength ratio computed in ANTEN
- o flag indicating type of antenna site
 - satellite
 - non-satellite

Outputs

- o the principal polarization gain in direction defined by the off axis angle

4.3.2.2 Single Variable Gain Model (SVGAIN)

Purpose

This routine calculates the principal polarization gain for a given off-axis angle by accessing data in the antenna pattern file.

Description

The details of this routine are described in reference 4.3/1.

Inputs

- o principal polarization on axis gain
- o off axis angle
- o record number of the pattern in the pattern file
- o the 3dB beamwidth half-angle
- o pattern file characteristic parameters
- o flag indicating type of antenna site
 - satellite
 - non- satellite
- o the diameter-to-wavelength ratio

Outputs

- o the principal polarization gain in direction θ
- o error return code

4.3.2.3 Contour Gain Model (CNGAIN)

Purpose

This routine calculates the principal polarization gain for given off-axis and rotation angles by accessing data in the antenna pattern file.

Description

The details of this routine are described in Reference 4.3/1.

Inputs

- ① the principal polarization on-axis gain
- ① the off-axis angle
- ① the rotation angle
- ① record number of the antenna pattern in the pattern file
- ① the 3dB beamwidth half-angle
- ① pattern file characteristic parameters
- ① diameter-to-wavelength ratio
- ① flag indicating type of antenna site
 - satellite
 - non-satellite

Outputs

- ① the principal polarization gain in direction θ , \emptyset
- ① error return code
- ① gain interpolated along first radial enclosing θ , G1
- ① gain interpolated along second radial enclosing θ , G2

4.3.2.4 General Polar Pattern Model (GPGAIN)Purpose

This routine calculates the principal polarization gain for given off-axis and rotation angles by accessing data stored in the antenna pattern file.

Description

This routine is almost identical to the contour gain model, in that it interpolates between stored values of the antenna gain to determine the principal polarization gain. Unlike the contour model, many fewer radial patterns are required to describe the antenna pattern, and these radial patterns need not be given at equal intervals $\Delta\theta$. A description of the user input data and pattern storage in the file is given in the next chapter.

Inputs

- ① same as for contour pattern described in section 4.3.2.3.

Outputs

- ① same as for contour pattern described in section 4.3.2.3.

4.3.2.5 Single Variable Cross Polarization Gain Model (SVDPOL)Purpose

This routine calculates the depolarization ratio and the cross polarization gain for a given off-axis angle by accessing data stored in the antenna pattern file.

Description

The details of this routine are described in reference 4.3/1.

Inputs

- ① principal polarization on-axis gain
- ① off-axis angle

- o 3dB beamwidth half-angle
- o record number of the pattern in the pattern file
- o pattern file characteristic parameters
- o principal polarization gain at off-axis angle θ
- o mainbeam, sidelobe, and backlobe depolarization ratios.

Outputs

- o error return code
- o depolarization ratio
- o cross polarization gain

4.3.2.6 Contour Cross Polarization Gain Model (CNDPOL)

Purpose

This routine calculates the depolarization ratio and the cross polarization gain for a given off-axis angle and rotation angle by accessing data in the antenna pattern file.

Description

The details of this routine are described in reference 4.3/1.

Inputs

- o principal polarization on-axis gain
- o off-axis angle
- o rotation angle
- o 3dB beamwidth half-angle
- o pattern file characteristic parameters
- o principal polarization gain at first radial enclosing θ , G1
- o principal polarization gain at second radial enclosing θ , G2
- o record number of pattern in antenna pattern file
- o mainbeam, sidelobe, and backlobe depolarization ratios.

Outputs

- o error return code
- o depolarization ratio
- o cross polarization gain

4.3.2.7 General Polar Pattern Depolarization Model (GPDPOL)Purpose

This routine calculates the depolarization ratio and cross polarization gain for a given off-axis and rotation angle by accessing data in the pattern file.

Description

This routine calculates the cross polarization antenna gain using the same interpolation algorithm as CNDPOL. The insertion and storage of user-input data used in this routine are discussed in Chapter 5.

Inputs

- o same as for contour pattern described in section 4.3.2.6

Outputs

- o same as for contour pattern described in section 4.3.2.6.

4.3.2.8 Depolarization Model Routine (DEPOL)Purpose

This routine is the default depolarization model which determines the depolarization ratio of an antenna.

Description

This routine is described in Reference 4.3/1.

Inputs

- ⊙ the principal polarization on-axis gain
- ⊙ the off-axis angle
- ⊙ the depolarization ratio of the mainbeam
- ⊙ the depolarization ratio of the near sidelobes
- ⊙ the depolarization ratio of the backlobes.

Outputs

- ⊙ depolarization ratio

4.3.2.9 Polarizer Mismatch Factor Routine (POLMIS)Purpose

This routine computes the principal and cross polarization mismatch factors between receiving and transmitting antennae.

Description

This routine uses the geometric algorithms and equations for the mismatch factors described in Chapters 2 and 3 of Reference 4.3/1.

Inputs

- ⊙ polarizer vector of transmitting antenna (for linearly polarized beams)
- ⊙ polarizer vector of the receiving antenna (for linearly polarized beams)

- 0 Faraday rotation angle
- 0 site-to-site vector
- 0 receiving antenna depolarization ratio
- 0 polarization of transmitting antenna (V, H, R or L)
- 0 polarization of the receiving antenna (V, H, R or L)

Outputs

- 0 principal polarization mismatch factor
- 0 cross polarization mismatch factor

References

- 4.3/1: SED 0710-44-TR-102, Issue 4; "Orbit Frequency Utilization Simulation - Volume 1 - Analytical Foundation", February 28, 1977.
- 4.3/2: SED 0710-44-SW-103, Issue 3; "Orbit Frequency Utilization Simulation - Volume 2 - Program Description", February 28, 1977.

4.4 Propagation Models

4.4.1 General

Three propagation phenomena are included in the discussions in this section, namely:

- o tropospheric absorption
- o ionospheric scintillation
- o Faraday Rotation

Models for all of these phenomena are discussed in detail in Reference 4.4/1. These models can be used almost directly in the simulation.

Of the three phenomena, tropospheric absorption is always considered along any path. The absorption due to the troposphere is assumed to be a non-fluctuating, or nominal, loss. The other two phenomena are not and hence are user-selectable. Of these, only Faraday rotation is applied to both interferers and link carriers.

4.4.2 Tropospheric Absorption Model (TROP)

Purpose

This routine is used to calculate the tropospheric absorption along the line-of-site connecting two sites.

Description

The main algorithms used in calculating the absorption are described in Section 4.2 of Reference 4.4/1. The implementation of the routine is illustrated in Figure 4.4/1.

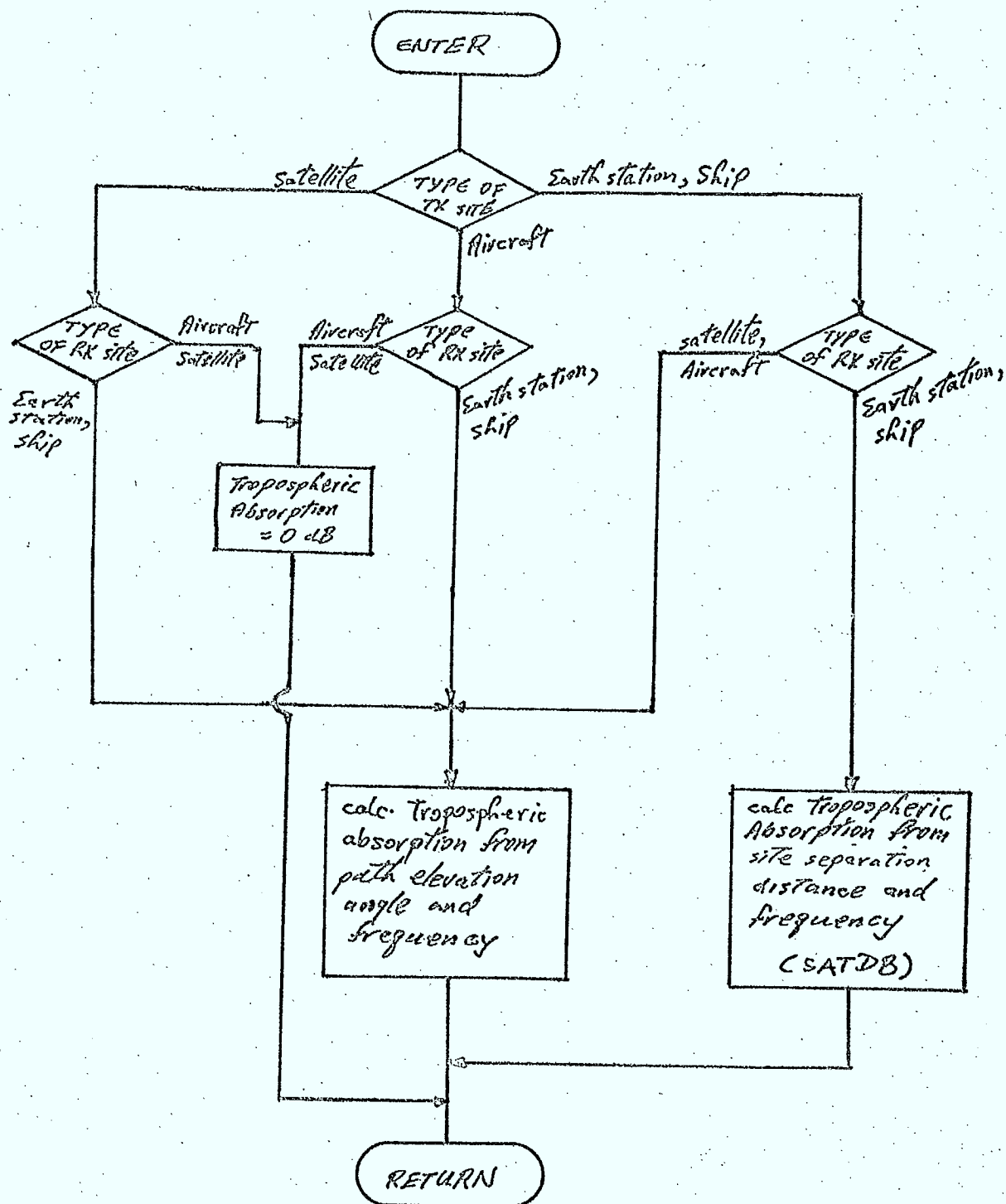
Inputs

- o flag indicating type of TX site
- o flag indicating type of RX site
- o elevation angle of path
- o great circle site separation distance
- o frequency

Outputs

- o nominal attenuation due to troposphere.

Figure 4.4/1 Flowchart of TROP



4.4.3 Ionospheric Scintillation Model (ISCINT)

Purpose

This routine calculates the scintillation loss experienced by signals transmitted via transionospheric paths.

Discription

The model used for this propagation phenomenon is discussed in detail in Section 4.6 of Reference 4.4/1. This model is only invoked for the wanted carrier in a LINK calculation. A simplified flowchart of the ionospheric scintillation routine (ISCINT) is illustrated in Figure 4.4/2.

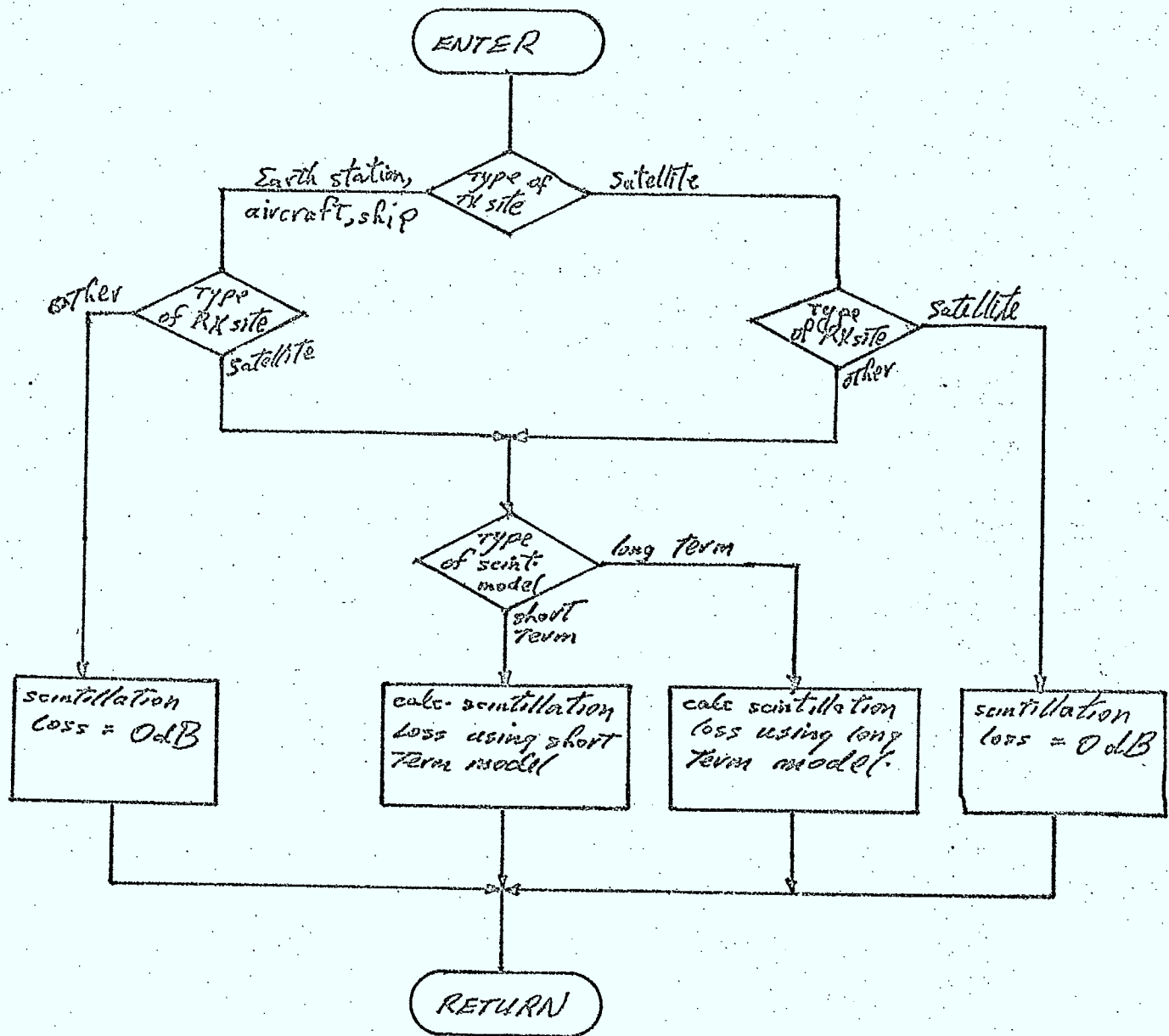
Inputs

- o type of RX site
- o type of TX site
- o site-to-site vector
- o location parameters of TX site (\vec{LOC} , lat, long, rad)
- o location parameters of RX site (\vec{LOC} , lat, long, rad)
- o type of scintillation model flag $\left\{ \begin{array}{l} \text{long term} \\ \text{short term} \end{array} \right.$
- o Greenwich mean time
- o day of year
- o sunspot number
- o fraction of time signal power is exceeded

Outputs

- o attenuation due to scintillation

Figure 4.4/2 Flowchart of ISCINT



4.4.4 Faraday Rotation Model (FARROT)

Purpose

This routine calculates the rotation angle of the electric field vector of a linearly polarized signal crossing the ionosphere.

Description

This model is discussed in detail in Section 4.7 of Reference 4.4/1. A simplified flowchart of the model is illustrated in Figure 4.4/3.

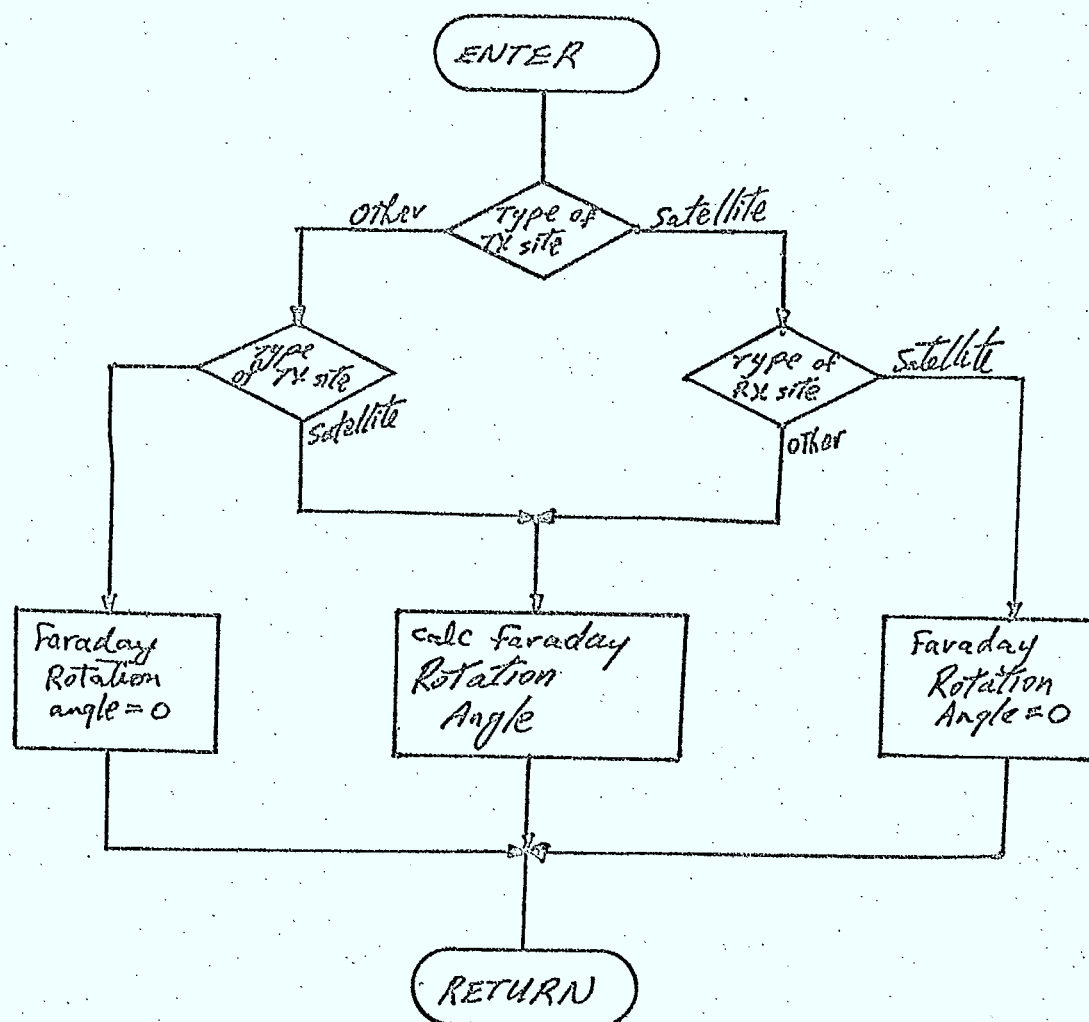
Inputs

- ① type of TX site
- ① type of RX site
- ① site-to-site vector
- ① TX location parameters (lat, long, rad, \overrightarrow{LOC})
- ① RX location parameters (lat, long, rad, \overrightarrow{LOC})
- ① sunspot number
- ① Greenwich mean time (GMT)
- ① day of year
- ① frequency

Outputs

- ① total Faraday rotation angle.

Figure 4.4/3 Flowchart of FARROT



4.5 Multipath Interference Model

4.5.1 General

In this section, a model is described that can be used to calculate the average diffuse and specular multipath interference power on paths between aircraft or ships and satellites. This model is only invoked in LINK calculations, and depends on a variety of geometric, antenna, propagation, and other models described elsewhere in this chapter.

4.5.2 Multipath Interference Path Loss Calculations

The situation under analysis is illustrated in Figure 4.5/1. The ratio of total received multipath power (diffuse plus specular)-to-transmitter power is called the path loss and denoted L_M . This ratio can be estimated for paths between mobile sites and satellites (or between two mobile sites) as follows:

Define the following parameters:

- o G_T principal polarization gain of TX antenna in direction of specular point
- o d_T distance from the TX site to the specular point
- o d_R distance from the RX site to the specular point
- o A_T tropospheric attenuation along the path (approximated by the one-way tropospheric path loss from the specular point to the satellite)
- o λ operating wavelength
- o D geometric power divergence factor (see Section 4.2.9)
- o ρ_0 total multipath reflection coefficient for a flat, smooth earth. (Note: this coefficient depends on the polarization of the transmitted signal)

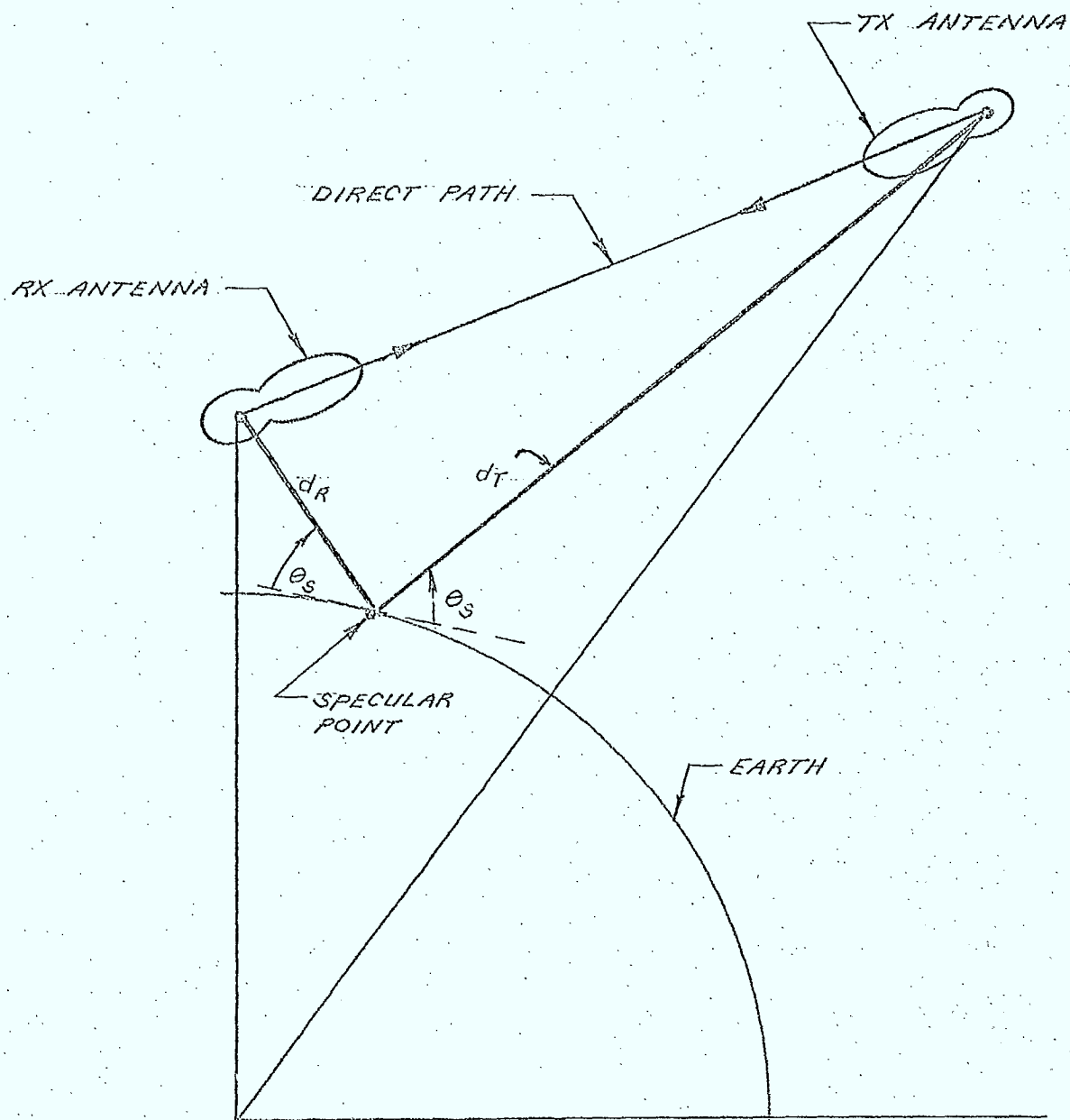


FIG. 4.5/1 MULTIPATH GEOMETRY

The flux at the receiver, coming from the direction of the specular point is given by:

$$F_m = \left[\frac{P_T G_T A_T D P_0^2}{4\pi (d_T + d_R)^2} \right] \quad (4.5.1)$$

where P_T is the transmitter power.

The power actually accepted by the receiving antenna depends on its gain in the direction of the specular point, the wavelength, and on the polarization of the reflected signal. For a circularly polarized wave, the sense of polarization is changed upon reflection if the specular incidence angle, θ_S , is greater than the "Brewster" angle for the reflecting surface. (References 4.5/1, 4.5/2, 4.5/3). As surface roughness and other factors influence the polarization state of the reflected signal (Reference 4.5/4), a simple model is now proposed for use in the simulation.

An effective receiving antenna gain, G_R' , can be defined that takes into account the polarization of the transmitted signal, and whether or not the sense of polarization of the reflected signal has been reversed. Values for G_R' are listed in Table 4.5/1 for various RX and TX antenna polarizations. In terms of G_R' , the path loss for the multipath power is given by:

$$L_m = \frac{G_T G_R' A_T D P_0^2 \lambda^2}{[4\pi (d_T + d_R)]^2} \quad (4.5.2)$$

The reflection coefficient, P_0 , depends on the polarization of the transmitted signal, and on the complex dielectric constant of the reflecting surface. In terms of P_V and P_H , the amplitudes of the reflection coefficients for vertically and horizontally polarized signals, P_0 is given by (Reference 4.5/4):

$$P_0 = \begin{cases} P_V ; & \text{vertical polarization} \\ P_H ; & \text{horizontal polarization} \\ \frac{1}{2} (P_V^2 + P_H^2 + 2P_V P_H)^{\frac{1}{2}} ; & \text{circular polarization} \end{cases} \quad (4.5.3)$$

TABLE 4.5/1

Effective RX Antenna Gain For
Multipath Interference Calculations

TX Polarization	RX Polarization	Effective RX Gain, G_R
Vertical	Vertical	G_P
	Horizontal	G_C
	Circular	$.5 G_P$
Horizontal	Vertical	G_C
	Horizontal	G_P
	Circular	$.5 G_P$
Right Hand Circular (no reversal)	linear	$.5 G_P$
	right circular	G_P
	left circular	G_C
Right Hand Circular (sense reversal)	linear	$.5 G_P$
	right circular	G_C
	left circular	G_P
Left Hand Circular (no reversal)	linear	$.5 G_P$
	right circular	G_C
	left circular	G_P
Left Hand Circular (sense reversal)	linear	$.5 G_P$
	right circular	G_P
	left circular	G_C

The term for circular polarization is a maximum since the product $\rho_v \rho_h$ does not include the phase angles of the reflection coefficients or those of the antennae.

4.5.3 Fresnel Reflection Coefficients ρ_v, ρ_h

The coefficients ρ_v and ρ_h for a plane surface are dependent on a number of factors including:

- incidence angle at the specular point (θ_s)
- operating frequency, f
- permittivity of the reflecting surface, ϵ
- conductivity of the reflecting surface, σ

From Reference 4.5/3, the coefficients ρ_v and ρ_h can be obtained from the Fresnel reflection coefficients expressed as:

$$\rho_v e^{i\delta_v} = \frac{(\epsilon - \frac{i4\pi\sigma}{\omega}) \sin \theta_s - \sqrt{(\epsilon - \frac{i4\pi\sigma}{\omega}) - \cos^2 \theta_s}}{(\epsilon - \frac{i4\pi\sigma}{\omega}) \sin \theta_s + \sqrt{(\epsilon - \frac{i4\pi\sigma}{\omega}) - \cos^2 \theta_s}} \quad (4.5.4)$$

$$\rho_h e^{i\delta_h} = \frac{\sin \theta_s - \sqrt{(\epsilon - \frac{i4\pi\sigma}{\omega}) - \cos^2 \theta_s}}{\sin \theta_s + \sqrt{(\epsilon - \frac{i4\pi\sigma}{\omega}) - \cos^2 \theta_s}} \quad (4.5.5)$$

where δ_v and δ_h are the phase angles of the reflection coefficients and ω is the angular frequency. (Note: ϵ and σ are in cgs units). Typical values for ϵ and σ are given in Table 4.5/2.

TABLE 4.5/2

Typical Values For ϵ and σ (cgs units)

Type of Surface	ϵ	$\sigma \times 10^6$
Sand	2 - 5	2 - 20
Dry Land	5 - 10	20 - 40
Moist Soil	10 - 30	20 - 6000
Fresh Water	80	20 - 100
Sea Water	60 - 80	10000 - 60000 *

* conductivity decreases very rapidly from UHF to ≈ 2 GHz.

Equation 4.5.4 can be rearranged to yield:

$$P_v = \frac{\sqrt{A_v^2 + B_v^2}}{\sqrt{D_v^2 + C_v^2}}$$

$$S_v = \tan^{-1}\left(\frac{D_v}{C_v}\right) - \tan^{-1}\left(\frac{B_v}{A_v}\right)$$

(4.5.6)

$$A_v = E \sin \theta_s - \cos\left(\frac{\tan^{-1}(K/a)}{2}\right) d$$

$$B_v = K \sin \theta_s - \sin\left(\frac{\tan^{-1}(K/a)}{2}\right) d$$

$$C_v = E \sin \theta_s + \cos\left(\frac{\tan^{-1}(K/a)}{2}\right) d$$

$$D_v = K \sin \theta_s + \sin\left(\frac{\tan^{-1}(K/a)}{2}\right) d$$

$$d = (a^2 + K^2)^{1/4}$$

$$a = E - \cos^2 \theta_s$$

$$K = 20 \times 10^{-6} / f_{\text{MHz}}$$

where f_{MHz} is the frequency in MHz.

Equation 4.5.5 can be rearranged to yield:

$$P_h = \frac{\sqrt{A_h^2 + B_h^2}}{\sqrt{C_h^2 + B_h^2}} \quad (4.5.7)$$

$$S_h = \tan^{-1}\left(\frac{B_h}{A_h}\right) - \tan^{-1}\left(\frac{B_h}{C_h}\right)$$

$$A_h = \sin \theta_s - \cos\left(\frac{\tan^{-1}(K/a)}{2}\right) d$$

$$B_h = \sin\left(\frac{\tan^{-1}(K/a)}{2}\right) d$$

$$C_h = \sin \theta_s + \cos\left(\frac{\tan^{-1}(K/a)}{2}\right) d$$

where a , k , and d are defined in equation 4.5.6. These coefficients and phase angles are illustrated in Figure 4.5/2 for several reflecting surfaces.

The Brewster angle, which is usually used to determine whether or not the sense of polarization of a circularly polarized wave reverses can only be evaluated when the conductivity is zero. For non-zero conductivities, the sense reversal is only an approximation. For simulation purposes, it will be assumed that the sense of polarization changes whenever δ_v , the phase angle of the vertical polarization reflection coefficient is greater than 90 degrees.

Fig. 29.4. Modulus and phase of the Fresnel reflection coefficients (solid curves, ρ_p and δ_p ; dot-dash curves, ρ_s and δ_s) as functions of the angle ψ for a land surface ($\epsilon = 4$, $\sigma = 9 \cdot 10^7$).

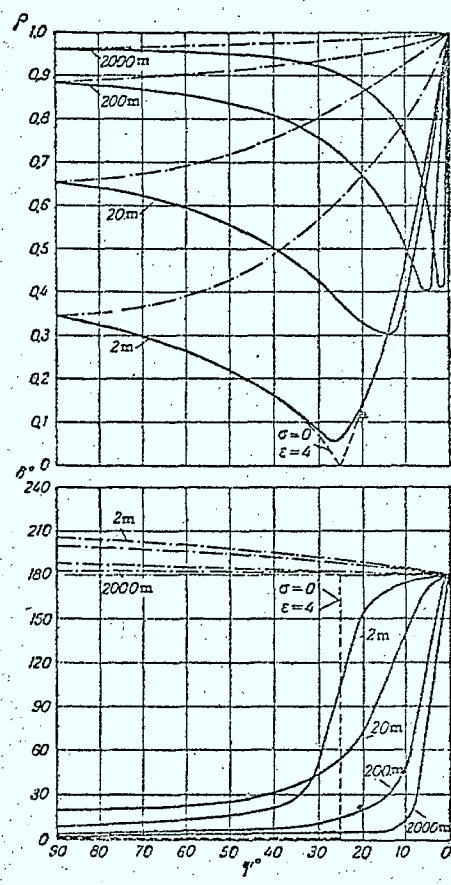


Fig. 29.5. Modulus and phase of the Fresnel reflection coefficients (solid curves, ρ_p and δ_p ; dot-dash curves, ρ_s and δ_s) as functions of the angle ψ for a sea surface ($\epsilon = 80$, $\sigma = 3.6 \cdot 10^{10}$).

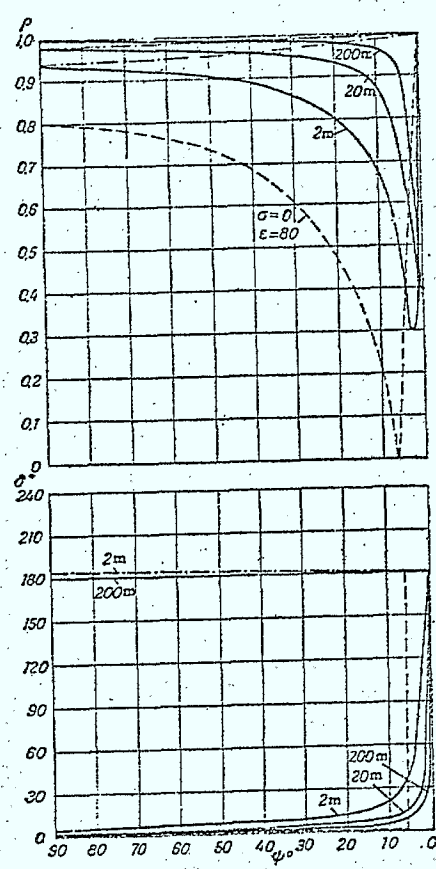
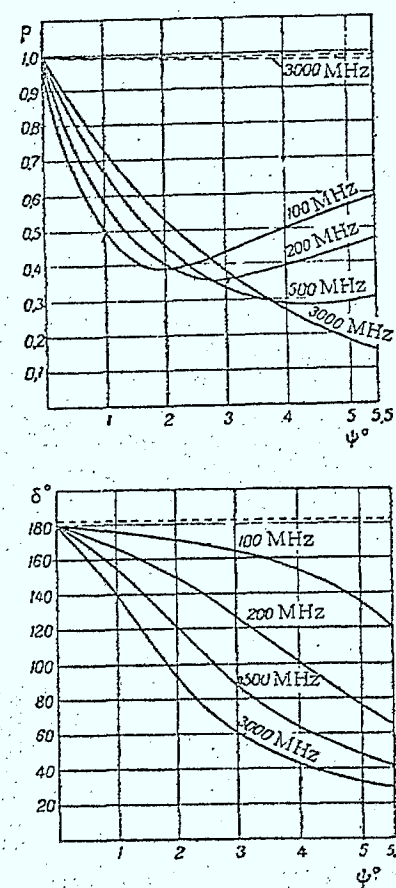


Fig. 29.6. Modulus and phase of the Fresnel reflection coefficients (solid curves, vertical polarization; dashed lines, horizontal polarization) as functions of the angle ψ for a sea surface at selected frequencies in the microwave range.



4.5.4 Diffuse and Specular Components

The diffuse and specular components of the received multipath power can be estimated as follows (Reference 4.5/1, 4.5/5). If Δh is the rms surface roughness, then the path loss for the specular component is given by:

$$L_{sp} = L_m e^{-16\pi^2 \left(\frac{\Delta h}{\lambda} \sin \theta_s \right)^2} \quad (4.5.8)$$

The sum of the diffuse and specular powers is approximately constant for all expected surface roughnesses (Reference 4.5.4) so:

$$L_{DIFF} = L_m \left(1 - e^{-16\pi^2 \left[\frac{\Delta h}{\lambda} \sin \theta_s \right]^2} \right) \quad (4.5.9)$$

Typical values for the rms surface roughness range from 0 (calm sea) to approximately 3 to 4 meters for very rough seas. Over land, values on the order of one meter are appropriate.

4.5.5 Doppler Spread

The performance of many data modems used in mobile communications systems is dependent on the Doppler spread of the multipath signal (Reference 4.5/1, 4.5/2, and Section 4.8). This Doppler spread, B_{DOP} , can be estimated from the velocity of the mobile station relative to the satellite, v , (or non-mobile terminal) from (References 4.5/2 and 4.5/3):

$$B_{DOP} = \frac{4 \alpha v \sin \theta_s}{\lambda} \quad (4.5.10)$$

where α is the rms surface slope. This parameter is related to the ratio of the rms surface height fluctuations-to-the spatial correlation length of surface height fluctuations. In the case of a sea surface, typical values of α range from 0.1 for a wind speed of 10 knots to 0.12 at 20 knots (Reference 4.5/5).

4.5.6 Implementation of the Multipath Model (MLTINT)

Purpose

This routine is used to calculate the diffuse and specular path losses (L_{sp} , L_{diff}) and the Doppler spread on paths involving ships or aircraft and satellites.

Description

The implementation of the multipath interference model discussed in Sections 4.5.1 to 4.5.5 is illustrated in Figure 4.5/3. The routine makes use of subroutine SPGEOM (see section 4.2) to calculate the geometric parameters required in the calculations as well as other geometry and antenna gain subroutines to determine the gains of the RX and TX antennae in the direction of the specular point. The reflection coefficient model and the effective RX antenna gain model are implemented as separate subroutines.

Inputs

- ◉ type of TX site
- ◉ type of RX site
- ◉ transmitter location and antenna parameters
- ◉ receiver location and antenna parameters
- ◉ frequency
- ◉ multipath report instructions

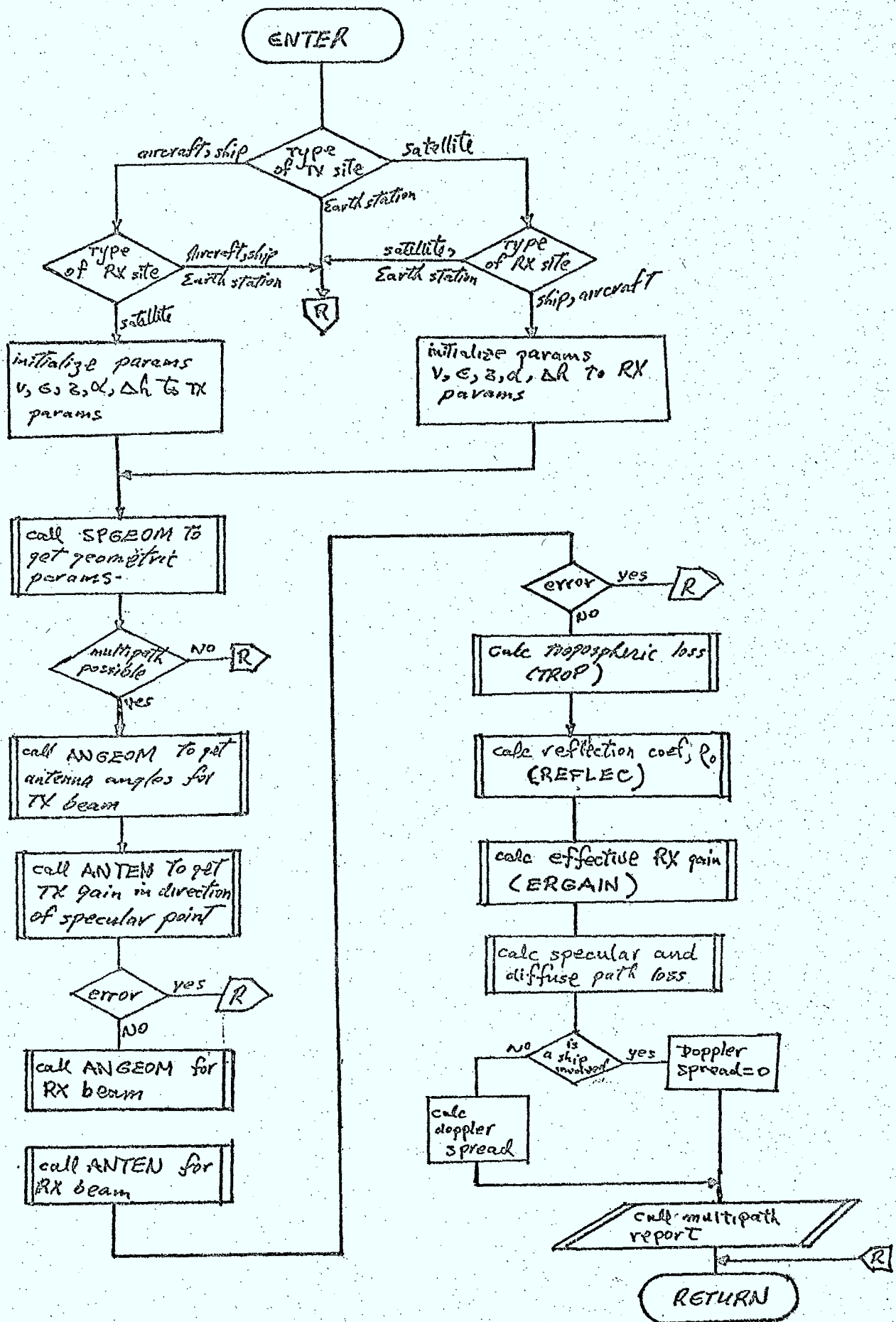
Outputs

- ◉ Doppler spread
- ◉ path loss for diffuse multipath, L_{diff}
- ◉ path loss for specular multipath, L_{spec}
- ◉ flag indicating whether or not multipath is involved

Reports

- ◉ prints detailed multipath interference report

Figure 4.5/3 Flowchart of MLTINT



4.5.7 Reflection Coefficient Routine (REFLEC)

Purpose

This routine is used to calculate the reflection coefficient, ρ_0 , for use in multipath interference calculations.

Description

The coefficient is calculated using equations 4.3.5, 4.5.6, and 4.5.7. The implementation is illustrated in Figure 4.5/4.

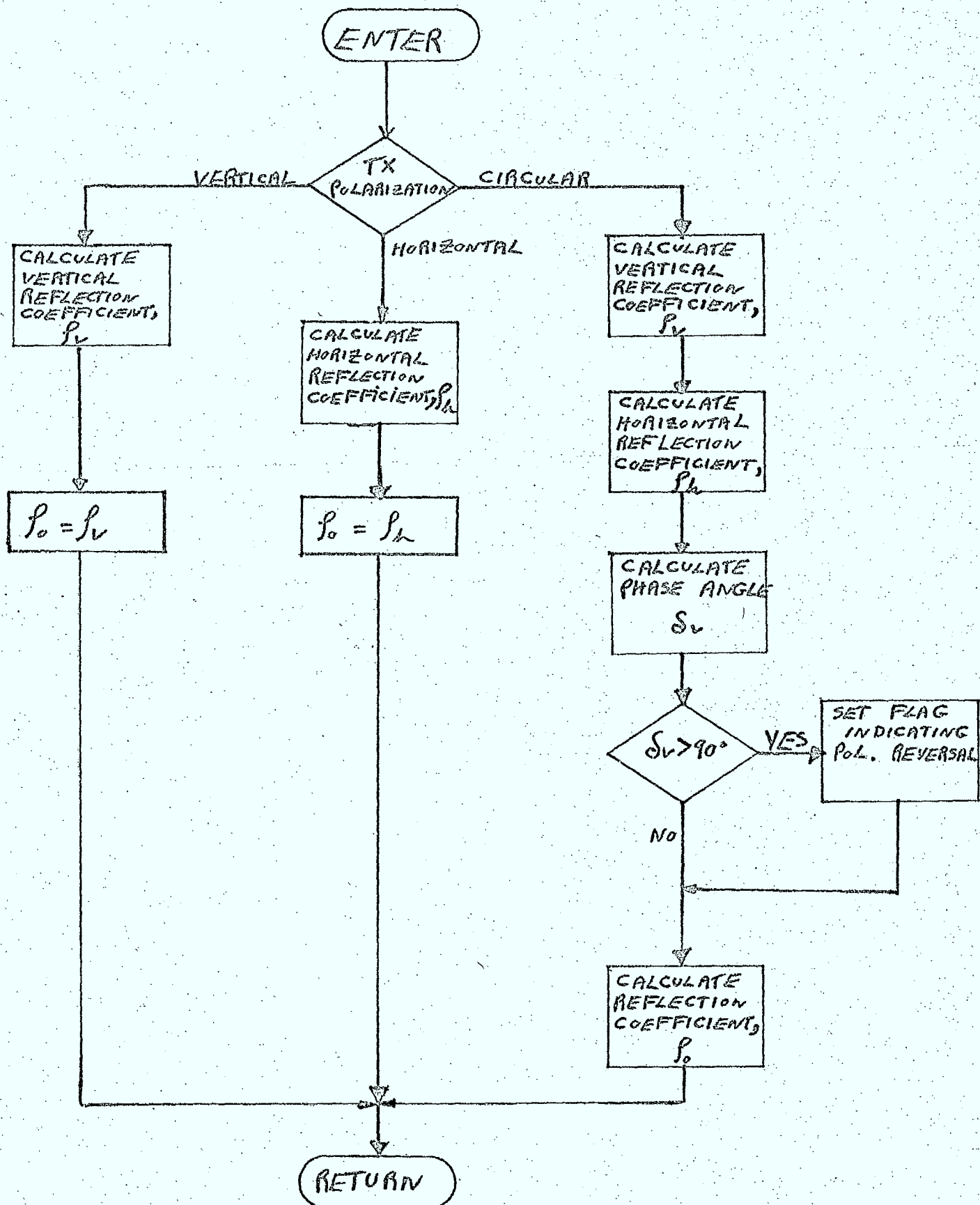
Inputs

- transmitter polarization
- incidence angle at specular point, θ_s
- frequency, f
- permittivity of surface, ϵ
- conductivity of surface, σ

Outputs

- reflection coefficient, ρ_0
- flag indicating whether or not circularly polarized signal will change sense of polarization upon reflection

Figure 4.5/4 Flowchart of REFLEC



4.5.8 Effective RX Antenna Gain Calculation (ERGAIN)Purpose

This routine is used to calculate the effective gain of a receiving antenna for use in multipath interference calculations.

Description

The effective gain is calculated from the values given in Table 4.5/1.

Inputs

- TX antenna polarization type
- RX antenna polarization type
- principal polarization gain of RX antenna in direction of the specular point, G_p
- cross polarization gain of the RX antenna in the direction of the specular point
- flag indicating whether or not polarization sense has reversed on reflection for circularly polarized signals

Outputs

- effective RX antenna gain

References

- 4.5/1: C.C.I.R. Report 501-1, "Technical Characteristics of Systems Providing Communications and/or Radio Determination Using Satellite Techniques for Aircraft and/or Ships", 1974.
- 4.5/2: I.L. Lebow, et. al., "Satellite Communications to Mobile Platforms", Proc. IEEE, Vol. 59, No. 2, February 1971.
- 4.5/3: Y.L. Al' Pert, "Radio Wave Propagation and the Ionosphere", Vol. 2, "Propagation of Electromagnetic Waves Near the Earth", Consultants Bureau, New York, 1974.
- 4.5/4: I. Katz, "Radar Reflectivity of the Ocean Surface for Circular Polarization", IEEE, Trans. Ant. Prop., 1963.
- 4.5/5: P.A. Bello, "Aeronautical Channel Characterization", IEEE, Trans. Comm. Vol. Com-21, pp 548-563, May 1973.

4.6 Baseband Signal Processing Models

This section describes the models required to simulate the baseband signal processing used in link calculations, for the following types of signals:

- o random binary digital data
- o analog voice signals

The types of baseband signal processing included in the simulation are:

- o Delta modulation coding and decoding of analog voice signals
- o Forward Error Correction (FEC) coding and decoding of digital signals
- o Companding of analog voice signals
- o Pre-emphasis and De-emphasis of analog voice signals

4.6.1 Delta Modulation Coding and Decoding of Analog Voice Signals

4.6.1.1 General

The Delta modulation encoder is characterized as a device with an output bit rate, R_0 , that is input by the user and stored in the ISI transmitter carrier record. It is assumed that the digital signal has the same characteristics as a binary data baseband.

The Delta modulation decoder is simulated as a separate subroutine (subroutine DLTDEC).

4.6.1.2 Delta Modulation Decoding Subroutine (DLTDEC)

Purpose: This routine calculates the signal quality (expressed as a test tone signal-to-noise ratio) at the output of a Delta modulation decoder.

Description: The Delta modulation decoder is modelled as a device which outputs an analog voice signal with the same power and bandwidth as the signal input to the decoder. Degradation in the resultant analog voice is due to several sources:

- o quantization noise of the coder-decoder system
- o bit errors resulting from demodulation of the RF carrier contaminated by RF interference, thermal noise, and distortion
- o baseband noise accompanying the voice signal that was input to the Delta modulation encoder.

It is assumed that the coder-decoder system has been designed so that signal degradation due to slope overload effects is negligible.

The signal-to-noise ratio due to quantization, $(S/N)_T$, is a function of the type of Delta modulation used (linear or adaptive, for example) and depends on design details (number of integrators used or integrator time constants, for example) (Reference 4.6/1, 4.6/2). As modelling such details is beyond the scope of this work, a simple method of handling these effects is recommended. As the quantization noise is independent of degradations introduced by the communications channel, a constant value, input by the user, will be used.

The signal to noise ratio due to channel bit errors, $(S/N)_B$, for linear Delta modulation is given by (Reference 4.6/3, 4.6/4):

$$\left(\frac{S}{N}\right)_B = \frac{K}{P_E} \quad (4.6.1)$$

where P_E is the bit error probability at the input to the decoder and K is a proportionality constant dependent of design parameters of the decoder.

For adaptive Delta modulation systems, it is assumed that equation (4.6.1) represents a lower bound for $\left(\frac{S}{N}\right)_B$.

Again, to allow the user to characterize the decoder, without knowledge of decoder design details, the user inputs the bit error probability, P_1 , which causes a 3dB drop in signal-to-noise ratio relative to the quantization signal-to-noise ratio (see Figure 4.6/1). At P_1 :

$$\left(\frac{S}{N}\right)_B = \left(\frac{S}{N}\right)_T = \frac{K}{P_1} \quad (4.6.2)$$

where K can now be computed and used to evaluate the signal to noise ratio due to channel bit errors from equation (4.6.1).

The total signal to noise ratio due to quantization and bit errors is given by:

$$\left(\frac{S}{N}\right)_S = \frac{1}{\left(\frac{N}{S}\right)_T + \left(\frac{N}{S}\right)_B} \quad (4.6.3)$$

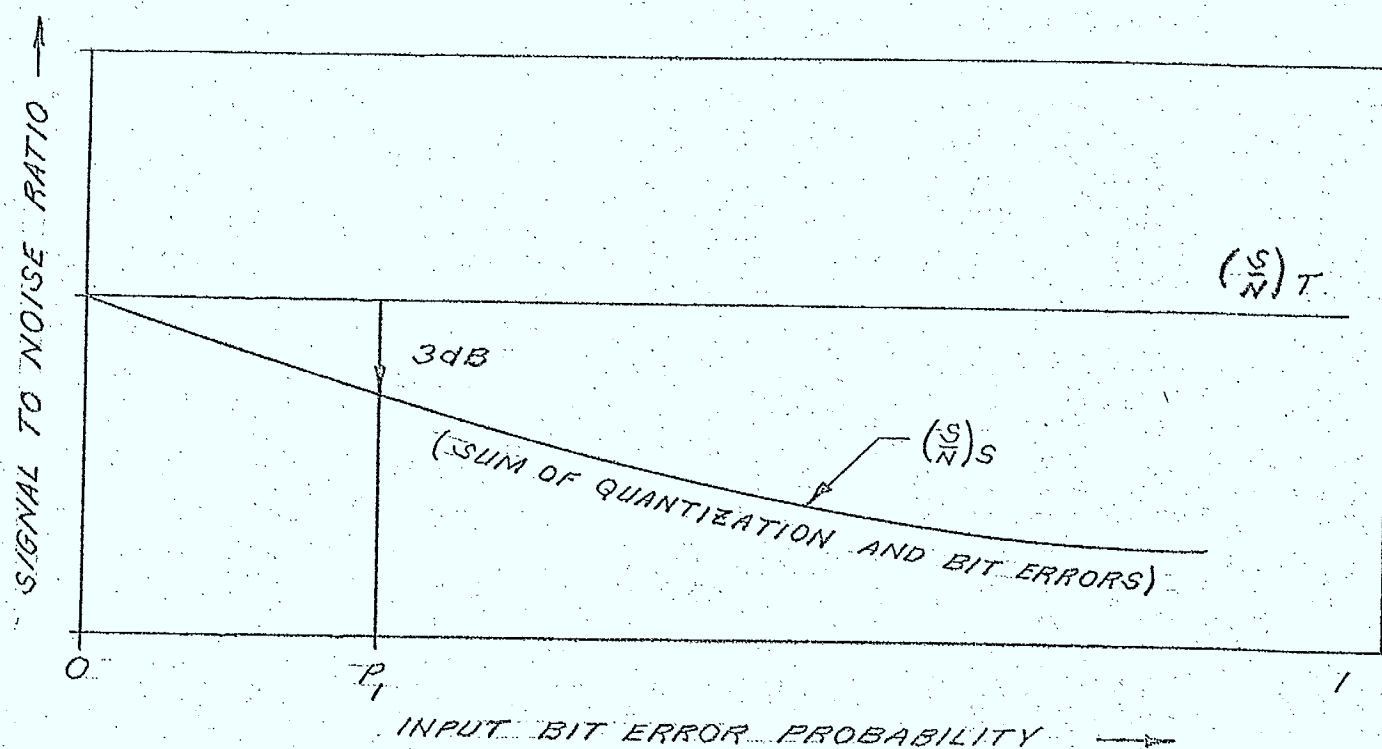


FIG. 4.6/1 CHARACTERIZATION OF DELTA MODULATION
SIGNAL TO NOISE RATIO DUE TO CHANNEL
BIT ERRORS.

The total signal to noise ratio at the output of the Delta modulation decoder is given by:

$$\left(\frac{S}{N}\right)_{\text{ToT}} = \frac{1}{\left(\frac{N}{S}\right)_S + \left(\frac{N}{S}\right)_i} \quad (4.6.4)$$

where $\left(\frac{N}{S}\right)_i$ is derived from the signal to noise ratio at the input to the Delta modulation encoder.

A general flowchart for this subroutine is shown in Figure 4.6/2.

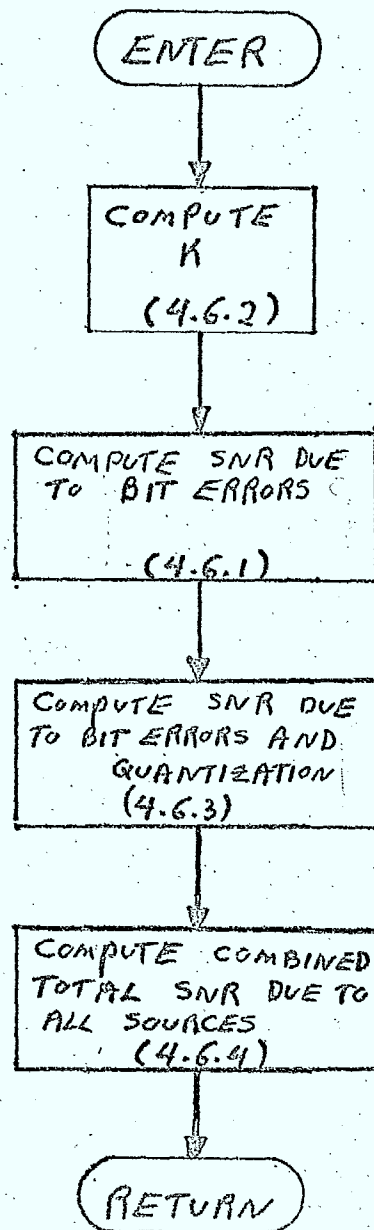
Inputs

- o $\left(\frac{S}{N}\right)_T$ - the quantization unweighted test tone signal-to-noise ratio. The default value of $\left(\frac{S}{N}\right)_T$ is chosen as 55 dB (computed from reference 4.6/1 for a typical case).
- o P_1 - the bit error probability (at the input to the decoder) which causes a 3dB drop in the output signal to noise ratio. The default value is chosen as 0.5×10^{-3} from reference 4.6/1.
- o P_E - the bit error probability at the input to the Delta modulation decoder.
- o $\left(\frac{S}{N}\right)_i$ - the signal to noise ratio at the input to the Delta modulation encoder.

Outputs

- o $\left(\frac{S}{N}\right)_{\text{ToT}}$ - the signal to noise ratio at the output of the Delta modulation decoder due to quantization noise, bit errors in the channel and the initial signal to noise ratio at the input to the encoder (from previous hops).

Figure 4.6/2 Flowchart of DLTDEC



4.6.2 Forward Error Correction (FEC) Coding and Decoding of Digital Signals

4.6.2.1 General

The FEC encoder is characterized as a device with an output bit rate, R_o , given by:

$$R_o = \frac{R_i}{r} \quad (4.6.5)$$

where, R_i is the input bit rate, and r is the code rate.
 r is given by:

$$r = \frac{k}{n+k} \quad (4.6.6)$$

where k is the number of information bits and n is the number of redundant bits in a given constraint length (convolutional codes) or block length (block codes).

The code rate, r , is stored in the ISI transmitter carrier record and used to modify the bit rate according to equation 4.6.5.

The FEC decoder is modelled as a separate subroutine (subroutine FECDEC). Two models are available for the decoder bit error probability input/output transfer function. The first model, which is valid when channel bit errors are independent of each other, is an analytical model used to estimate the performance of a variety of standard coding schemes. The second model is a parametric model which allows the user to specify the input/output decoder transfer characteristic.

4.6.2.2 FEC Decoding Subroutine (FECDEC)

Purpose: This routine calculates the bit error probability and the bit rate at the output of a FEC decoder.

Description: The binary FEC decoder is modelled as a device which outputs a bit stream at rate R_o , with bit error probability P_o .
 R_o is given by:

$$R_o = rR_i \quad (4.6.7)$$

where r is the code rate defined by equation (4.6.6) and R_i is the bit rate into the FEC decoder.

Analytical Model:

In addition to r , the "analytical" FEC decoder is characterized by the following parameters (Reference 4.6/6):

- N - the total number of information and redundant bits in a coded sequence length. This is referred to as the constraint length (convolutional codes) or block length (block codes).
- e - the error correction capability of the code. This is the number of bit errors in a given constraint length or block length that can be corrected by the decoder.

The error correction capability is frequently written in terms of the code minimum distance by:

$$e = \frac{d}{2} - 1 \quad ; d \text{ even} \quad (4.6.8)$$

or

$$e = \frac{d-1}{2} \quad ; d \text{ odd} \quad (4.6.9)$$

where d is the minimum number of bits that will be different between any two coded words.

If it is assumed that channel bit errors are independent, the relationship between the bit error probability, P_o , at the output of the FEC decoder and the bit error probability, P_i , at the input of the decoder is given by (from Reference 4.6/6):

$$P_o \leq \frac{d}{2N} \left(\frac{N}{\frac{d}{2}} \right) P_i^{d/2} \quad ; d \text{ even} \quad (4.6.10)$$

$$P_o \leq \left[\frac{\delta d + (1-\delta) \left(\frac{d+1}{2} \right)}{N} \right] \left(\frac{N}{\frac{d+1}{2}} \right) P_i^{\frac{d+1}{2}} \quad ; d \text{ odd} \quad (4.6.11)$$

where δ is related to the number of code words of minimum distance d , and is generally not easily obtainable.

However, it is pointed out in Reference 4.6/6 that setting $\delta=1$ in equation (4.6.11) only slightly weakens the accuracy. Thus equation

(4.6.11) becomes:

$$P_o \leq \frac{d}{N} \left(\frac{N}{\frac{d+1}{2}} \right) P_i^{\frac{d+1}{2}} \quad ; d \text{ odd} \quad (4.6.12)$$

For simulation purposes, strict equality is used in the above expressions to estimate an upper bound on P_o .

Equation (4.6.12) is plotted in Figure 4.6/3 along with measured data for the SPADE CODEC employing convolutional error correction (Reference 4.6/5).

In deriving equations (4.6.10) and (4.6.11) it is assumed that $NP_i < 1$. Thus, these equations break down at large P_i . In the simulation, a threshold value for P_i is specified above which the channel is declared unusable and the link computation terminates.

Parametric Model

To allow the user to specify P_o as a function of P_i directly when measured decoder characteristics are available, the parametric model can be used. The decoder output bit error probability is approximated as:

$$P_o = KP_i^{\lambda} \quad (4.6.13)$$

where K is a proportionality constant and λ is some power of P_i . This equation can be written as:

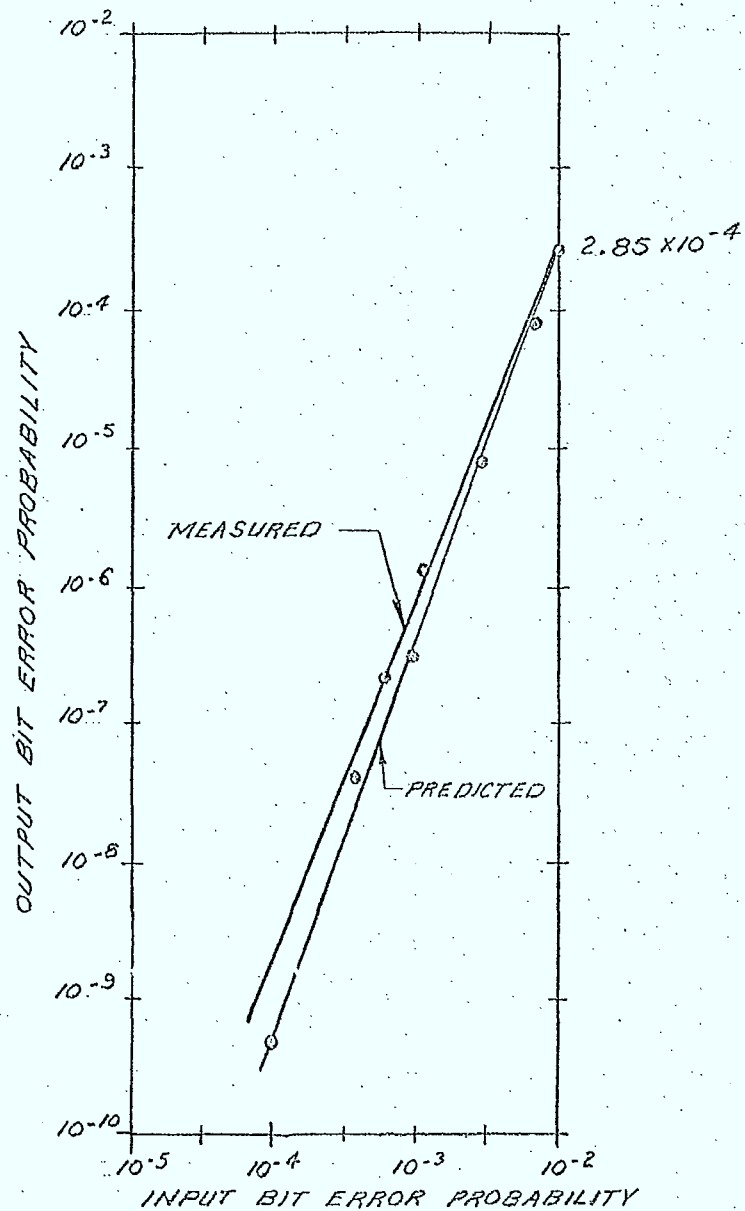
$$\log_{10} P_o = \lambda \log_{10} P_i + \log_{10} K \quad (4.6.14)$$

Figure 4.6/4 is a sketch showing how curves derived from equation (4.6.14) for fixed K , variable λ ; and for fixed λ , variable K , would appear.

Given a decoder transfer curve of some type similar to the one shown in Figure 4.6/4, the user specifies $(P_o^1, P_i^1)_2$; $(P_o^2, P_i^2)_2$ for two separated points on the curve. From this data, equation (4.6.14) can be solved simultaneously for K and λ and used to calculate P_o for any value of the input error probability.

A threshold value for P_i is also specified for this model, above which the channel is declared unusable.

A general flowchart for this subroutine is shown in Figure 4.6/5.

NOTE:

FOR SPADE CODEC: -N = 20 (HIGHEST ORDER IN GENERATOR POLYNOMIAL + 1)

-R = 3/4

-d = 5

FIG: 4.6/3 COMPARISON OF PREDICTED ERROR TRANSFER CHARACTERISTICS TO ACTUAL MEASUREMENTS

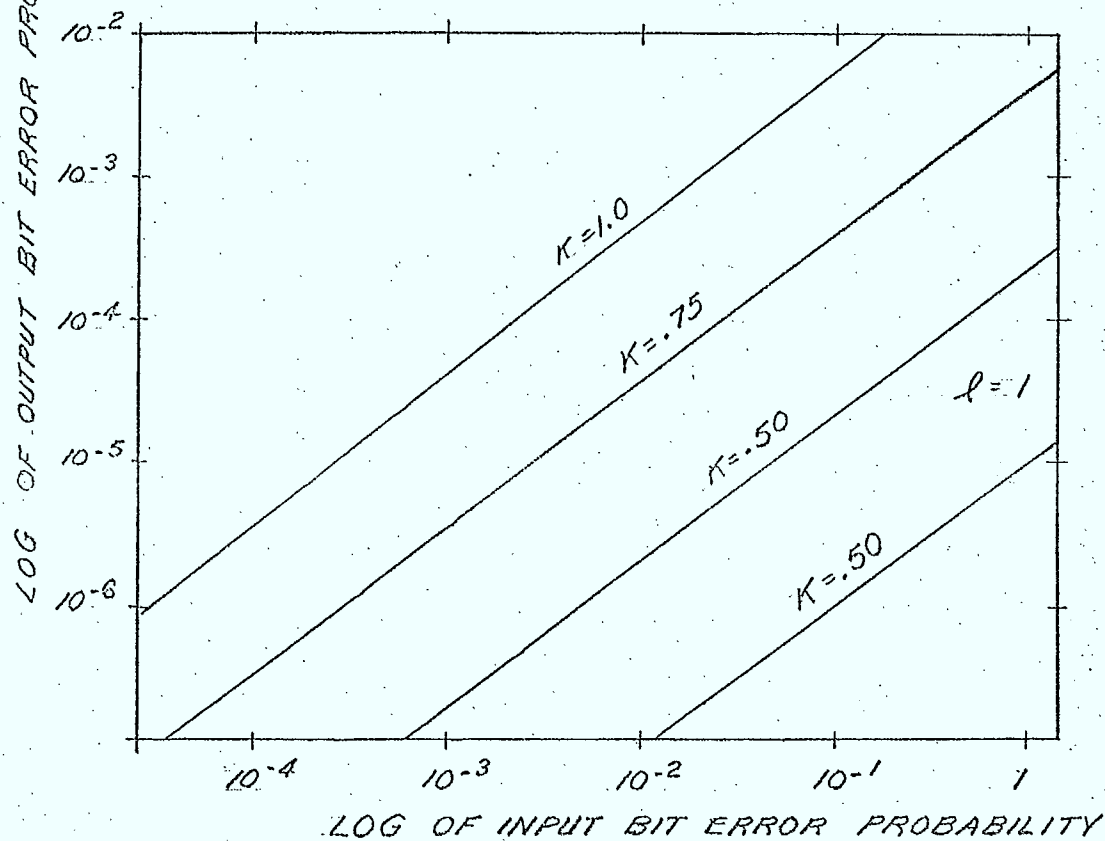
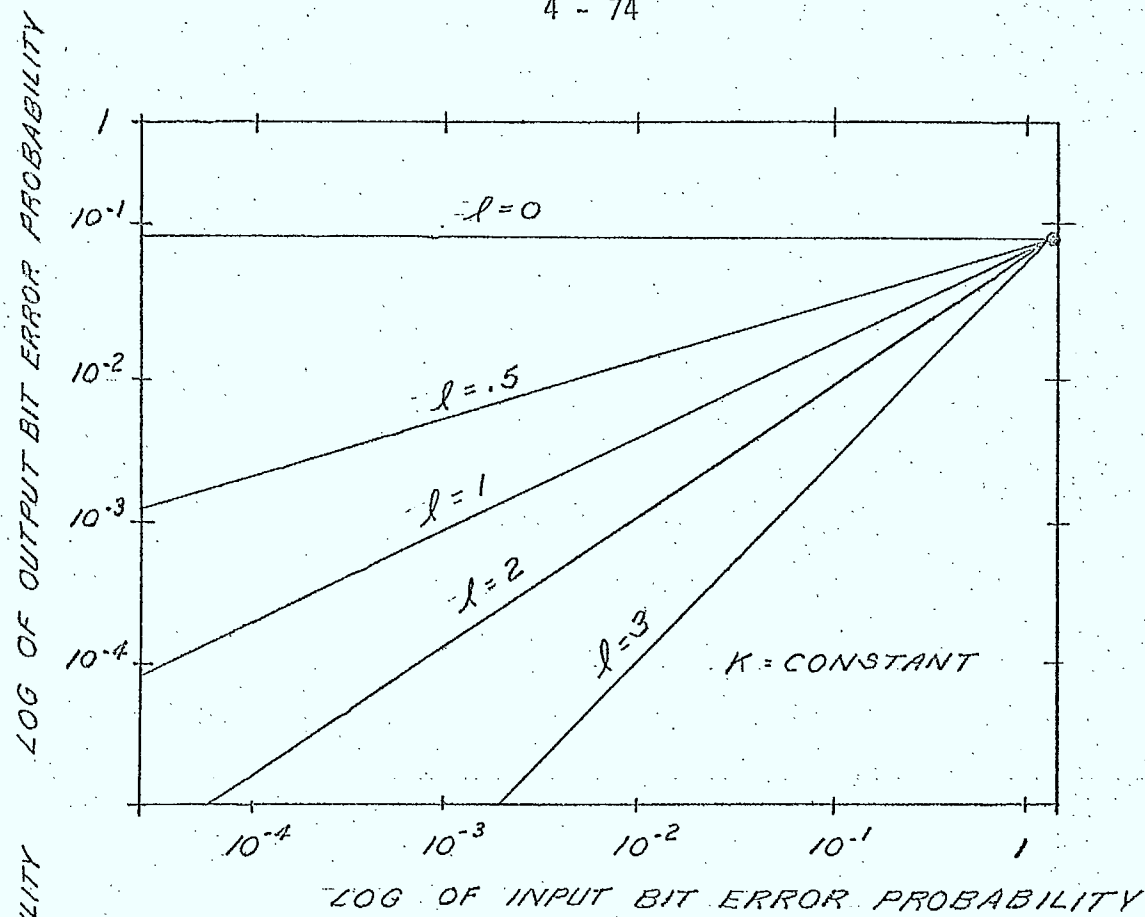
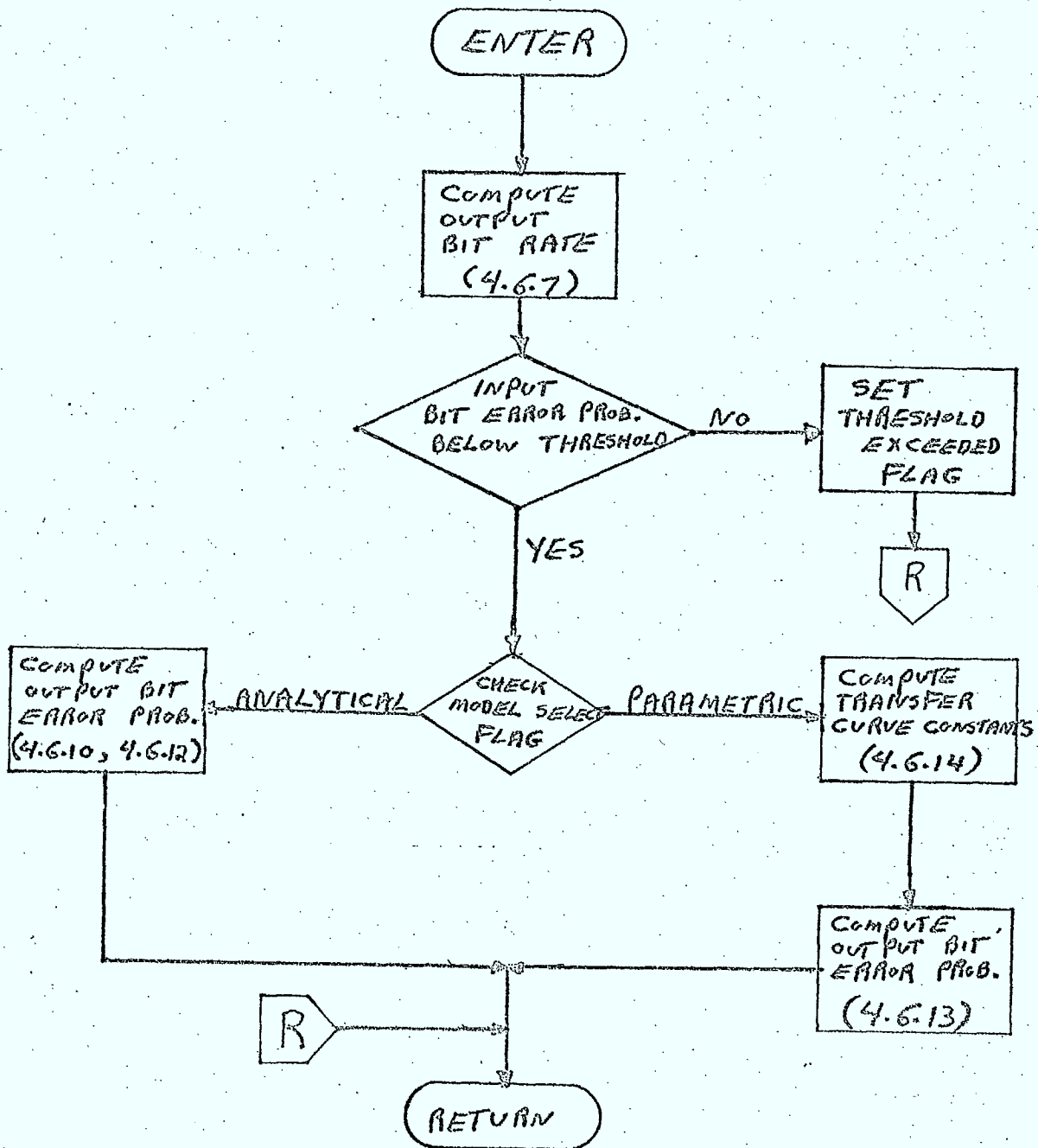


FIG. 4.6/4 P_o / P_i TRANSFER CURVES FOR PARAMETRIC
FEC DECODER MODEL

Figure 4.6/5 Flowchart of FECDEC



Inputs

- o r - the code rate used to compute the output bit rate. The default value is chosen as 3/4 (from Reference 4.6/5 for the SPADE CODEC)
- o - flag selecting bit error probability transfer curve:
 - o user specified curve
 - o simulation model
- o P_i - the bit error probability at the input to the FEC decoder
- o R_i - the bit rate at the input to the FEC decoder
- o N - the constraint length or block length of the code. The default value is chosen as 20 (Reference 4.6/5)
- o e - the error correction capability of the code (defaults to 2) (Reference 4.6/5)
- o P_T - the threshold bit error probability at an input to the decoder, above which the channel is declared unusable (default value is 10^{-2})
- o $(P_o', P_i')_1; (P_o', P_i')_2$ - the parameters representing the input-output bit error probability transfer characteristic defined by two separated points on the transfer curve. P_o' is the error probability after correction; P_i' is the error probability before correction.

Outputs

- o R_o - the bit rate at the output of the FEC decoder
- o P_o - the bit error probability at the output of the FEC decoder
- o - flag indicating whether or not decoder below threshold

4.6.3 Companding of Analog Voice Signals

The effectiveness of compressing the analog message power range at the transmitter and complementary expansion at the receiver (referred to as companding), is frequently measured in terms of an improvement factor or noise reduction factor. The noise reduction factor is a function of the compressor characteristics and average speech power (Reference 4.6/7). As modelling such details is beyond the scope of this work, the companding improvement factor is specified directly in the ISI receiver carrier record. A default value of 18.8dB reported in Reference 4.6/8 will be used. This improvement is only applied to the signal-to-noise ratio if the SNR at the compander input is greater than the threshold level for the device.

The use of companding will alter the voice signal into the FM modulator, and thereby modify the shape of the transmitted spectrum. This effect is modelled in an approximate fashion by assuming that the compressor alters the peak-to-average power ratio of the baseband voice signal, Δ_B , into the modulator. A default value of 8dB will be used (Reference 4.6/9); for no companding a default of 12dB is used.

4.6.4 Pre-emphasis and De-emphasis Models

For simulation purposes, pre-emphasis is modelled by a power transfer characteristic,

$$G_p(f) = \begin{cases} af^2 & , f_l < f < f_m \\ 0 & , \text{elsewhere} \end{cases} \quad (4.6.15)$$

that reshapes the baseband voice spectrum at the input to the FM modulator. The combined effect of pre-emphasis and de-emphasis is modelled by an improvement factor that is applied to the signal-to-noise ratio at the receiver. A default value for this improvement factor of 6dB will be used unless overridden by the user.

References

- 4.6/1: Lindholm, C.R., "Multiple Access Techniques for Communication Satellites: Digital Modulation, Time-Division Multiplexing, and Related Signal Processing", The Rand Corporation, RM-4997-NASA, September 1966.
- 4.6/2: Tomozawa, A. and Kaneko, H., "Companded Delta Modulation for Telephone Transmission", IEEE Transactions on Communication Technology, Vol. Com-16, No. 1, February 1968.
- 4.6/3: Campanella, S.J. and Sciulli, J.A.- "A Comparison of Voice Communication Techniques for Aeronautical and Marine Applications", Comsat Technical Review, Volume 2, Number 1, 1972.
- 4.6/4: Reinhart, E.E., "Radio Relay System Performance in an Interference Environment", The Rand Corporation, RM-5786-NASA, October 1968.
- 4.6/5: Wu, W.W., "New Convolutional Codes - Part 1", IEEE Transactions on Communications, Vol. Com-23, No. 9, September 1975.
- 4.6/6: Chase, D., "Digital Signal Design Concepts for a Time Varying Rician Channel", IEEE Transactions on Communications, Vol. Com-24, No. 2, February 1976.
- 4.6/7: Sunde, E.D., "Communications Systems Engineering Theory", John Wiley and Sons Inc., New York, 1969.
- 4.6/8: "UHF-SHF Satellite Communications Link Calculations", Bell-Northern Research, July, 1975, D.O.C..
- 4.6/9: C.C.I.R. Report 597, "Technical Characteristics of Systems Providing Communication and/or Radiodetermination using Satellite Techniques for Aircraft and/or Ships", 1974

4.7 RF Spectrum Models

4.7.1 General

In this section, models are presented for the following RF spectra:

- o FM single channel voice (with and without pre-emphasis and companding)
- o binary continuous phase FSK (including FFSK)
- o binary and M-ary PSK
- o FM/TV
- o Gaussian noise spectrum
- o band limited white noise spectrum
- o general RF spectrum model

These spectra are calculated across a predefined "simulation bandwidth" specified by a lower frequency, F_L , and an upper frequency F_M . The spectra are normalized such that their total power is 1 watt. Any portion of this may be contained within the simulation bandwidth, as illustrated in Figure 4.7/1.

4.7.2 FM Single Channel Voice (FMVOIC)

Purpose

This routine is used to calculate the normalized RF spectrum across the simulation bandwidth, of an FM carrier modulated by a voice signal.

Description

The RF spectrum at the output of an FM modulator is dependent on the statistics of the modulating signal, its bandwidth, and the modulation index. For rms modulation indices, β , greater than unity, the spectrum is approximately Gaussian in shape and will be modelled by the high-index FM spectrum model described in Section 6.2 of Reference 4.7/1. For rms modulation indices less than 1, the spectrum is much more complex. For simulation purposes, the voice signal will be modelled as a band of noise with a power spectrum, $W_{eB}(f)$, given by (Reference 4.7/2):

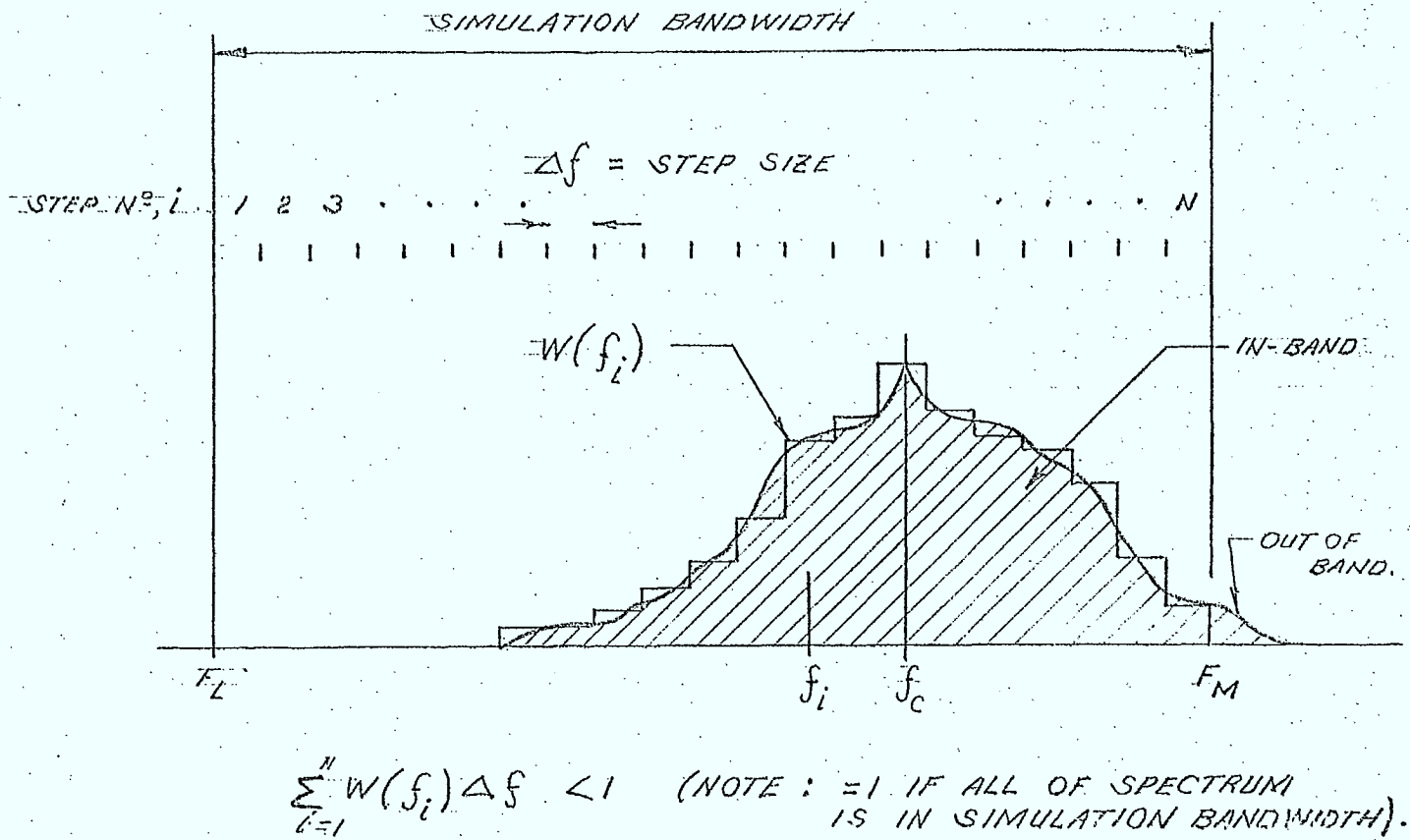


FIG: 4.7/1 : SIMULATION BANDWIDTH AND RF SPECTRA

$$W_{e_B}(f) = \begin{cases} 0 & , f < f_\ell \\ a_1 & , f_\ell < f < 500\text{Hz} \\ \frac{a_2}{f^2} & , 500\text{Hz} < f < 1500\text{Hz} \\ \frac{a_3}{f^4} & , 1500\text{Hz} < f < 2500\text{Hz} \\ 0 & , f > f_m \end{cases} \quad (4.7.1)$$

where a_1 , a_2 , and a_3 are constants, f_ℓ is the lower baseband frequency, and f_m is the highest baseband frequency. When preemphasis is used, this baseband spectrum is multiplied by the power transfer characteristic, $G_p(f)$, where

$$G_p(f) = \begin{cases} 0 & , f < f_\ell \\ bf^2 & , f_\ell < f < f_m \\ 0 & , f > f_m \end{cases} \quad (4.7.2)$$

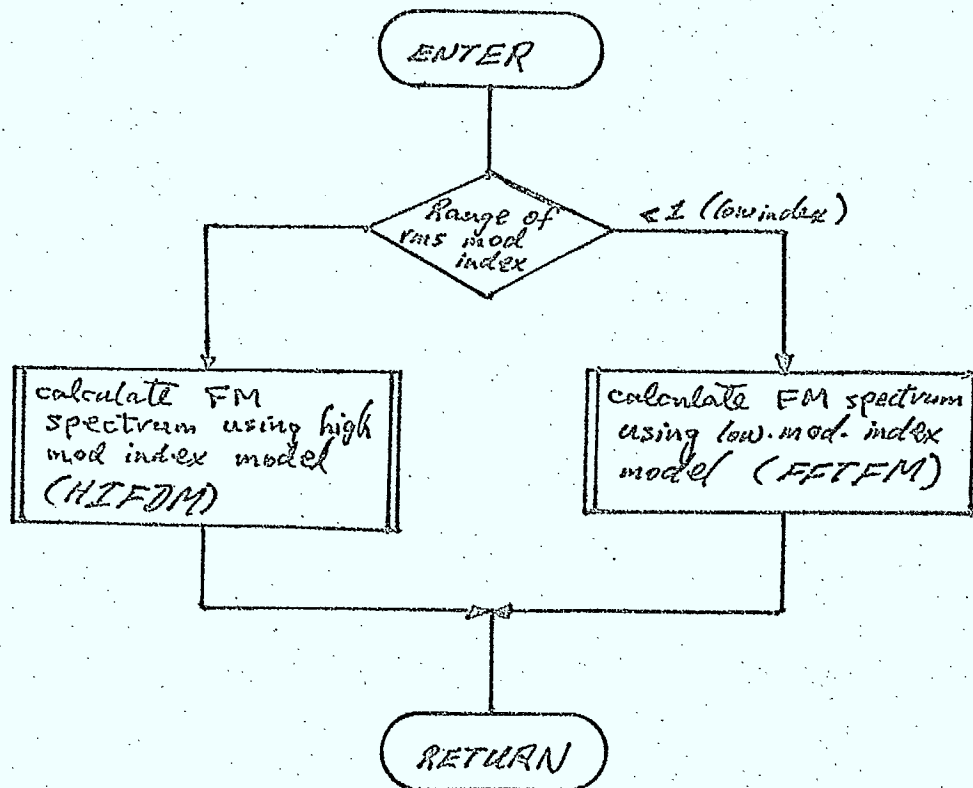
and b is a constant.

The RF spectrum at the output of the modulator can then be determined using the Fast Fourier Transform algorithm described in Section 6.2.2 of Reference 4.7/1. A flowchart of the FM voice spectrum model is illustrated in Figure 4.7/2.

Inputs

- o lower baseband frequency, f_ℓ
- o upper baseband frequency, f_m
- o rms modulation index, β
- o peak-to-average baseband power ratio, A_B
- o flag indicating whether or not pre-emphasis is used
- o carrier frequency, f_c
- o lower simulation frequency bound, F_L
- o upper simulation frequency bound, F_M
- o number of steps across simulation bandwidth, N
- o frequency step size across simulation bandwidth, Δf

Figure 4.7/2 Flowchart of FMVOIC



Outputs

o normalized RF spectrum across the simulation bandwidth, $W(f_i), i=1, \dots, N$

4.7.3 Binary FSK Model (FSKSPC)Purpose

This routine is used to calculate the normalized power spectrum across the simulation bandwidth, at the output of a binary continuous phase FSK modulator.

Description

The spectrum model is based on that described in Reference 4.7/3. The frequency modulating baseband is assumed to be a random sequence of binary pulses, each of duration T ($=1/\text{Bit Rate}$). The FSK modulator is characterized by the deviation ratio, D , defined as:

$$D = \frac{2\Delta f}{R_b} \quad (4.7.3)$$

where R_b is the bit rate and Δf is the difference between the two possible values of the instantaneous frequency. Fast Frequency Shift Keying (FFSK) is just binary FSK with a deviation ratio $D=0.5$.

From Reference 4.7/3, the normalized RF spectrum is given by:

$$W(f) = \begin{cases} \frac{4}{R_b} \left[\frac{D}{\pi(D^2 - X^2)} \right]^2 \frac{(\cos \pi D - \cos \pi X)^2}{(1 - 2\cos \pi D \cos \pi X + \cos^2 \pi D)} & , \begin{matrix} |\cos \pi D| \approx 1 \\ |D-X| > .01 \end{matrix} \\ \frac{1}{R_b} \left(\frac{D \sin \pi X}{X} \right)^2 \frac{1}{(1 - 2\cos \pi D \cos \pi X + \cos^2 \pi D)} & , \begin{matrix} |\cos \pi D| < 1, \\ |D-X| \leq .01 \end{matrix} \\ \frac{1}{4} \delta(X+D) + \frac{1}{4} \delta(X-D) + \frac{2}{R_b} \left[\frac{D}{\pi(D^2 - X^2)} \right]^2 (1 - \cos \pi D \cos \pi X) & , \begin{matrix} |\cos \pi D| = 1 \\ |D-X| \approx .01 \end{matrix} \\ \frac{1}{4} \delta(X+D) + \frac{1}{4} \delta(X-D) + \frac{D}{4R_b} & , \begin{matrix} |\cos \pi D| = 1 \\ |D-X| \approx .01 \end{matrix} \end{cases} \quad (4.7.4)$$

$$\text{where } X = \frac{2(f-f_c)}{R_b}$$

(4.7.5)

and f_c is the carrier frequency.

For deviation ratios equal to 1, 2, 3, ..., one-half of the carrier power is contained in two spectral lines, one on each side of the carrier frequency, while the other half of the power is contained in the continuous portion of the spectrum. For other deviation ratios, no spectral lines are present.

Inputs

- o bit rate into modulator, R_b
- o deviation ratio, D
- o carrier frequency, f_c
- o lower simulation frequency bound, F_L
- o upper simulation frequency bound, F_M
- o number of steps across the simulation bandwidth, N
- o frequency step size, Δf

Outputs

- o normalized RF spectrum across simulation bandwidth, $W(f_i)$, $i=1, \dots, N$.

4.7.4 PSK Spectrum Model (PSKSPC)

Purpose

This routine is used to calculate the normalized RF power spectrum across the simulation bandwidth due to binary or M-ary CPSK or DPSK modulated by a random bit sequence.

Description

The PSK spectrum model for rectangular input pulse shapes, described in Section 6.4.2 of Reference 4.7/1 will be used.

Inputs

- o bit rate, R_b
- o number of phases, M
- o carrier frequency, f_c
- o lower simulation frequency bound, F_L
- o upper simulation frequency bound, F_M
- o number of steps across simulation bandwidth, N
- o frequency step size, Δf

Outputs

- o normalized RF spectrum across simulation bandwidth, $W(f_i)$, $i=1,N$.

4.7.5 FM Television Spectrum Model (FMTV)Purpose

This routine is used to calculate the normalized RF spectrum of an FM/TV signal across the simulation bandwidth.

Description

The FM/TV model described in Section 6.3 of Reference 4.7/1 will be used to model the spectrum. The model has been simplified however by assuming that the peak-to-peak frequency deviation of the dispersal waveform (if any), is included in the peak-to-peak frequency deviation of the video signal.

Inputs

- o peak-to-peak frequency deviation, f_{pp}
- o upper baseband frequency, f_m
- o carrier frequency, f_c
- o lower simulation frequency bound F_L
- o upper simulation frequency bound, F_M
- o number of steps across simulation bandwidth, N
- o frequency step size, Δf

Outputs

- o normalized RF spectrum across simulation bandwidth, $W(f_i)$, $i=1,\dots,N$.

4.7.6 Gaussian Noise Spectrum Model (GAUSS)Purpose

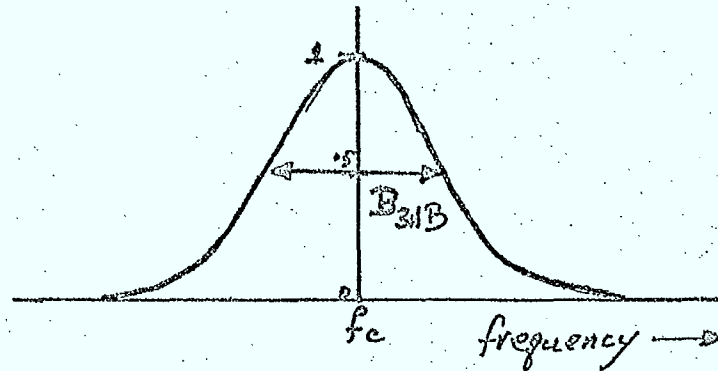
This routine calculates the RF spectrum across the simulation bandwidth, of a noise-like signal whose power spectrum is Gaussian in shape.

Description

If B_{3dB} is the 3-dB bandwidth of the RF spectrum (see sketch), then the normalized spectral density is given by

$$W(f) = \frac{0.93944}{B_{3dB}} e^{-\left[2.77259 \left(\frac{f-f_c}{B_{3dB}}\right)^2\right]} \quad (4.7.6)$$

where f_c is the carrier frequency

Inputs

- o 3-dB bandwidth, B_{3dB}
- o carrier frequency, f_c
- o lower simulation frequency bound, F_L
- o upper simulation frequency bound, F_M
- o number of steps across simulation bandwidth, N
- o frequency step size, Δf

Outputs

- o normalized RF spectrum across simulation bandwidth, $W(f_i)$, $i=1, \dots, N$.

4.7.7 Bandlimited White Noise Model (WHITE)Purpose

This routine calculates the RF spectrum across the simulation bandwidth, of a carrier whose spectrum can be approximated by a band of white noise.

Description

If the noise-like spectrum is limited to a band of width, W , centered about the carrier frequency, f_c , the normalized spectrum is given by:

$$W(f) = \begin{cases} 0, & |f-f_c| \geq \frac{W}{2} \\ \frac{1}{W}, & |f-f_c| < \frac{W}{2} \end{cases} \quad (4.7.7)$$

Inputs

- o RF spectrum bandwidth, W
- o carrier frequency, f_c
- o lower simulation frequency, F_L
- o upper simulation frequency, F_M
- o number of steps across simulation bandwidth, N
- o frequency step size, Δf

Outputs

- o normalized RF spectrum across the simulation bandwidth, $W(f_i)$, $i=1, \dots, N$.

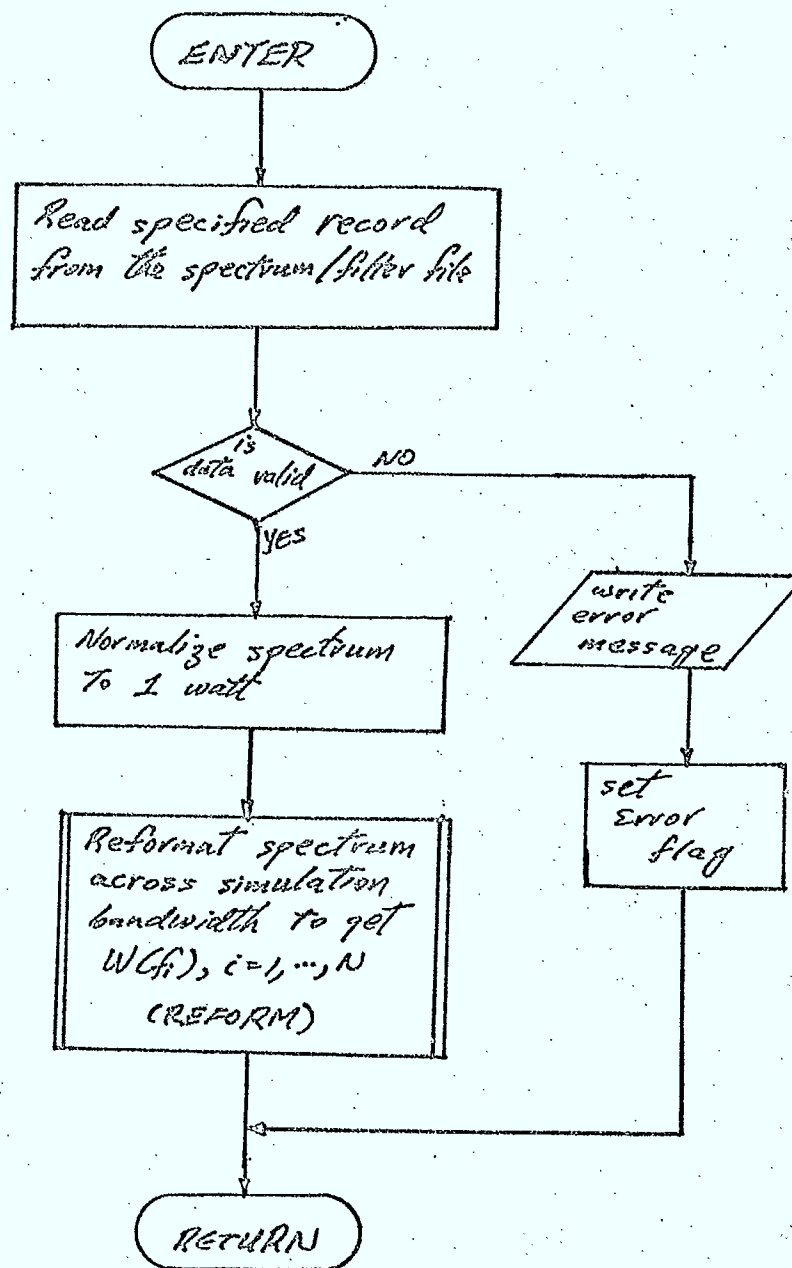
4.7.8 General Spectrum Model (GENSPC)Purpose

This routine calculates the RF spectrum across the simulation bandwidth for arbitrary spectra stored on a disk file.

Description

This routine first reads a specified record from the general spectrum file and normalizes the spectrum to 1 watt. It is assumed that this spectrum is centered about the carrier frequency f_c , and has a bandwidth W . The portion lying in the simulation bandwidth is then determined using the subroutine REFORM described in Reference 4.7/4. A flowchart of the general spectrum routine is illustrated in Figure 4.7/3 while the layout of the spectrum file is discussed in Chapter 5.

Figure 4.7/3 Flowchart of GENSPC



Inputs

- o RF bandwidth of carrier, W
- o record number of spectrum in the spectrum file
- o logical unit number of spectrum file
- o carrier frequency, f_c
- o lower simulation frequency bound, F_L
- o upper simulation frequency bound, F_M
- o number of steps across simulation bandwidth, N
- o frequency step size, Δf

Outputs

- o normalized RF spectrum across simulation bandwidth, $W(f_i)$, $i=1, \dots, N$
- o error flag indicating whether or not correct data was read from the file

References

- 4.7/1: SED 0710-44-TR-102, Issue 4; "Orbit Frequency Utilization Simulation - Volume 1 - Analytical Foundation", February 28, 1977.
- 4.7/2: C.C.I.R. Report 597, 1974.
- 4.7/3: M.G. Pelchat, "The Autocorrelation Function and Power Spectrum of PCM/FM with Random Binary Modulation Waveforms", IEEE Trans. Space Elec. Tel., Vol-10, 1963.
- 4.7/4: SED 0710-44-SW-103, Issue 3; "Orbit Frequency Utilization Simulation - Volume 2 - Program Description", February 28, 1977.

4.8 DEMULATOR MODELS

4.8.1 General

In this section, models are presented for FSK, PSK, and FM demodulators operating in an environment of thermal noise, intermodulation distortion, interference, and multipath interference (both specular and diffuse). The main purpose of these models is to establish the quality of the signal transmitted over the preceding non-ideal communications channel.

For digital signals, the bit error probability is used to measure receiver performance, while the unweighted test-tone signal-to-noise ratio is used for FM demodulators.

4.8.2 Digital Demulator Models

The FSK and PSK demodulator models are based on the results of References 4.8/1, 4.8/2, 4.8/3, and 4.8/4, in which analyses are presented that can be used to estimate the bit error probability of DPSK and non-coherent FSK demodulators operating in the presence of multipath interference. Although these models were intended for ideal receivers in the absence of RF interference and intermodulation distortion noise, an empirical model will be presented here in which these effects are also considered. This model is based on the use of an effective carrier-to-noise ratio which contains contributions from thermal noise, RF interference, and intermodulation distortion noise from non-linear amplifiers, as well as a contribution to model the effects of non-ideal receiver performance in the absence of all other degradations. This last term is required so that unrealistically low bit error probabilities will not be calculated under conditions of very high carrier-to-noise ratios.

The basic digital demodulator model (routine DIGDMD), on which the FSK and PSK models are based will now be presented. The basic model is a function of three ratios, defined as:

SNR - signal-to-noise ratio

SDR - carrier power-to-average diffuse multipath power ratio

SSR - carrier power-to-specular multipath power ratio

These ratios will be determined in terms of actual carrier power, receiver implementation margins, etc., for FSK and PSK receivers in later sections.

From Reference 4.8/3, it has been shown that the bit error probability of the basic digital demodulator, P_e , can be obtained from:

$$P_e = \frac{1}{\left(2 + \frac{SNR}{SDR}\right)} I_0 \left\{ \frac{2\sqrt{(SNR)(SSR)}}{2 + \frac{SNR}{SDR}} \right\} \exp \left\{ - \frac{\left(SNR + \frac{SNR}{SSR}\right)}{\left(2 + \frac{SNR}{SDR}\right)} \right\} \quad (4.8.2)$$

where $I_0(x)$ is the zeroeth order modified Bessel function of the first kind. This equation is based on the assumption that the multipath fading rate is much less than the transmitted bit rate. (ie: nonselective fading). The assumption is also made that the relative multipath delay and the delay spread are small compared to the bit duration. As the delay spread on aeronautical links is less than $5\mu s$ (Reference 4.8/5), this last assumption will be valid for bit rates ≤ 100 kHz. The relative multipath delay is approximately (Reference 4.8/6):

$$\tau = \frac{2h}{c} \sin \theta_s, \quad (4.8.3)$$

where h is the aircraft height and c is the speed of light. (For ships, this delay is negligible). For an aircraft at 70000 ft. at the subsatellite point, the delay is approximately 140μ sec (Reference 4.8/6). Thus in this instance, the relative delay is greater than the bit period for bit rates greater than ≈ 7 kHz. For lower aircraft heights and elevation angles typical of those expected for mid to high latitude locations, higher bit rates can be used before the assumption that the relative multipath delay

is less than the bit period is invalid. In any case, other models for receiver performance have not been found that can consider large multipath delays.

The model presented in equation 4.8.2 has been extended in Reference 4.8/4 to remove the assumption of slow fading. Assuming the nonflat fading can be characterized by the Doppler spread, B_{DOP} , of the fading process, it is possible to substitute for the SNR and SDR, an equivalent signal-to-noise ratio, $(SNR)_{eq}$ and equivalent signal-to-diffuse ratio $(SDR)_{eq}$. These equivalent ratios depend on the Doppler spread, the bit period, T , and on the carrier-to-noise and carrier-to-diffuse ratios, ie:

$$(SNR)_{eq} = \frac{1}{\left(\frac{1}{SNR}\right) + SDR \cdot f_1(a, T)} \quad (4.8.4)$$

$$(SDR)_{eq} = SDR \cdot f_2(a, T) \quad (4.8.5)$$

where

$$a = \pi B_{DOP} / \sqrt{2} \quad (4.8.6)$$

$$\begin{aligned} f_1(a, T) = & \frac{1}{aT} \left[\frac{\exp(-aT)}{aT} (\cos aT - \sin aT) - \frac{1}{aT} + 2 \right] \\ & - \frac{1}{(aT)^2} \left[\frac{\exp(-2aT)}{aT} \sin 2aT - \frac{2 \exp(-aT)}{aT} \cdot \sin aT \right. \\ & \left. + 2aT \right] \\ & + \frac{1}{(aT)^3} \left[\frac{4(aT)^3}{3} + \frac{2 \exp(-aT)}{aT} (\cos aT + \sin aT) \right. \\ & \left. - \frac{3}{2aT} - \frac{\exp(-2aT)}{2aT} (\sin 2aT + \cos 2aT) \right] \\ f_2(a, T) = & \frac{1}{aT} \left[\frac{\exp(-aT)}{aT} (\cos aT - \sin aT) - \frac{1}{aT} + 2 \right] \quad (4.8.8) \end{aligned}$$

The bit error probability can be obtained from SNR, SDR, SSR, B_{DOP} , and T by calculating $(SNR)_{eq}$ and $(SDR)_{eq}$ using equations 4.8.4 and 4.8.5 and substituting these values into equation 4.8.2 in place of SNR and SDR. The results of this model have been verified (Reference 4.8/4) against those obtained from the AEROSAT channel simulator, as shown in Figure 4.8/1. A flowchart illustrating the sequence of calculations is shown in Figure 4.8/2.

Inputs

- o SNR, SDR, SSR
- o Doppler spread
- o bit rate

Outputs

- o bit error probability

4.8.3 FSK Demodulator Model (FSKDMD)

Purpose

This routine is used to calculate the bit error probability of a binary, continuous phase, noncoherent FSK or FFSK receiver.

Description

As in section 9.5 of Reference 4.8/7, the non-ideal FSK demodulator will be characterized by an "implementation margin", m , and a "limiting error probability", P_0 . The implementation margin measures the increase in carrier power required for the non-ideal receiver to obtain the same bit error probability as an ideal receiver, when the receiver operates in a white noise environment, (see Figure 4.8/3). The noise calculated by the simulation must be increased by this factor m to allow for non-ideal receiver performance. At very low noise powers, ie, very high carrier-to-noise ratios, the performance of most receivers is limited by

Figure 4.8/1 Results of Basic Digital Demodulator
for DPSK Receiver

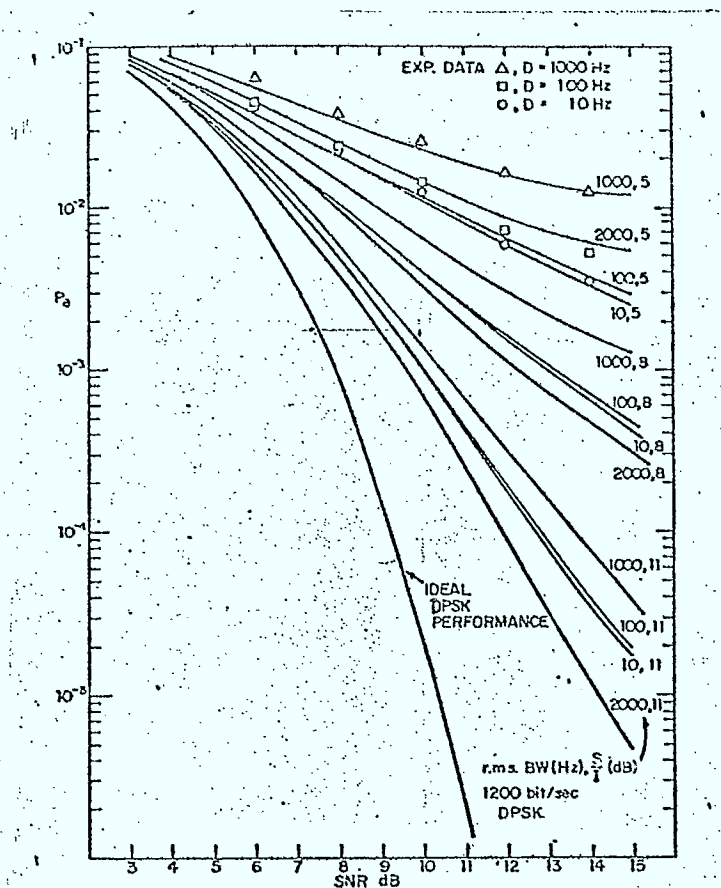
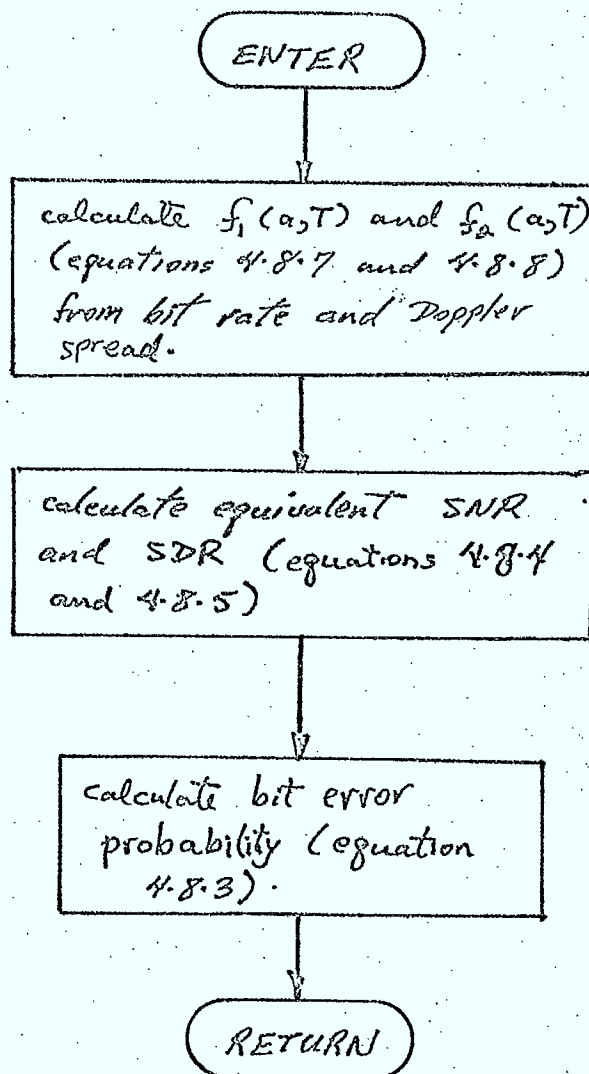


Fig. 2. Probability of bit error versus SNR with direct path signal power to multipath power ratio, S/I , and multipath Doppler spread, D , as parameters. ($SNR = E/N_0$.)

Figure 4.8/2 Flowchart of DIGDMD



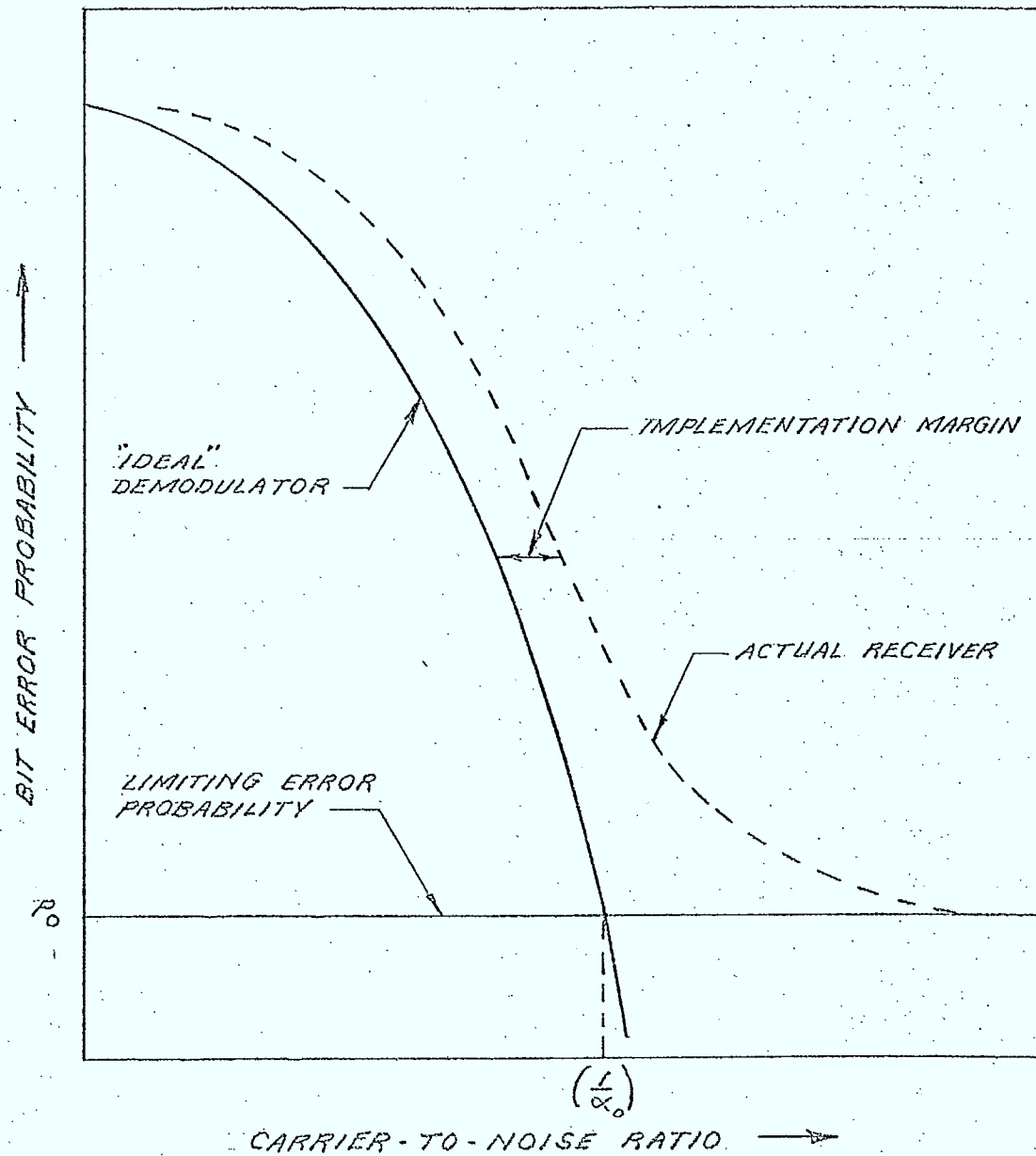


FIG: 4.8/3 ILLUSTRATION OF IMPLEMENTATION MARGIN AND LIMITING ERROR PROBABILITY FOR NON-IDEAL RECEIVERS.

intersymbol interference and other factors so that the bit error probability of the receiver approaches a limiting value, P_0 , as the input carrier power is increased. For simulation purposes, this limiting error rate is modelled as being due to an additional noise term that is proportional to the input carrier power. In a white noise environment, the bit error probability at the output of an ideal noncoherent FSK receiver is given by (Reference 4.8/8):

$$P_e = \frac{1}{2} e^{-\frac{1}{2} C/N} \quad (4.8.9)$$

where C/N is the carrier-to-noise power ratio into the receiver. Based on the assumptions just mentioned, the limiting error probability, P_0 , is given by:

$$P_0 = \lim_{C \rightarrow \infty} \left[\frac{1}{2} \exp \left(-\frac{1}{2} \left[\frac{C}{N + \alpha_0 C} \right] \right) \right] \quad (4.8.10)$$

where α_0 is a constant to be determined. Rearranging this expression yields:

$$\alpha_0 = -\frac{1}{2 \ln 2P_0} \quad (4.8.11)$$

The signal-to-noise ratio, SNR, required as an input for the basic digital demodulator discussed in Section 8.8.2 is then given by:

$$SNR = \frac{P_C}{m(P_T + P_I + P_D) + \alpha_0 P_0} \quad (4.8.12)$$

where:

P_C is the carrier power into the FSK demodulator

P_T is the thermal noise power

P_I is the RF interference noise power

P_D is the intermodulation distortion noise power

m is the FSK receiver implementation margin

α_0 is given by equation 4.8.11 and ensures that a limiting error probability of P_0 results whenever the carrier power is much greater than the unwanted noise power.

The other inputs to the basic demodulator are:

$$\left. \begin{aligned} \text{SDR} &= P_{\text{diff}} / P_c \\ \text{SSR} &= P_{\text{spec}} / P_c \end{aligned} \right\} \quad (4.8.13)$$

where P_{diff} is the average diffuse multipath power and P_{spec} is the specular multipath power.

A flowchart illustrating the implementation of the FSK demodulation model is shown in Figure 4.8/4.

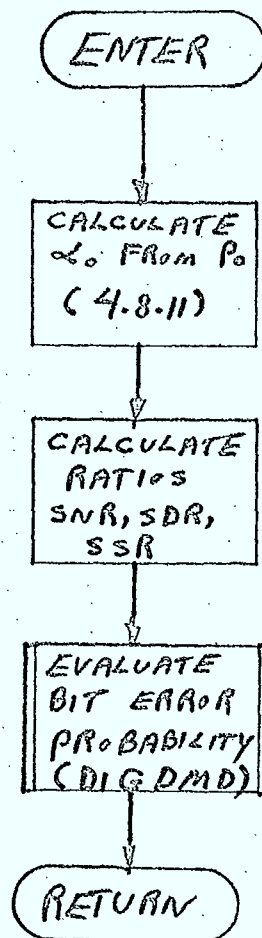
Inputs

- o average carrier power
- o thermal noise power
- o intermodulation distortion noise power
- o RF interference noise power
- o ratio of diffuse-to-carrier power
- o ratio of specular-to-carrier power
- o receiver implementation margin
- o limiting error probability of the receiver
- o Doppler spread
- o bit rate

Outputs

- o bit error probability

Figure 4.8/4 Flowchart of FSKDMD



4.8.4 PSK Demodulator Routine (PSKDMD)

Purpose

This routine is used to calculate the bit error probability for non-ideal binary and M-ary CPSK and DPSK receivers operating in a thermal noise, RF interference, intermodulation distortion, and multipath fading environment.

Description

The PSK receiver models that will be considered in this simulation are:

- ◉ binary DPSK
- ◉ M-ary DPSK
- ◉ binary CPSK
- ◉ M-ary CPSK

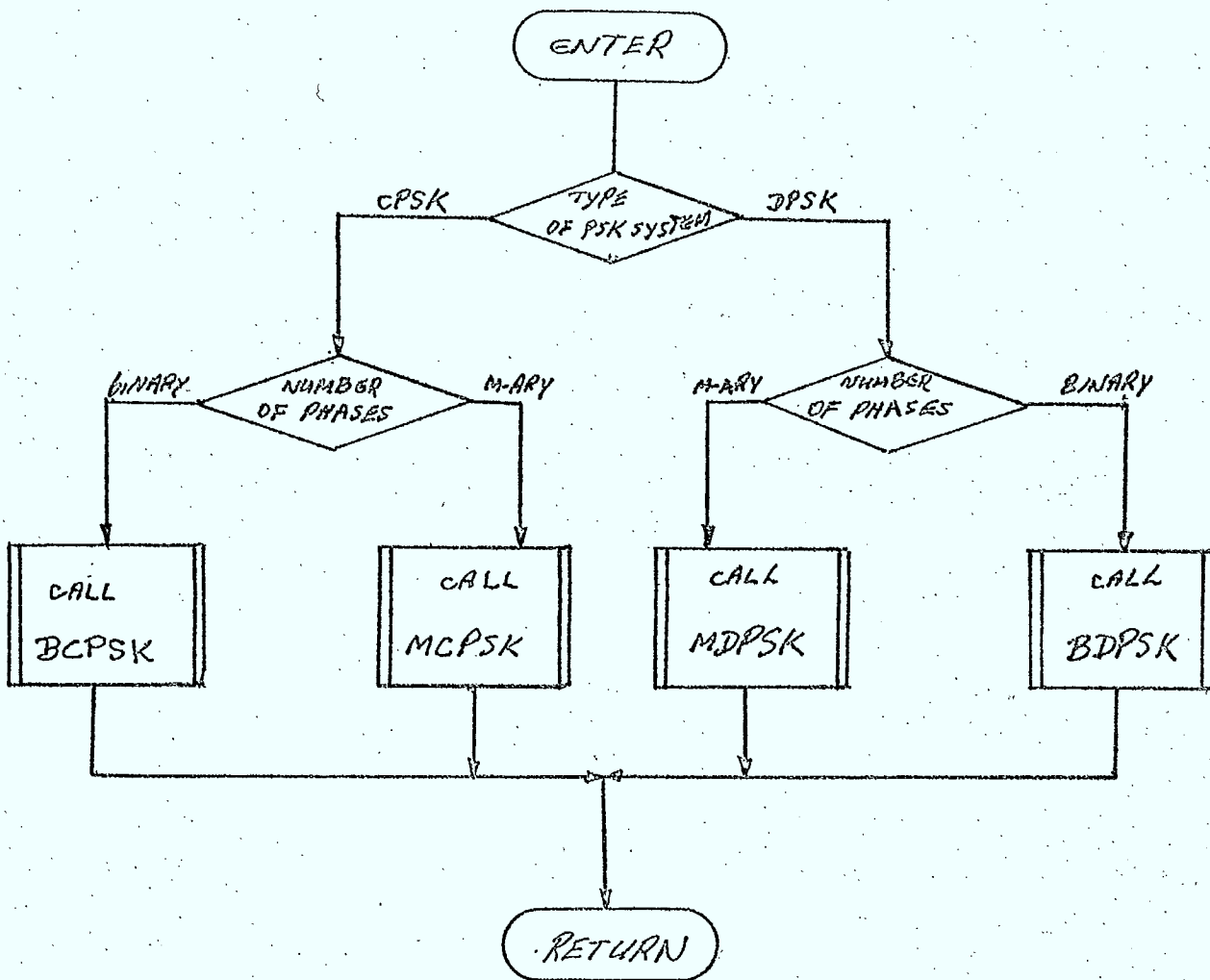
All of these models are based on an equivalent binary DPSK model, since the basic digital demodulator model described in Section 4.8.2 applies to both binary DPSK and noncoherent FSK receivers (References 4.8/2, 4.8/3, 4.8/4). Descriptions of the four PSK receivers follow in the next subsections.

A flowchart of the PSKDMD is shown in Figure 4.8/5.

Inputs

- ◉ type of PSK receiver (CPSK or DPSK)
- ◉ number of phases, M
- ◉ bit rate
- ◉ carrier power
- ◉ thermal noise power
- ◉ intermodulation distortion noise power
- ◉ RF interference noise power
- ◉ ratio of diffuse-to-carrier power
- ◉ ratio of specular-to-carrier power
- ◉ receiver implementation margin
- ◉ limiting error probability
- ◉ Doppler spread /

Figure 4.8/5 Flowchart of PSKDMD



Outputs

- bit error probability

4.8.5 Binary DPSK Demodulator Routine (BDPSK)Purpose

This routine calculates the bit error probability of a non-ideal binary DPSK demodulator.

Description

This routine calls the basic digital demodulator routine to determine the bit error probability. It first calculates the ratios SNR, SDR, and SSR required by routine DIGDMD. Making the same assumptions as used in the FSK demodulator model, together with the results of Reference 4.8/4 relating FSK to DPSK, these ratios for a non-ideal binary DPSK receiver are given by:

$$SNR = \frac{2P_c}{m(P_T + P_I + P_B) + \alpha_0 P_c} \quad (4.8.14)$$

where

$$\alpha_0 = - \frac{1}{\ln 2P_0}$$

$$SDR = P_{aff} / P_c$$

$$SSR = P_{spec} / P_c$$

where m is the implementation margin for the binary DPSK receiver and P_0 is the limiting error probability.

Inputs

- same as for FSK demodulator

Outputs

- bit error probability

4.8.6 Binary CPSK Demodulator (BCPSK)Purpose

This routine is used to calculate the bit error probability of a non-ideal binary CPSK receiver.

Description

The bit error probability of an "ideal" binary CPSK receiver operating in a white noise environment is (Reference 4.8/7) given by:

$$P_e = \frac{1}{2} \operatorname{erfc} \left[\sqrt{\frac{C}{N}} \right] \quad (4.8.15)$$

If the receiver implementation margin is m and the limiting error probability is P_0 , then it can be shown (Section 9.5, Reference 4.8/7) that:

$$P_e = \frac{1}{2} \operatorname{erfc} \left[\frac{P_c}{m(P_T + P_D + P_I) + \alpha_0 P_c} \right] \quad (4.8.16)$$

where P_c is the carrier power, P_T is the thermal noise power, P_I is the RF interference noise power, P_D is the distortion noise power, and α_0 is given by:

$$\alpha_0 = \frac{1}{\left[\operatorname{erfc}^{-1}(2P_0) \right]^2} \quad (4.8.17)$$

It is possible to estimate the error probability of this receiver in the presence of multipath interference, using the basic digital demodulator routine, by determining C/N for an ideal binary DPSK receiver that gives the same error probability as does equation 4.8.16. The bit error probability of an ideal binary DPSK receiver is given by:

$$P_e = \frac{1}{2} e^{-C/N} \quad (4.8.18)$$

So

$$\left(\frac{C}{N}\right) = -\ln \left[\operatorname{erfc} \left(\sqrt{\frac{P_e}{m(P_T + P_I + P_D) + d_0 P_e}} \right) \right] \quad (4.8.19)$$

The ratio SNR required by the basic digital demodulator is given by:

$$SNR = 2 \left(\frac{C}{N} \right) \quad (4.8.20)$$

where (C/N) is given by equation 4.8.19.

Inputs

- o same at FSK receiver

Outputs

- o bit error probability

4.8.7 M-ary DPSK Receiver Model (MDPSK)

Purpose

This routine is used to calculate the bit error probability of a non-ideal M-ary ($M \geq 4$) DPSK receiver.

Description

This routine makes use of the basic digital demodulator routine discussed in Section 4.8.2.

The symbol error probability of an ideal M-ary DPSK receiver operating in a white noise environment (Reference 4.8/7) is given by:

$$P_{SM} = \text{erfc} \left[\sqrt{\frac{C}{N}} \sin \left(\frac{\pi}{\sqrt{2} M} \right) \right] \quad (4.8.21)$$

In terms of the implementation margin m , and the limiting symbol error probability, P_0 , and following the approach taken in Section 4.8.6, the ratio SNR is given by:

$$SNR = -2 \ln \left[\frac{1}{\log_2 M} \cdot \text{erfc} \left(\sqrt{\frac{P_c}{m(P_f + P_c + P_b) + \alpha_0 P_c}} \sin \left(\frac{\pi}{\sqrt{2} M} \right) \right) \right] \quad (4.8.22)$$

where

$$\alpha_0 = \frac{1}{\left[\frac{\text{erfc}^{-1}(P_0 \log_2 M)}{\sin \left(\frac{\pi}{\sqrt{2} M} \right)} \right]^2} \quad (4.8.23)$$

The term $\log_2 M$ in these equations is required to relate the symbol error probability to the bit error probability.

Inputs

- o same as for FSKDMD plus M (number of phases)

Outputs

- o bit error probability

4.8.8 M-ary CPSK Receiver Model (MCPSK)

Purpose

This routine is used to calculate the bit error probability of a non-ideal M-ary ($M \geq 4$) CPSK receiver.

Description

This routine makes use of the basic digital demodulator routine to calculate the bit error probability.

The symbol error probability of an ideal M-ary ($M \geq 4$) CPSK demodulator is given by:

$$P_{e,M} = \text{erfc} \left[\sqrt{\frac{C}{N}} \sin \frac{\pi}{M} \right] \quad (4.8.24)$$

Given the implementation margin m , and the limiting bit error probability for the receiver, the ratio SNR is given by:

$$\text{SNR} = -2 \ln \left[\frac{1}{\log_2 M} \cdot \text{erfc} \left(\sqrt{\frac{P_c}{m(P_T + P_B + P_X) + \alpha_0 P_c}} \sin \frac{\pi}{M} \right) \right] \quad (4.8.25)$$

where

$$\alpha_0 = \frac{1}{\left[\frac{\text{erfc}^{-1}(P_0 \log_2 M)}{\sin \pi/M} \right]^2} \quad (4.8.26)$$

Inputs

- same as for FSKDMD plus the number of phases, M

Outputs

- bit error probability

4.8.9 FM Demodulator Model (FMDMD)

Purpose

The FM demodulator model is used to calculate the signal-to-noise ratio at the output of an FM demodulator operating in the presence of thermal noise, RF interference, intermodulation distortion noise, and multipath interference. Two models will be included in the simulation. The first is the narrow-band FM demodulator (NBFM), used for the reception of analog single-channel voice basebands. The other model is the adaptive narrow-band FM demodulator (ANBFM), also used for analog single-channel voice basebands.

Description

The models for these demodulators are empirical in nature, based on both measurements and theoretical performance characteristics. Unlike the FM demodulator model used in OFUS, the models described here can be used for carrier-to-noise ratios above and below the threshold C/N of the receiver.

The effect of multipath interference on the performance of these demodulators depends on the relative magnitudes of the specular and diffuse components of the multipath signal. For analog voice systems, the relative time delay of the reflected signal is short compared with the top modulating frequency, and causes negligible distortion in the demodulated signal (Reference 4.8/9), and thus will be ignored in the simulation models.

The reflected multipath signal interferes with the direct signal to cause amplitude fading at the input to the demodulator. The specular component causes a slow, quasi-periodic fade, with a period on the order of several seconds (References 4.8/10, 4.8/11). The diffuse component is characterized by a Rayleigh amplitude probability distribution function (Reference 4.8/8) and results in more rapid, noise-like fluctuations in the amplitude of the received signal.

As fluctuations caused by the diffuse component are much faster than those due to the specular component, and the performance of the demodulator under worst case specular interference is of interest in LINK calculations, the median signal level will be used in calculating the carrier-to-noise ratio at the input to the demodulator. The median carrier power is given by:

$$\hat{P}_c = P_c \left[1 - \sqrt{\frac{P_{diff}}{P_c}} - \sqrt{\frac{P_{spec}}{P_c}} \right]^2 \quad (4.8.27)$$

where

P_c is the average received carrier power,

P_{diff} is the average diffuse multipath power, and

P_{spec} is the average specular multipath power.

The effective carrier-to-noise ratio at the demodulator input is then given by:

$$\left(\frac{C}{N}\right) = \frac{\hat{P}_c}{P_T + P_I + P_D}, \quad (4.8.28)$$

where

P_T is the thermal noise power in the receiver bandwidth,

P_I is the RF interference power, and

P_D is the RF intermodulation distortion noise power.

NBFM Demodulator Model

The narrow band FM demodulator is modelled as a conventional discriminator, allowing use of the standard FM equation to predict the signal-to-noise ratio at the demodulator output. The unweighted test-tone signal-to-noise ratio, for an FM demodulator operating above threshold, is

given by (References 4.8/7, 4.8/12, 4.8/13):

$$\left(\frac{S}{N}\right)_{TT} = 32 \left(\frac{C}{N}\right) \frac{f_m \beta^2 (\sqrt{\Lambda_B} \beta + 1)}{(f_m - f_c)} \quad , \quad (4.8.29)$$

where

f_m is the upper baseband frequency (~ 3000 Hz)

f_c is the lower baseband frequency (~ 300 Hz)

β is the rms modulation index, and

Λ_B is the peak-to-average baseband power ratio.

The performance of a typical NBFM demodulator is shown in Figure 4.8/6. For C/N less than the threshold value for the receiver, $(C/N)_{Th}$, the signal-to-noise ratio degrades much faster than that predicted by equation 4.8.29. For simulation purposes, the signal-to-noise ratio is assumed to be proportional to the n -th power of the carrier-to-noise ratio in this region (see Figure 4.8/6) ie:

$$\left(\frac{S}{N}\right)_{TT} = k \left(\frac{C}{N}\right)^n \quad , \quad \frac{C}{N} < (C/N)_{Th} \quad (4.8.30)$$

where the proportionality constant, k , is determined from the signal-to-noise ratio at threshold, ie:

$$k = \frac{\left(\frac{S}{N}\right)_{Th}}{\left(\frac{C}{N}\right)_{Th}^n} \quad . \quad (4.8.31)$$

The constant n can be determined from FM demodulator performance curves presented in Reference 4.8/12. For modulation indices typical of those used in mobile-satellite system applications, a value of $n=5$ has been determined.

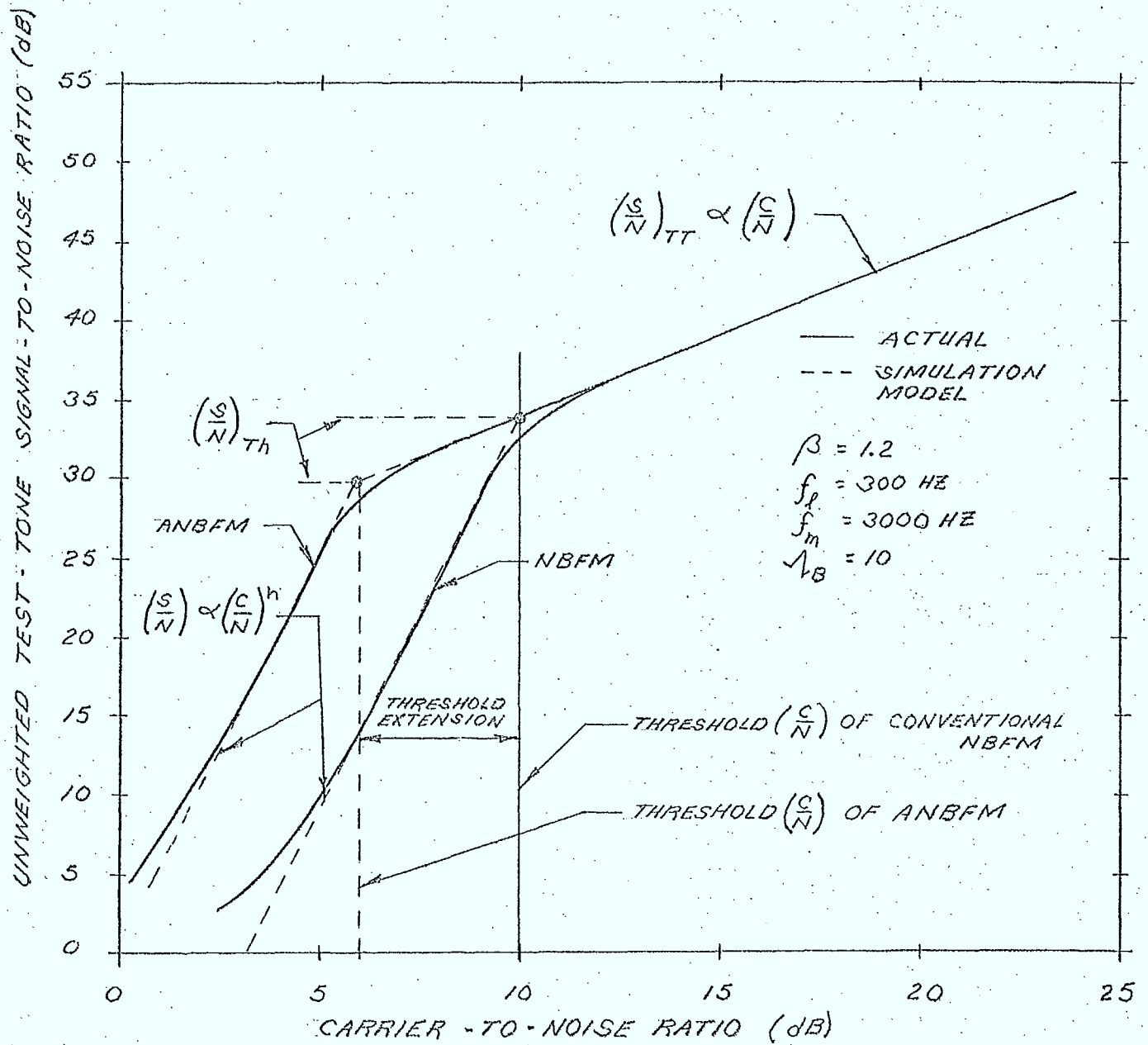


FIG: 4.8/6 FM DEMODULATOR MODEL

ANBFM Demodulator Model

The adaptive NBFM demodulator is basically a threshold-extension FM demodulator. Threshold extension is provided by a phase-locked loop demodulator whose loop bandwidth is dependent on the received carrier power (Reference 4.8/9). The receiver threshold can be decreased by approximately 4dB when compared with that of a conventional NBFM demodulator.

The signal-to-noise ratio at the output of an ANBFM demodulator is given by equation 4.8.29 for operation above threshold, and by equation 4.8.30 for operation below threshold. The threshold C/N is given by:

$$\left(\frac{C}{N}\right)_{TR} = \left(\frac{C}{N}\right)_{Th, CONV} \cdot \epsilon \quad , \quad (4.8.32)$$

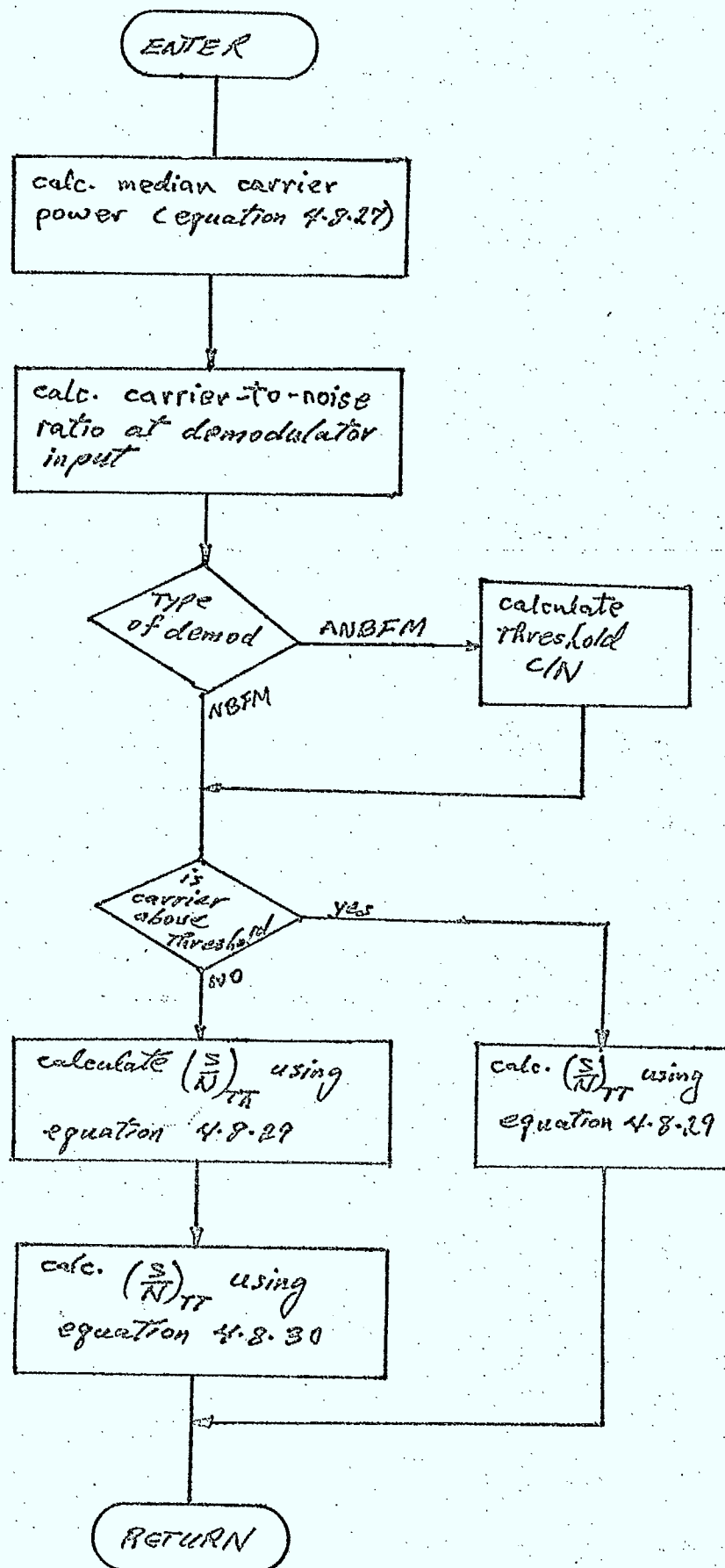
where $(C/N)_{Th, CONV}$ is the threshold C/N of a conventional NBFM demodulator, and ϵ is the threshold extension factor of the ANBFM (or other threshold extension) demodulator.

The implementation of the FM demodulator model is illustrated in Figure 4.8/7.

Inputs

- o rms modulation index
- o peak-to-average baseband power ratio
- o lower baseband frequency
- o upper baseband frequency
- o threshold C/N of convention NBFM demodulator
- o threshold extention factor
- o flag indicating type of FM modulator
- o average carrier power
- o RF interference power
- o RF thermal noise power
- o RF intermodulation distortion power
- o diffuse-to-carrier power ratio (average)
- o specular-to-carrier power ratio

Figure 4.8/7 Flowchart of FMDMD



Outputs

- o unweighted test-tone signal-to-noise ratio

References

- 4.8/1: J.J. Jones, "FSK and DPSK Performance in a Mixture of CW Tone and Random Noise", IEEE Trans. Comm. Tech., October 1970.
- 4.8/2: S.G. Wilson, et.al., "DPSK Performance on L-Band Aeronautical Satellite Channels: Test Results and a Coding Evaluation", IEEE Trans. Comm., March, 1976.
- 4.8/3: J.J. Jones, "Multichannel FSK and DPSK Reception with Three Component Multipath", IEEE Trans. Comm. Tech., Vol. Com-16, No. 6, December 1968.
- 4.8/4: H. Salwein, "DPSK Performance Under Time - Selective Multipath Fading", IEEE Trans. Comm., March 1975.
- 4.8/5: "Aeronautical L-Band Technology Tests with the ATS-6 Satellite", J.M. Gutwein, and R.G. Bland, U.S. Dept. of Trans/Transportation Systems Center, 1976.
- 4.8/6: H.C. Salwein, and C.B. Duncombe, "Performance Evaluation of Data Modems for the Aeronautical Satellite Channel", IEEE Trans. Comm. Vol. COM-23, No. 7, July 1975.
- 4.8/7: SED 0710-44-TR-102, Issue 4; "Orbit Frequency Utilization Simulation - Volume 1 - Analytical Foundation", February 28, 1977.
- 4.8/8: M.J. Massaro, "The Distribution of Error Probability for Rayleigh Fading and Gaussian Noise", IEEE Trans. Comm., November 1974.
- 4.8/9: "UHF-SHF Satellite Communications Link Calculations", Bell-Northern Research, Study Contract No. PL36100-4-0995, DOC, Government of Canada, July 1975.

- 4.8/10: G.T. Bergemann and H.L. Kucera, "Signal Characteristics of a Very-High-Frequency Satellite-to-Aircraft Communications Link", IEEE Trans. Comm. Tech., Vol. COM-17, No. 6, December, 1969.
- 4.8/11: "Link Factors for Antenna and Propagation Phenomena for MUSAT", W.D. Hindson, C.R.C. Tech. Memorandum SS20, August 1976.
- 4.8/12: C.C.I.R. Report 601, "Technical Characteristics of Systems Providing Communications and/or Radiodetermination Using Satellite Techniques for Aircraft and/or Ships", 1974.
- 4.8/13: "A Multi-Beam SHF Satellite Communications System for Canada (1977-1985)", Bell Northern Research, Study Contract No. PL36100-2-0067, D.O.C., October 1972.

4.9 Filter Models

4.9.1 General

In this section, models are presented for the power transfer characteristics of the following filters:

- Butterworth nth-order filter (BUTFIL)
- Chebyshev nth-order filter (CHBFIL)
- Ideal bandpass filter (IBPFIL)
- General filter model (GENFIL)

The selection of any of these filter models is done using subroutine FILTER, that returns the filtered RF power spectrum across the simulation bandwidth.

4.9.2 Filter Model Selector Routine (FILTER)

Purpose

This routine is used to calculate the RF power spectrum at the output of the specified filter.

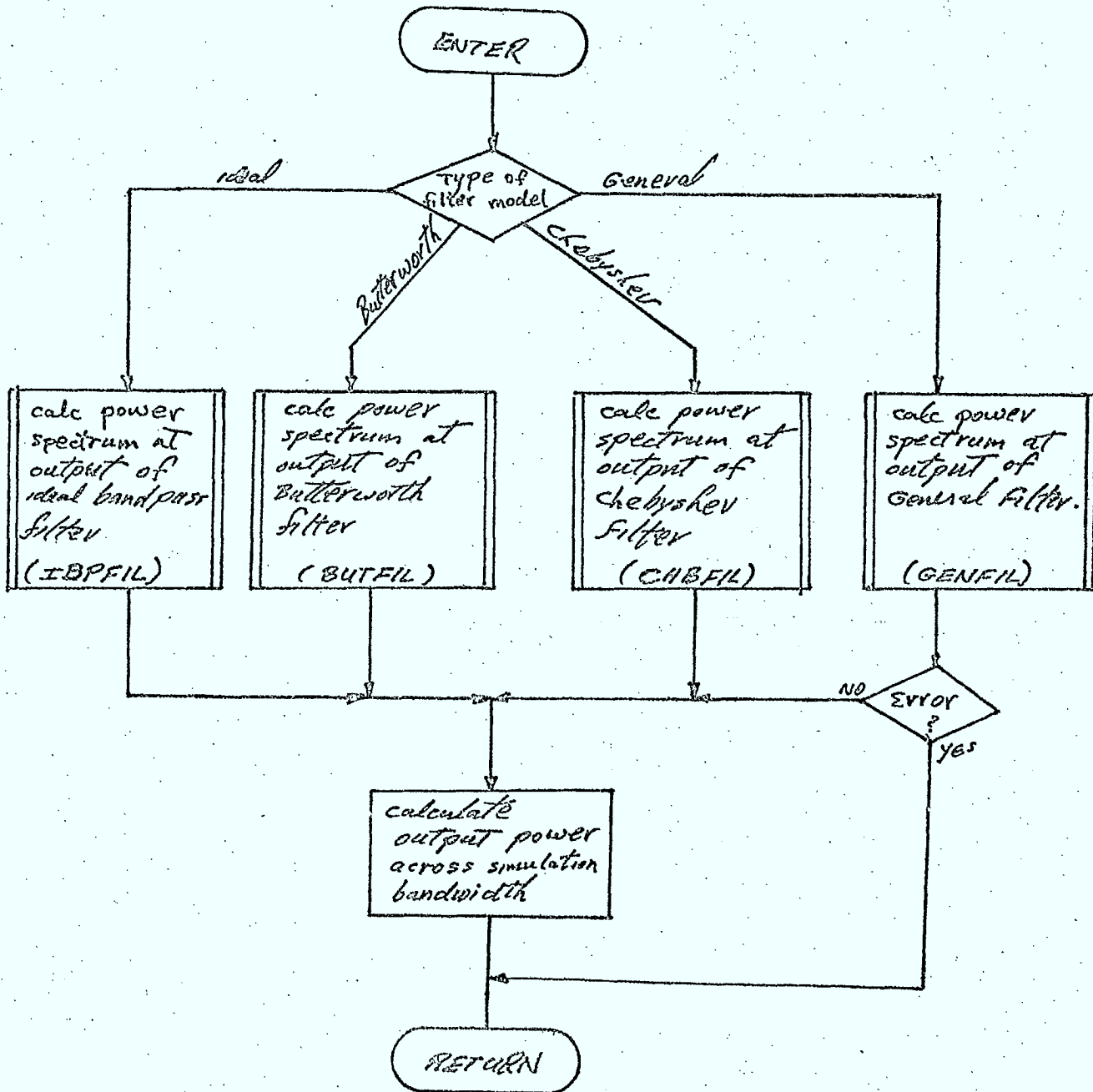
Description

This routine simply selects the appropriate filter model, as indicated in Figure 4.9/1.

Inputs

- $W(f_i)$, $i=1, \dots, N$ spectrum to be filtered
- N number of steps across the simulation bandwidth
- Δf frequency step size
- F_L lower frequency limit of simulation bandwidth
- F_M upper frequency limit of simulation bandwidth
- center frequency of filter, f_0
- type of filter model. One of:
 - Butterworth
 - Chebyshev
 - Ideal Bandpass
 - General

Figure 4.9/1 Flowchart of FILTER



- n number of poles (Butterworth and Chebyshev)
- B_{3dB} 3-dB bandwidth (Butterworth and Chebyshev)
- B_F filter bandwidth (ideal band pass, general)
- Record number of general filter
- α_i insertion loss (ie: ratio of output spectral density at mid-band-to-input spectral density) (Default = 1)

Outputs

- $W(f_i)$, $i=1, \dots, N$ RF spectrum at filter output
- output power across simulation bandwidth
- flag indicating whether or not input data for the general filter model was valid

4.9.3 Ideal Bandpass Filter Model (IBPFIL)

Purpose

This routine calculates the power spectrum across the simulation bandwidth at the output of an ideal band pass filter.

Description

The filter is characterized by its bandwidth, B_F , and the center frequency, f_0 . If α_i is the insertion loss, then the output power spectrum is given by:

$$W_{out}(f) = \begin{cases} W_{in}(f) \alpha_i & ; |f - f_0| < B_F/2 \\ 0 & ; \text{elsewhere} \end{cases} \quad (4.9.1)$$

Inputs

- $F_L, F_M, N, \Delta f, B_F, f_0, \alpha_i, W(f_i), i=1, N$
(defined in previous section)

Outputs

- $W(f_i), i=1, \dots, N$ output filtered spectrum

4.9.4 Butterworth Filter Model (BUTFIL)Purpose

This routine calculates the power spectrum across the simulation bandwidth at the output of an n^{th} order Butterworth filter.

Description

The Butterworth filter (Reference 4.9/1) is characterized by its 3-dB bandwidth, B_{3dB} , and n , the number of poles. If α_i is the insertion loss, then the output power spectrum is given by:

$$W_{out}(f) = \begin{cases} \frac{W_{in}(f) \alpha_i}{1 + \left[\frac{f - f_0}{B_{3dB}/2} \right]^{2n}} & ; F_L < f < F_M \\ 0 & ; \text{elsewhere} \end{cases} \quad (4.9.2)$$

where F_L and F_M are the lower and upper bounds of the simulation bandwidth.

Inputs

- $F_L, F_M, N, \Delta f, B_{3dB}, \alpha_i, f_0, n, W(f_i), i=1, \dots, N$
(described in Section 4.9.2)

Outputs

- $W(f_i), i=1, \dots, N$ output filtered power spectrum

4.9.5 Chebyshev Filter Model (CHBFIL)Purpose

This routine calculates the power spectrum across the simulation bandwidth at the output of an n^{th} order Chebyshev filter.

Description

The Chebyshev filter (Reference 4.9/2) is characterized by its 3-dB bandwidth, $B_{3\text{-dB}}$, and n , the number of poles. If α_i is the mid-band insertion loss and f_0 is the center frequency of the filter, then the output power spectrum is given by:

$$W_{\text{out}}(f) = \begin{cases} \frac{W_{\text{in}}(f) a_n}{1 + C_n^2 \left[\frac{f - f_0}{B_{3\text{dB}}/2} \right]} & ; F_L < f < F_H \\ 0 & ; \text{elsewhere} \end{cases} \quad (4.9.3)$$

where $C_n(x)$ is the n^{th} order Chebyshev polynomial given by:

$$C_n(x) = \begin{cases} \cos(n \cos^{-1}(x)) & ; |x| \leq 1 \\ \cosh(n \cosh^{-1}(x)) & ; |x| > 1 \end{cases} \quad (4.9.4)$$

and a_n is related to the insertion loss by:

$$a_n = \begin{cases} d_i & ; n = 0, 2, 4, \dots \\ 2 d_i & ; n = 1, 3, 5, \dots \end{cases} \quad (4.9.5)$$

The term a_n is required to ensure that:

$$\frac{W_{OUT}(f=f_0)}{W_{IN}(f=f_0)} = \mathcal{L}_i$$

for all filter orders, n .

Equation 4.9.4 is not a useful expression for simulation purposes. Instead the recursion relation for Chebyshev polynomials will be employed:

$$\begin{aligned} C_0(z) &= 1 \\ C_1(z) &= z \\ C_2(z) &= 2z^2 - 1 \\ &\vdots \\ C_{n+1}(z) &= 2z C_n(z) - C_{n-1}(z) \end{aligned} \quad (4.9.6)$$

The implementation of this routine is illustrated in Figure 4.9/2.

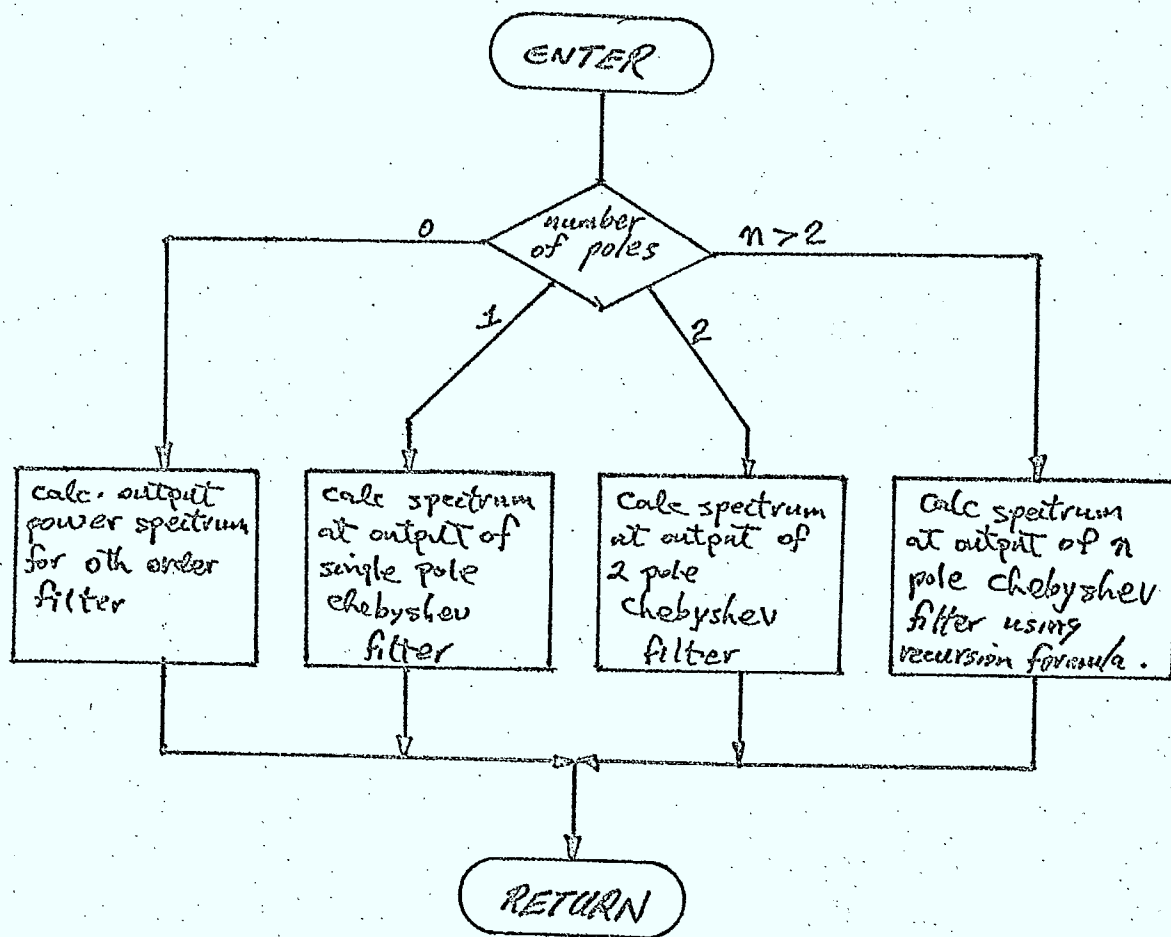
Inputs

o $F_L, F_M, \Delta f, N, i, f_0, n, B_{3\text{-dB}}, W(f_i), i=1, \dots, N$
(described in Section 4.9.2)

Outputs

o $W(f_i), i=1, \dots, N$ output filtered power spectrum across the simulation bandwidth

Figure 4.9/2 Flowchart of CHBFIL



4.9.6 General Filter Model (GENFIL)

Purpose

This routine is used to calculate the RF power spectrum at the output of a specified general filter.

Description

The general filter model is characterized by:

- the record number of the filter in the general filter file
- the bandwidth, B_F , of the filter
- the insertion loss, α_i
- the center frequency of the filter, f_0

If $G(f-f_0)$ is the power transfer function stored in the filter file, then the output RF power spectrum is given by:

$$W_{out}(f) = \begin{cases} \alpha_i W_{in}(f) G(f-f_0) & ; |f-f_0| < \frac{B_F}{2} \\ 0 & ; \text{elsewhere} \end{cases} \quad (4.9.7)$$

The implementation of this routine is illustrated in Figure 4.9/3. A description of the filter file record layout is contained in Chapter 5.

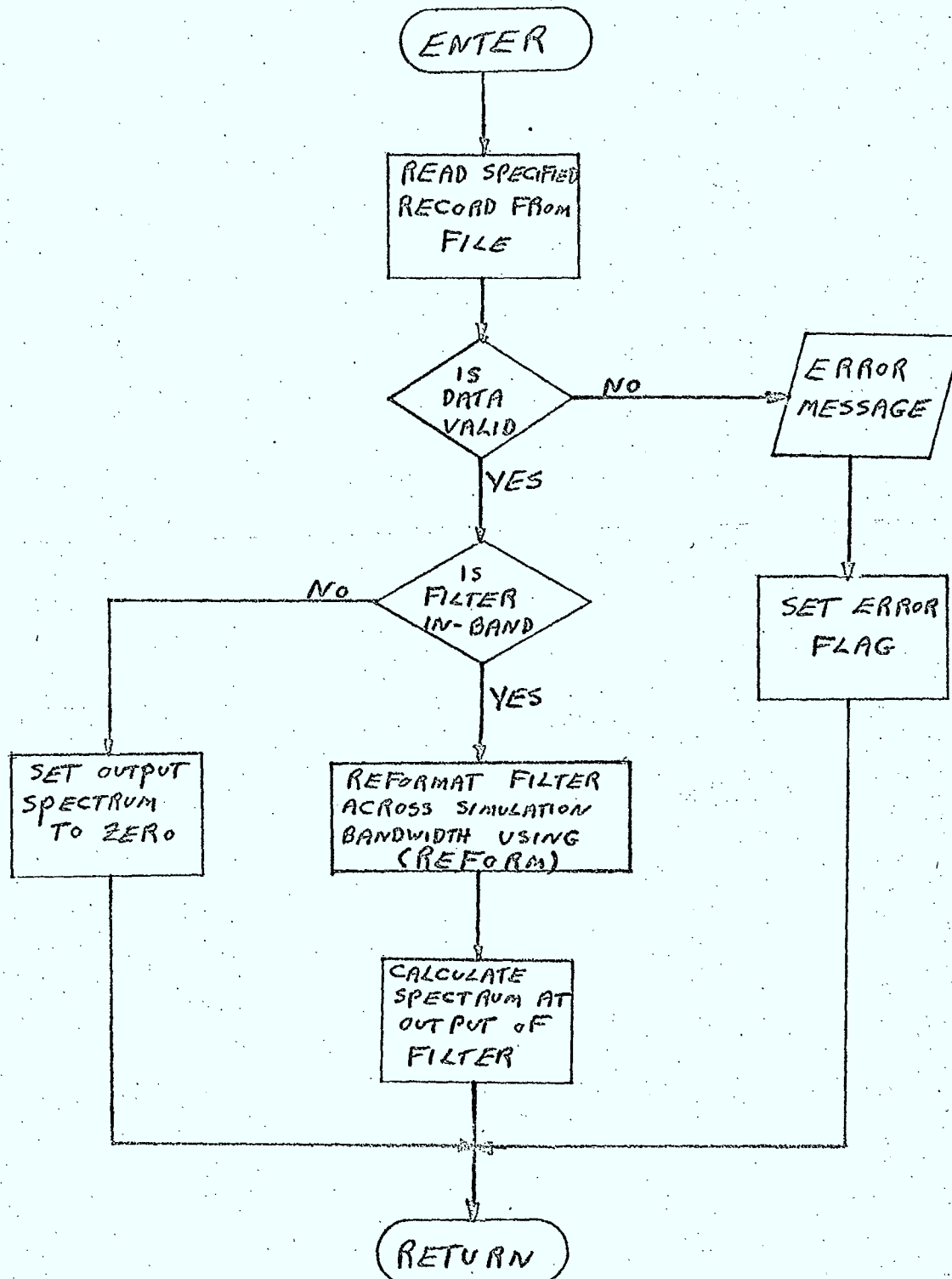
Inputs

- F_L , F_M , Δf , N , f_0 , B_F , rec.no. of filter, $W(f_i)$, $i=1, \dots, N$, α_i (described in Section 9.4.2)

Outputs

- $W(f_i)$, $i=1, \dots, N$, RF spectrum at output of filter
- flag indicating whether or not valid data was read from the filter file

Figure 4.9/3 Flowchart of GENFIL



References (

- 4.9/1: "Introduction to Modern Network Synthesis", M.E. Van Valkenburg,
Publ. John Wiley and Sons, New York, 1960

4.10 High Power Amplifier Models (HPA)

4.10.1 General

The two major subroutines modelling the HPA are:

- a model simulating the power transfer characteristics of linear, soft-limiting, and hard-limiting HPA's. (subroutine HPAPWR)
- a model for the intermodulation distortion noise spectrum for each of the above amplifiers. (subroutine HPAIMD)

These routines are required for link and ISI interference calculations. For ESI interference calculations, detailed HPA models are not required, since the ESI carrier is simply characterized by its nominal output power (stored in the ESI transmitter carrier record).

Before describing each model in detail, several of the main assumptions made in developing the models for use in link calculations will be discussed.

An HPA can be used in either a baseband transmitter or in an IF-type repeater. When used in a baseband transmitter, it is assumed that the amplifier operates at its nominal operating point. The output power of the carrier is then always equal to its nominal value. Similarly, the distortion-to-carrier ratio is assumed to remain at its nominal value, and is assumed to have a spectrum that is uniform across the carrier's RF bandwidth. (Note: this is identical to the OFUS HPA model for baseband transmitters)

When an HPA is used in an IF repeater, a different model must be employed, because the output power of the carrier depends on its input power. This change in input power is due to fading of the signal caused by a variety of propagation phenomena. The output carrier power is thus dependent on the input carrier power relative to its nominal value, the power of other carriers (if any) also being amplified by the HPA, and whether or not the amplifier employs automatic gain control (AGC).

For simulation purposes, it is assumed that the input power of these other carriers (if any) remains at some nominal value, and that if AGC is employed, the total output power of the amplifier remains constant. Note that the output power of a particular carrier (namely the one simulated in a link calculation) may change even with AGC, if the HPA is amplifying other carriers.

For interference calculations it is assumed that the output power of the carrier equals its nominal output power.

The intermodulation distortion model, which is only invoked in link calculations, also makes use of the assumptions made above. One further assumption that has been made is that for multi-carrier IF repeaters, the intermodulation distortion spectrum can be approximated by a Gaussian spectrum centered in the amplifier bandwidth. As the level of the distortion power is a function of the amplifier operating point, parametric models for each of the amplifiers described above are included in the HPA intermodulation distortion model.

4.10.2 HPA Power Transfer Characteristic (HPAPWR)

Purpose

This routine calculates the carrier output power, the total amplifier output power (required for the distortion model), and the change in amplifier operating point due to changes in the input carrier power level.

Description

This routine contains models for the following type of amplifiers:

- o baseband transmitter amplifiers
- o linear, single or multi-carrier amplifiers with AGC
- o linear, single or multi-carrier amplifiers without AGC
- o biased, soft-limiting, single or multi-carrier amplifiers with AGC
- o biased, soft-limiting, single or multi-carrier amplifiers without AGC
- o biased, hard-limiting, single or multi-carrier amplifiers

The main logic paths to be employed in implementing these models are illustrated in the flowchart in Figure 4.10/1.

For baseband type amplifiers, the output carrier power does not have to be calculated, as it is stored in the ISI TX carrier record. For the other amplifiers, the output carrier power depends on a variety of factors. The following discussion applies to these amplifiers.

Under nominal (ie: non-fading) conditions, the carrier power into the amplifier is some fraction, r , of the total input power. For single carrier operation, $r=1$. For multi-carrier operation r is less than 1.

If the nominal input carrier power is denoted ϕ , then the total nominal input power to the amplifier, $P_{IN,NOM}$, is given by:

$$P_{IN,NOM} = \frac{\phi}{r} \quad (4.10.1)$$

If the input carrier power is less than its nominal value, by some fraction, δp_i , where:

$$\delta p_i = \left(\frac{\text{actual input carrier power}}{\text{nominal input carrier power}} \right),$$

then assuming that the remaining carriers (if any) remain at their nominal values, the total input power to the amplifier is:

$$P_{IN} = (P_{IN,NOM} - \phi) + (\delta p_i \phi) \quad (4.10.2)$$

The ratio of the total input power to the nominal total input power is then given by:

$$\Delta P_{IN} = \frac{P_{IN}}{P_{IN,NOM}} = (1 - r + \delta p_i r) \quad (4.10.3)$$

The ratio of the input carrier power to the total input power, denote r' , is given by:

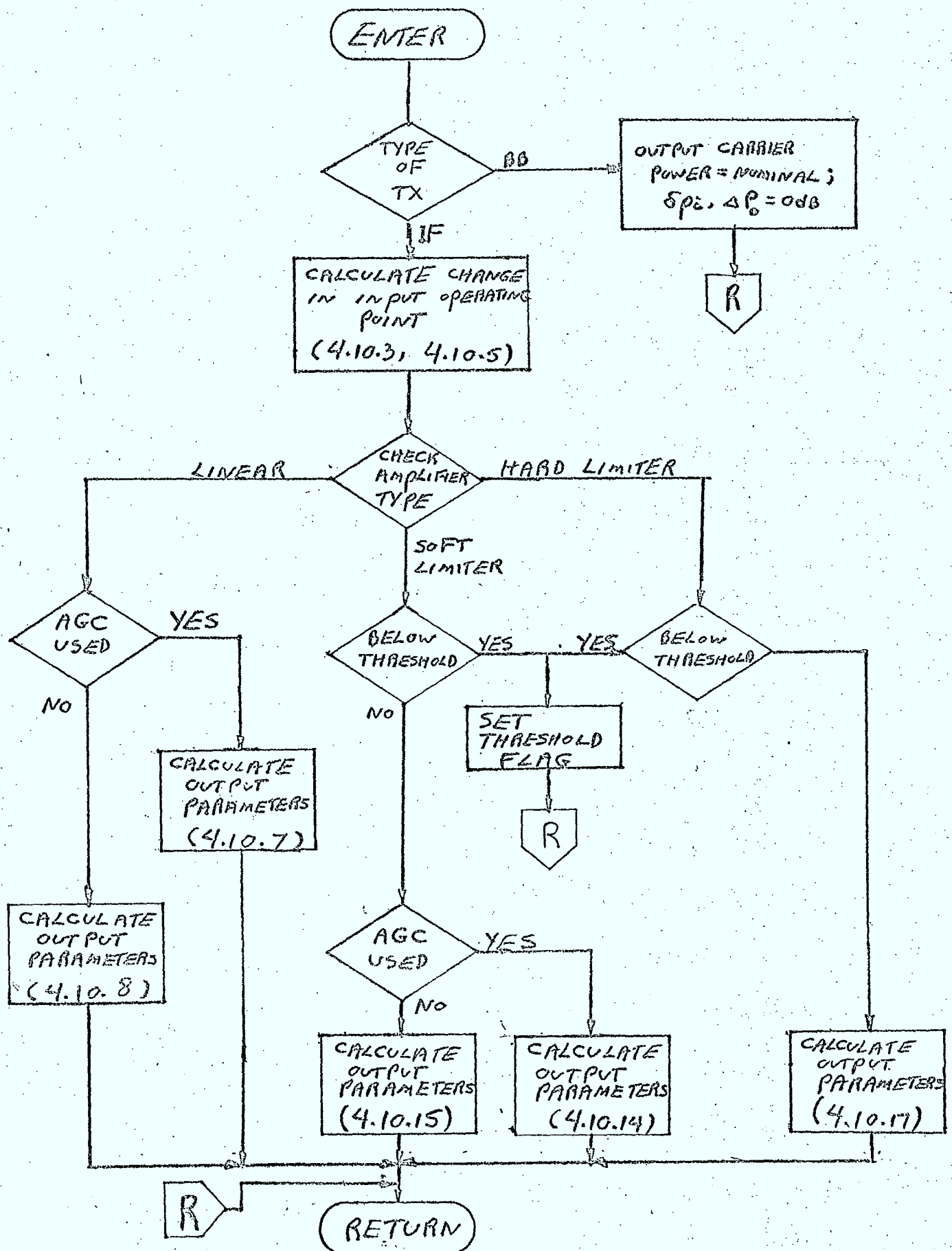
$$r' = \frac{\phi \delta p_i}{P_{IN}} \quad (4.10.4)$$

or

$$r' = \left(\frac{\delta p_i r}{\Delta P_{IN}} \right) \quad (4.10.5)$$

Figure 4.10/1

Flowchart of HPAPWR



The two parameters, r' and ΔP_{IN} , characterize the change in input operating point for all of the amplifiers listed previously. The output parameters required of the amplifier models are:

- carrier output power, P_0
- total output power of the amplifier, P_{TOT}
- $\left(\frac{\text{carrier output power}}{\text{nominal carrier output power}} \right)$, δp_0
- $\left(\frac{\text{total output power of the amplifier}}{\text{nominal total output power of the amplifier}} \right)$, ΔP_0

The quality δp_0 is required since it affects the value of δp_i used at the next amplifier in the link. The quantities P_{TOT} , and ΔP_0 are required for the intermodulation distortion model described in the next section.

The remainder of this subsection presents the models and algorithms used to evaluate these parameters for each of the amplifiers, together with a description of the parameters required to characterize the amplifier power transfer characteristics.

Baseband Transmitter

$$\begin{aligned}
 p_0 &= P_{0,NOM} \quad (\text{user input}) \\
 \delta p_0 &= 1 \\
 P_{TOT} &= P_{0,NOM} \\
 \Delta P_0 &= 1
 \end{aligned}
 \tag{4.10.6}$$

Linear Amplifier

A linear amplifier is characterized by the total nominal output power of the amplifier. If the amplifier employs AGC, then:

$$\begin{aligned}
 p_0 &= P_{NOM} r' \\
 \delta p_0 &= \frac{r' P_{NOM}}{r P_{NOM}} = \left(\frac{r'}{r} \right) \\
 P_{TOT} &= P_{NOM} \\
 \Delta P_0 &= 1 \quad (\text{ie.: 0dB})
 \end{aligned}
 \tag{4.10.7}$$

If AGC is not used, then:

$$\begin{aligned}
 p_0 &= r^i p_{\text{NOM}} \Delta p_{\text{IN}} \\
 \delta p_0 &= \delta p_i \\
 p_{\text{TOT}} &= \Delta p_{\text{IN}} p_{\text{NOM}} \\
 \Delta p_0 &= \Delta p_{\text{IN}}
 \end{aligned}
 \tag{4.10.8}$$

Soft-Limiter

A biased, soft-limiting amplifier (Reference 4.10/1) can be characterized by the following parameters:

$$\begin{aligned}
 \circ P_{\text{SAT}} &= \text{total amplifier saturated output power} \\
 \circ \Delta p_{\text{IN,BIAS}} &= \left(\frac{\text{total input power at which the output power is zero}}{\text{nominal total input power}} \right) \\
 \circ \Delta p_{\text{IN,SAT}} &= \left(\frac{\text{total input power required to reach saturation}}{\text{nominal total input power}} \right) \\
 \circ \Delta p_{\text{NOM}} &= \left(\frac{\text{nominal total output power}}{\text{saturated total output power}} \right)
 \end{aligned}$$

The power transfer characteristic for a typical soft limiting amplifier is shown in Figure 4.10/2. The transfer curve can be expressed analytically by:

$$p_{\text{TOT}} = \begin{cases} 0 & ; \Delta p_{\text{IN}} < \Delta p_{\text{IN,BIAS}} \\ K(\Delta p_{\text{IN}} - \Delta p_{\text{IN,BIAS}})^n, & \Delta p_{\text{IN,BIAS}} \leq \Delta p_{\text{IN}} \leq \Delta p_{\text{IN,SAT}} \\ P_{\text{SAT}} & \Delta p_{\text{IN}} > \Delta p_{\text{IN,SAT}} \end{cases}
 \tag{4.10.9}$$

where K and n are constants. K and n can be obtained by solving the following set of simultaneous equations:

$$P_{\text{SAT}} = K(\Delta p_{\text{IN,SAT}} - \Delta p_{\text{IN,BIAS}})^n
 \tag{4.10.10}$$

$$P_{\text{NOM}} = K(1 - \Delta p_{\text{IN,BIAS}})^n
 \tag{4.10.11}$$

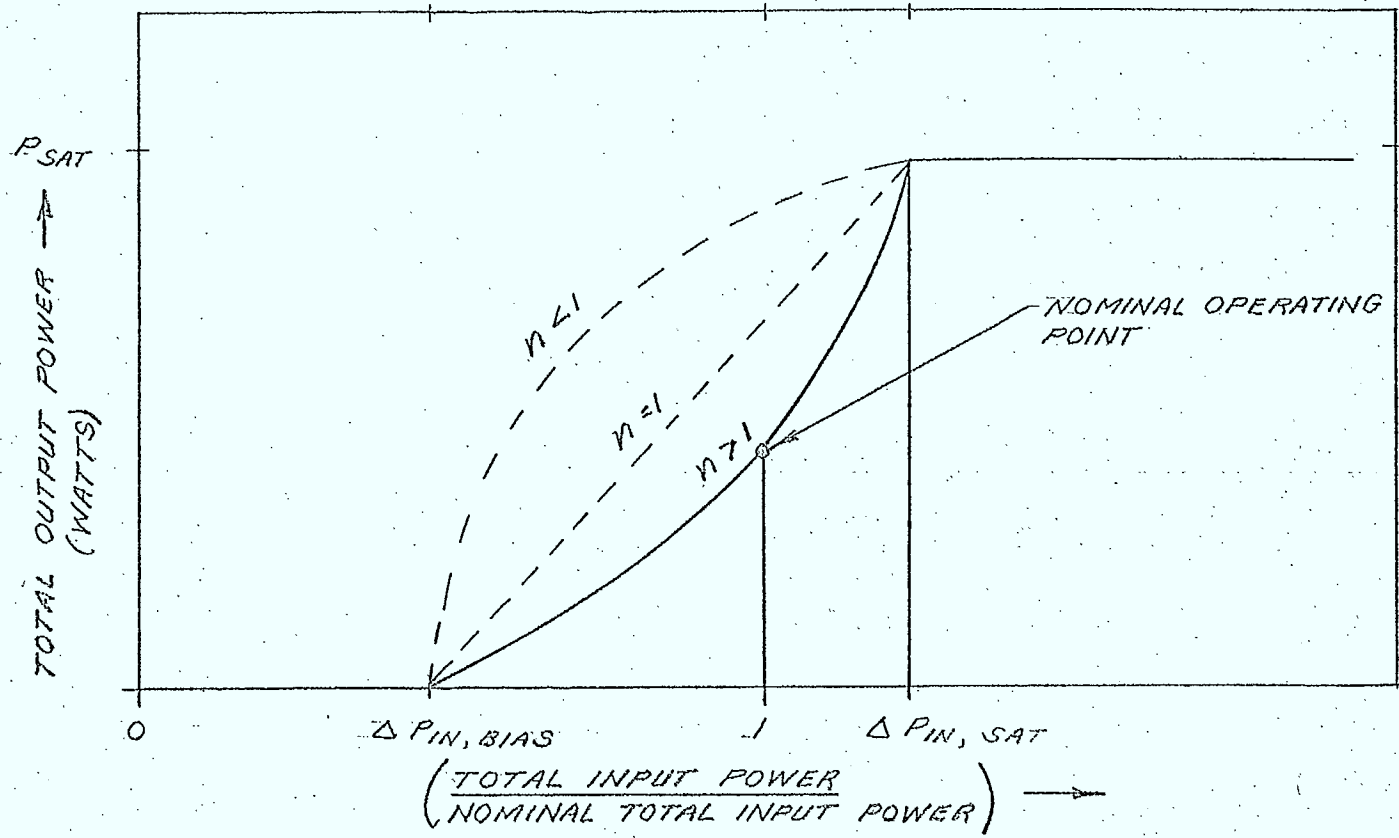


FIG. 4.10/2 BIASED, SOFT-LIMITING AMPLIFIER CHARACTERISTIC

These equations can be solved to give:

$$n = \frac{\log \Delta P_{\text{NOM}}}{\log \left[\frac{1 - \Delta P_{\text{IN,BIAS}}}{\Delta P_{\text{IN,SAT}} - \Delta P_{\text{IN,BIAS}}} \right]} \quad (4.10.12)$$

$$K = \frac{P_{\text{SAT}}}{(\Delta P_{\text{IN,SAT}} - \Delta P_{\text{IN,BIAS}})^n} \quad (4.10.13)$$

It should be noted that whenever ΔP_{IN} is less than $\Delta P_{\text{IN,BIAS}}$, the amplifier output power is zero. Whenever this "threshold" effect is encountered, a flag is set indicating this condition, and is used as a signal to the calling routine to stop the link calculation in progress.

The output parameters for a soft-limiting amplifier employing AGC are given by:

$$\begin{aligned} p_o &= P_{\text{SAT}} \Delta P_{\text{NOM}} r' \\ S_{p_o} &= r'/r \\ P_{\text{TOT}} &= P_{\text{SAT}} \Delta P_{\text{NOM}} \\ \Delta P_o &= 1 \end{aligned} \quad (4.10.14)$$

If AGC is not used, then

$$\begin{aligned} p_o &= P_{\text{TOT}} r' \\ S_{p_o} &= \frac{r' P_{\text{TOT}}}{r P_{\text{SAT}} \Delta P_{\text{NOM}}} \end{aligned} \quad (4.10.15)$$

P_{TOT} = given by equation (4.10.9)

$$\Delta P_o = \frac{P_{\text{TOT}}}{\Delta P_{\text{NOM}} P_{\text{SAT}}}$$

Hard-Limiter

A biased, hard-limiting amplifier (Reference 4.10/1) can be characterized by the following parameters:

- o P_{SAT} = total saturated output power
- o $\Delta P_{IN, BIAS}$ = $\left(\frac{\text{total input power at which output power is zero}}{\text{total nominal input power}} \right)$

The power transfer characteristic for a typical hard limiting amplifier is shown in Figure 4.10/3. The transfer curve can be expressed analytically as:

$$P_{TOT} = \begin{cases} 0 & \Delta P_{IN} < \Delta P_{IN, BIAS} \\ P_{SAT} & \Delta P_{IN} \geq \Delta P_{IN, BIAS} \end{cases} \quad (4.10.16)$$

The output parameters of the hard limiter are:

$$\begin{aligned} p_o &= r' P_{TOT} \\ s_{p_o} &= r' / r \end{aligned} \quad (4.10.17)$$

P_{TOT} - given by equation (4.10.16)

$\Delta P_{TOT} = 1$ or 0 (below threshold)

Inputs

- o δp_i = $\left(\frac{\text{carrier input power}}{\text{nominal carrier input power}} \right)$
- o r = $\left(\frac{\text{input carrier power}}{\text{total input power due to all carriers}} \right)_{\text{nominal}}$
- o flag indicating the type of amplifier:
 - linear
 - soft limiter
 - hard limiter
- o flag indicating if AGC is used

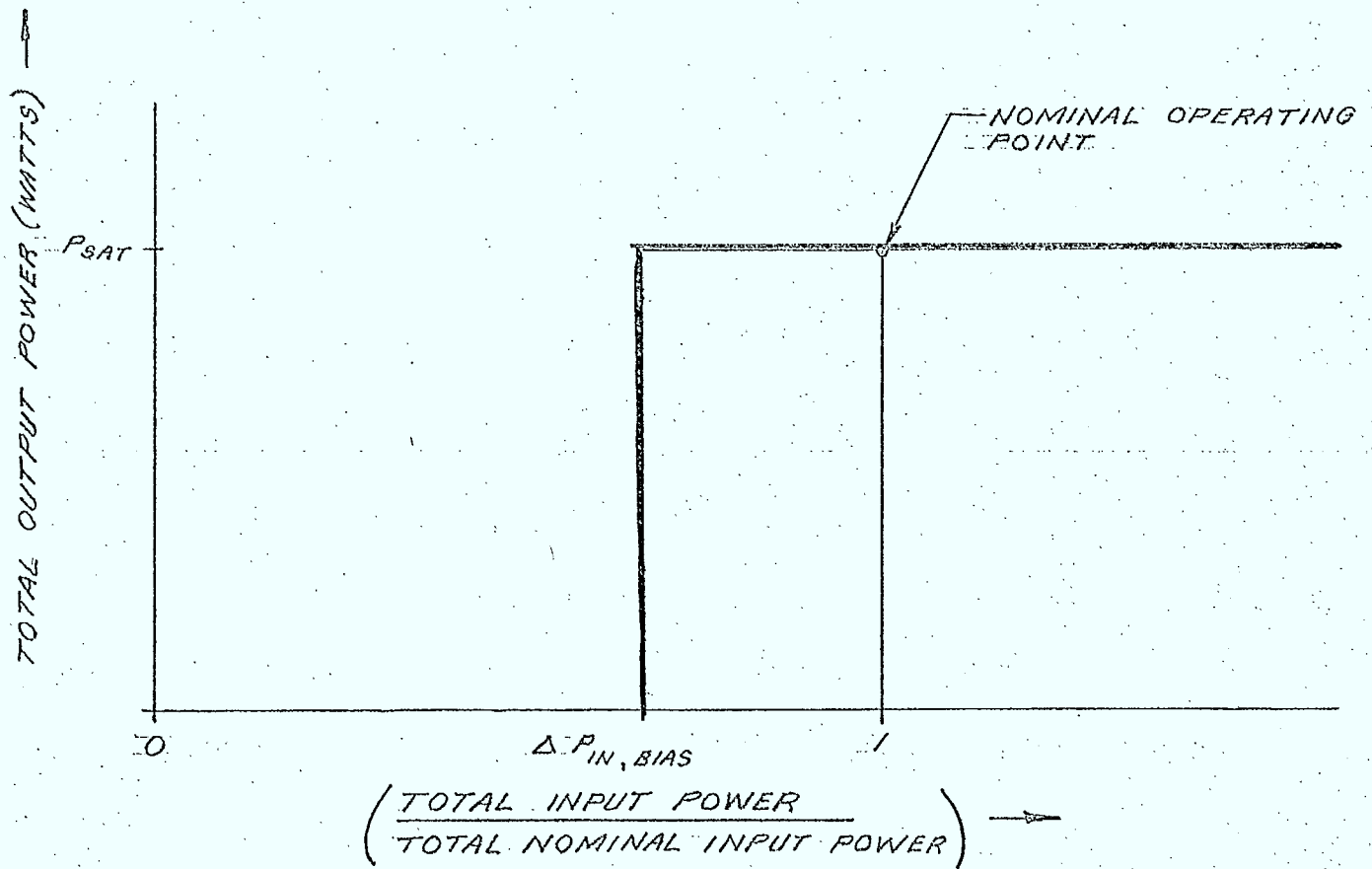


FIG. 4.10/3 POWER TRANSFER CHARACTERISTIC FOR A HARD-LIMITING AMPLIFIER.

- $P_{O,NOM}$ = the nominal carrier output power (baseband transmitters)
- P_{NOM} = the nominal amplifier total output power (linear amplifiers)
- P_{SAT} = total amplifier saturated output power (limiting amplifiers)
- ΔP_{NOM} = $\left(\frac{\text{nominal total output power}}{\text{saturated total output power}} \right)$; (soft-limiter)
- $\Delta P_{IN,BIAS}$ = $\left(\frac{\text{input power at which total output power is zero}}{\text{nominal total input power}} \right)$; (limiting amplifiers)
- $\Delta P_{IN,SAT}$ = $\left(\frac{\text{total input power at saturation}}{\text{total nominal input power}} \right)$; (soft-limiter)

Outputs

- P_{TOT} = the total output power of the amplifier
- p_0 = output power of the carrier
- ΔP_0 = $\left(\frac{\text{total amplifier output power}}{\text{total nominal amplifier output power}} \right)$
- δp_0 = $\left(\frac{\text{carrier output power}}{\text{nominal carrier output power}} \right)$
- flag indicating if the total input power is below threshold (for biased limiter models).

4.10.3 HPA Intermodulation Distortion Routine (HPAIMD)

Purpose

This subroutine calculates the intermodulation distortion spectrum in watts/Hz across the simulation bandwidth for ISI transmitters used in link calculations.

Description

This routine contains models for the intermodulation distortion noise spectrum of "linear", soft-limiter, and hard-limiter HPA's. For baseband-type transmitters, a simple distortion model is also included. This model can also be used, as an option, to describe the distortion of the other amplifiers. The assumptions made in the previous sections also apply for these models.

The main logic paths to be employed in implementing these models are illustrated in Figure 4.10/4.

For a multiple carrier amplifier such as those used in satellite repeaters, the intermodulation distortion spectrum can be approximated by a Gaussian shaped noise spectrum (Reference 4.10/2) as illustrated in Figure 4.10/5. This assumption is valid when the number of carriers is very large. For simulation purposes, it will be assumed that this approximation is valid for any number of carriers.

If it is assumed that the total output power of the amplifier, P_{TOT} , is uniformly distributed across the amplifier bandwidth, B_A , then at the center of the amplifier passband, the intermodulation distortion noise density is given by:

$$W_D(f_A) = \left(\frac{D}{C}\right)_0 \frac{P_{TOT}}{B_A}, \text{ Watts/Hz, (4.10.18)}$$

where $\left(\frac{D}{C}\right)_0$ is the distortion-to-carrier ratio at the center of the amplifier passband and f_A is the center frequency of the amplifier. At any frequency the distortion noise spectral density is given by:

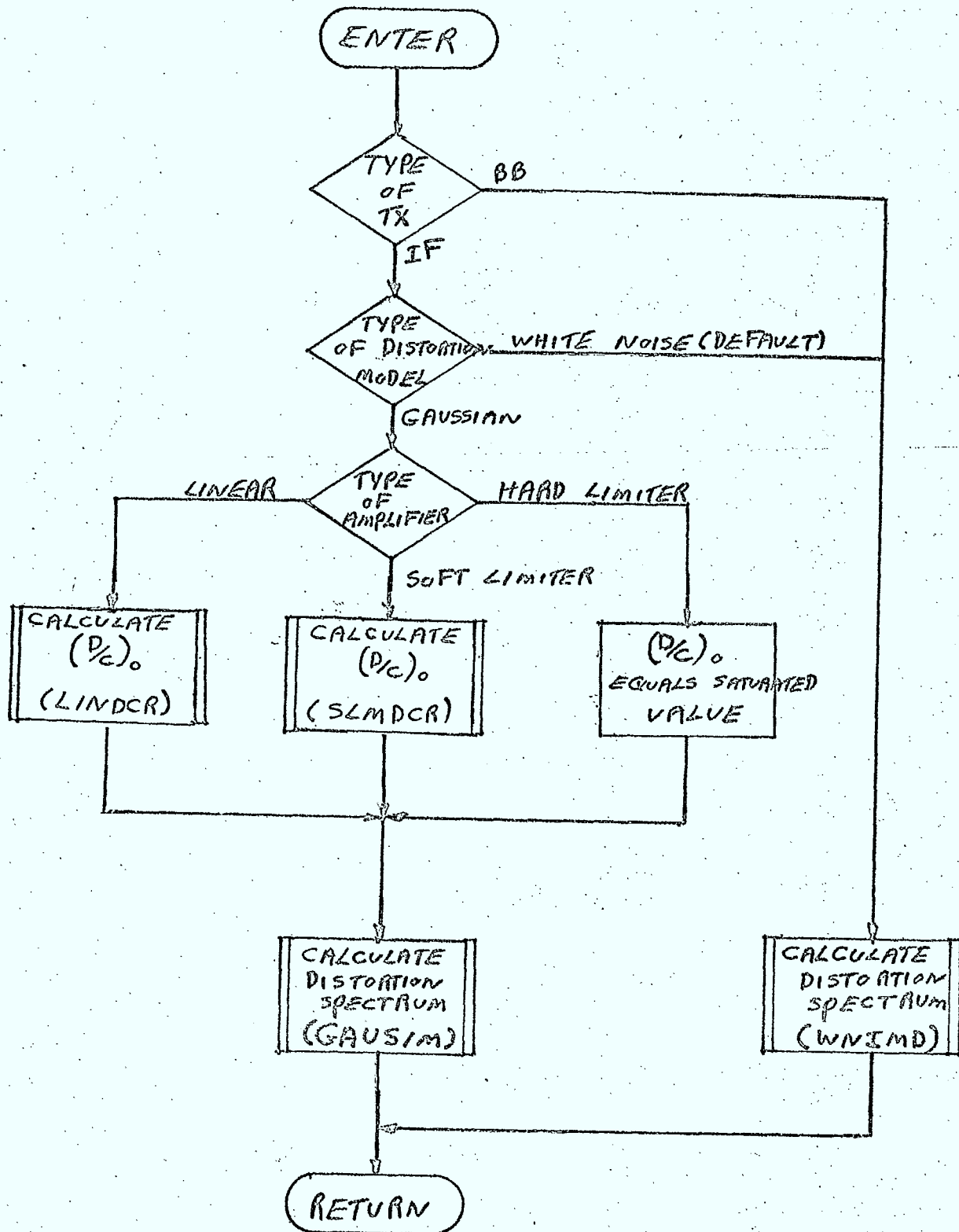
$$W_D(f) = \begin{cases} \left(\frac{D}{C}\right)_0 \frac{P_{TOT}}{B_A} \exp\left\{-\frac{(f-f_A)^2}{2\sigma^2}\right\}; & \text{Watts/Hz, } |f-f_A| \leq B_A/2 \\ 0 & ; |f-f_A| > \frac{B_A}{2} \end{cases} \quad (4.10.19)$$

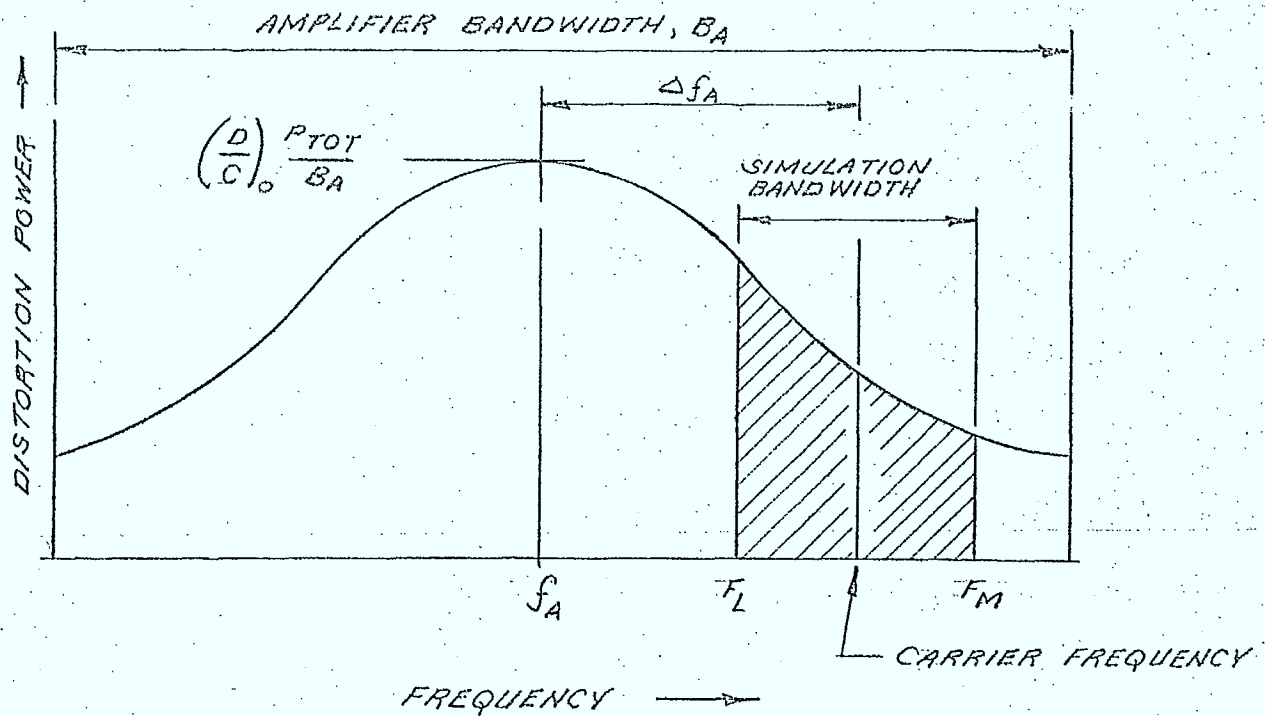
The parameter $(D/C)_0$ depends on the amplifier operating point and the type of amplifier. For a hard-limiting amplifier,

$$\left(\frac{D}{C}\right)_0 = \left(\frac{D}{C}\right)_{SAT} \quad (4.10.20)$$

where $(D/C)_{SAT}$ is the saturated output distortion-to-carrier ratio at the center of the amplifier passband. For "linear" and soft-limiting amplifiers, $(D/C)_0$ is a function of the output operating point, ΔP_0 (see previous subsection). For a "linear" amplifier, a routine, LINDCR, is used to determine $(D/C)_0$ from a parametric model. A subroutine, SLMDCR, is used to determine $(D/C)_0$ from a parametric model for soft limiter amplifiers. These routines are described in later subsections.

Figure 4.10/4 Flowchart of HPAIMD





GAUSSIAN IM DISTORTION MODEL

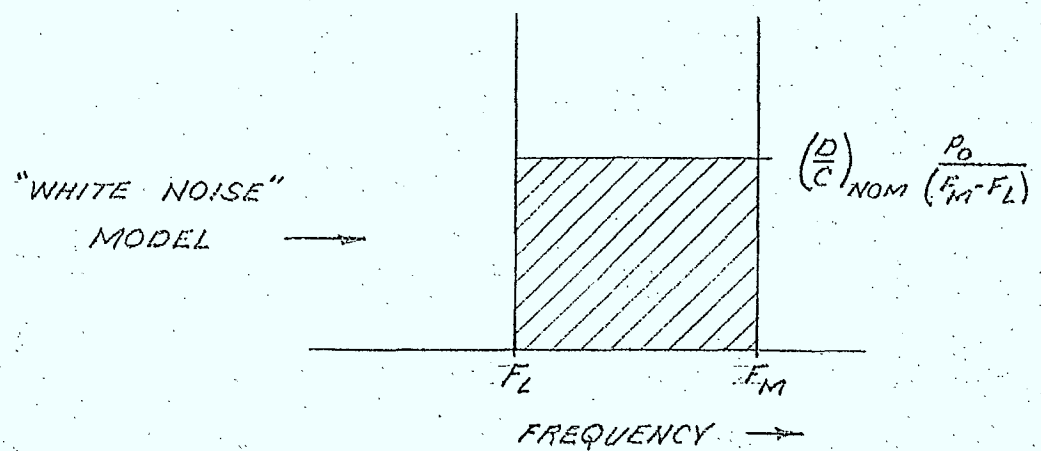


FIG: 4.10/5. IM DISTORTION SPECTRUM MODELS

The parameters B_A , σ , and Δf_A ($=f_A$ - carrier frequency) must be input by the user for this distortion spectrum model.

For baseband transmitters, and as an optional model for other HPA's, a simpler distortion model is used. This model assumes that the distortion spectrum is uniform across the RF bandwidth of the carrier (equal to the simulation bandwidth). The assumption is also made that the distortion-to-carrier ratio is independent of the amplifier input operating point. The intermodulation noise spectral density is given by:

$$W_D(f) = \begin{cases} \left(\frac{P}{C}\right)_{\text{nom}} \frac{P_o}{F_M - F_L} ; F_L < f < F_M \\ 0 ; \text{elsewhere} \end{cases} \quad (4.10.21)$$

where p_o is the output carrier power, F_L and F_M are the lower and upper frequency bounds of the simulation bandwidth. This spectrum is also illustrated in Figure 4.10/5.

Inputs

- ⊙ flag indicating type of transmitter:
 - ⊙ IF repeater
 - ⊙ baseband repeater
- ⊙ flag indicating type of distortion spectrum model selected:
 - ⊙ white noise spectrum
 - ⊙ Gaussian spectrum
- ⊙ flag indicating the type of amplifier:
 - ⊙ linear
 - ⊙ soft limiter
 - ⊙ hard limiter

- o P_{TOT} total amplifier output power (for Gaussian model)
- o ΔP_0 the change in the output operating point of the amplifier (for Gaussian model)
- o p_0 carrier output power (for white noise model)
- o F_L lower frequency bound of simulation bandwidth
- o F_M upper frequency bound of simulation bandwidth
- o Δf frequency step size
- o N number of steps across simulation bandwidth
- o B_A the amplifier bandwidth (Gaussian model)
- o σ the standard deviation of the Gaussian intermodulation distortion spectrum
- o Δf_A the center frequency of the amplifier relative to the carrier frequency (Gaussian model)
- o $\left(\frac{C}{D}\right)_{NOM}$ the carrier to distortion ratio (for the white noise spectrum model)
- o $\left(\frac{C}{D}\right)_{SAT}$ the saturated carrier to distortion ratio for hard and soft limiting amplifiers (Gaussian model)
- o $\left\{ \left(\frac{C}{D}\right)_1, \Delta P_1 \right\}$ the parameters representing the soft limiter carrier to distortion curve as a function of output backoff (measured at center frequency) (Gaussian model)
- o $\left\{ \left(\frac{C}{D}\right)_2, \Delta P_2 \right\}$
- o ΔP_{NOM} the nominal output backoff (Gaussian model)
- o $\left\{ \left(\frac{C}{D}\right)_1, \Delta P_1 \right\}$ the parameters representing the "linear" amplifier carrier-to-distortion curve as a function of the change in output operating point. (measured at center frequency) (Gaussian model)
- o $\left\{ \left(\frac{C}{D}\right)_2, \Delta P_2 \right\}$
- o $\left\{ \left(\frac{C}{D}\right)_3, \Delta P_3 \right\}$

Outputs

- o $W_{P,HPA}(f_i), i=1 \text{ to } N$ the intermodulation distortion spectrum across the simulation bandwidth

4.10.4 "Linear" Amplifier Distortion to Carrier Ratio Subroutine (LINDCR)Purpose

This subroutine calculates the distortion to carrier ratio
 $\left(\frac{D}{C}\right)_0$ at the center frequency of a "linear" amplifier.

Description

For amplifiers with approximately linear transfer characteristics, an intermodulation distortion model similar to that of section 7.2 of reference 4.10/3 is recommended. It is assumed that the user can parametrically characterize the carrier-to-intermodulation distortion as a function of the change in the output operating point by specifying 3 points on the transfer curve (see Figure 4.10/6).

Thus, for any ΔP_0 , (expressed in dB), $\left(\frac{C}{D}\right)_0$ (in db), is found by linear interpolation.

Inputs

- ΔP_0 the change in the output operating point of the amplifier
- $\left\{ \left(\frac{C}{D}\right)_1, \Delta P_1 \right\}$ the parameters representing the "linear" amplifier carrier-to-distortion curve as a function of the change in the output operating point (measured at center frequency)
- $\left\{ \left(\frac{C}{D}\right)_2, \Delta P_2 \right\}$
- $\left\{ \left(\frac{C}{D}\right)_3, \Delta P_3 \right\}$

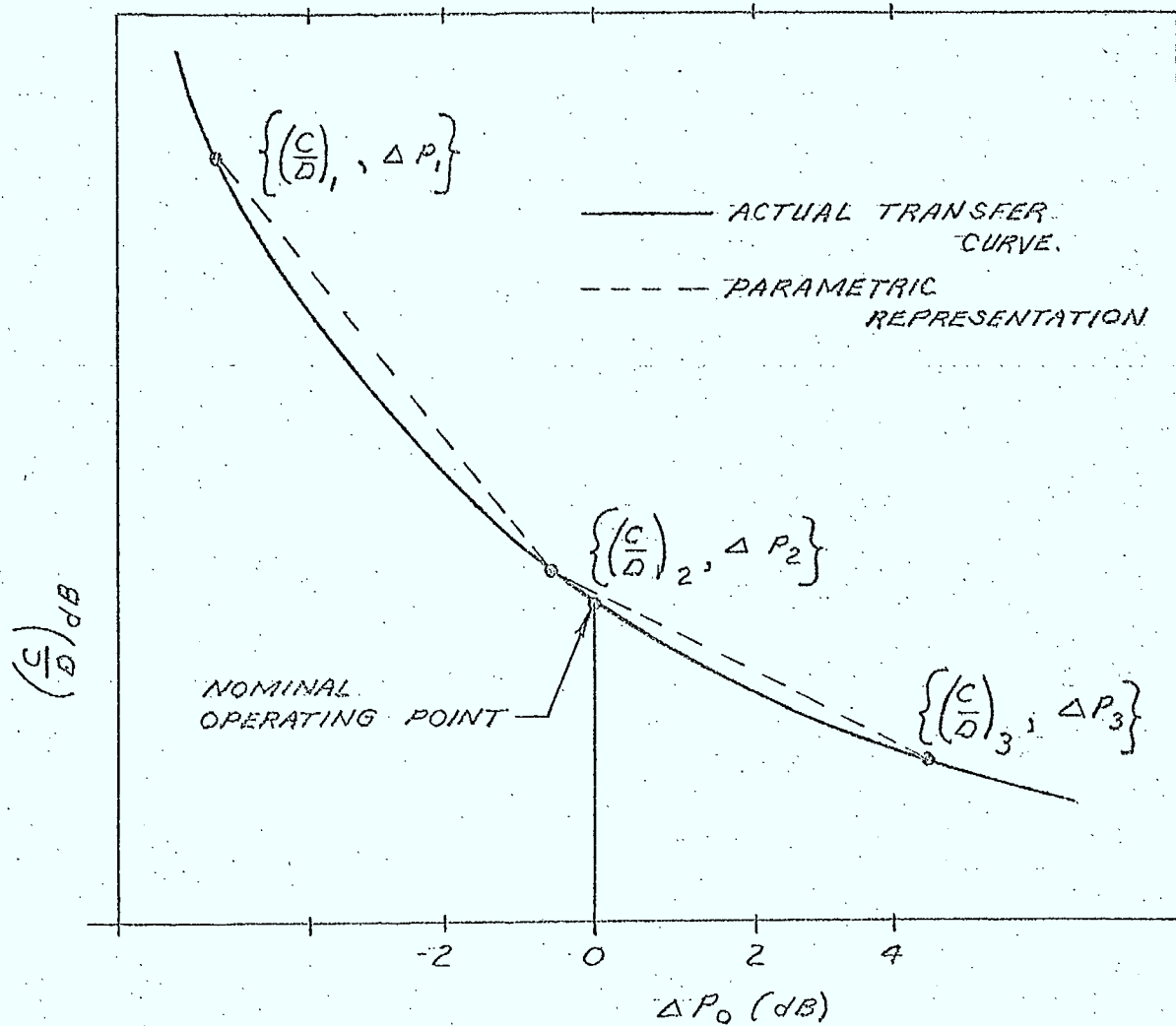


FIG: 4.10/6 $\frac{C}{D}$ AS A FUNCTION OF ΔP_0 FOR A "LINEAR" AMPLIFIER.

Outputs

$\odot \left(\frac{D}{C}\right)_0$ the distortion to carrier ratio at the center of the amplifier

4.10.5 Soft Limiter Distortion to Carrier Ratio Subroutine (SLMDCR)Purpose

This subroutine calculates the distortion to carrier ratio at the center frequency of a soft limiting amplifier.

Description

Measurements of carrier-to-intermodulation distortion for soft limiting devices can be expressed in terms of the amplifier output backoff. (reference 4.10/4, 4.10/5). Figure 4.10/7 illustrates the results of such a measurement for a typical HPA (from reference 4.10/4). This figure shows that $\frac{C}{D}$ is approximately linear over a large range of output backoff.

It is assumed that the user will characterize the $\frac{C}{D}$ curve as a function of output backoff by specifying 2 points on the transfer curve in addition to the value at saturation, $(C/D)_{SAT}$. (see Figure 4.10/8)

Thus, for any ΔP_0 , expressed in dB, the amplifier backoff is given by:

$$\Delta P \text{ (dB)} = \Delta P_{NOM} \text{ (dB)} + \Delta P_0 \text{ (dB)} \quad (4.10.22)$$

$\left(\frac{C}{D}\right)_0$ is obtained by linear interpolation.

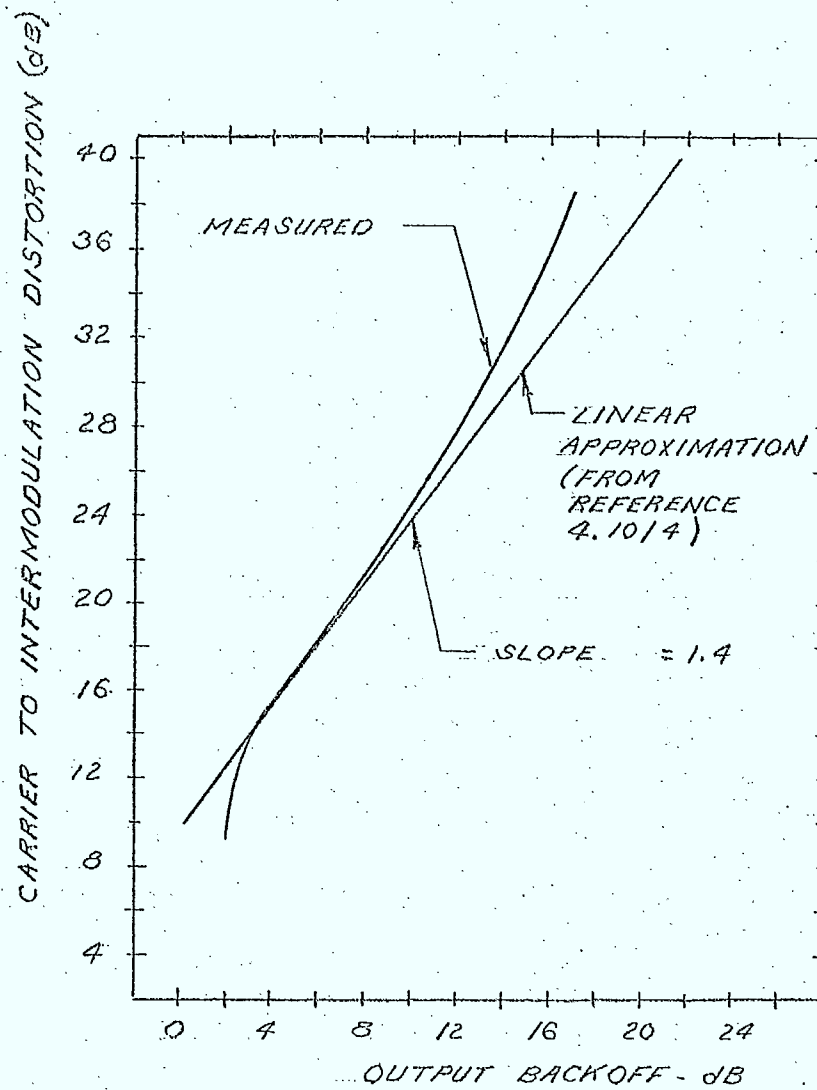


FIG: 4.10/7 CARRIER TO INTERMODULATION DISTORTION AS A FUNCTION OF OUTPUT BACKOFF

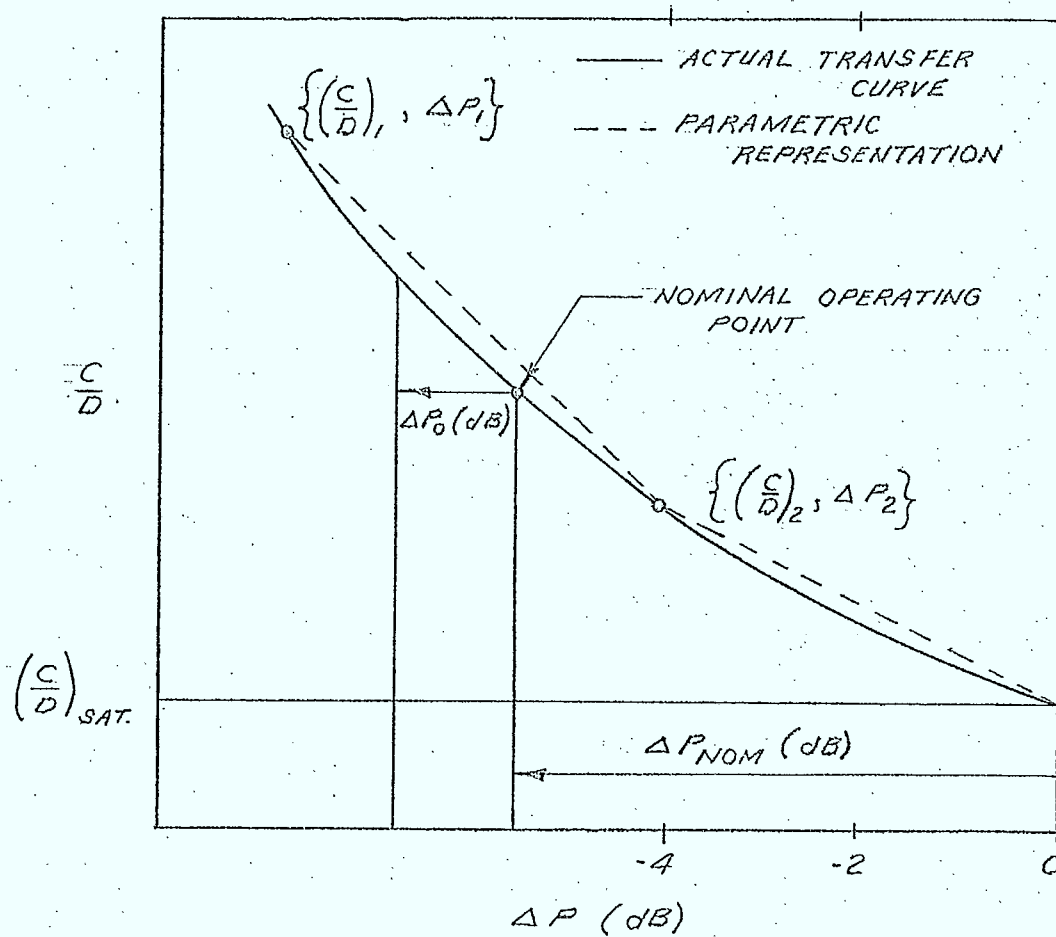


FIG: 4.10/8 PARAMETRIC REPRESENTATION OF $\frac{C}{D}$ AS A FUNCTION OF ΔP .

Inputs

- ΔP_0 the change in the output operating point of the amplifier
- ΔP_{NOM} the nominal output backoff defined as

$$\left(\frac{\text{nominal output power}}{\text{saturated output power}} \right)$$
- $\left(\frac{C}{D} \right)_{SAT}$ the saturated carrier to distortion ratio
- $\left\{ \left(\frac{C}{D} \right)_1, \Delta P_1 \right\}$ the parameters representing the soft limiter carrier-to-distortion curve as a function of output backoff (measured at center frequency)
- $\left\{ \left(\frac{C}{D} \right)_2, \Delta P_2 \right\}$

Outputs

- $\left(\frac{D}{C} \right)_0$ the distortion to carrier ratio at the center of the amplifier

4.10.6 Gaussian Distortion Spectrum Model (GAUSIM)Purpose

This routine computes the intermodulation distortion spectrum across the simulation bandwidth for the Gaussian distortion spectrum model.

Description

The distortion noise spectral density for the Gaussian distortion model is given in a previous section as (see Figure 4.10/5):

$$W_D(f) = \begin{cases} \left(\frac{D}{C} \right)_0 \frac{P_{TOT}}{B_A} \exp \left\{ -\frac{(f-f_A)^2}{2\sigma^2} \right\}; \text{ watts/Hz}, |f-f_A| < B_A/2 \\ 0 & ; |f-f_A| > B_A/2 \end{cases} \quad (4.10.23)$$

The intermodulation distortion spectrum across the simulation bandwidth is computed by evaluating this expression at frequencies given by:

$$f_i = F_L + (i - \frac{1}{2})\Delta f \quad i=1 \text{ to } N \quad (4.10.24)$$

Inputs

- o F_L lower frequency bound of simulation bandwidth
- o F_M upper frequency bound of simulation bandwidth
- o Δf frequency step size
- o N number of steps across simulation bandwidth
- o B_A amplifier bandwidth
- o σ standard deviation of intermodulation distortion spectrum
- o Δf_A center frequency of amplifier relative to carrier frequency
- o $\left(\frac{D}{C}\right)_0$ distortion to carrier ratio at centre frequency of amplifier
- o P_{TOT} the total amplifier output power

Outputs

- o $W_{D,HPA}(f_i); i=1 \text{ to } N$ the intermodulation distortion spectrum across the simulation bandwidth in watts/Hz

4.10.7 White Noise Distortion Spectrum Model (WNIMD)

Purpose

This routine computes the intermodulation distortion spectrum across the simulation bandwidth for the white noise distortion spectrum model.

Description

The distortion noise spectral density for this model is given in a previous section as (see Figure 4.10/5):

$$W_D(f) \begin{cases} \left(\frac{D}{C}\right)_{\text{NOM}} \frac{P_0}{(F_M - F_L)} & , F_L < f < F_M \\ 0 & , \text{elsewhere} \end{cases} \quad (4.10.25)$$

Inputs

- F_L lower frequency bound of simulation bandwidth
- F_M upper frequency bound of simulation bandwidth
- Δf frequency step size
- N number of steps across the simulation bandwidth
- $\left(\frac{D}{C}\right)_{\text{NOM}}$ the nominal carrier to distortion ratio
- P_0 carrier output power

Outputs

- $W_{D,\text{HPA}}(f_i); i=1 \text{ to } N$ the intermodulation distortion spectrum across the simulation bandwidth

References

- 4.10/1: Johannsen, K.G., Paulsen, F.L., Dutcher, G.L.,
"Signal to Intermodulation Noise in Biased Limiting Amplifiers",
IEEE Transactions on Communications, July 1975
- 4.10/2: Cahn, C.R., "Calculation of Intermodulation Due to Amplitude
Limiting of Multiple Carriers", Concise Papers, IEEE
Transactions on Communication Technology, December 1968
- 4.10/3: SED 0710-44-TR-102, Issue 4; "Orbit Frequency Utilization
Simulation - Volume 1 - Analytical Foundation", February 28,
1977
- 4.10/4: Weinberger, H.I. and Kanehira, E.M., "Single Channel Per
Carrier Satellite Repeater Channel Capacity", IEEE Transactions
on Aerospace and Electronic Systems, Vol. AES-11, No. 5,
September 1975
- 4.10/5: Dicks, J.L., Schultze, P.H., and Schmitt, C.H., "Systems
Planning", Comsat Technical Review, Volume 2, Number 2, 1972

4.11 Low Noise Amplifier Model (LNA)

4.11.1 General

The major subroutine modelling the LNA simulates the power transfer characteristics of a "linear" amplifier (subroutine LNA). An intermodulation distortion model identical to that developed for the "linear" HPA (see section 4.10) is also used. Thus, this routine calls the following routines described in section 4.10:

- o LINDCR "Linear" amplifier distortion-to-carrier ratio subroutine
- o GAUSIM Gaussian distortion spectrum model
- o WNIMD white noise distortion spectrum model

This subroutine and its associated subprograms are required in link analyses.

The LNA is assumed to have a nominal gain of 1. The intermodulation distortion model makes the same assumptions similar to those described for the HPA intermodulation distortion model in section 4.10.

4.11.2 Low Noise Amplifier Subroutine (LNA)

Purpose

This routine calculates the output power of the LNA and its intermodulation distortion power spectrum (Note: noise temperature of the LNA is input by the user and thus is not modelled in this routine).

Description

This routine contains models for the following type of low noise amplifiers:

- o "linear", single or multi-carrier LNA's with AGC
- o "linear", single or multi-carrier LNA's without AGC

A Gaussian or white noise intermodulation distortion spectrum model can be selected by the user. The major logic paths of this subroutine are shown in Figure 4.11/1.

The ratio of total input power to the nominal total input power is given by (derived in section 4.10):

$$\Delta P_{in} = (1 - r + \sum \delta p_i r) \quad (4.11.1)$$

The ratio of input carrier power to the total input power is given by (derived in section 4.10):

$$r' = \frac{\sum \delta p_i r}{\Delta P_{in}} \quad (4.11.2)$$

The output parameters calculated in this routine are:

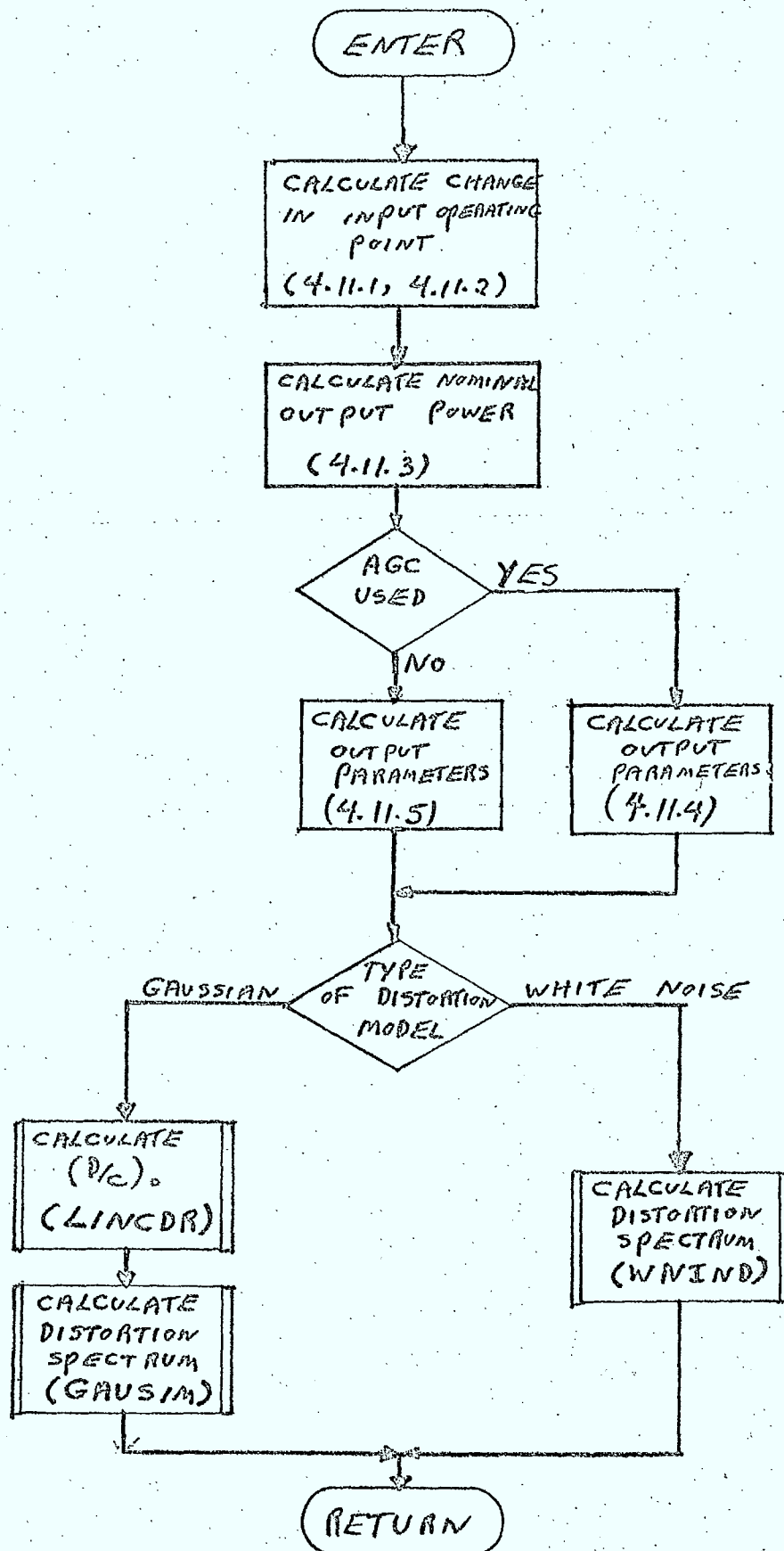
- o $\left(\frac{\text{the output carrier power}}{\text{nominal output carrier power}} \right) \cdot \delta p_0$
- o the distortion power spectrum across the simulation bandwidth in watts/Hz, $W_{D,LNA}(f_i)$; $i=1$ to N

δp_0 is required since it affects the input power to the next amplifier in the link.

Several internal parameters are computed which are required by the intermodulation distortion models. These are:

- o $\left(\frac{\text{total output power of the amplifier}}{\text{nominal total output power of amplifier}} \right) \cdot \Delta P_0$
- o the carrier output power, P_0
- o the total output power of the amplifier, P_{TOT}

Figure 4.11/1 Flowchart of LNA



The nominal output power of the amplifier, P_{NOM} , is given by:

$$P_{NOM} = \left(\frac{P_{IN}}{r} \right) \left(\frac{1}{S p_i} \right) \quad (4.11.3)$$

where P_{IN} is the actual carrier input power.

Thus, for an LNA, using AGC, δp_0 and the other internal parameters listed above are given by:

$$\begin{aligned} p_o &= r' P_{TOT} = \frac{r' P_{IN}}{r S p_i} \\ S p_o &= \frac{r' P_{TOT}}{r P_{NOM}} = r'/r \\ P_{TOT} &= P_{NOM} = P_{IN}/r S p_i \\ \Delta P_o &= 1 \quad (0 \text{ dB}) \end{aligned} \quad (4.11.4)$$

If AGC is not used, then:

$$\begin{aligned} p_o &= r' P_{TOT} = \frac{r' \Delta P_o P_{IN}}{r S p_i} \\ S p_o &= \frac{r' P_{TOT}}{r P_{NOM}} = S p_i \\ P_{TOT} &= \Delta P_o P_{NOM} = \frac{\Delta P_o P_{IN}}{r S p_i} \\ \Delta P_o &= \Delta P_{IN} \end{aligned} \quad (4.11.5)$$

If the default white noise distortion spectrum model is not overridden by the user, subroutine WNIMD, described in section 4.10.7, is called to compute the spectrum across the simulation bandwidth.

If the Gaussian distortion spectrum model has been selected, subroutine LINCDR described in section 4.10.4, is called to compute the distortion to carrier ratio, $\left(\frac{D}{C}\right)_0$, at the center frequency of the amplifier.

Once $\left(\frac{D}{C}\right)_0$ is calculated, subroutine GAUSIM, described in section 4.10.6, is called to compute the intermodulation noise spectrum across the simulation bandwidth.

Inputs

- o P_{IN} input carrier power (actual) in watts
- o r $\left(\frac{\text{input carrier power}}{\text{total input power due to all carriers}}\right)_{\text{nominal}}$
- o δp_i $\left(\frac{\text{actual input carrier power}}{\text{nominal input carrier power}}\right)$
- o flag indicating whether or not AGC is used
- o flag indicating type of distortion model
 - white noise
 - Gaussian
- o B_A amplifier bandwidth
- o Δf_A center frequency of amplifier relative to carrier frequency
- o σ standard deviation of the Gaussian intermodulation distortion spectrum
- o $\left\{\left(\frac{C}{D}\right)_1, \Delta P_1\right\}$ the parameters representing the "linear" amplifier carrier-to-distortion curve as a function of the change in output operating point (measured at center frequency) (Gaussian model)
- o $\left\{\left(\frac{C}{D}\right)_2, \Delta P_2\right\}$
- o $\left\{\left(\frac{C}{D}\right)_3, \Delta P_3\right\}$

- F_L lower frequency bound on simulation bandwidth
- F_M upper frequency bound on simulation bandwidth
- Δf frequency step size
- N number of steps across simulation bandwidth

Outputs

- δp_0 $\left(\frac{\text{output carrier power}}{\text{nominal output carrier power}} \right)$
- $W_{D,LNA}(f_i)$, $i=1$ to N the intermodulation distortion spectrum across the simulation bandwidth in watts/Hz

4.12 Antenna Noise Temperature

4.12.1 General

In this section, the antenna noise temperature models for receiving antennas located at earth stations, ships or on aircraft, and spacecraft are discussed. Noise sources to be considered are:

- ⊙ sky (tropospheric)
- ⊙ ground
- ⊙ galactic
- ⊙ solar
- ⊙ man made

The user can directly specify the antenna noise temperature for the various types of receiving sites, by entering the noise temperature into the ISI receiver carrier record.

An analytical model is presented, which can be used to calculate the antenna noise temperature as a function of antenna on-axis gain, frequency, and boresight elevation angle, for earth station, aircraft, or ship receiving antennae. Major assumptions made are:

- ⊙ the noise temperature of a spacecraft antenna is given by the physical temperature of the earth (290°K). The user may over-ride this value by specifying a new noise temperature in the ISI receiver carrier record.
- ⊙ the antenna gain pattern is assumed to be a symmetric Gaussian shaped pattern, unless specified as an isotropic antenna.
- ⊙ for on-axis gains less than 3 ($\approx 4.7\text{dB}$) the antenna gain pattern is assumed to be isotropic.

4.12.2 Antenna Noise Temperature Subroutine (ANTEMP)Purpose

This subroutine calculates the antenna noise temperature for receiving antennae located at earth stations, ships, or aircraft.

Description

The general expression for antenna noise temperature is given by (Reference 4.12/1) (see Figure 4.12/1):

$$T_A = \frac{1}{4\pi} \int_0^{2\pi} \int_0^{\pi} T(\theta, \phi) G(\theta, \phi) \sin \theta d\theta d\phi \quad (4.12.1)$$

where $T(\theta, \phi)$ is the temperature distribution function and $G(\theta, \phi)$ is the normalized antenna directivity such that:

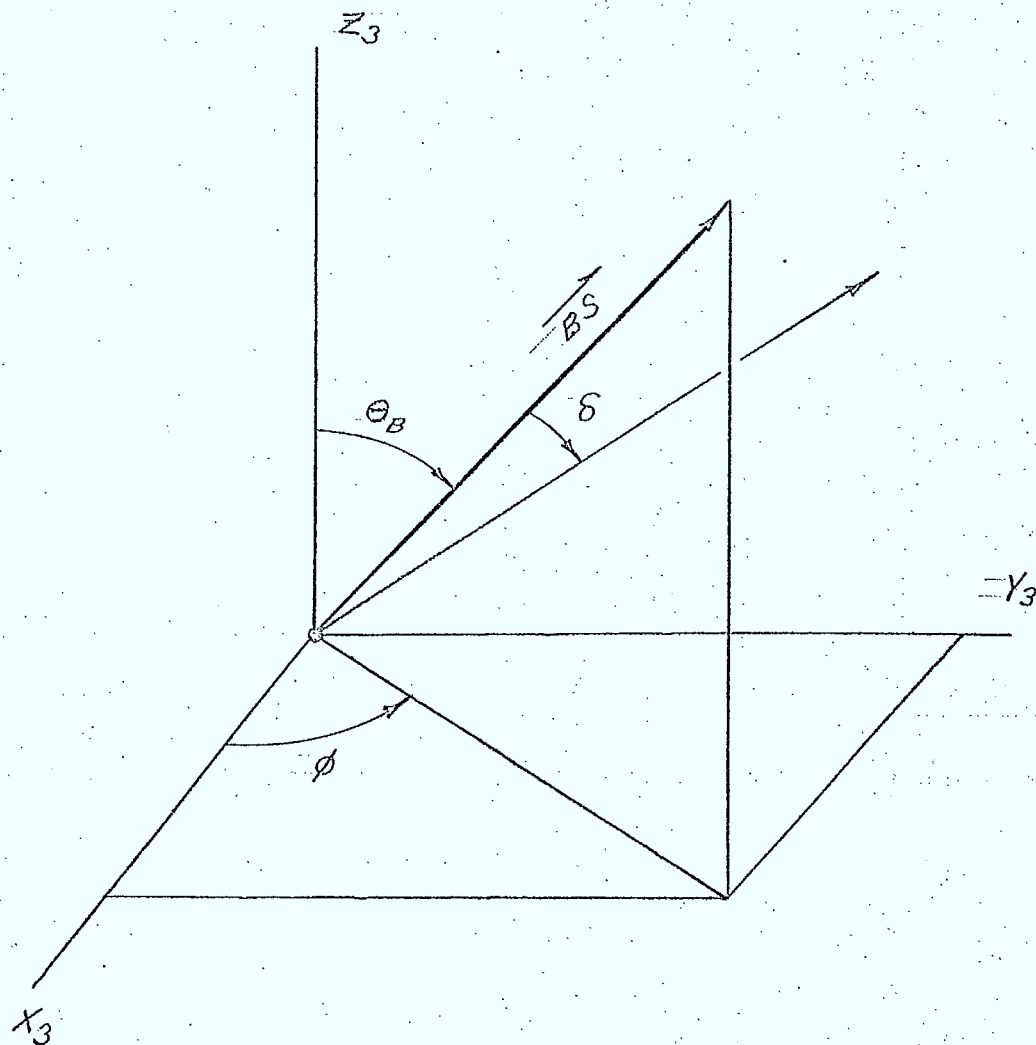
$$\int_0^{2\pi} \int_0^{\pi} G(\theta, \phi) \sin \theta d\theta d\phi = 4\pi \quad (4.12.2)$$

Normalization of Gain Pattern

For moderate to high gain antennas, the gain will be written as:

$$G(\theta, \phi) = G_0 e^{-a' G_0 \delta^2(\theta, \phi)} \quad (4.12.3)$$

where G_0 is the on-axis gain, δ is the off-axis angle, and a' is a normalization constant.



\overrightarrow{BS} - ANTENNA BORESIGHT

δ - OFF AXIS ANGLE (CAN
BE EXPRESSED IN TERMS
OF θ, ϕ).

θ, ϕ - SPHERICAL POLAR CO-ORDINATES
ON A LOCAL VERTICAL REFERENCE
FRAME

Z_3 - LOCAL VERTICAL

Y_3 - DUE SOUTH

FIG. 4.12/1 ANTENNA NOISE TEMPERATURE GEOMETRY.

For low gain ($G_0 < 3$) or isotropic antennas, it is assumed that $G(\theta, \phi)$ can be written as:

$$G(\theta, \phi) = 1 \quad (4.12.4)$$

The normalization condition for equation (4.12.3) can be written:

$$\int_0^{2\pi} \int_0^\pi G_0 e^{-a' G_0 \delta^2} \sin \delta \, d\delta \, d\phi' = 4\pi \quad (4.12.5)$$

$$2\pi \int_0^\pi G_0 e^{-a' G_0 \delta^2} \sin \delta \, d\delta = 4\pi$$

By assuming that the exponential in the integrand is very small at $\delta = \pi$, the integral can be written as:

$$2\pi \int_0^\infty G_0 e^{-a' G_0 \delta^2} \sin \delta \, d\delta = 4\pi \quad (4.12.6)$$

This integral has been reduced to the Dawson's integral form (reference 4.12/2) and tabulated values have been used to determine a' as a function of G_0 (see Figure 4.12/2). It can be seen from Figure 4.12/2 that a' is well behaved from $G_0 \approx 3$ (~ 4.7 dB).

Equation (4.12.3) has been plotted in Figure 4.12/3, for several values of G_0 , together with the CCIR antenna patterns, (reference 4.12/3).

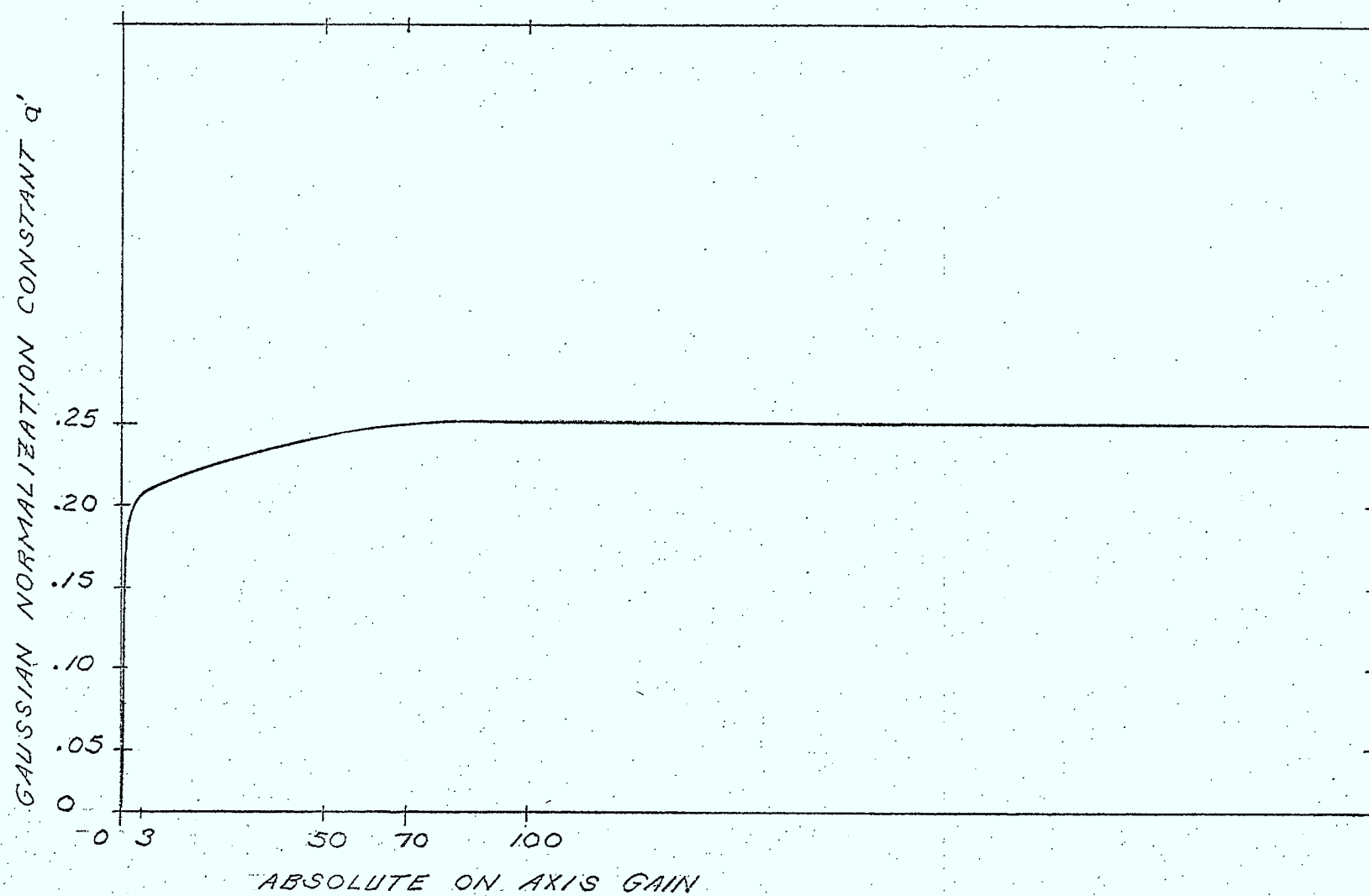


FIG. 4.12/2 - NORMALIZATION CONSTANT q' AS FUNCTION OF G_0

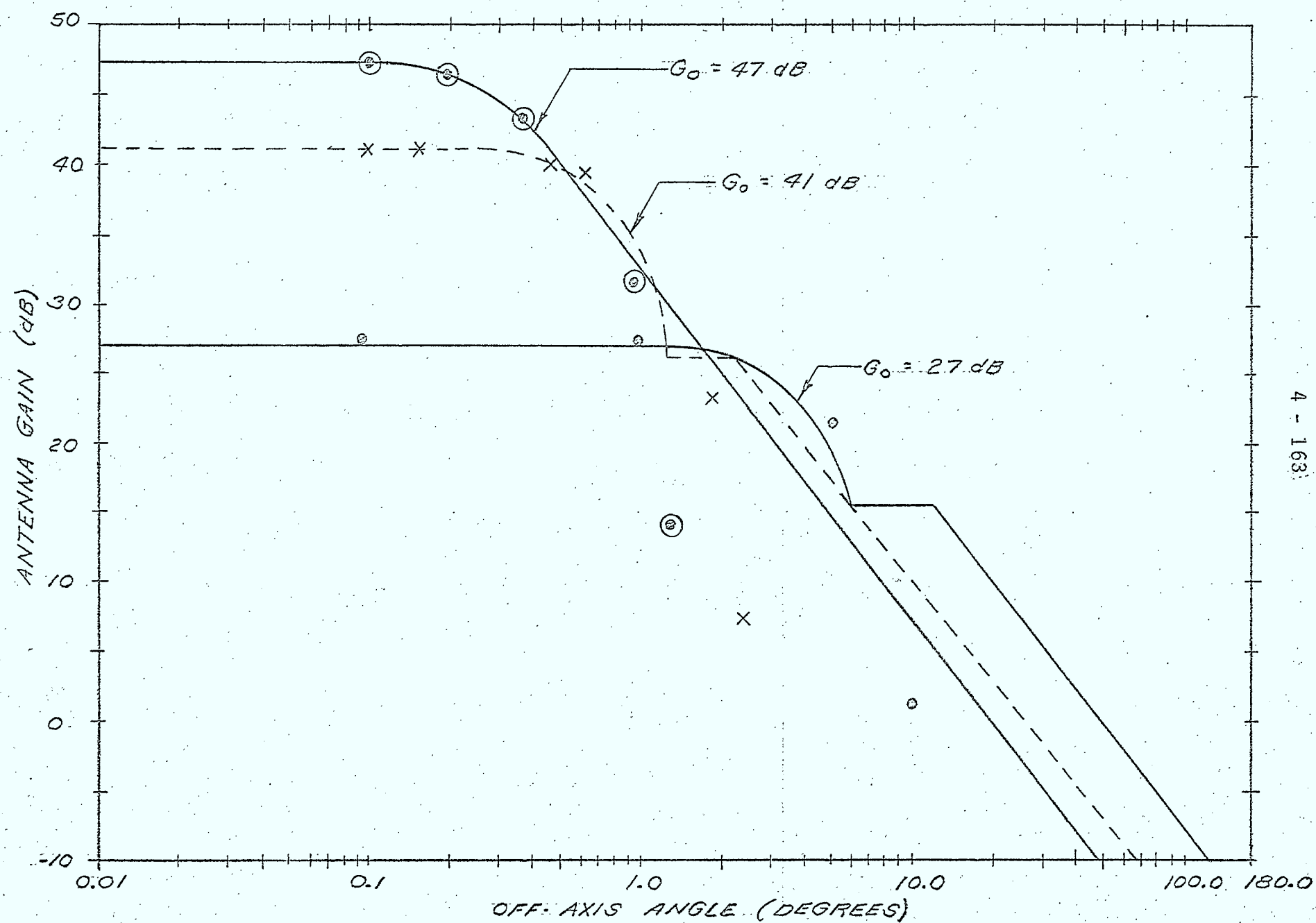


FIG. 4.12/3 CCIR ANTENNA PATTERNS VERSUS GAUSSIAN ANTENNA MODEL

The gain pattern predicted by equation (4.12.3) is over idealized since the gain in the far sidelobe and back lobe regions is negligible, which is not true of actual antennae.

To use the gain pattern expressed by equation (4.12.3) in noise temperature calculations (equation 4.12.1), the off-axis angle δ must be expressed in terms of spherical polar coordinates θ, ϕ . By suitable choice of a coordinate system (which can be done if it is assumed that the temperature distribution $T(\theta, \phi)$ has no azimuthal dependence), the antenna boresight vector can be written as:

$$\vec{B_s} = \sin \theta_B \hat{x} + \cos \theta_B \hat{z} \quad (4.12.7)$$

where θ_B is the zenith angle of the boresight. Similarly, any arbitrary direction can be written as:

$$\vec{D_i} = \cos \phi \sin \theta \hat{x} + \sin \phi \sin \theta \hat{y} + \cos \theta \hat{z} \quad (4.12.8)$$

Thus, $\delta(\theta, \phi)$ is found by:

$$\begin{aligned} \delta(\theta, \phi) &= \cos^{-1} (\vec{B_s} \cdot \vec{D_i}) \\ &= \cos^{-1} (\sin \theta_B \cos \phi \sin \theta + \cos \theta_B \cos \theta) \end{aligned} \quad (4.12.9)$$

Equation (4.12.1) can now be evaluated numerically once the temperature distribution function is known.

Antenna Noise Temperature for Earth Station and Ship Receiving Antennae

The antenna noise temperature for an earth station (or ship) receiving antenna can be written as:

$$T_A = \frac{1}{4\pi} \int_0^{2\pi} \int_0^{\pi} T(\theta) G_0 e^{-a' G_0 \delta^2} \sin \theta d\theta d\phi \quad (4.12.10)$$

δ can be expressed in terms of θ , ϕ , and the boresight zenith angle using equation (4.12.9).

The integral can be evaluated numerically over the following distributed temperature sources:

- sky (tropospheric)
- ground
- cosmic

The source data of Figure 4.12/4 (from reference 4.12/4), extended down to 200 MHz, will be used in a curve fitting technique to derive an analytical expression, $T_T(\theta, f)$, for tropospheric noise temperature as a function of a zenith angle and frequency, similar to that given in section 8.2 of reference 4.12/3. Thus, the tropospheric noise temperature is given by:

$$T_T = \begin{cases} T_T(\theta, f) & ; 0 \leq \theta \leq \frac{\pi}{2} \\ 0 & ; \frac{\pi}{2} < \theta \leq \pi \end{cases} \quad (4.12.11)$$

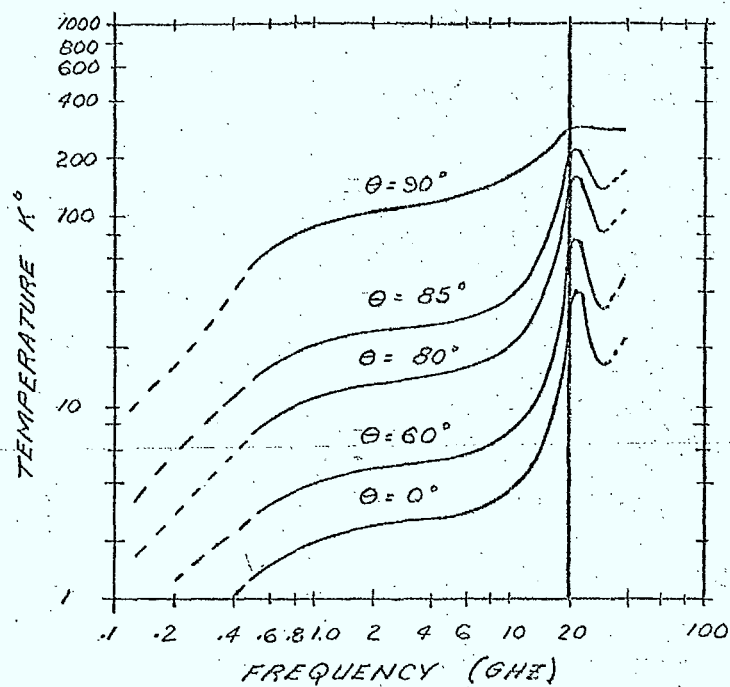


FIG: 4.12/4 SKY NOISE TEMPERATURE DUE TO OXYGEN AND WATER VAPOUR.

The noise temperature of the ground, T_G , is assumed to be a constant for a particular type of terrain and will be user specified (defaults to 290°K).. Thus:

$$T_G = \begin{cases} 0 & ; 0 \leq \theta \leq \frac{\pi}{2} \\ \text{constant} & ; \frac{\pi}{2} < \theta \leq \pi \end{cases} \quad (4.12.12)$$

The average galactic noise temperature is derived from Reference 4.12/4 and is given by:

$$T_{GAL} = \begin{cases} \frac{26.1}{f^2} & ; 0 \leq \theta \leq \frac{\pi}{2} \\ 0 & ; \frac{\pi}{2} < \theta \leq \pi \end{cases} \quad (4.12.13)$$

where f is the frequency in GHz.

The antenna temperature contribution due to these distributed sources is given by:

$$\begin{aligned} T_{A,D} = & \frac{1}{4\pi} \left[\int_0^{2\pi} \int_0^{\frac{\pi}{2}} T_T(\theta, \phi) G_0 e^{-a' G_0 S^2(\theta, \phi)} \sin \theta d\theta d\phi \right. \\ & + T_G \int_0^{2\pi} \int_{\frac{\pi}{2}}^{\pi} G_0 e^{-a' G_0 S^2(\theta, \phi)} \sin \theta d\theta d\phi \\ & \left. + \frac{26.1}{f^2} \int_0^{2\pi} \int_{\frac{\pi}{2}}^{\pi} G_0 e^{-a' G_0 S^2(\theta, \phi)} \sin \theta d\theta d\phi \right] \quad (4.12.14) \end{aligned}$$

Each of the integral terms in equation (4.12.14) will be evaluated numerically (off line) for various on-axis gains, frequencies, and over the 0° to 90° boresight elevation range. The data generated from these runs will be used as source data, for curve fitting techniques, from which, the antenna temperature due to the distributed sources, $T_{A,D}(G_0, \theta_B, f)$, can be expressed analytically.

The first two terms of equation (4.12.14) have been evaluated numerically for the temperature distribution function illustrated in Figure 4.12/5.

The functional form for $0 \leq \theta < \pi_a$ was chosen to give reasonable agreement with the results at 2 GHz derived from Reference 4.12/3.

Figure 4.12/6 shows the antenna temperature calculated for different low gain (broad beam) antennas, as a function of elevation angle using this temperature distribution function. The limiting case for very high gain antennae and isotropic antennae is also shown.

As pointed out previously, the antenna gain pattern expressed by the Gaussian is over idealized and predicts a negligible antenna noise temperature contribution from the backlobes. To compensate for this, the antenna temperature is corrected by adding a constant temperature contribution T_B , chosen to give good agreement with measurements (defaults to 250K from Reference 4.12/5). Thus the antenna temperature due to distributed sources is given by:

$$T_{A,D} = T_{A,D}(G_0, \theta_B, f) + T_B \quad (4.12.15)$$

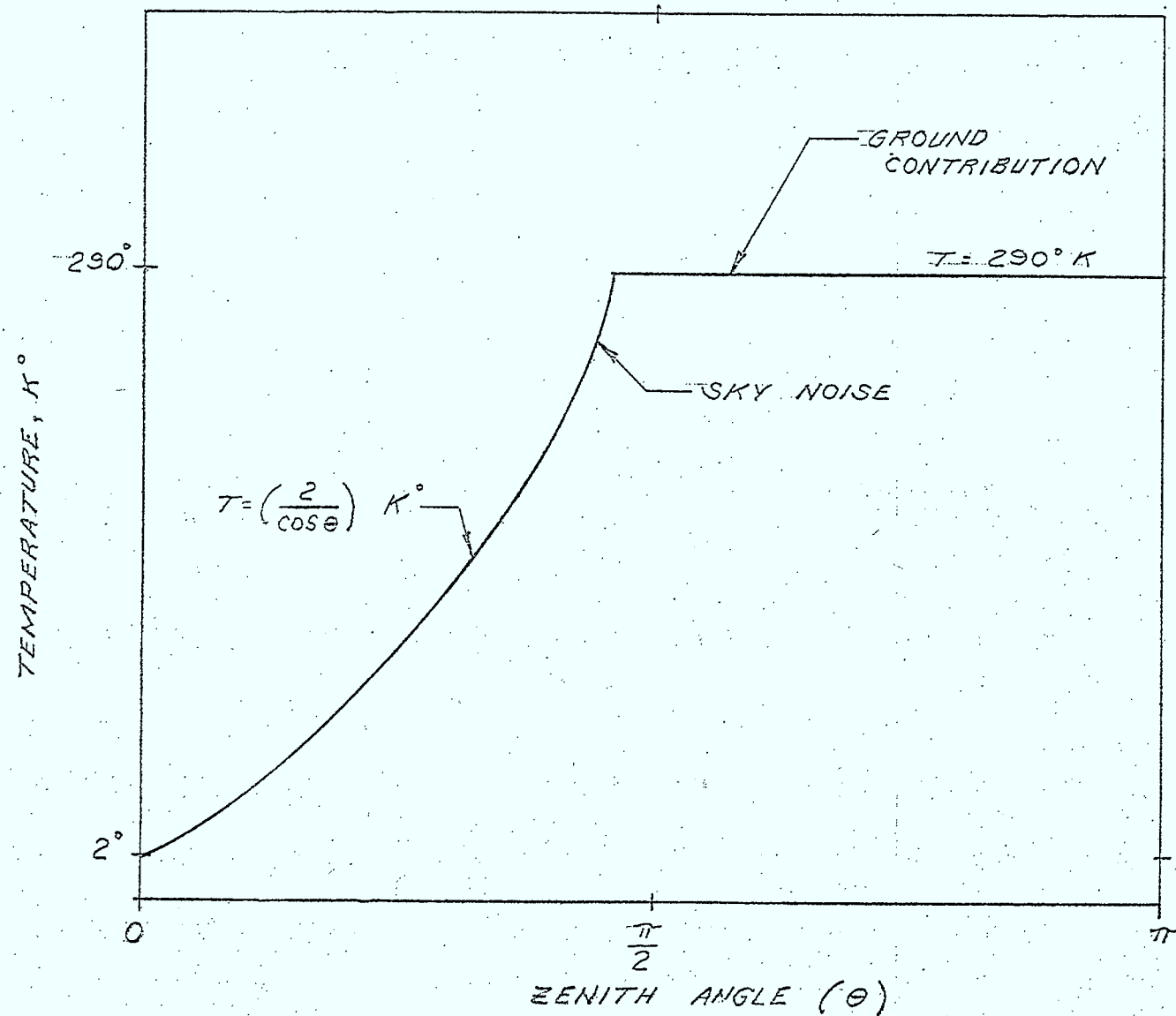


FIG. 4.12/5 TEMPERATURE DISTRIBUTION FOR TEST OF ANTENNA NOISE TEMPERATURE MODEL.

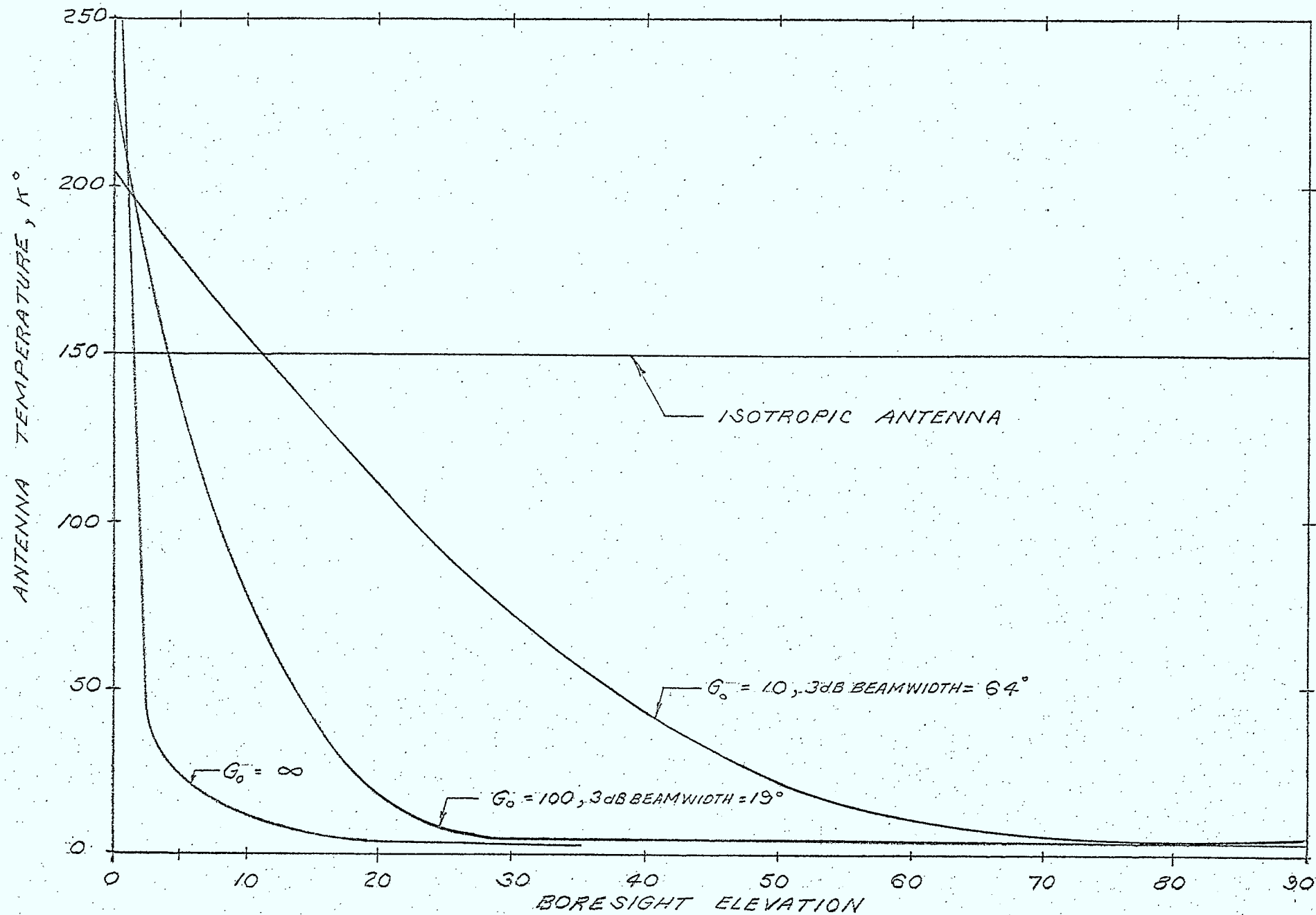


FIG. 4.12/6 MAIN BEAM AND NEAR SIDELobe ANTENNA NOISE TEMPERATURE DUE TO TROPOSPHERIC AND GROUND SOURCES EVALUATED USING EQUATION (4.12.16)

In addition to the distributed sources mentioned above, other noise temperature sources to the receiver antenna are:

- o solar
- o man made

The solar contribution to the antenna noise temperature is written as:

$$T_{A,S} = \frac{T_S G_S}{4\pi} \iint \sin \theta d\theta d\phi \quad (4.12.16)$$

solid angle subtending sun

$$= \frac{T_S G_S \Omega_S}{4\pi}$$

where T_S is assumed to be constant over the solar disc and zero elsewhere, G_S is the antenna gain in the direction of the sun (assumed to be constant over the solar disc), and Ω_S is the solid angle subtended by the sun (6.8×10^{-5} steradians).

T_S is given in reference 4.12/4 as:

$$T_S = \frac{675 \times 290}{f} \text{ , } K^\circ \text{ (quiet sun)} \quad (4.12.17)$$

where f is in GHz.

G_S is determined by:

- o calling subroutine SUNLOC, described in section 4.2.7, to determine the location vector and zenith angle of the sun (a function of time of day and time of year)
- o if the sun is visible (zenith angle $< 90^\circ$), the angle δ_S , between the sun location vector and boresight vector is:

$$\delta_S = \cos^{-1} (\vec{L}_0 \cdot \vec{B}_S) \quad (4.12.18)$$

- o if the sun is visible, δ_S is used in equation (4.12.3) to find G_S

If the sun is not visible, the solar contribution to the antenna temperature is zero.

If the antenna is isotropic or can be approximated as isotropic ($G_0 < 3$), the evaluation of equation (4.12.14) is greatly simplified. In this case, the integral can be readily evaluated and expressed analytically as a function of frequency. Similarly, when the sun is visible to the antenna, the solar contribution to the antenna temperature for an isotropic antenna is given by equation (4.12.16) with $G_S = 1$.

The contribution to antenna noise temperature due to man made sources, $T_{A,M}$, is a user specified parameter which defaults to 00K.

Thus, the total antenna noise temperature of an earth station or ship antenna due to all sources is:

$$T_A = T_{A,D} + T_{A,S} + T_{A,M} \quad (4.12.19)$$

Antenna Noise Temperature for Aircraft Receiving Antennas

The antenna noise temperature model used for aircraft receiving antennas is exactly analogous to that described for the earth station antenna. However, it is assumed that the aircraft is above the troposphere (ie: $h \geq 20000$ ft.) and thus:

$$T_T(\theta, f) = 0 \quad 0 \leq \theta \leq \frac{\pi}{2} \quad (4.12.20)$$

where θ is the zenith angle.

For zenith angles greater than $\pi/2$, the tropospheric contribution to the noise temperature can be obtained from equation (4.12.11) by replacing θ by $(\pi - \theta)$.

Antenna Noise Temperature for Spacecraft Receiving Antenna

A rigorous determination of the antenna noise temperature for spacecraft receiving antenna would be analogous to that performed for earth station antennae. However, the geometry is considerably more complicated since the solid angle of the earth is now a function of the spacecraft location and boresight pointing, thus complicating the integrations for the distributed sources (ground and galactic).

As this model is very complex, it will be assumed that the noise temperature of the spacecraft receiving antenna is given by the physical temperature of the earth (290°K) unless otherwise specified by the user.

A flowchart of the antenna noise temperature subroutine is given in Figure 4.12/7.

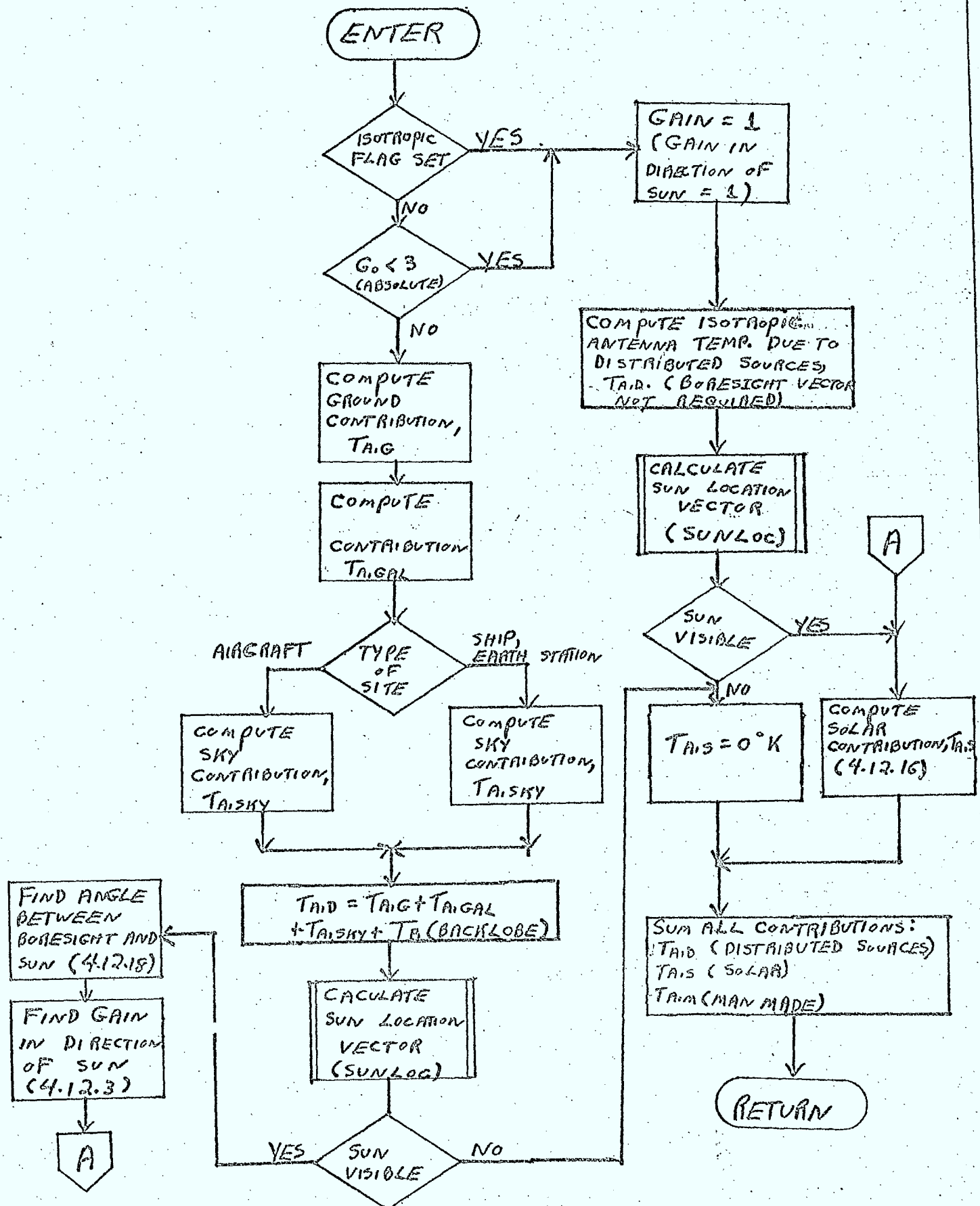
Inputs

- ⊙ flag indicating type of site
- ⊙ flag indicating if antenna is isotropic
- ⊙ antenna on-axis gain
- ⊙ boresight elevation angle
- ⊙ frequency
- ⊙ earth's surface temperature
- ⊙ antenna temperature contribution due to the far lobe and back lobe regions
- ⊙ antenna temperature contribution due to man made sources
- ⊙ antenna boresight vector
- ⊙ time of day (GMT)
- ⊙ day of the year
- ⊙ latitude of site
- ⊙ longitude of site

Outputs

- ⊙ the antenna noise temperature (K⁰)

Figure 4.12/7 Flowchart of ANTEMP



References

- 4.12/1: Reed, H.H., "Noise Curves for High Gain Antennas", Microwaves, April, 1967.
- 4.12/2: "Handbook of Mathematical Functions", U.S. Department of Commerce, National Bureau of Standards, Applied Mathematics Series - 55.
- 4.12/3: SED 0710-44-TR-102, Issue 4, "Orbit Frequency Utilization Simulation - Volume 1 - Analytical Foundation", February 28, 1977.
- 4.12/4: Hogg, D.G. and Mumford, W.W., "The Effective Noise Temperature of the Sky", The Microwave Journal, March, 1960.
- 4.12/5: Cuccia, C.L., Gill, W.J., Wilson, L.H., "Sensitivity of Microwave Earth Stations for Analog and Digital Communications", Microwave Journal, Vol. 12, No. 1, 1969.

5.0 FILE DESIGN

5.1 Introduction

The simulation will make use of three FORTRAN direct access files:

- a database, storing information on receivers and transmitters belonging to the specific UHF communications system under study, and on interfering transmitters belonging to other communications systems,
- a pattern file, storing digitized gain response patterns for those antennas which cannot be characterized by the analytic models provided by the program,
- a spectrum and filter file, providing data characterizing the shapes of spectra and filters for those cases where the spectrum or filter cannot be described by any of the program models.

The database and pattern file will be maintained by the program. This requires that the program be capable of performing the typical sort of operations (create, insert, delete, update, etc) involved in file maintenance.

The spectrum and filter file will not be maintained by the program. If the user of the program chooses to make use of this file, he must make it available to the simulation, with its contents in the format expected by the simulation.

The following sections describe the structure and organization, record formats, and file maintenance operations pertinent to the database (Section 5.2) and the pattern file (Section 5.3); Section 5.4 deals with the spectrum and filter file.

5.2 Database

5.2.1 File Organization and Record Format

The database will exhibit a hierarchical structure with cross-linking modelled on the structure possessed by the database used in OFUS. The structure employed by this simulation will, however, be somewhat simpler than that used in OFUS. Section 8.2 of Reference 5.2/1 discusses the OFUS database structure.

Records contained within the database will be of the following types:

- o file header record - containing data required for file maintenance operations and providing access to the various system records
- o system records - providing access to the sites that are part of a particular communications system
 - ISI system record - header for the specific communications system under study; link calculations can be specified only for transmitters and receivers in this system
 - ESI system records - headers for other communications systems whose transmitters act only as interferers
- o site records - containing location information for sites in a communications system and providing access to antenna beam records
 - satellite site records - for satellite sites
 - non-satellite site records - for earth stations, aircraft, ships, etc.
- o beam records - containing various antenna parameters and providing access to the carrier records associated with the beam
 - satellite beam records - for antennas on satellites
 - either RX or TX beams
 - non-satellite beam records - for antennas at earth stations, on aircraft, ships, etc.
 - either TX or RX beams

- o carrier records - containing parameters characterizing transmitters or receivers
 - ISI TX carrier records - for transmitters within the ISI system. These transmitters can be used as interferors or as components of a communications link.
 - RX carrier records - for receivers in the ISI system. These receivers are used as components of a communications link.
 - ESI TX carrier records - for transmitters in an ESI system. These transmitters can only serve as interfering transmitters.

Figure 5.2/1 is a diagram illustrating the organization of the database; it shows the hierarchy imposed by having records point to other records.

In addition to this hierarchical structure, the database can also have a cross-linked structure involving certain non-satellite beam records, satellite beam records, and satellite site records. Non-satellite beam records of appropriate type can reference satellite site records to establish the direction their boresights point and also satellite beam records to establish an orientation for their polarizers. Those records involved in such referencing of satellite sites and beams are linked together into chains in order to permit access to all those non-satellite beams involved in referencing a particular satellite site record or beam record. Figure 5.2/2 is a diagram indicating the pointer fields involved in this satellite referencing and chain formation.

Each type of record in the database has a unique organization for the data contained within it. The tables on the following pages give these record formats.

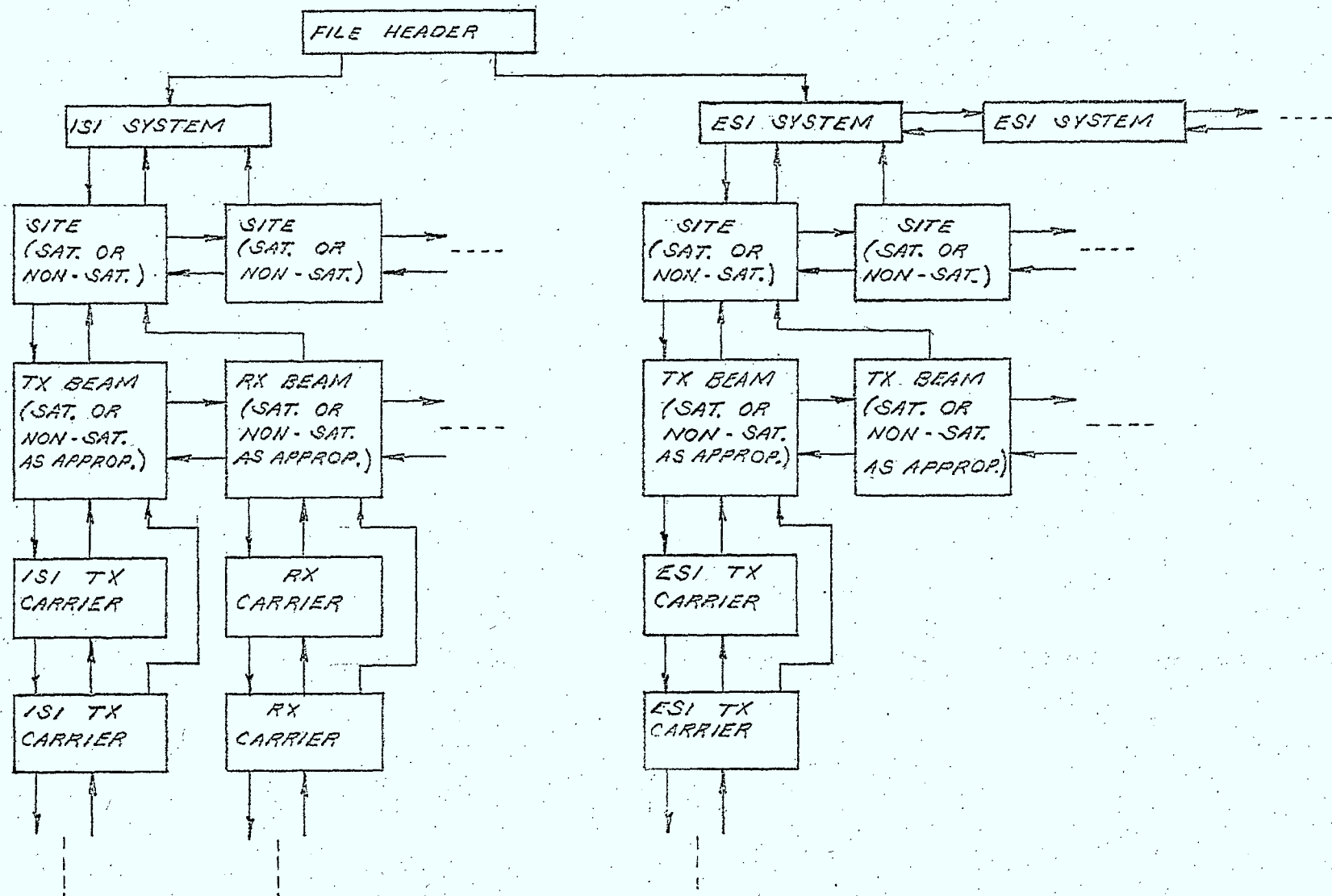


FIG: 5.2/1 DATABASE ORGANIZATION HIERARCHY

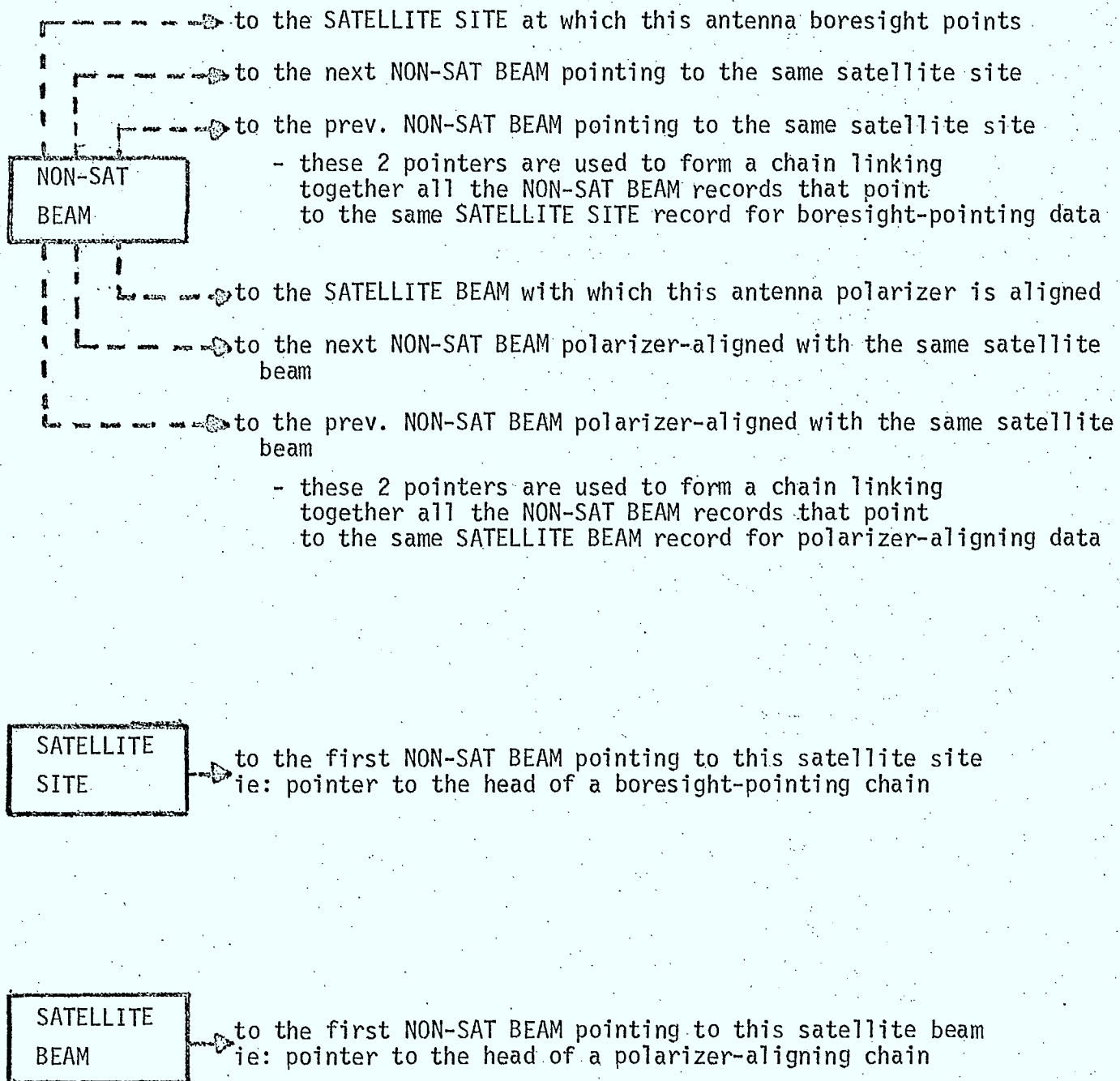


Figure 5.2/2 DATABASE CROSS-LINKED ORGANIZATION

-GIVING BORESIGHT-POINTING AND POLARIZER-ALIGNING DATA

TABLE 5.2/1 SYSTEM RECORD

<u>FIELD</u>	<u>CONTENTS</u>
1	type code (ISI or ESI)
2	pointer to next system (ESI only)
3	pointer to prev. system (ESI only)
4	pointer to first site record in the system
5-8	name of system (16 symbols max., no embedded quote mark)
9-17	comment (36 symbols max., no embedded quote mark)

TABLE 5.2/2 SATELLITE SITE RECORD

<u>FIELD</u>	<u>CONTENTS</u>
1	type code
2	pointer to next site in the system
3	pointer to prev. site in the system
4	pointer to first beam record at the site
5	pointer to parent system
6-9	name of site (16 symbols max.; no embedded quote mark)
10	pointer to head of a boresight-pointing chain
11	latitude of site
12	longitude of site
13	distance of site from center of earth

TABLE 5.2/3 NON-SATELLITE SITE RECORD

<u>FIELD</u>	<u>CONTENTS</u>
1	type code
2	pointer to next site in system
3	pointer to prev. site in system
4	pointer to first beam record at the site
5	pointer to parent system
6-9	name of site (16 symbols max.; no embedded quote mark)
10	latitude of site
11	longitude of site
12	type of site (earth station, ship, aircraft)
13	height above earth surface
14	speed (ISI aircraft only)
15	surface slope (ISI aircraft only)
16	surface roughness (ISI aircraft, ship only)
17	ground conductivity (ISI aircraft, ship only)
18	ground permittivity (ISI aircraft, ship only)

TABLE 5.2/4 SATELLITE BEAM RECORD

<u>FIELD</u>	<u>CONTENTS</u>
1	type code (TX or RX {ISI only})
2	pointer to next beam at site
3	pointer to prev. beam at site
4	pointer to first carrier record on-beam (TX or RX as approp.)
5	pointer to parent satellite site
6	beam ident. number
7	pointer to head of a polarizer-aligning chain
8	on-axis gain
9	beam symmetry (symmetric, elliptical, contour, polar)
10	major-axis beamwidth (elliptical only)
11	minor-axis beamwidth (elliptical only)
12	model flag (CCIR, single-variable)(symm., ellip., only)
13	pointer to princ. pol. pattern (single-var., contour, polar)
14	pointer to cross pol. pattern (single-var., contour, polar)
15	main beam depol. ratio
16	sidelobe depol. ratio
17	backlobe depol. ratio
18	antenna noise temp. (RX only)
19	polarization type (R, L, V, H)
20	polarizer rotation angle (V, H only)
21	boresight target latitude
22	boresight target longitude
23	distance of boresight target from center of earth
24	reference target latitude (ellip., contour, polar)
25	reference target longitude (ellip., contour, polar)
26	distance of ref. target from center of earth (ellip., contour, polar)

TABLE 5.2/5 NON-SATELLITE BEAM RECORD

<u>FIELD</u>	<u>CONTENTS</u>
1	type code (TX or RX {ISI only})
2	pointer to next beam at site
3	pointer to prev. beam at site
4	pointer to first carrier record on beam (TX or RX as approp.)
5	pointer to parent non-satellite site
6	beam ident. number
7	on-axis gain
8	beam symmetry (isotropic, symmetric, elliptical, polar)
9	major-axis beamwidth (elliptical only)
10	minor-axis beamwidth (elliptical only)
11	model flag (CCIR, single-variable)(symm., ellip. only)
12	pointer to princ. pol pattern (single-var., polar)
13	pointer to cross pol. pattern (single-var., polar)
14	mainbeam depol. ratio
15	sidelobe depol. ratio (symm., ellip., polar only)
16	backlobe depol. ratio (symm., ellip., polar only)
17	antenna noise temp. type (simple, detailed)(RX only)
18	antenna noise temp (simple model, RX only)
19	temp. of backlobes (detailed, RX only, not isotropic)
20	temp. of ground or sea (detailed, RX only)
21	man-made temp. (detailed, RX only)
22	polarization (R, L, V, H)
23	type of polarizer data (sat. frame, earth frame)(non-iso. V, H only)
24	polarizer rotation angle (earth frame)
25	pointer to satellite beam polarizer is aligned with (sat. frame)
26	forward pointer in polarizer-aligning chain
27	backward pointer in polarizer-aligning chain

Table 5.2/5 Continued

<u>FIELD</u>	<u>CONTENTS</u>
28	type of boresight pointing data (target coords, az & el, pointer)
29	boresight target latitude (non-isotropic only)
30	boresight target longitude (non-isotropic only)
31	distance of boresight target from center of earth (non-iso only)
32	reference target latitude (ellip., polar only)
33	reference target longitude (ellip., polar only)
34	distance of ref. target from center of earth (ellip, polar only)
35	boresight azimuth (non-isotropic only)
36	boresight elevation (non-isotropic only)
37	reference azimuth (ellip., polar only)
38	reference elevation(ellip., polar only)
39	pointer to satellite site boresight is aimed at (symm. only)
40	forward pointer in boresight-pointing chain
41	backward pointer in boresight-pointing chain

TABLE 5.2/6 ISI TX CARRIER RECORD

<u>FIELD</u>	<u>CONTENTS</u>
1	type code
2	pointer to next ISI TX carrier on beam
3	pointer to prev. ISI TX carrier on beam
4	pointer to parent ISI TX beam
5	carrier ident. number
6	carrier frequency
7	RF bandwidth of carrier
8	type of TX (IF, baseband)
9	type of baseband signal (voice, digital)
10	delta-mod flag (voice only)
11	bit rate (digital, delta-mod voice)
12	forward error correcting flag (digital, delta-mod voice)
13	code rate (for forward error correcting)
14	preemphasis flag (voice only)
15	companding flag (voice only)
16	peak-to-average baseband ratio after companding (voice only)
17	modulator type (FSK, PSK, FM, other)
18	deviation ratio (FSK)
19	no. of phases (PSK)
20	lower baseband frequency (FM)
21	upper baseband frequency (FM)
22	rms mod. index (FM)
23	pointer to other spectrum model (other)
24	first filter (none, Butterworth, Chebyshev, ideal bandpass, general)
25	no. of poles (Butterworth, Chebyshev)
26	3-dB filter bandwidth (Butterworth, Chebyshev)
27	pointer to general filter model (general)
28	filter bandwidth (ideal bandpass, general)
29	nominal carrier output power (baseband only)
30	ratio of carrier power to total amp. output power (IF only)

TABLE 5.2/6 Continued

<u>FIELD</u>	<u>CONTENTS</u>
31	type of HPA (linear, soft-limiter, hard-limiter)(IF only)
32	nominal amp. output power (linear only)
33	input bias rel. to saturation (soft-limiter only)
34	input oper. point rel. to sat. (soft, hard-limiter)
35	total amp. sat. output power (soft, hard-limiter)
36	nominal output backoff (soft-limiter)
37	auto. gain control (on, off)(linear, soft-limiter)
38	distortion model (simple, detailed)
39	(C/D) _{NOM} (baseband, IF simple model)
40	amp. bandwidth (detailed IF)
41	amp. center freq. rel. to carrier freq. (detailed IF)
42	std. deviation of inter-mod spectrum (detailed IF)
43	(C/D) _{SAT} (soft, hard-limiter)
44	B ₁ (soft-limiter)
45	B ₂ (soft-limiter)
46	(C/D) ₁ (linear, soft-limiter)
47	(C/D) ₂ (linear, soft-limiter)
48	(C/D) ₃ (linear)
49	P ₁ (linear)
50	P ₂ (linear)
51	P ₃ (linear)
52	second filter (none, Butterworth, Chebyshev, ideal bandpass, general)
53	insertion loss
54	filter center freq. relative to carrier freq.
55	no. of poles (Butterworth, Chebyshev)
56	3-dB filter bandwidth (Butterworth, Chebyshev)
57	pointer to general filter model (general)
58	filter bandwidth (ideal pandpass, general)

TABLE 5.2/7 RX CARRIER RECORD

<u>FIELD</u>	<u>CONTENTS</u>
1	type code
2	pointer to next RX carrier on beam
3	pointer to prev. RX carrier on beam
4	pointer to parent ISI RX beam
5	carrier ident. number
6	type of RX (IF, baseband)
7	first filter (none, Butterworth, Chebyshev, ideal bandpass, general)
8	insertion loss
9	filter center freq. rel. to carrier freq.
10	no. of poles (Butterworth, Chebyshev)
11	3-dB filter bandwidth (Butterworth, Chebyshev)
12	pointer to general filter model (general)
13	filter bandwidth (ideal bandpass, general)
14	LNA noise temp.
15	auto. gain control (on, off)
16	ratio of carrier power to total amp. output power
17	distortion model (simple, detailed)
18	$(C/D)_{\text{NOM}}$ (simple, detailed)
19	$(C/D)_1$ (detailed)
20	$(C/D)_2$ (detailed)
21	$(C/D)_3$ (detailed)
22	P_1 (detailed)
23	P_2 (detailed)
24	P_3 (detailed)
25	Δf_A (detailed)
26	α (detailed)
27	B_A (detailed)

TABLE 5.2/7 Continued

<u>FIELD</u>	<u>CONTENTS</u>
28	second filter (none, Butterworth, Chebyshev, ideal bandpass, general)
29	filter center freq. rel. to carrier freq.
30	no. of poles (Butt., Cheb.)
31	3-dB filter bandwidth (Butt., Cheb.)
32	pointer to general filter model (general)
33	filter bandwidth (ideal bandpass, general)
34	demodulator type (FSK, DPSK, CPSK, ANBFM, NBFM) (baseband only)
35	nominal threshold C/N (NBFM, ANBFM)
36	threshold extension factor (ANBFM)
37	deemphasis flag (on, off) (NBFM, ANBFM)
38	pre/deemphasis improvement factor (NBFM, ANBFM)
39	companding flag (on, off) (NBFM, ANBFM)
40	companding improvement factor (NBFM, ANBFM)
41	$(S/N)_{TH}$ (NBFM, ANBFM)
42	bit rate (FSK, DPSK, CPSK)
43	implementation margin (FSK, DPSK, CPSK)
44	limiting error probability (FSK, DPSK, CPSK)
45	no. of phases (DPSK, CPSK)
46	Δ -demod flag (FSK, DPSK, CPSK)
47	$(S/N)_{\pi}$ due to quantization (Δ -demod)
48	$(BER)_{3-dB}$ (Δ -demod)
49	forward error correcting (none, sim. model, user-specified)
50	$(BER)_{TH}$ (sim. model, user-specified)
51	P_{in1} (user-spec.)
52	P_{out1} (user-spec.)
53	P_{in2} (user-spec.)
54	P_{out2} (user-spec.)
55	constraint or block length (sim. model)
56	code rate (sim. model)
57	error correction capability of code (sim. model)

TABLE 5.2/8 ESI TX CARRIER RECORD

<u>FIELD</u>	<u>CONTENTS</u>
1	type code
2	pointer to next ESI TX carrier on beam
3	pointer to prev. ESI TX carrier on beam
4	pointer to parent ESI TX beam
5	carrier ident. number
6	carrier freq.
7	RF bandwidth of carrier
8	nominal carrier putput power
9	spectrum type (FSK,PSK,FM/VOICE,FM/TV,Gaussian noise,white noise, general)
10	deviation ratio (FSK)
11	no. of phases (PSK)
12	bit rate (FSK, PSK)
13	companding flag (FM/VOICE)
14	peak-to-avg. baseband power ratio after companding (FM/VOICE)
15	preemphasis flag (FM/VOICE)
16	rms mod. index (FM/VOICE)
17	lower baseband freq. (FM/VOICE)
18	upper baseband freq. (FM/VOICE, FM/TV)
19	peak-to-peak freq. deviation (FM/TV)
20	pointer to other spectrum model (general)
21	3-dB bandwidth (Gaussian Noise)
22	filter (none, Butterworth, Chebyshev, ideal bandpass, general)
23	no. of poles (Butt., Chev.)
24	3-dB filter bandwidth (Butt., Chev.)
25	pointer to general filter model (general)
26	filter bandwidth (ideal bandpass, general)

5.2.2 Creation (CREATE)

The user will be able to initialize the database in the same manner as is now done in OFUS. Section 4.8 of Reference 5.2/1 and Section 3.2.1 of Reference 5.2/2 describe and illustrate this operation.

5.2.3 Insertion

5.2.3.1 Introduction (INSERT)

Just as in OFUS, the user will be able to insert records into the simulation database by issuing the appropriate command and then presenting the data for insertion as a separate input file.

To reduce the volume of data that would be required, default values are provided for many of the required items, including many values which might prove difficult to obtain.

Keywords are used wherever possible in preference to numeric code values so that the user is able to characterize his system in familiar terminology rather than in obscure codes.

Data items entered by the user will be checked for validity (eg; falling within established validity bounds, being a legal keyword, being a legal reference to other records in the database, being consistent with other data items in the record, etc.).

In short, the philosophy followed in OFUS:

- of attempting to ease the data collection burden of the user, and
- of attempting to ensure the integrity of the database structure and the validity of the data contained within will be followed in this simulation. Section 8.3 of Reference 5.2/1 expands upon this.

Subroutine INSERT performs an insertion operation primarily by calling the appropriate record insertion routines (described in the following subsections).

5.2.3.2 System Record Insertion (SYSI)

Purpose

The function of SYSI is to read the data that constitutes a system record to be inserted into the database and to perform all required validity tests.

Description

The method to be followed consists primarily of reading the sequence of data items input by the user, with the determination of which items to expect being made in the light of previously entered items and the presence or absence of certain keywords.

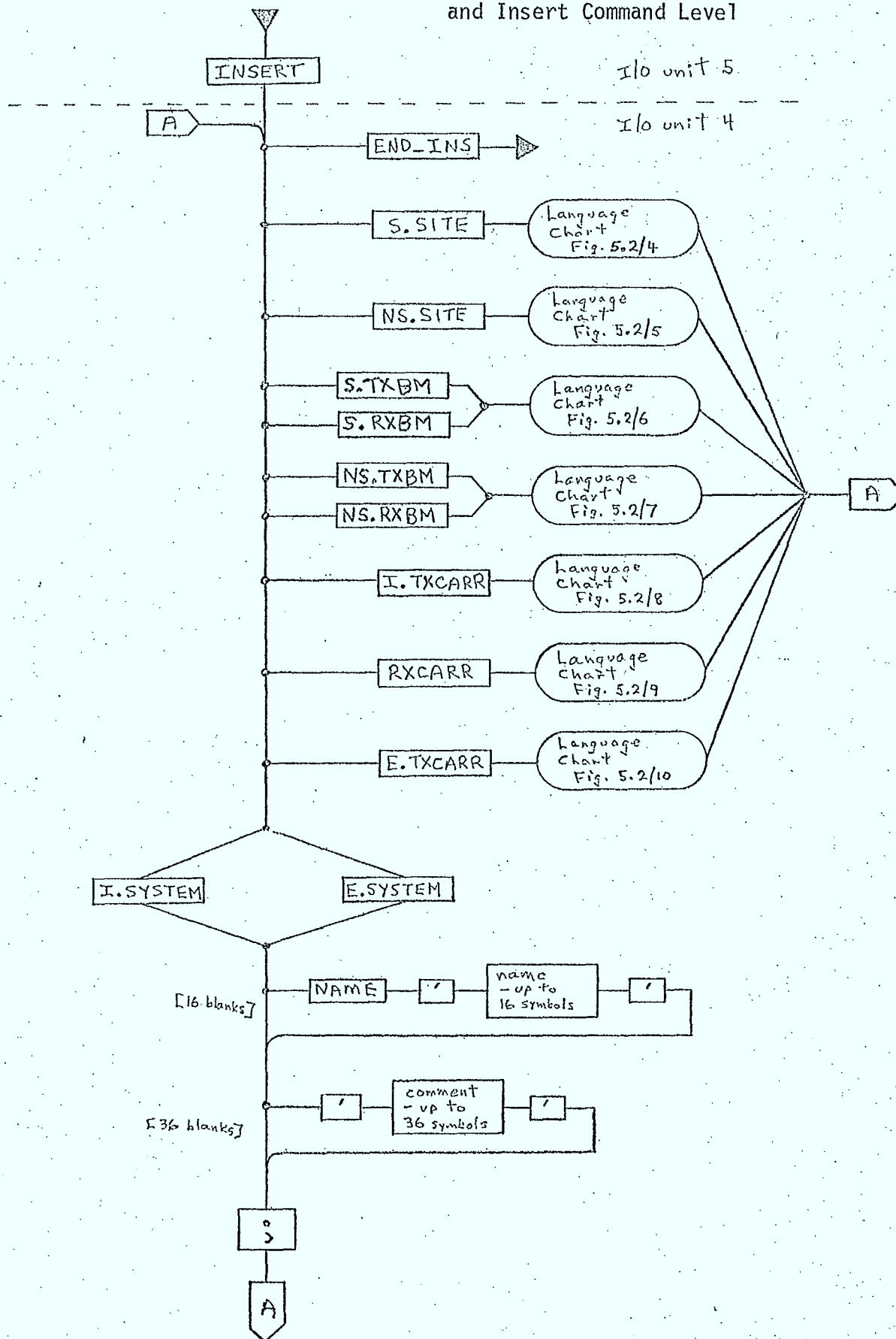
Since the form of the processing logic involved in this subroutine is a function of the language it must accept, the language chart in Figure 5.2/3 will serve to indicate both the logical form of the subroutine and the syntactic form of the input data.

Inputs

- input device unit no. and characteristic parameters

Outputs

- record buffer array

Figure 5.2/3 Language Chart for System Record Insertion
and Insert Command Level

5.2.3.3 Satellite Site Record Insertion (SSITI)

Purpose

Subroutine SSITI reads the data items that constitute a satellite site record to be inserted into the database and performs validity tests.

Description

The language chart in Figure 5.2/4 can be used to illustrate the logic of the subroutine and the language form required for the data items.

Inputs

- o input device unit no. and characteristic parameters

Outputs

- o record buffer array

5.2.3.4 Non-Satellite Site Record Insertion (NSSITI)

Purpose

To read the data items that form a non-satellite site record to be inserted into the database and to perform validity testing.

Description

The logic and required language form can both be determined from the language chart in Figure 5.2/5.

Figure 5.2/4 Language Chart for Satellite Site Record Insertion

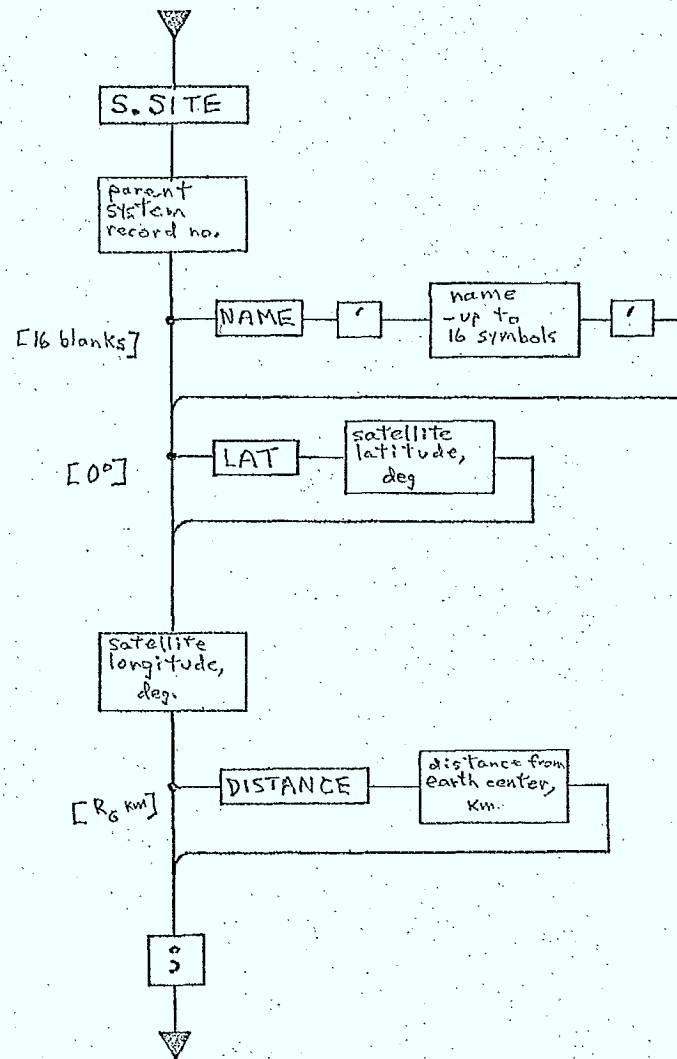
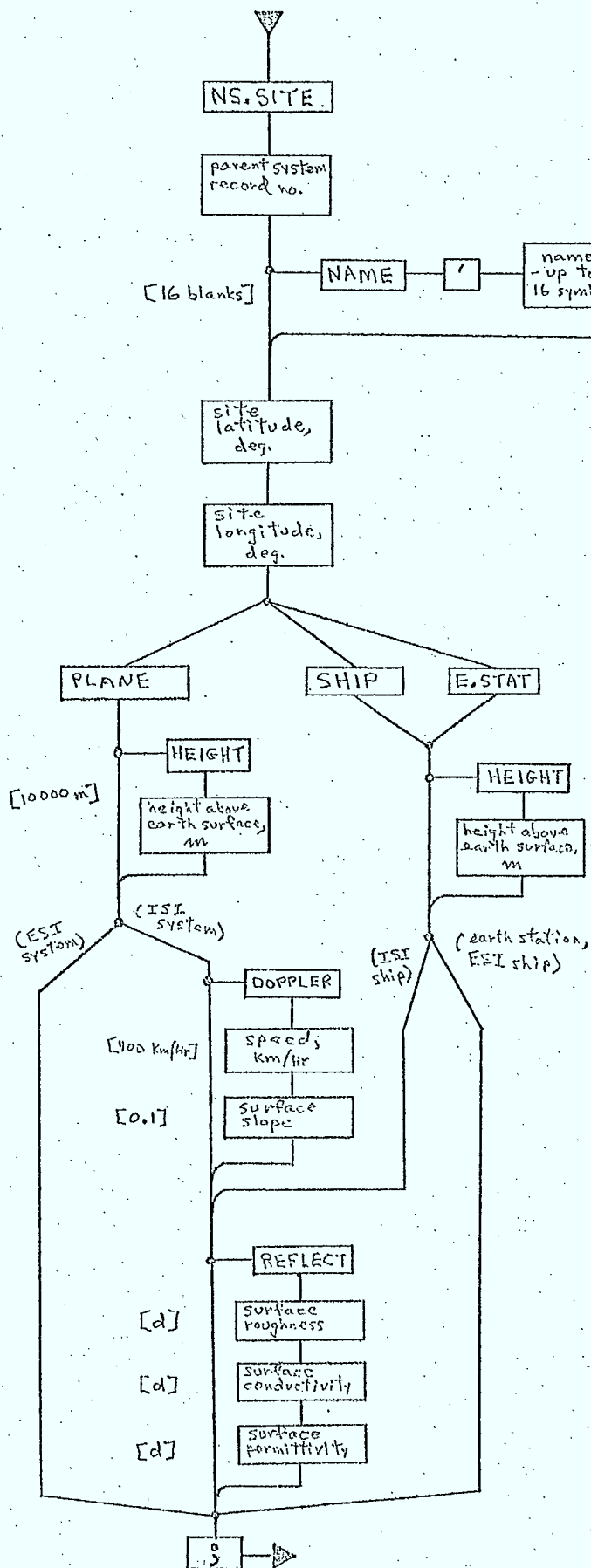


Figure 5.2/5 Language Chart for Non-Satellite Site
Record Insertion



Inputs

- o input device unit no. and characteristic parameters

Outputs

- o record buffer array

5.2.3.5 Satellite Beam Record Insertion (SBMI)Purpose

To read and test for validity the data items that form a satellite beam record to be inserted into the database.

Description

As given by the language chart in Figure 5.2/6.

Inputs

- o input device unit no. and characteristic parameters

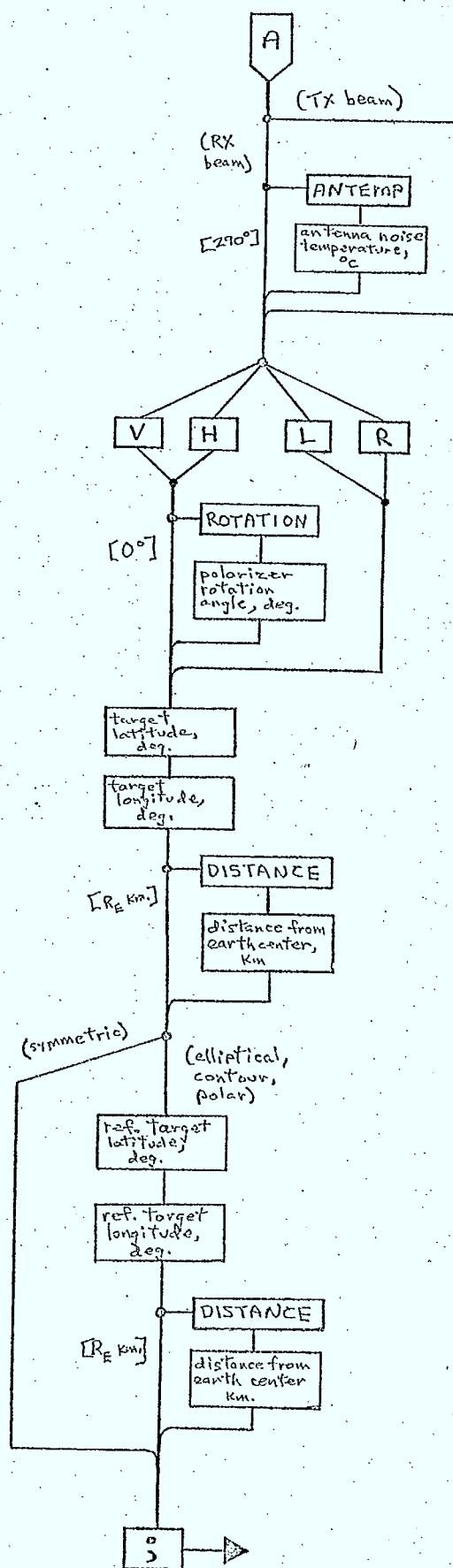
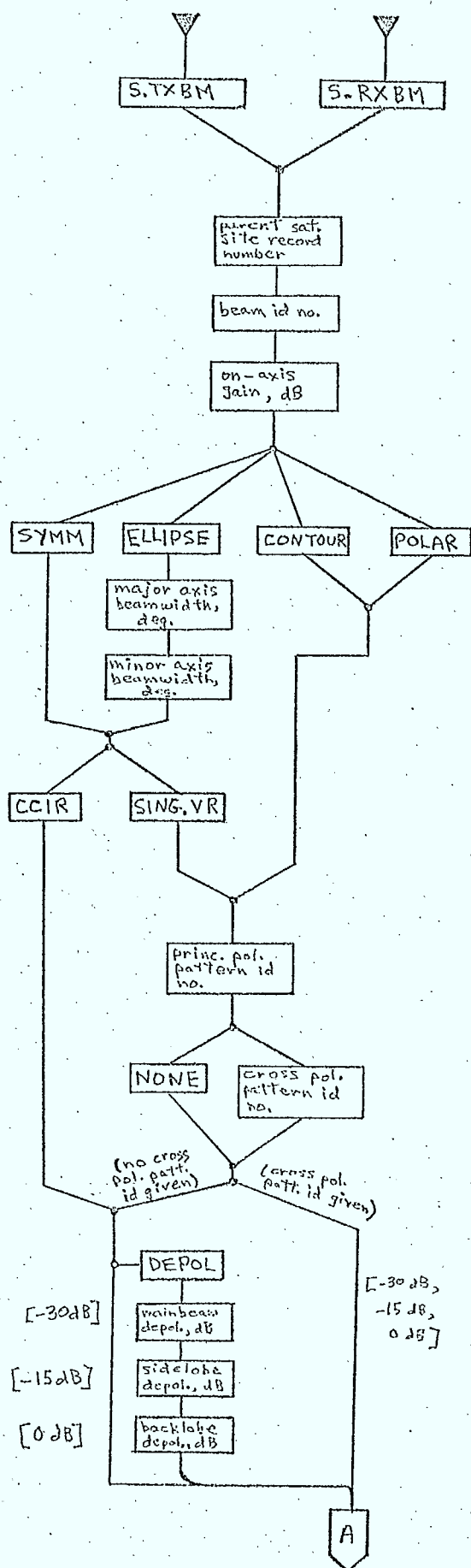
Outputs

- o record buffer array

5.2.3.6 Non-Satellite Beam Record Insertion (NSBMI)Purpose

To read data items forming a non-satellite beam record to be inserted into the database and to perform validity tests.

Figure 5.2/6 Language Chart for Satellite Beam
Record Insertion



Description

As given by the language chart in Figure 5.2/7.

Inputs

- o input device and database unit nos. and characteristic parameters

Outputs

- o record buffer array

5.2.3.7 ISI TX Carrier Record Insertion (ITXCRI)Purpose

To read and test for validity the data items forming a transmit carrier record for the ISI system.

Description

The language chart in Figure 5.2/8 indicates the structure of the subroutine ITXCRI and the form of language assumed for the data items.

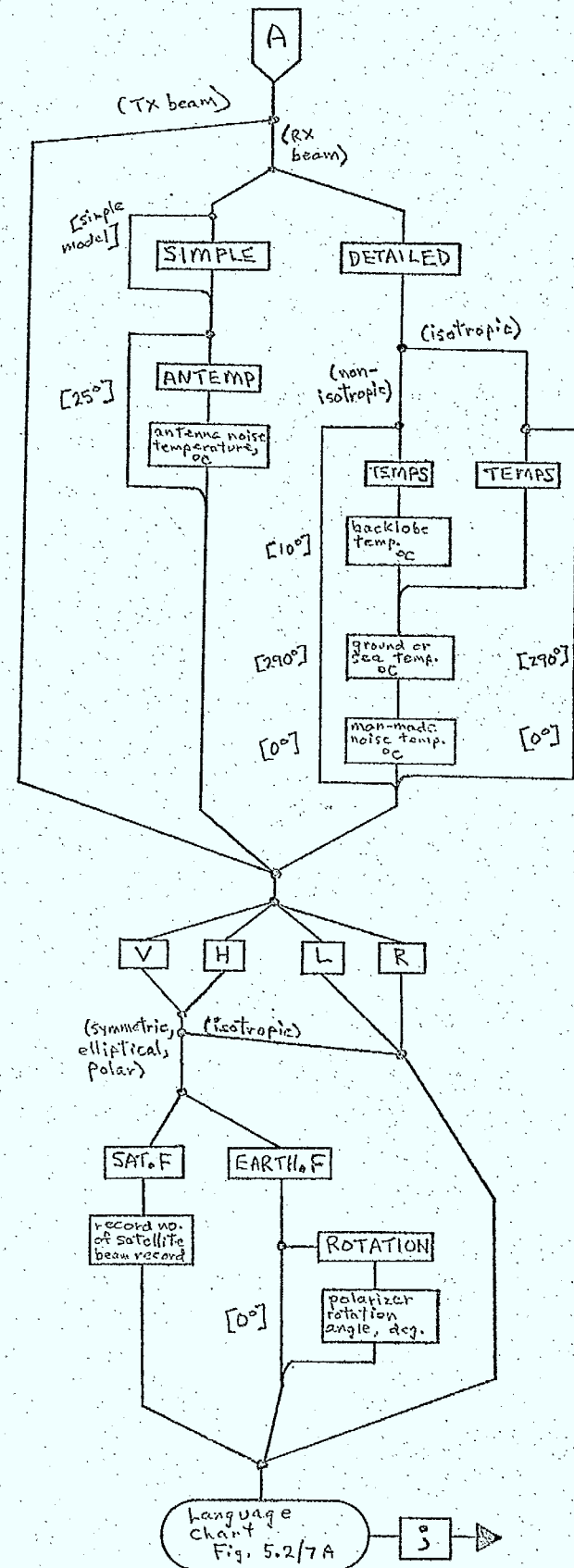
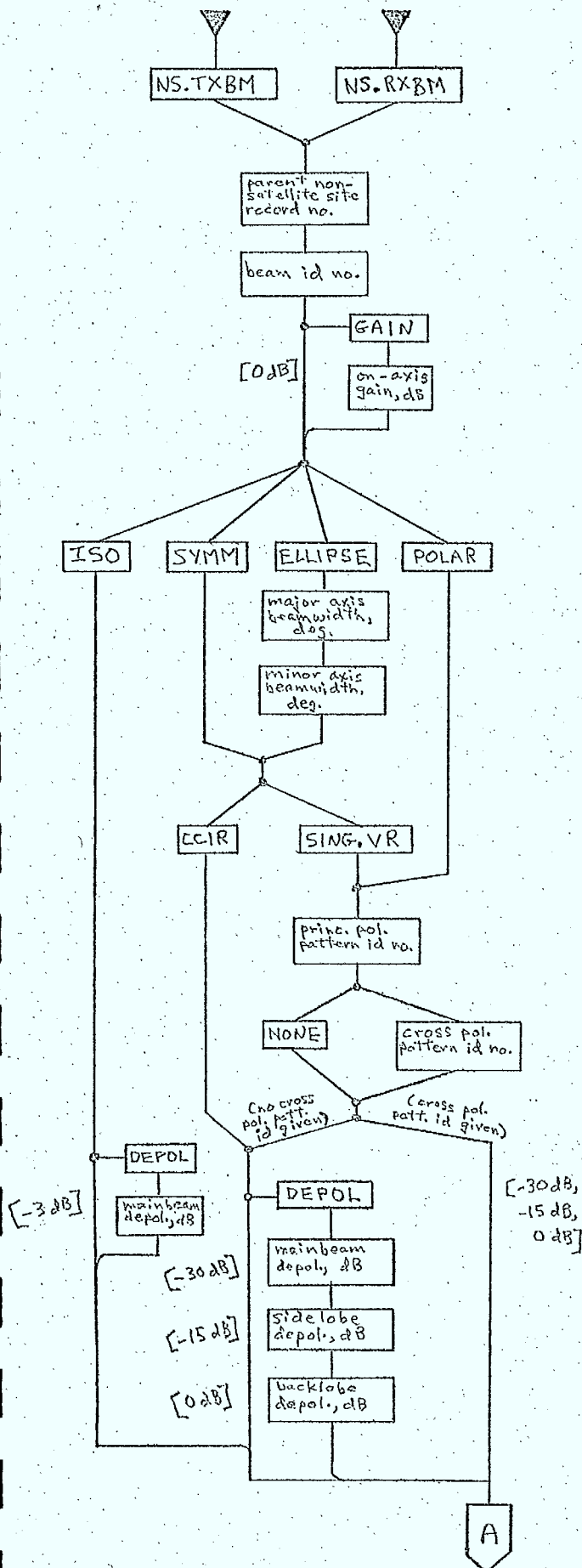
Inputs

- o input device unit no. and characteristic parameters

Outputs

- o record buffer array

Figure 5.2/7 Language Chart for Non-Satellite Beam
Record Insertion

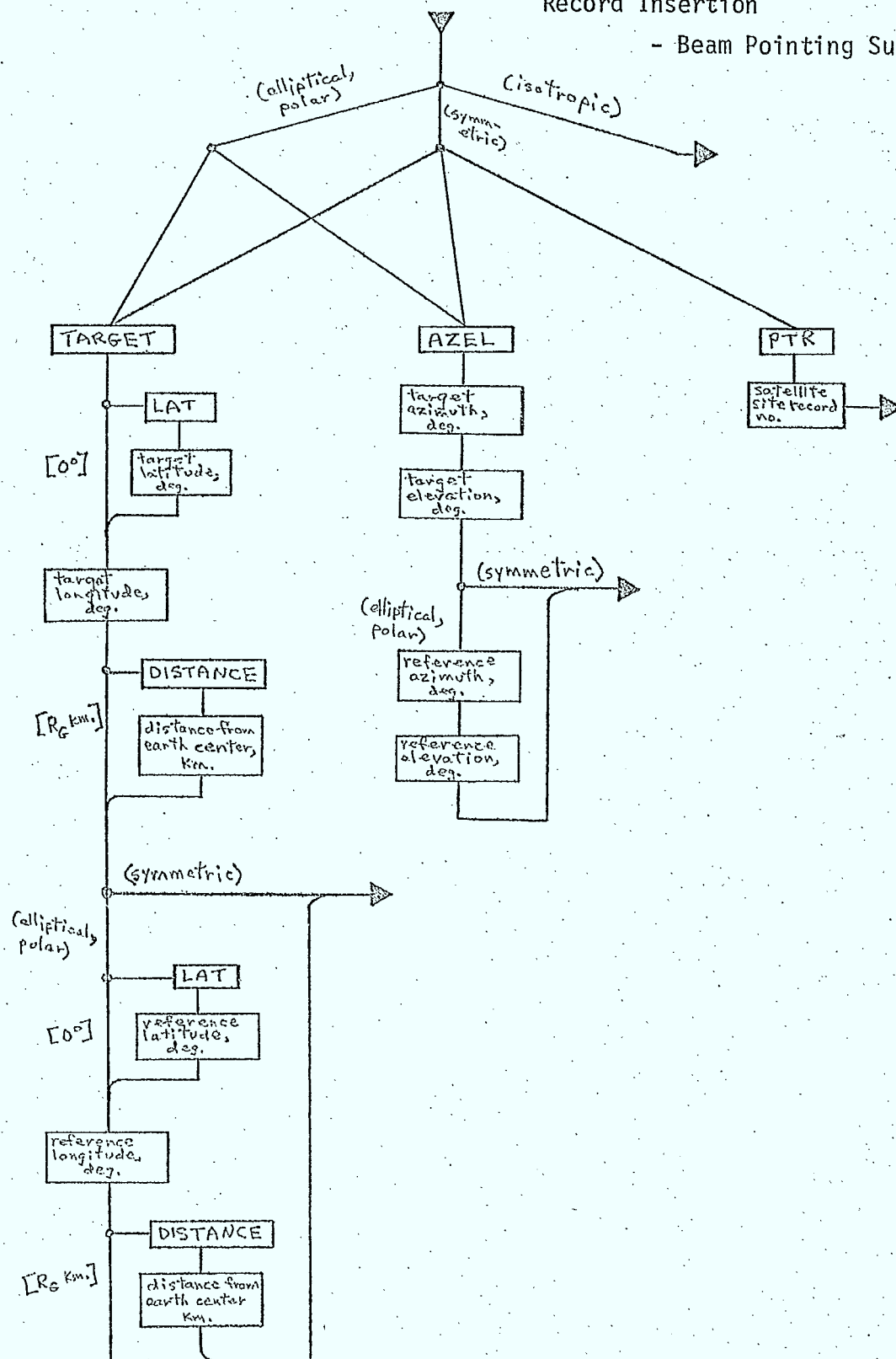


Language
chart
Fig. 5.2/7A

Figure 5.2/7A Language Chart for Non-Satellite Beam

Record Insertion

- Beam Pointing Sub-Chart



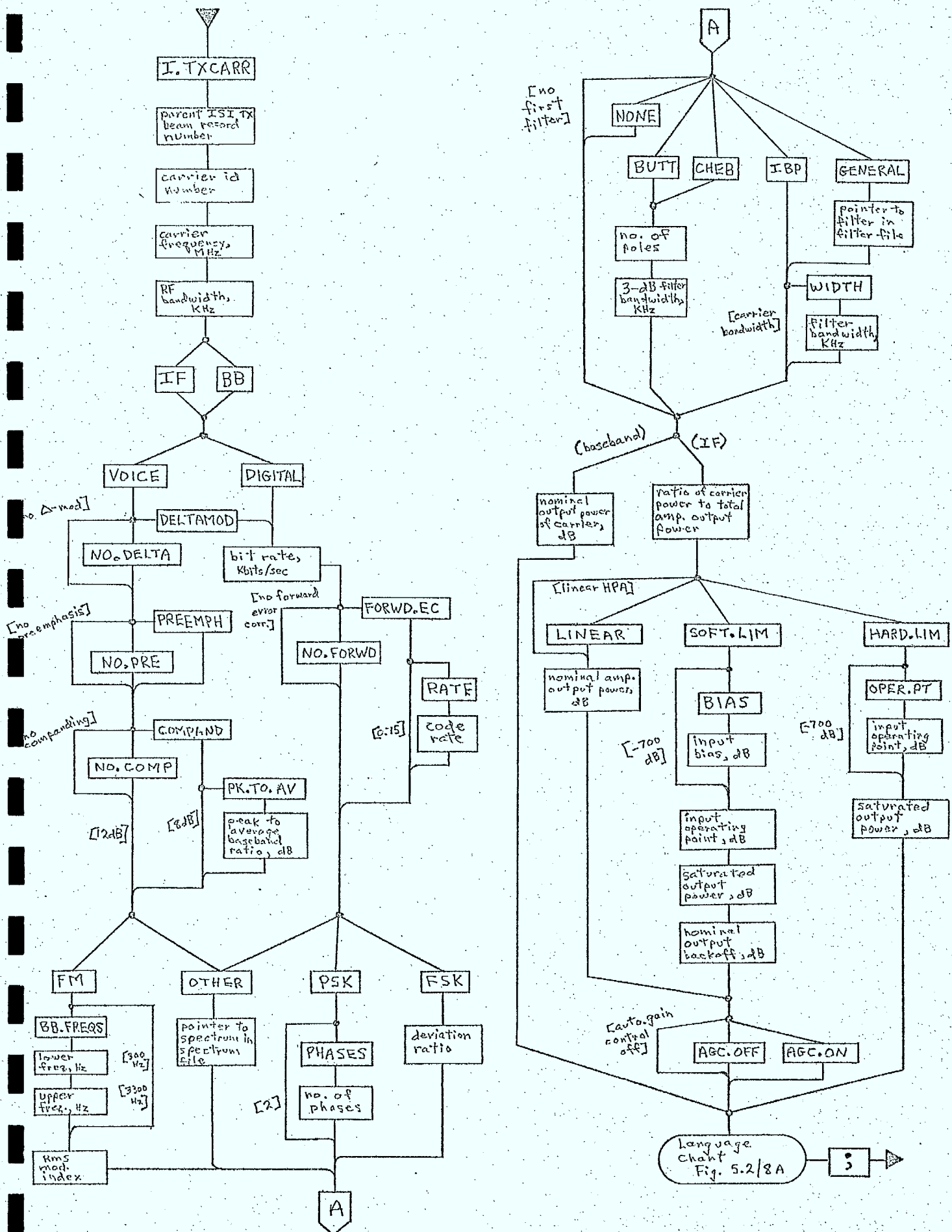
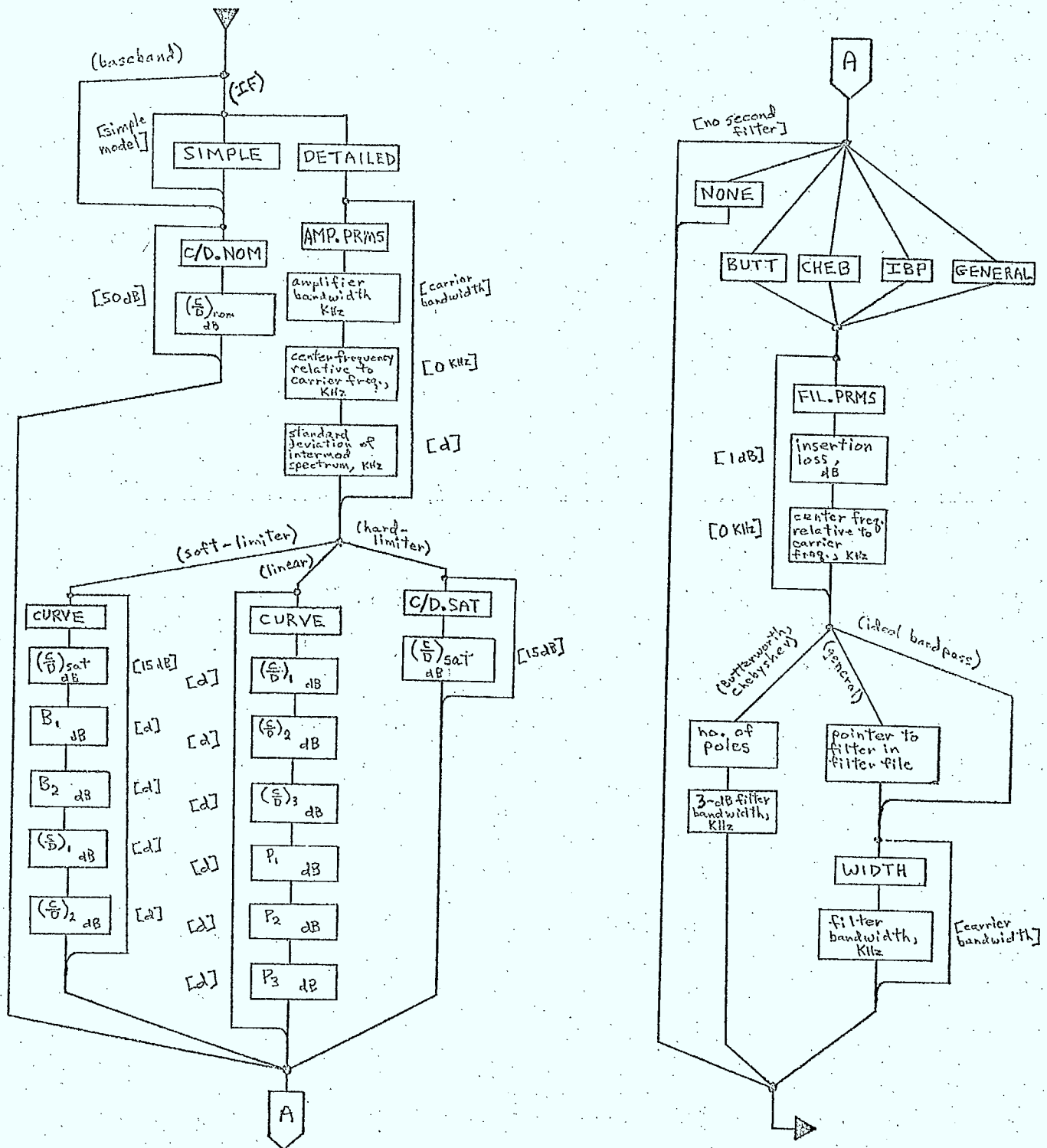


Figure 5.2/8A Language Chart for ISI TX Carrier Record Insertion
- Distortion Model and Second Filter Sub-Chart



5.2.3.8 RX Carrier Record Insertion (IRXCRI)

Purpose

To read and test for validity the data items forming a receiver carrier record for the ISI system.

Description

As given by the language chart in Figure 5.2/9.

Inputs

- input device unit no. and characteristic parameters

Outputs

- record buffer array

5.2.3.9 ESI TX Carrier Record Insertion (ETXCRI)

Purpose

To read and validity test the data items forming a transmit carrier record for the ISI system.

Description

As given by the language chart in Figure 5.2/10.

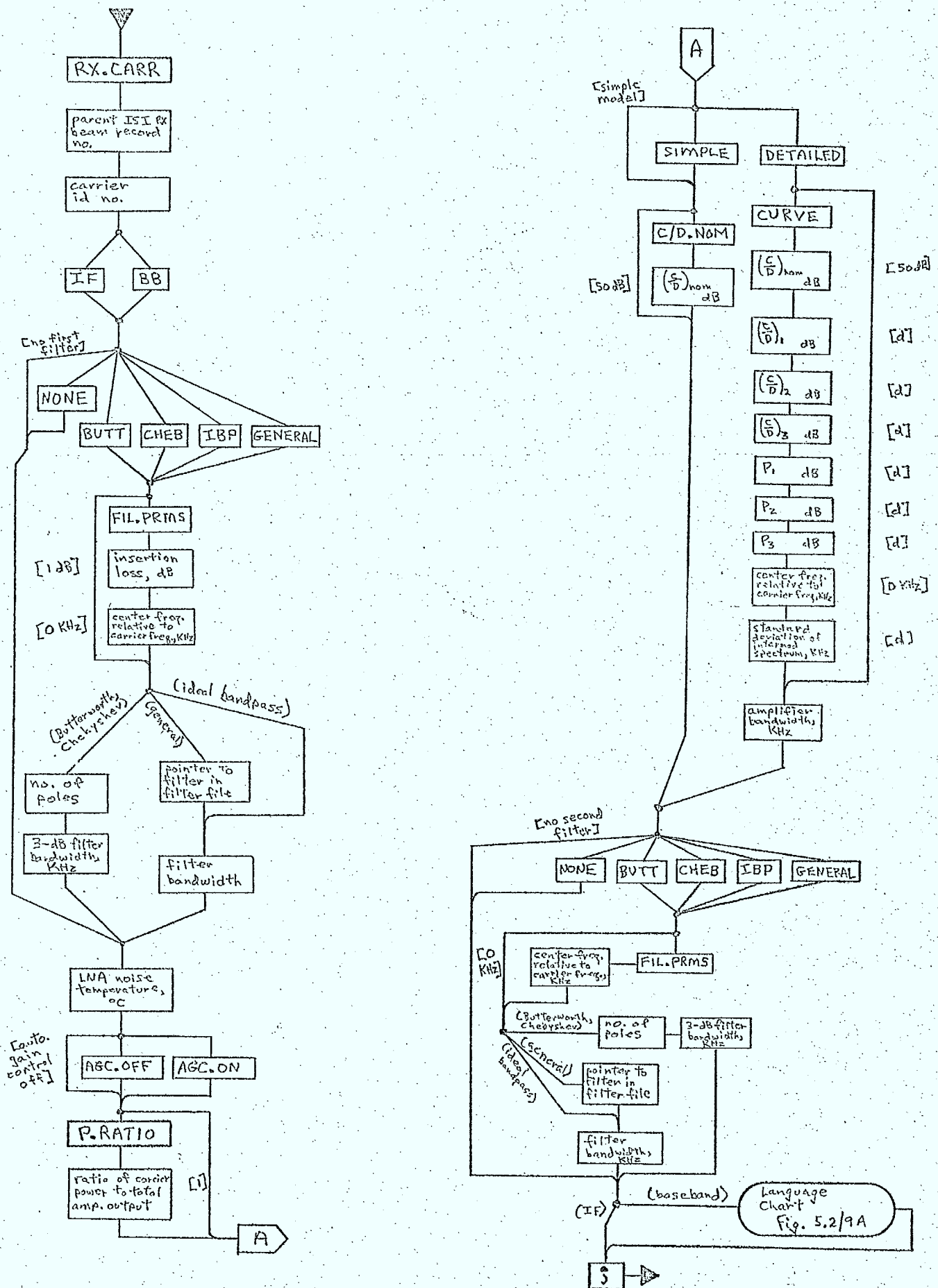
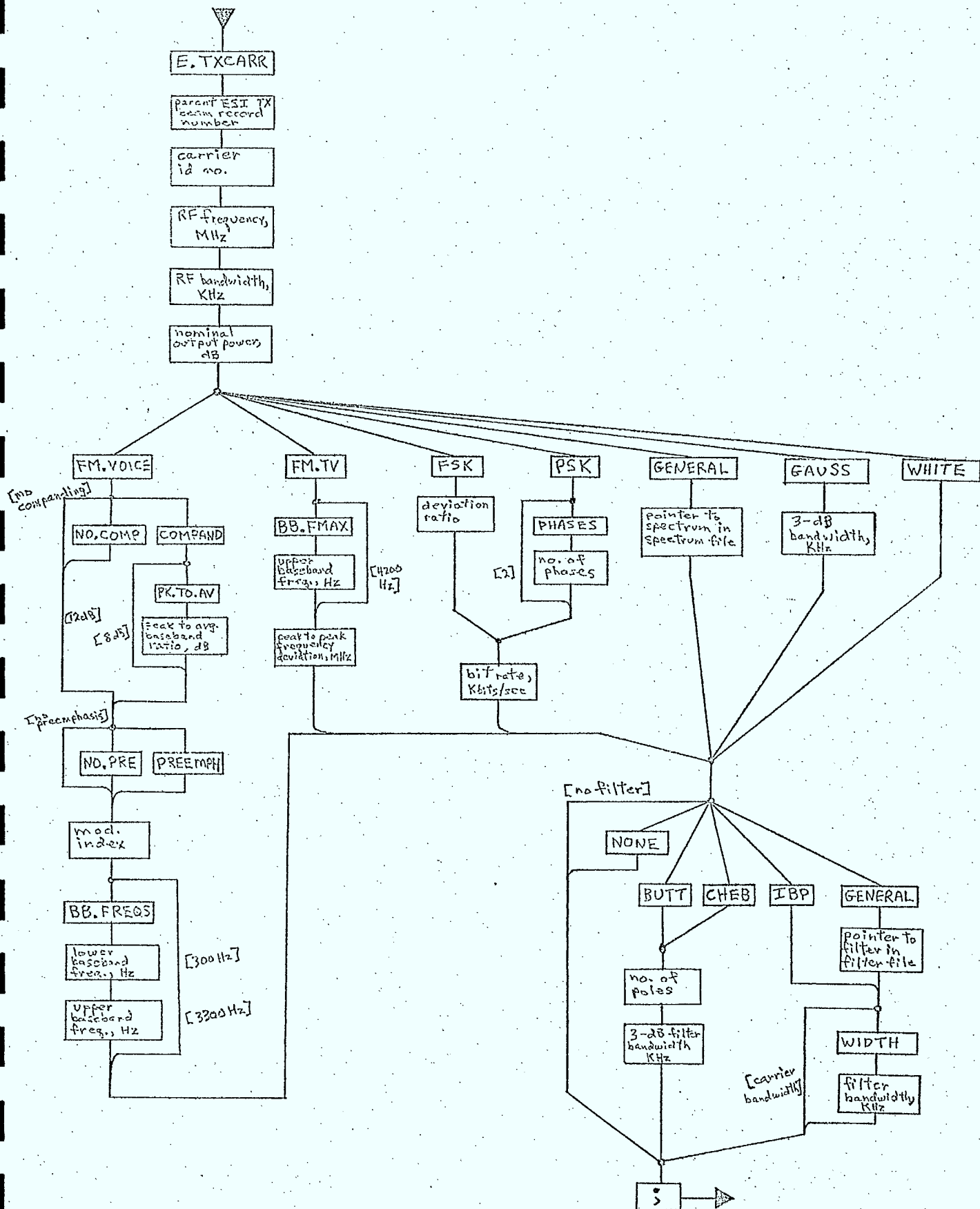


Figure 5.2/10 Language Chart for ESI TX Carrier Record Insertion



Inputs

- o input device unit no. and characteristic parameters

Outputs

- o record buffer array

5.2.4 Deletion (DELETE)

This operation will be carried out as it is in OFUS. Section 4.3 of Reference 5.2/1 describes how this operation can be performed. The language chart in Figure 5.2/11 gives the form of the command language available to the user.

5.2.5 Dumping (DUMP)

This database operation will be the same as the corresponding operation in OFUS. Section 4.5 in Reference 5.2/1 describes this operation in more detail. The language chart in Figure 5.2/12 illustrates the form of the command language available.

5.2.6 Updating (UPDATE)

Though the command language available to the user will remain almost the same as that used by OFUS, the method of implementation will be completely different.

The processing of the language items indicating the record to be updated and the field numbers within that record will remain approximately the same as in OFUS, but the new value items for those fields will be read by the appropriate segments of the insertion routines (with transfer to them being via ENTRY statements). In this way, the user will be able to input data items used to update records in the same units and

Figure 5.2/11 Language Chart for Deleting Database or Pattern File Records

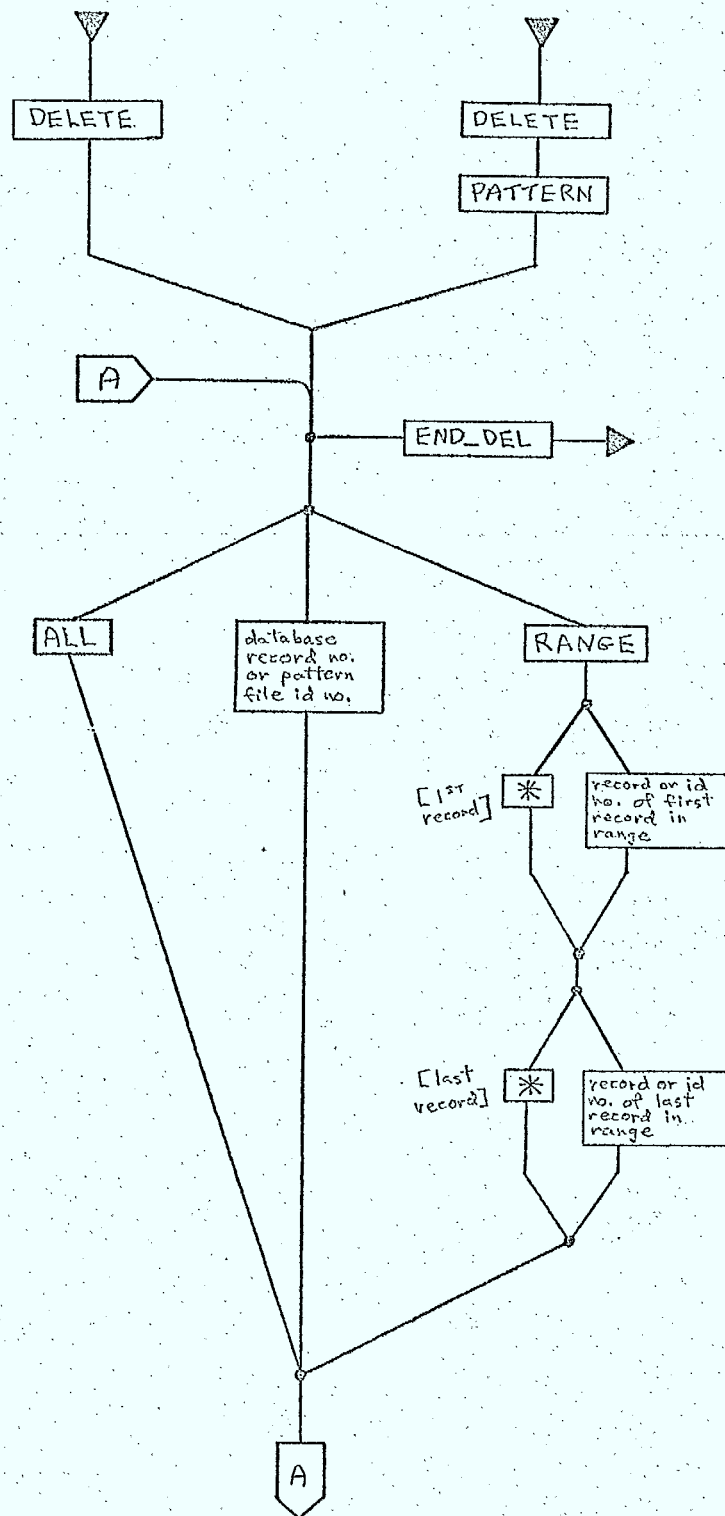
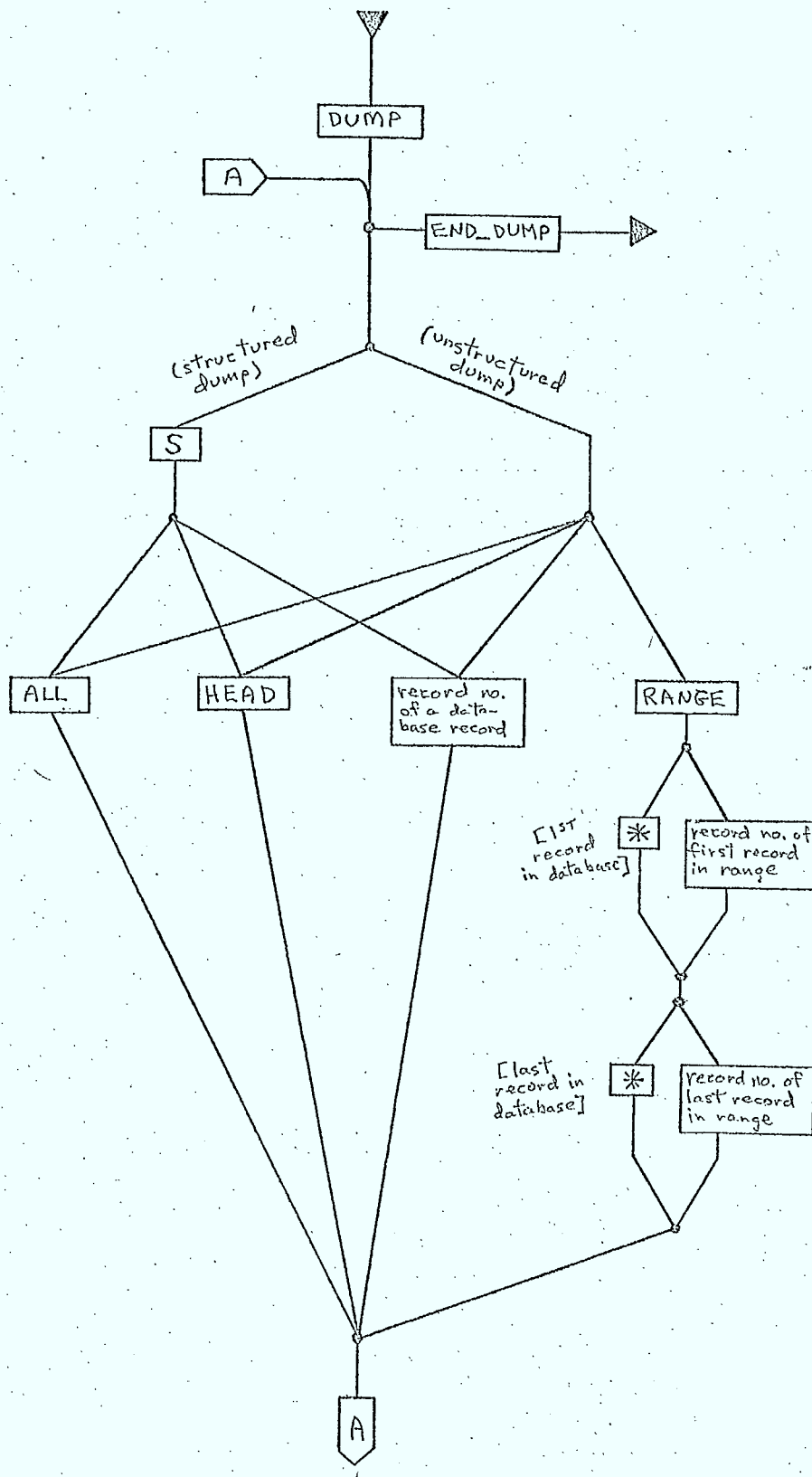


Figure 5.2/12 Language Chart for Dumping Database Records



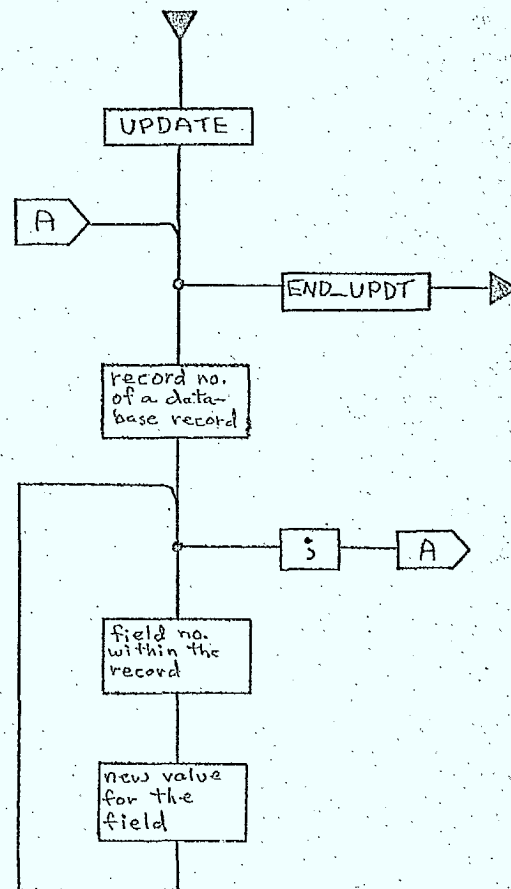
the same form as for insertion. The processing and validity checking required for insertion would then be available to read and test items for update.

The language chart in Figure 5.2/13 shows the form of the language available to the user for doing updates to database records.

5.2.7 Reorganization (REORG)

This operation will be implemented as in the OFUS program. Section 4.6 of Reference 5.2/1 describes this procedure in more detail.

Figure 5.2/13 Language Chart for Updating Database Records



References

- 5.2/1: SED 0710-44-SW-103, Issue 3; "Orbit Frequency Utilization Simulation - Volume 2 - Program Description", February 28, 1977.
- 5.2/2: SED 0710-44-SW-105, Issue 3; "Orbit Frequency Utilization Simulation - Volume 4 - User's Guide", February 28, 1977.

5.3 Pattern File

5.3.1 File Organization and Record Format

The pattern file used by this simulation will be almost the same as that used by the OFUS program. Section 8.5 of Reference 5.3/1 describes this pattern file.

To incorporate general polar patterns, there will have to be certain modifications made. Among these modifications are:

- o changes to the directory records to accommodate a polar pattern type code and the number of radials that a polar pattern can use (eg; 3 to 60)
- o a new type of "1st radial record" for each radial of a polar pattern. This record would be organized as:

<u>Field</u>	<u>Contents</u>
1	- a type code
2	- no. of data points in the radial
3	- rotation angle assoc. with the radial
4	- pointer to first continuation data record
2i+3	- G/G_0 , dB beginning with the on-axis
2i+4	- θ/θ_0 values, and ordered by increasing
for $1 \leq i \leq 15$	off-axis ratio (θ/θ_0)

The record size and data form parameters would remain unchanged (34 words, binary data). File size (default length of 600 records) would also remain the same.

5.3.2 Creation (CREATE)

File creation would be accomplished in the same way as in OFUS. This creation operation is described in Section 4.8 of Reference 5.3/1 and Section 3.2.1 of Reference 5.3/2.

5.3.3 Insertion

5.3.3.1 Single Variable and Contour Patterns (PATINS, PATT, CNTOUR, CONVRT, STORE)

These routines, described in Section 4.9 of Reference 5.3/1 and illustrated in Section 3.3.5 of Reference 5.3/2, would be used in almost their present form to insert single variable and contour patterns into the pattern file. Minor changes would be required to handle the slight changes and additions to the language (changes made to maintain consistency with the language style used elsewhere in this simulation and additions made necessary by the incorporation of the capability to insert polar patterns).

Since polar patterns can be described as a group of single variable patterns, each with an associated rotation angle giving the plane of rotation about the boresight in which the pattern lies, much of the processing used for a single variable pattern can be reused for polar patterns. The existing OFUS routines would require minor changes to permit this modification of processing control.

Figures 5.3/1 and 5.3/2 are language charts indicating the form of the input for inserting single variable and contour patterns respectively.

5.3.3.2 Polar Patterns (POLPAT)

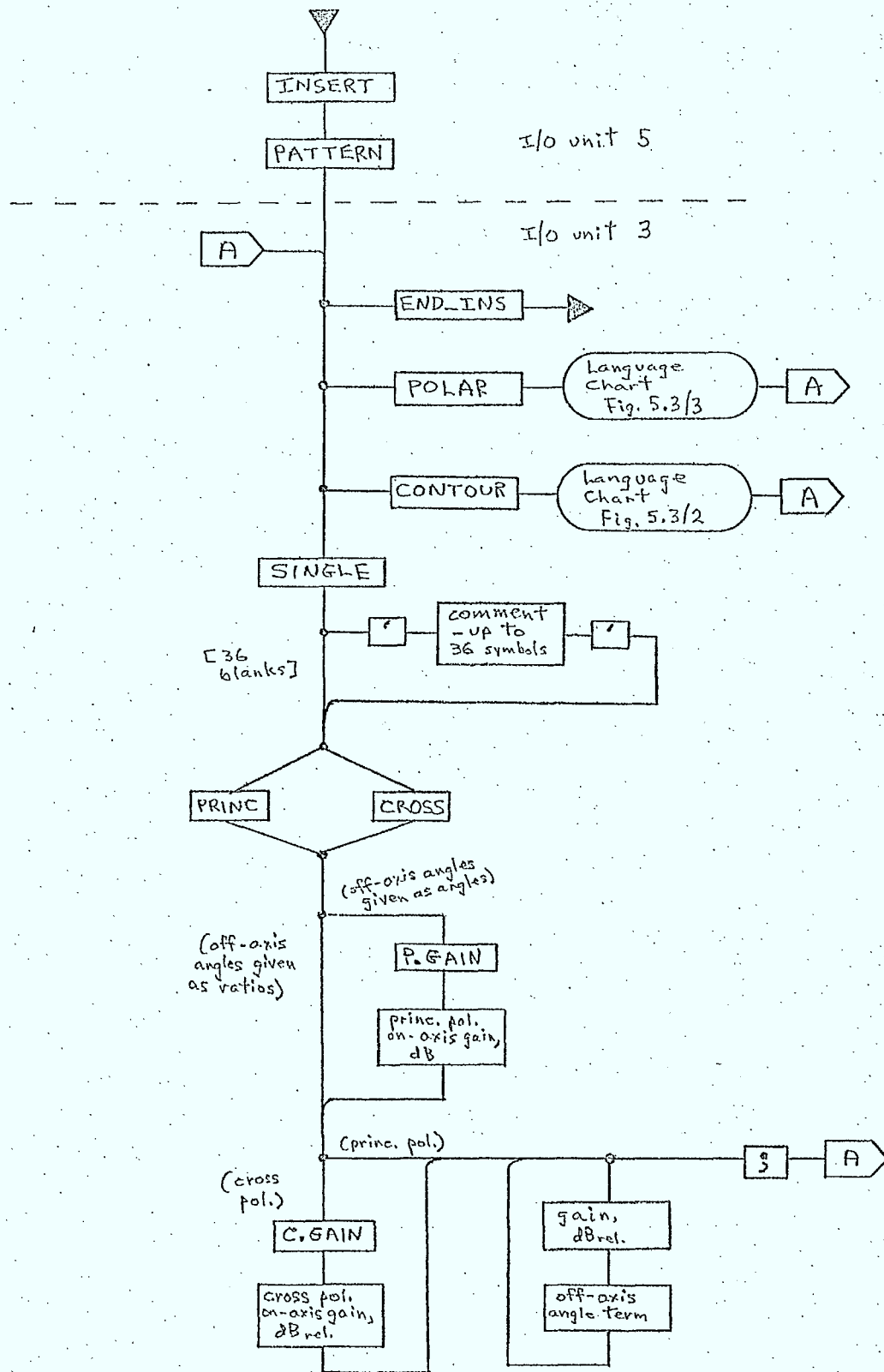
Purpose

The purpose of POLPAT is to read and process the data that forms one radial pattern associated with a polar pattern.

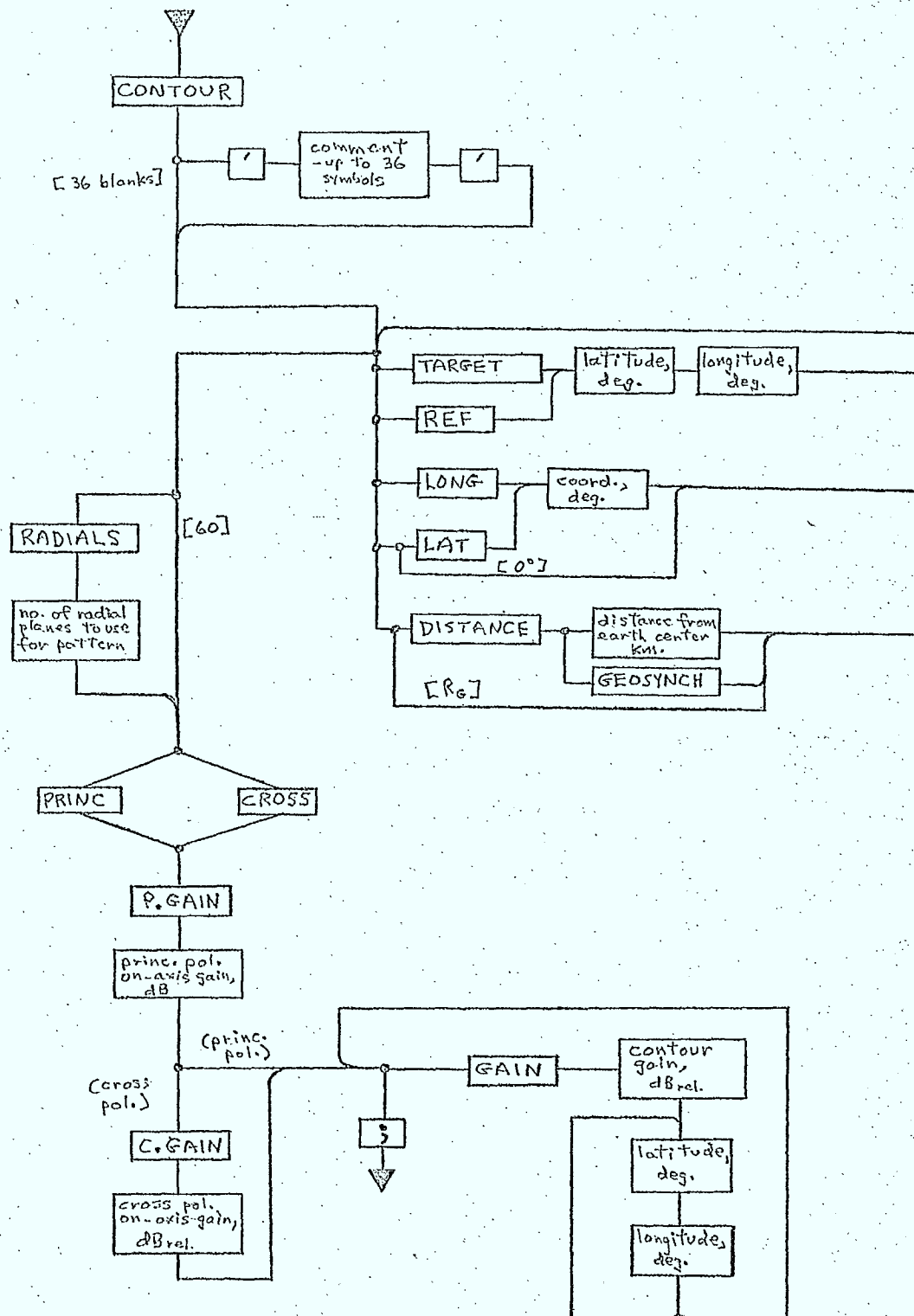
Description

The processing performed by this routine would be very similar to that performed by certain segments of subroutine PATT in Reference 5.3/3 in processing single variable pattern data.

Figure 5.3/1 Language Chart for Single-Variable Antenna Pattern Insertion and Insert Command Level



100



The user would be required to provide polarization type and on-axis gain data, along with (gain, off-axis angle) data for a least three radial patterns, together with the rotation angles to be associated with each radial. The input data for polarization type, gains, and off-axis angles would be the same (with the same options) as for the single variable patterns described in Table 4.9/1 in Reference 5.3/1.

The same validity checking of input data as is done in OFUS will be done by this simulation.

Figure 5.3/3 is a language chart describing the form of the language that would be required for the insertion of a polar pattern.

Inputs

- o input device unit number and associated parameters
- o pattern storage array
- o 3dB half angle

Outputs

- o pattern storage array

5.3.4 Deletion (PATDEL)

The deletion of a pattern from the pattern file would be done as in OFUS. This operation is described in Section 4.10 of Reference 5.3/1. Figure 5.3/11 is the relevant language chart.

5.3.5 Dumping (PATDMP)

Again, this operation can be performed by an already existing sub-program in OFUS with only minor changes to accommodate polar patterns in the file. Section 4.11 of Reference 5.3/1 describes this operation. Figure 5.3/4 is the appropriate language chart.

Figure 5.3/3 Language Chart for Polar Antenna Pattern Insertion

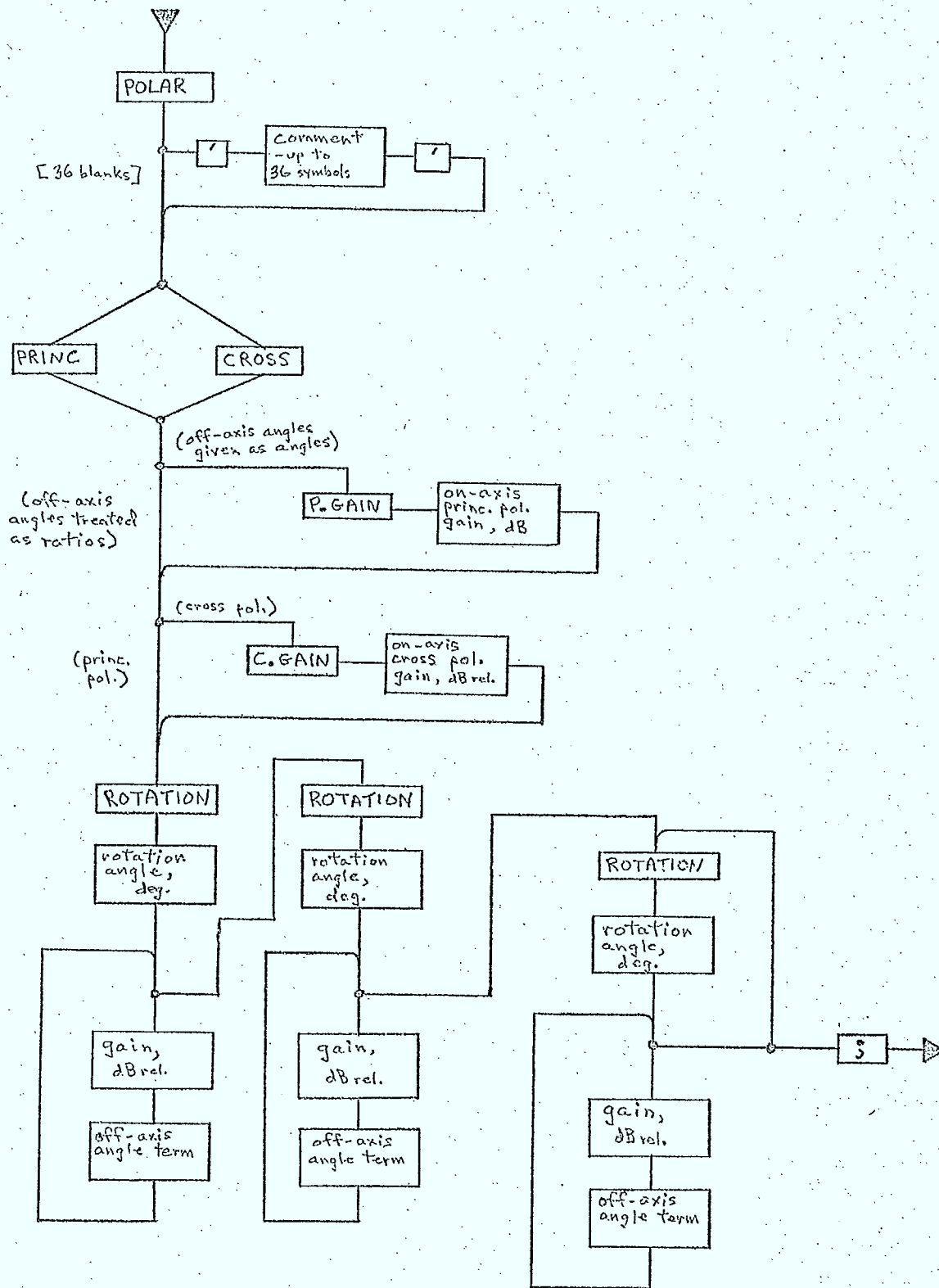
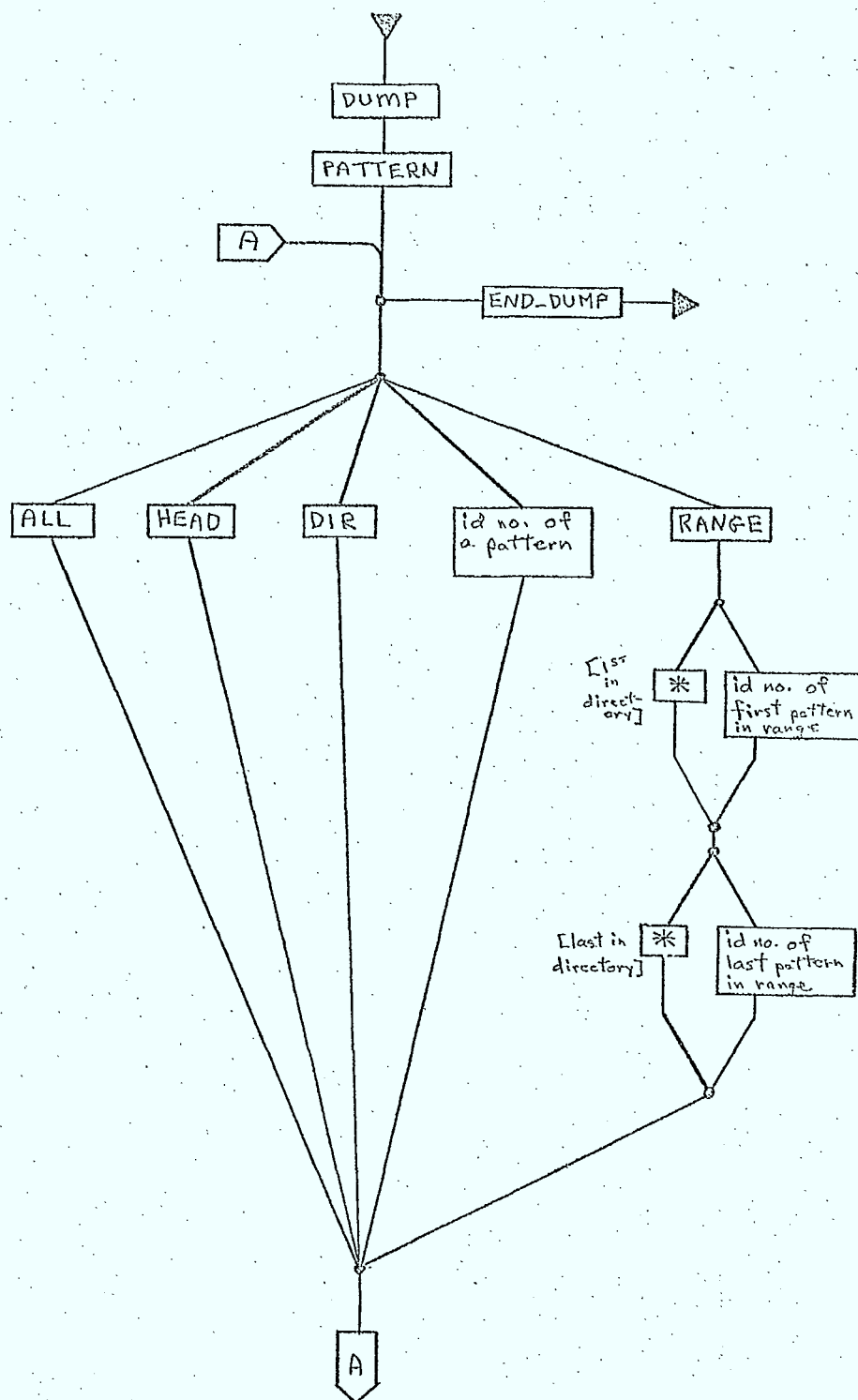


Figure 5.3/4 Language Chart for Dumping Pattern File Records



5.3.6 Reorganization (PATRG)

Since the pattern file used by this simulation has the same organization as that used by OFUS, the same routine can be used to effect the reorganization of the pattern file. This operation is described in Section 4.12 of Reference 5.3/1.

References

- 5.3/1: SED 0710-44-SW-103, Issue 3; "Orbit Frequency Utilization Simulation - Volume 2 - Program Description", February 28, 1977.
- 5.3/2: SED 0710-44-SW-105, Issue 3; "Orbit Frequency Utilization Simulation - Volume 4 - User's Guide", February 28, 1977.
- 5.3/3: SED 0710-44-SW-104, Issue 3; "Orbit Frequency Utilization Simulation - Volume 3 - Program Listing", February 28, 1977.

5.4 Spectrum and Filter File

This FORTRAN direct access file is used to store data describing spectra and filters of arbitrary shapes.

The simulation will do no maintenance operations on this file. Its creation and the insertion, deletion, updating, etc., of data in it, is the responsibility of the user. The data in this file must be organized in the format described in this section. To use this data in calculations, the user must insert the record number of the appropriate filter or spectrum in the carrier records in the database, as indicated on the insertion language charts described in Section 5.2.

The simulation will treat the spectrum and filter file as a FORTRAN direct access file.

A simulation default will set the size of this file to 50 records each of which describes one filter or spectrum. Each record is 202 words (808 bytes) long, with its data contents stored in binary form. (ie; the simulation will use unformatted READs to read data from this file.)

Each record must have the following data format:

<u>Field</u>	<u>Contents</u>
1	a type code - integer 0: filter data 1: spectrum data
2	number of data values, n - integer - the simulation will read as many of the following fields in this record as is specified here - minimum value of 2 - maximum value of 200
3	- filter or spectrum data, sampled at equally spaced
4	frequency intervals across the RF bandwidth of the
5	filter or spectrum (Note, this bandwidth is stored
.	in carrier records in the database). For filters,
.	the data must be normalized so that a value of 1 is
.	stored at the filter center frequency. For RF spectra,
.	no normalization is required.
202	

Upon reading n points from a record in this file, the simulation will process this data as described in Chapter 4.

6.0 MISCELLANEOUS

6.1 Antenna Pattern Display

6.1.1 Display Command Processor (DSPLAY)

Purpose

This routine displays antenna gain response patterns by producing page plots of gain vs. off-axis angle for antenna beams stored in the database.

Description

User instructions are read and interpreted to determine:

- o which beams are to be plotted
- o for which polarizations the gains are to be computed
- o for non-symmetric beams, the angle of rotation about the bore-sight that describes the plane in which the gain response is to be determined.

These parameters, once specified, remain in effect until overridden by subsequent specifications. When the desired parameters have all been specified, the plots are produced by calling subroutine PATPLT.

Because subroutine ANTEN, used in the calculation routines to obtain gain values, is also used here for the same purpose, the gain values that are plotted are those that would be used in actual calculations.

Note that for an isotropic antenna, a message is written instead of producing a plot that would be a horizontal line.

This subroutine is a modification of the one described in Section 6.10 of Reference 6.1/1 and in Reference 6.1/2. Figure 6.1/1 is a flowchart indicating the structure of subroutine DSPLAY; Figure 6.1/2 is a language chart indicating the form of the commands available to the user.

Figure 6.1/2 Language Chart for Pattern Display

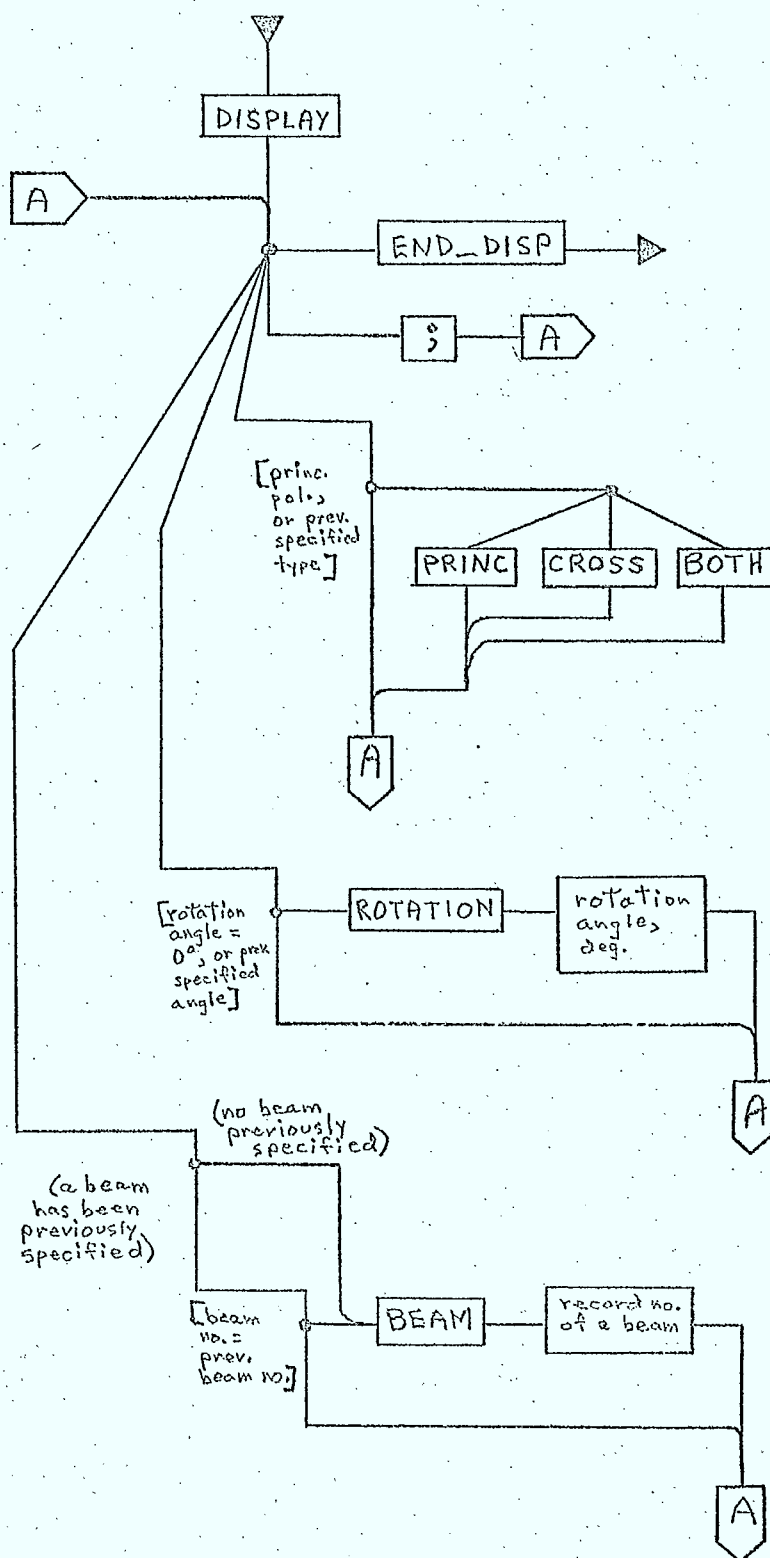
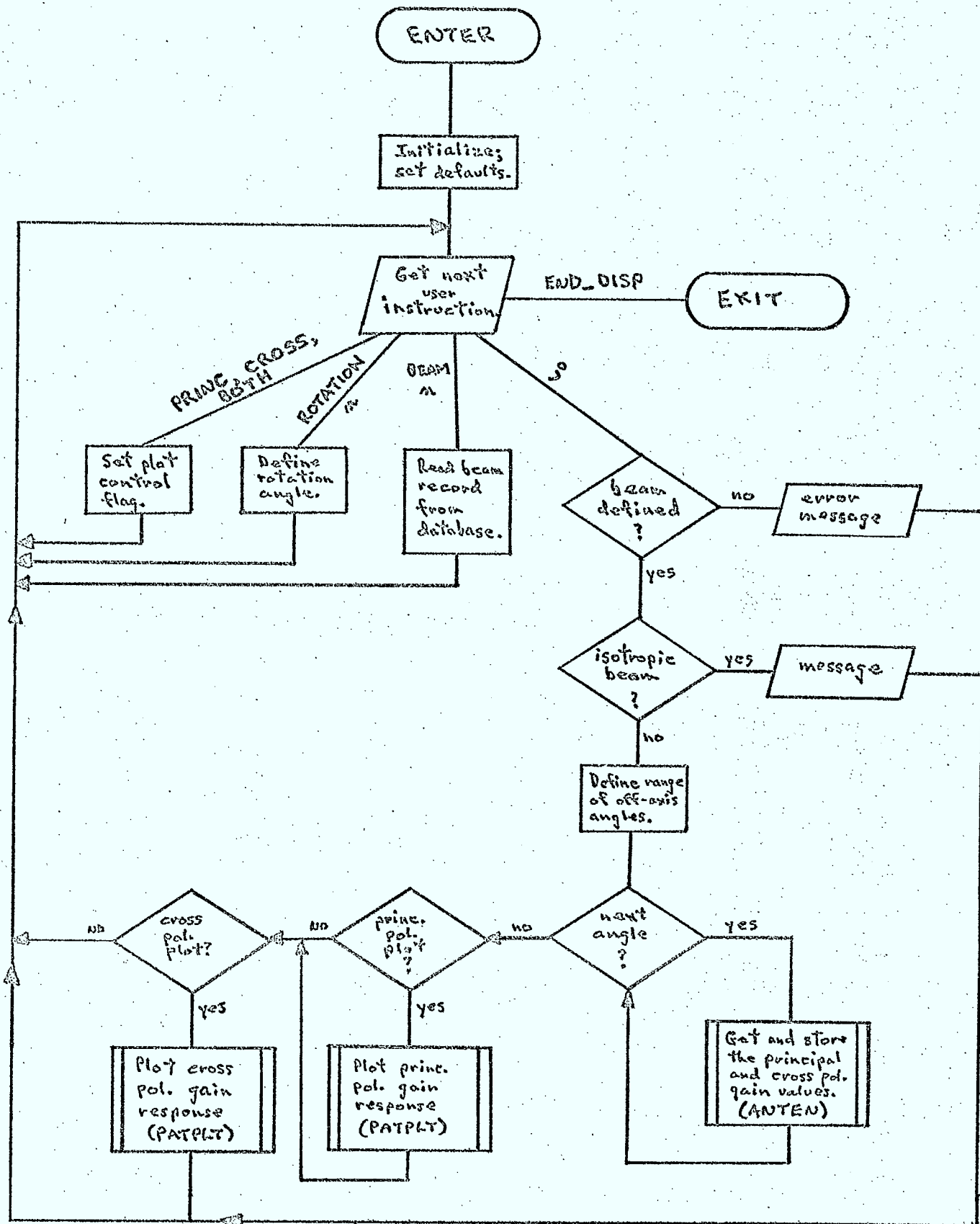


Figure 6.1/1 Flowchart of DSPLAY



Inputs

- o I/O devices, database, pattern file
 - unit no., characteristic parameters
- o user instructions

Outputs

- o page plot header lines
- o message lines

6.1.2 Display Plot Utility (PATPLT)Purpose

This routine formats an array of gain values into a page plot of gain vs. off-axis angle.

Description

The method used is described in Section 6.10 of Reference 6.1/1 and in Reference 6.1/2.

Inputs

- o array of gain values
- o size of the array
- o output device unit no.
- o no. of lines per page

Outputs

- o page plot of gain vs. off-axis angle

References

- 6.1/1: SED 0710-44-SW-103, Issue 3; "Orbit Frequency Utilization Simulation - Volume 2 - Program Description", February 28, 1977
- 6.1/2: SED 0710-44-SW-104, Issue 3; "Orbit Frequency Utilization Simulation - Volume 3 - Program Listing", February 28, 1977

6.2 Status and Error Messages

A status message is a short note from the program to the user intended to provide information which, generally, he would find useful or desirable to have.

An error message is a consequence of an error condition arising. Generally, this type of message describes the error as the program encountered it and indicates the nature of any recovery action attempted.

Among the typical error messages would be those arising from attempts to insert invalid data into the database or pattern file. Error messages may also be generated if erroneous data is read from the various files during SITE or LINK calculations.

Status messages produced by the program are generally required to inform the user of why calculations have been terminated. Such messages appear when sites used in LINK calculations are not visible to each other, or when signal levels fall below equipment threshold levels.

Section 6.9 in Reference 6.2/1 provides a more detailed characterization of status and error messages.

References

- 6.2/1: SED 0710-44-SW-103, Issue 3; "Orbit Frequency Utilization Simulation - Volume 2 - Program Description", February 28, 1977.

7.0 SYSTEM RESOURCE REQUIREMENTS

7.1 Device and Memory Requirements

Given certain points of similarity between this simulation and the OFUS program:

- both are batch programs, not interactive, though limited interactive capability is provided;
- both require user input and produce reports, plots, and messages;
- both make use of a program - maintained database and pattern file;
- the size of this simulation is expected to be comparable to that of OFUS;

it is not surprising that the computer hardware requirements of this simulation would be similar to those of OFUS, as outlined in Section 2.2 of Reference 7.1/1.

7.1.1 Input

Input to the simulation consists of:

- user commands and instructions specifying and controlling the operation of the simulation;
- data to be inserted into the program - maintained database;
- data to be inserted into the program - maintained pattern file.

These three sources of input data are distinguished by the program from one another, and each is assigned a different FORTRAN logical I/O unit number. Each is treated as a sequential dataset with a record length equal to a value established by program default (initially, 80 characters, but adjustable downwards to 32 characters or upwards to 132 characters).

Prior to program execution, the FORTRAN logical I/O unit numbers must be associated with the actual devices from which the three input datasets will be obtained. These devices can be:

- terminal, where the user types in the input as it becomes required during program execution;
- card reader, where the user has prepared his input as card decks which the program reads during its execution;
- disk, where the user has prepared his input as sequential datasets stored on disk, which the program then reads during execution. (Tape or drum devices could replace the disk unit).

7.1.2 Output

The program produces:

- reports, detailing the calculations performed and the results obtained in site or link analyses;
- plots, of spectra or antenna response;
- status messages and error messages.

These outputs are considered to form just one sequential output dataset, with reports, plots, and messages appearing in the order in which the program produced them. Record length will be set to a value established by program default (initially, 108 characters to accomodate one carriage control character and a maximum printed line length of 107 characters, but adjustable upwards to 132 characters).

Prior to program execution, the FORTRAN logical I/O unit number attached to this output dataset must be associated with the device on which the output is to be produced. This device could be:

- terminal, where the output is written on the terminal as it is produced. Note that most terminals do not make use of carriage control; consequently, the "vertical forms control" provided by carriage control characters will not be available.
- line printer, where the output is written on a line printer. In this case, carriage control would normally be operative, so that the output would exhibit the desired spacing and pagination.
- disk, where the output is written onto a sequential disk dataset. This permits the user to produce many copies of the output by printing the disk dataset as often as desired at either a terminal or on a line printer. (Tape or drum devices could replace the disk unit)

7.1.3 Processing

Since this simulation will be of comparable size to the OFUS program, and since it also maintains a database and a pattern file, the hardware requirements would be comparable to those of OFUS. These requirements would include:

- CPU and associated subsystems, to support the processing requirements of the simulation. Because of the size of the program, this requirement would likely be met only by a larger general purpose computer;
- memory, for program and variable storage during execution. Again, the size of the program indicates that the memory requirement could be substantial. The OFUS program, with no overlay structure, forms a load module of approximately 100K words (1K=1024). Overlaying could reduce this, but even with overlaying, memory requirements would remain quite large;
- disk, for the program - maintained database and pattern file. These two files are treated by the program as FORTRAN direct access datasets, and each with its own logical I/O unit number. (A drum could replace the disk for these direct access files).
- disk, for the user-maintained spectrum and filter file. This would also be a FORTRAN direct access file from which the program could obtain data giving RF spectra shapes or filter characteristics, though the simulation would not have the capability to maintain these files. (Again, a drum could replace the disk).

References

7.2/1: SED-0710-44-SW-105, Issue 3; "Orbit Frequency Utilization Simulation - Volume 4 - User's Guide", February 28, 1977.

7.2 Language Requirements

The simulation will be written in FORTRAN IV, using those language features that are compatible with the compilers on the computers on which the simulation is initially intended to run (the IBM System 370-158 for program development, and the XDS Sigma 9 for DOC use).

Section 2.3 of Reference 7.2/1 indicates both the language features that will likely be used and the supporting FORTRAN library functions that will likely be required.

References

7.2/1: SED 0710-44-SW-105, Issue 3; "Orbit Frequency Utilization Simulation - Volume 4 - User's Guide", February 28, 1977.

81941

System level design of the mobile-satellite simulation.

P
91
C655
P533
1977

DATE DUE
DATE DE RETOUR[illegible]

LOWE-MARTIN No. 1137

